UNIVERSITY OF AMSTERDAM

UvA-DARE (Digital Academic Repository)

The holographic correspondence

Probing bulk gravitational physics with Wilson lines and geodesic Witten diagrams

Llabrés Llambías, E.M.

[Link to publication](#)

THE HOLOGRAPHIC CORRESPONDENCE

probing bulk gravitational physics
with Wilson lines and geodesic Witten diagrams

Eva Llabrés Llambías

THE HOLOGRAPHIC CORRESPONDENCE

PROBING BULK GRAVITATIONAL PHYSICS WITH
WILSON LINES AND GEODESIC WITTEN DIAGRAMS

The Holographic Correspondence

probing bulk gravitational physics with Wilson lines and geodesic Witten diagrams

Academisch Proefschrift

ter verkrijging van de graad van doctor

aan de Universiteit van Amsterdam

op gezag van de Rector Magnificus

prof. dr. ir. K.I.J. Maex

ten overstaan van een door het College voor Promoties

ingestelde commissie,

in het openbaar te verdedigen in de Agnietenkapel

op dinsdag 6 november 2018, te 12.00 uur

door

Eva Maria Llabrés Llambías

geboren te Maó, Spanje

Promotiecommissie

Promotor

    prof. dr. J. de Boer   Universiteit van Amsterdam

Co-Promotor

    dr. A. Castro Anich   Universiteit van Amsterdam

Overige leden

dr. A.M.F. Belin	Universiteit van Amsterdam
prof. dr. E.A. Bergshoeff	Rijksuniversiteit Groningen
dr. B.W. Freivogel	Universiteit van Amsterdam
dr. N. Iqbal	Durham University
prof. dr. P. Kraus	University of California
prof. dr. C.J.M. Schoutens	Universiteit van Amsterdam
prof. dr. E.P. Verlinde	Universiteit van Amsterdam

PUBLICATIONS

THIS THESIS IS BASED ON THE FOLLOWING PUBLICATIONS:

[1] A. Castro, E. Llabrés, and F. Rejon-Barrera,
"Geodesic Diagrams, Gravitational Interactions & OPE Structures",
JHEP06 (2017), 099, `arXiv:1702.06128 [hep-th]`.
Presented in Chapter **2**.

[2] A. Castro, N. Iqbal, and E. Llabrés,
"Wilson Lines and Ishibashi states in AdS_3/CFT_2",
JHEP09 (2018), 066, `arXiv:1805.05398 [hep-th]`.
Presented in Chapter **3**.

[3] A. Castro, N. Iqbal, and E. Llabrés,
"Eternal Higher Spin Black Holes: a Thermofield Interpretation",
JHEP08 (2016), 022, `arXiv:1602.09057 [hep-th]`.
Presented in Chapter **4**.

OTHER PUBLICATIONS BY THE AUTHOR:

[4] A. Castro, and E. Llabrés,
"Unravelling Holographic Entanglement Entropy in Higher Spin Theories",
JHEP03 (2015), 124, `arXiv:1410.2870 [hep-th]`.

[5] J. de Boer, E. Llabrés, J. F. Pedraza, and D. Vegh,
"Chaotic strings in AdS/CFT",
Phys. Rev. Lett. **120** no. 20, (2018), 201604, `arXiv:1709.01052 [hep-th]`.

SUMMARY

This thesis focuses on aspects of the AdS/CFT correspondence which are directly relevant to problems in quantum and classical gravity. Specifically, we use geodesic Witten diagrams, and gravitational Wilson lines in AdS/CFT to explore bulk gravitational physics. Here, we will very briefly summarize our results.

Introduction

In Chapter 1, we start by reviewing the holographic correspondence, focusing on the features that are essential to this thesis. This will establish the context for the novel results that are presented in the rest of the chapters. This introduction, as well as the thesis, has two distinguishable parts. The first one examines some aspects of the duality in general dimensions, and the second one focuses on the peculiarities of AdS_3/CFT_2. A recurrent leitmotiv is higher spin fields. We will use theories containing spinning fields, as a framework to study the AdS/CFT correspondence.

Spinning geodesic Witten diagrams

In conformal field theories, symmetries play a crucial role. The exploitation of the conformal group gives an efficient organizational principle for the observables in the theory. An example of such a principle is the conformal block decomposition of four-point correlation functions, which makes an explicit distinction among portions that are purely determined by symmetries and the theory dependent data. A very natural question arises in holography: can we organize observables in gravity as efficiently as we do in the dual CFTs? This issue has been addressed

since the beginning of holography using, for example, Witten diagrams. However, it was not until very recently that geodesic Witten diagrams were proposed as the dual of the conformal blocks. Geodesic Witten diagrams shed new light in the program of holographic reconstruction: they give a holographic meaning to the conformal block decomposition of four-point Witten diagrams, and they allow us to write the complicated d-dimensional volume integrals of the Witten diagrams in terms of simpler line integrals.

While the original proposal of geodesic Witten diagrams was formulated for only external scalar fields, we extended it to spinning external legs in Chapter 2. We found a systematic way to evaluate geodesic Witten diagrams for external fields of arbitrary spin, and we decomposed the original Witten diagrams in terms of those. Despite the success of geodesic Witten diagrams, we found some problems that remain unsolved. We observed that the same spinning conformal block can be expressed in terms of different geodesic Witten diagram with inequivalent bulk interactions. This shows that geodesic Witten diagrams do not treat bulk interactions as fundamental.

Wilson lines in AdS$_3$/CFT$_2$

In Chapter 3 and 4, we focus on gravity in three dimensions. In this case, gravity does not have propagating degrees of freedom, and it can be recasted as a Chern-Simons theory of gauge connections. This is in general much simpler to manipulate that the formalism of Einstein's general relativity. In Chern-Simons formulation, the coupling of matter is done by using gravitational Wilson lines. In the context of AdS/CFT, these objects are considered to properly probe the bulk from the boundary degrees of freedom, since they are related to quantities such as CFT correlation functions, and entanglement entropy.

In this thesis, we will exploit gravitational Wilson lines in AdS$_3$/CFT$_2$ with two different, but related purposes. In Chapter 3, we will show that they can be used to compute the overlap of two local bulk states. This g. In Chapter 4, we use the Wilson line in the context of higher spin theories. We use them to explicitly provide a notion of causality in higher spin gravity, which allows us to associate a Penrose diagram to higher spin black holes.

CONTENTS

1

INTRODUCTION

OR HOW I LEARNED TO STOP WORRYING AND LOVE HIGHER SPIN THEORIES

This Chapter is a self-contained introduction to topics and concepts that are relevant for this thesis. We start by presenting the AdS/CFT correspondence, and we later focus on an specific case: the $\text{AdS}_3/\text{CFT}_2$ duality. We will review as well some aspects of higher spin theories in AdS backgrounds, and their role in the context of holography.

1.1 Motivation

Einstein's theory of General Relativity provides a successful description of classical gravity, which treats the gravitational force as a geometric property of space-time. However, General Relativity fails to describe interactions at a subatomic scale. A reason is that gravity is non-renormalizable, and the tools of QFT are not useful to explore its high energy behavior. One of the most ambitious goals of modern physics is to find a UV complete theory of gravity, or *quantum gravity*, which describes the quantum behavior of the graviton. At high energies, this theory should suppress the non-renormalizable terms of General relativity, and describe interactions in quantum field theory. And at low energies, it should recover classical gravity.

There are other aspects we do not understand about gravity, even at the semi-classical level. A notorious example is that of the *black holes* space-times. They

are solutions to the classical Einstein field equations which have curvature singularities at the origin, and event horizons. The event horizon is a region of the space-time beyond which light cannot scape, and therefore their interiors are not accessible to an external observer. Even though unexpected from Einstein's formalism of general relativity, black holes have a thermodynamical interpretation. Their entropy is given by the Bekenstein-Hawking formula [6–8]:

$$S_{\text{BH}} = \frac{A}{4G_N} \, , \tag{1.1}$$

where A is area of the event horizon, and G_N is Newton's constant. This is an example of *holographic* behaviour, where all the information contained inside a volume is represented over the surface that surrounds it, just like in traditional holograms. Formula (1.1) contradicts classical expectations: due to the no-hair theorem, black holes are single-state systems which would have associated a null entropy. One expected resolution is to find the *space-time as emergent* from an effective description of some underlying microscopic theory, with all degrees of freedom encoded in the area of the black hole.

Holography does not only make its appearance in black hole space-times, but it is conjectured to be a general property of quantum gravity [9,10]. This statement is known as the *holographic principle* and states that all the information contained in a region of space-time in quantum gravity can be described by the degrees of freedom of its boundary. A concrete realisation of this principle is the *AdS/CFT correspondence*, conjectured in [11]. This is a duality that relates quantum and classical gravity theories in AdS_{d+1} backgrounds to quantum field theories with conformal symmetry living in d-dimensions (CFT_d). AdS space-times have a flat conformal *boundary*, where the CFT_d is thought to live in. The gravitational theory in the interior AdS_{d+1} spacetime is commonly regarded as the *bulk* theory. This correspondence is a very valuable theoretical framework in which we can ask crucial questions about quantum and classical gravity. The two main reasons are:

AdS/CFT is a powerful toolbox. The correspondence allows us to write gravitational theories of gravity using quantum field theory variables, and vice-versa. Therefore, depending on the problem we are addressing, we can choose the formalism which is more convenient for us. This property will serve us to answer questions in (quantum) gravity by recasting them in the language of the dual boundary theory. Moreover, the correspondence has a weak/strong character, which means that a theory of strong interactions has a weakly coupled dual description. For example, this has been exploited to analytically study strongly coupled field theories using simpler tools from classical gravity, which was the primary motivation in [11].

quantum field theory (boundary)	gravity (bulk)
conformal transformations	AdS isometries
operators $\mathcal{O}$	fields ϕ
conformal dimension Δ	mass m
correlation functions	Witten diagrams
algebra of conserved charges	asymptotic symmetries
conserved current	gauge symmetries
thermal state	black hole geometry

Figure 1.1: *A sample of entries of the AdS/CFT dictionary.*

AdS/CFT is a toy model for emergence. The AdS/CFT correspondence is a concrete example of the holographic principle, over which we possess a lot of control. The study of this duality can serve us to achieve a better understanding of the holographic behavior of gravity, and how the gravitational degrees of freedom should emerge from a quantum field theory. In particular, in a theory of quantum gravity, the graviton can be thought of as arising in the low-energy effective theory from the degrees of freedom of the UV. AdS/CFT is a wonderful framework to investigate this behavior. For example, an interesting idea arising from AdS/CFT is that the space-time should emerge from entangling the degrees of freedom of the quantum field theory [12].

In this chapter we will review basic aspects of the holographic duality; specifically, we will focus on some entries of the *AdS/CFT dictionary*. This dictionary is a map between bulk and boundary quantities, which allows us to switch from gravitational to quantum field theoretical language at our convenience. Some of the equivalences are collected in the table in Fig. 1.1. The first four lines in Fig. 1.1 will be carefully developed in Sections 1.2 and 1.3. In section 1.4 and 1.5, we will focus the rest of the entries in the context of AdS_3/CFT_2 holography.

We have outlined some of the advantages of the AdS/CFT correspondence. However, the holographic duality is as powerful as puzzling: the lack of understanding of some fundamental issues in gravity generates problems in the formulation of the holographic duality itself. Many elemental aspects of the correspondence remain still unclear 20 years after its formulation. This thesis addresses questions in the AdS/CFT correspondence and its relevance to problems in gravity. We work in the weak field expansion of gravity, and the conformal field theories are strongly coupled.

In Chapters 2, 3, and 4, we will refine some details of the holographic conjecture

in this limit, and our findings will lead us to learn about gravitational theories. Especially, we will focus on theories with *higher spin fields*, and *3-dimensional gravity*. Both of them will be reviewed later on in this chapter. We will use them as a framework to study holography, but at the same time, we will learn more about them by using this very powerful duality.

1.2 The AdS/CFT Correspondence

In this section, we reproduce the first entries of the AdS/CFT dictionary in Fig. (1.1). We start by reviewing some basic features of conformal field theories in 1.2.1. Then, in Sec. 1.2.2 we focus on the study of a scalar field in AdS background. We show that it can be interpreted as a source field in a conformal field theory that lives in the AdS boundary. In Sec. 1.2.3, we introduce Witten diagrams, which are used to compute CFT correlation functions holographically.

1.2.1 Correlation functions in CFT

We consider a *d*-dimensional space with line element $ds^2 = g_{ij}(x)dx^i dx^j$. A conformal transformation is defined as the coordinate change that leaves the metric $g_{ij}(x)$ invariant up to a scale, i.e.,

$$g_{ij}(x') = \Omega^2(x)g_{ij}(x) \,. \tag{1.2}$$

The scaling factor $\Omega(x)$ guarantees that angles between vectors do not change after this type of transformations. In this thesis we will focus in quantum field theories in flat backgrounds, i.e. $g_{ij} = \eta_{ij}$, where η_{ij} is Minkowski's metric. In this case, the conformal transformations are:

$$
\begin{aligned}
&\text{\textit{translations}} &&x'^i = x^i + a^i \,, \\
&\text{\textit{Lorentz}} &&x'^i = \Lambda^i{}_j \, x^j \,, \\
&\text{\textit{scalings}} &&x'^i = \alpha \, x^i \,, \\
&\text{\textit{special conformal transformations}} &&x'^i = \frac{x^i - b^i \, x^2}{1 - 2b \cdot x + b^2 x^2} \,,
\end{aligned}
\tag{1.3}
$$

where $\Lambda^i{}_j$ are the matrices of Lorentz rotations, and a^i, b^i, α are real and constant parameters. The generators of these transformations follow the algebra of $SO(d, 2)$ in Lorentzian signature $(-, +, .., +)$. In Euclidean signature $(+, +, .., +)$ the group

would be $SO(d+1,1)$. The scale factor in (1.2) is related to the Jacobian of the transformations as:

$$\left|\frac{\partial x'}{\partial x}\right| = \Omega^{-d}(x)\,. \tag{1.4}$$

A central element in the study of CFTs are local scalar operators that transform as:

$$\mathcal{O}'(x') = \left|\frac{\partial x'}{\partial x}\right|^{-\Delta/d} \mathcal{O}(x)\,. \tag{1.5}$$

under conformal transformations. These are called *quasi-primary* operators, and Δ is its conformal or scaling dimension. For simplicity and abuse of notation, we will often call them *primary* operators [1]. In CFTs we have an extensive control over correlation functions of primaries due to the symmetries (1.3). For example, the correlator of two primary operators can be fully determined by requiring invariance under the conformal transformations:

$$\langle \mathcal{O}(x_1)\mathcal{O}(x_2)\rangle = \frac{1}{x_{12}^{\Delta}}\,, \tag{1.6}$$

where we define $x_{12} \equiv |x_1 - x_2|$, and Δ is the conformal dimension of both operators. If the operators have different dimension, the correlator would be zero. Three-point functions can also be found by requiring invariance:

$$\langle \mathcal{O}_1(x_1)\mathcal{O}_2(x_2)\mathcal{O}_3(x_3)\rangle = \frac{\lambda_{123}}{(x_{12})^{(\Delta_1+\Delta_2-\Delta_3)/2}(x_{23})^{(\Delta_2+\Delta_3-\Delta_1)/2}(x_{13})^{(\Delta_1+\Delta_3-\Delta_2)/2}}\,. \tag{1.7}$$

where λ_{123} is a dynamical coefficient. For higher point functions, the solution is not uniquely fixed by conformal invariance. However, we can exploit an important property of conformal field theories: the *operator product expansion* (OPE). This expansion states that we can approximate two local operators at different points by a sum of operators at one of the points:

$$\mathcal{O}_1(x_1)\mathcal{O}_2(x_2) = \sum_{\mathcal{O}} \lambda_{12\mathcal{O}}\, C(x_{12}, \partial_{x_2})_{i_1\ldots i_l}\, \mathcal{O}^{i_1\ldots i_l}(x_2)\,, \tag{1.8}$$

where the sums runs over all primaries $\mathcal{O}^{i_1\ldots i_l}$ contained in the theory characterized by their dimension Δ, and spin l. The OPE coefficients $\lambda_{12\mathcal{O}}$ are theory dependent factors that appear in the three-point functions, and the differential operators $C(x_{12}, \partial_{x_2})_{i_1\ldots i_l}$ are determined by the form of the two, and three-point functions. Using OPEs for the pairs $\mathcal{O}_1\mathcal{O}_2$, and $\mathcal{O}_3\mathcal{O}_4$, we can decompose four-point functions as

$$\langle \mathcal{O}_1(x_1)\mathcal{O}_2(x_2)\mathcal{O}_3(x_3)\mathcal{O}_4(x_4)\rangle = \sum_{\mathcal{O}} \lambda_{12\mathcal{O}}\lambda_{34\mathcal{O}} W_{\Delta|l}(x_1, x_2, x_3, x_4)\,, \tag{1.9}$$

---

[1] Primary and quasi-primary are different operators in the context of CFT$_2$. We explain the details in Sec. 1.4.1.

where $W_{\Delta|l}(x_1, x_2, x_3, x_4)$, it is known as *conformal partial wave*, and it is defined through the differential operators in the OPEs, and two-point point functions of the exchanged operators [13–15]. Using conformal invariance, the conformal partial wave can be reduced to a function of two variables:

$$W_{\Delta|l}(x_1, x_2, x_3, x_4) = \left(\frac{x_{24}}{x_{14}}\right)^{\frac{\Delta_1-\Delta_2}{2}} \left(\frac{x_{14}}{x_{13}}\right)^{\frac{\Delta_3-\Delta_4}{2}} \frac{G_{\Delta|l}(u, v)}{(x_{12})^{(\Delta_1+\Delta_2)/2}(x_{34})^{(\Delta_3+\Delta_4)/2}},$$
(1.10)

with

$$u \equiv \frac{x_{12}x_{34}}{x_{13}x_{24}}, \quad v \equiv \frac{x_{14}x_{23}}{x_{13}x_{24}}.$$
(1.11)

$G_{\Delta|l}(u, v)$ is known as a *conformal block*, and explicit expressions can be found in e.g. [16–18] among many other places.

1.2.2 Scalar fields in AdS

Now we take a turn, and analyse theories of gravity. In particular, we start by considering the Einstein-Hilbert action in $(d+1)$-dimensions, with no matter, and negative cosmological constant Λ:

$$S_{EH} = \frac{1}{16\pi G_N} \int dy^{d+1} \sqrt{g}(R - 2\Lambda),$$
(1.12)

where $g = \det(g_{\mu\nu})$ in Euclidean signature, R is the Ricci scalar, and G_N is the gravitational constant. The solutions to (1.12) that are maximally symmetric with constant negative curvature, are known as Anti de Sitter spaces-times (AdS_{d+1}). They can be thought as embedded in the $(d+2)$-dimensional hyperboloid:

$$-Y_0^2 + Y_{d+1}^2 + Y_i Y^i = -\ell^2,$$
(1.13)

where ℓ is the AdS radius defined as $\Lambda = -d(d-1)/2\ell^2$, and $Y_i Y^i = \delta^{ij} Y_i Y_j$, with $i = 1, ..., d$. The metric on this geometry is $(d+2)$-dimensional Minkowski:

$$ds^2 = -dY_0^2 + dY_{d+1}^2 + dY_i dY^i.$$
(1.14)

We can parametrize the hyperboloid using a $(d+1)$-dimensional set of coordinates $y^\mu = (z, x^i)$, with the following change

$$Y^0 = \ell\,\frac{z^2 + x^2 + 1}{2z}, \quad Y^{d+1} = \ell\,\frac{1 - z^2 - x^2}{2z}, \quad Y^i = \ell\,\frac{x^i}{z}.$$
(1.15)

where $x^2 = x^i x_i$. This results in the AdS_{d+1} Poincare metric:

$$ds^2 = \frac{\ell^2}{z^2}(dz^2 + dx^i dx_i).$$
(1.16)

with boundary located at $z \to 0$. The isometry group of Euclidean AdS$_{d+1}$ is the d-dimensional conformal group $SO(d+1,1)$. For simplicity we have restricted ourselves to AdS with Euclidean signature, but everything is easily generalizable to Lorentzian signature via the appropriate Wick rotations. The isometries of AdS$_{d+1}$ match with the symmetries of a CFT$_d$. This is the first indication that there are relations between gravity theories in AdS backgrounds, and quantum field theories with conformal symmetries. In the following, we will see more examples of this.

Free scalar field in AdS

The AdS/CFT correspondence describes conformal field theories as living in the boundary of gravity theories in AdS background. In the following, we will explain explain basic aspects of the correspondence using a specific simple example. Consider a massive free scalar field in AdS background:

$$S\left[\phi\right] = \int d^{d+1}y \sqrt{g} \left(\frac{1}{2} \nabla_\mu \phi \nabla^\mu \phi + \frac{m^2}{2} \phi^2 \right), \qquad (1.17)$$

where ∇_μ is the AdS$_{d+1}$ covariant derivative, and m is the mass of the field. The previous action has :

$$(\nabla^2 - m^2)\phi(y) = 0. \qquad (1.18)$$

In this section we use Poincare coordinates (1.16), and $y^\mu = (z, x^i)$. Considering the equation (1.18) close to the boundary $z \to 0$, we observe that the field behaves asymptotically:

$$\phi(z,x) \sim z^{\Delta_\pm}, \qquad \Delta_\pm = \frac{d}{2} \pm \sqrt{\frac{d^2}{4} + m^2}, \qquad (1.19)$$

where $\Delta_\pm$ are the positive and negative roots of $m^2 \ell^2 = \Delta(\Delta - d)$. We choose the negative root, since it is the dominant contribution at the boundary $z \to 0$. We define $\Delta \equiv \Delta_+$, and impose the following boundary conditions:

$$\lim_{z \to 0} z^{\Delta - d} \phi(z,x) = \bar{\phi}(x), \qquad \Delta = \frac{d}{2} + \sqrt{\frac{d^2}{4} + m^2}. \qquad (1.20)$$

We refer to $\bar{\phi}(x)$ as the boundary value of $\phi(y)$. For simplicity we fixed $\ell = 1$, and we will restore it if needed. A solution to (1.18), which fulfils the boundary conditions (1.20) is:

$$\phi(y) = \int d^d x' G^\Delta_{b\partial}(y, x') \bar{\phi}(x'), \qquad (1.21)$$

where $G_{b\partial}^{\Delta}(y, x)$ is a bulk-to-boundary propagator which solves the wave equation (1.18) for the bulk coordinate y. Its explicit expression is:

$$G_{b\partial}^{\Delta}(z, x; x') = \left(\frac{z}{z^2 - (x - x')^2} \right)^{\Delta}, \qquad (1.22)$$

which has the appropriate asymptotic behaviour:

$$\lim_{z \to 0} z^{\Delta - d} G_{b\partial}^{\Delta}(z, x; x') = \delta(x - x'). \qquad (1.23)$$

So far in this section Δ is just a quantity defined in terms of m. However, we have already chosen it to match the notation for the scaling dimension of CFT primary operators, and we will explain the reason in Sec. 1.2.3. It will be important to keep in mind that for scaling transformations the boundary field behaves as

$$\bar{\phi}'(x') = \alpha^{\Delta - d} \bar{\phi}(x). \qquad (1.24)$$

The previous can be found imposing that $\phi(y)$ transforms as a scalar in (1.21).

Scalar field with cubic interaction

We will now analyse the AdS/CFT correspondence beyond the free fields. For example, let us consider a cubic interaction:

$$S[\phi] = \int d^{d+1}y \sqrt{g} \left(\frac{1}{2} \nabla_{\mu} \phi \nabla^{\mu} \phi + \frac{m^2}{2} \phi^2 + \frac{\lambda}{3} \phi^3 \right). \qquad (1.25)$$

We would like to find solutions to the classical action in terms of the boundary fields $\bar{\phi}(x)$, as we did in (1.21). In the interacting case the equations of motion are difficult to solve exactly, but expanding perturbatively around $\lambda \to 0$ we find the solution:

$$\phi(y) = \phi_1(y) + \lambda \int d^{d+1}y' G_{bb}^{\Delta}(y, y') \phi_1(y') + \dots,$$

$$\phi_1(y) \equiv \int d^d x' G_{b\partial}^{\Delta}(z, x - x') \bar{\phi}(x'), \qquad (1.26)$$

where ... stands for higher orders corrections in λ. G_{bb}^{Δ} is a bulk-to-bulk propagator which follows equation:

$$(\nabla_y^2 - m^2) G_{bb}^{\Delta}(y, y') = -\frac{\delta(y, y')}{\sqrt{g}}, \qquad m^2 = \Delta(\Delta - d). \qquad (1.27)$$

where ∇_y^2 is the covariant laplacian in the coordinate y. It is interesting to note that the bulk-to-bulk and the bulk-to-boundary are related by:

$$\lim_{z' \to 0} \frac{z'^{\Delta}}{2\Delta - d} \, G_{bb}^{\Delta}(z, x; z', x') = G_{b\partial}^{\Delta}(z, x; x') \,. \tag{1.28}$$

It is important to notice that the boundary conditions in (1.20) still hold for interacting solution (1.26).

1.2.3 Boundary correlators in AdS: Witten diagrams

It is crucial to notice that the following term is invariant to conformal transformations:

$$\int d^d x \, \mathcal{O}(x) \bar{\phi}(x) \,. \tag{1.29}$$

This can be shown for scalings considering (1.24), together with $d^d x' = \alpha^d d^d x$, and $\mathcal{O}'(x') = \alpha^{-\Delta} \mathcal{O}(x)$, and similarly for the other conformal transformations. The fact that the term (1.29) is invariant under conformal transformations suggests that there is a relation between partition functions of conformal field theories, and gravitational theories in AdS. Based on this observation, it was conjectured [19]:

$$Z_{\text{CFT}} \left[\bar{\phi}(x) \right] = \langle e^{\int d^d x \, \mathcal{O}(x) \bar{\phi}(x)} \rangle_{\text{CFT}} = Z_{\text{AdS}} \left[z^{\Delta - d} \phi(y) \big|_{z \to 0} = \bar{\phi}(x) \right] \,. \tag{1.30}$$

where $\bar{\phi}(x)$ behaves as a source field for primary operator $\mathcal{O}(x)$, with dimension Δ. The gravity partition function corresponds to the following path integral:

$$Z_{\text{AdS}} = \int \mathcal{D}\phi \exp \left[-\frac{1}{G_N} S_{\text{AdS}} \left[\phi \right] \right] \,, \tag{1.31}$$

where S_{AdS} is defined as:

$$\frac{1}{G_N} S_{\text{AdS}} \equiv S_{\text{EH}} + \frac{1}{G_N} S_{\text{matter}} \,. \tag{1.32}$$

where S_{EH} is the Einstein-Hilbert action (1.12), and S_{matter} is the action corresponding to the matter fields in AdS background. For the CFT partition function, Z_{CFT}, the fields $\bar{\phi}$ act as sources, and $\langle ... \rangle_{\text{CFT}}$ stands for the path integral over boundary fundamental fields weighted by the CFT action. Formula (1.30) proposes that n-point correlation functions of CFT operators $\mathcal{O}(x)$ can be computed using the partition function of the gravitational theory with

$$\langle \mathcal{O}_1(x_1) ... \mathcal{O}_n(x_n) \rangle = \frac{\delta^n Z_{\text{AdS}} \left[\bar{\phi}(x) \right]}{\delta \bar{\phi}(x_1) ... \delta \bar{\phi}(x_n)} \bigg|_{\bar{\phi}=0} \,. \tag{1.33}$$

We will be intereseted in connected n-point functions. Therefore, we consider the free energy density $F = -\log Z$:

$$\langle \mathcal{O}_1(x_1)...\mathcal{O}_n(x_n)\rangle_{\text{conn}} = \frac{\delta^n F_{\text{AdS}}\left[\bar{\phi}(x)\right]}{\delta\bar{\phi}(x_1)...\delta\bar{\phi}(x_n)}\bigg|_{\bar{\phi}=0}. \tag{1.34}$$

The path integral in (1.31) is generally very difficult to perform exactly in terms of the fields. We will work in the classical limit, $G_N \to 0$, and perform the saddle point approximation

$$Z_{\text{AdS}}[\bar{\phi}(x)] = \exp\left[-\frac{1}{G_N}S_{\text{AdS}}\left[\phi[\bar{\phi}]\right]\right], \tag{1.35}$$

where $\phi[\bar{\phi}]$ is the classical solution to the action in terms of the boundary source. The gravity constant G_N dividing in the exponent causes the need for a rescaling of the fields. For concreteness, we consider the massive scalar field in (1.25) as the only matter content of the theory. We see we need $\phi \to \sqrt{G_N}\,\phi$ to get the quadratic term to be zero-th order in G_N.

$$\frac{1}{G_N}S_{\text{AdS}}\left[\phi\right] = S_{EH} + \int d^{d+1}y\sqrt{g}\left(\frac{1}{2}\nabla_\mu\phi\nabla^\mu\phi + \frac{m^2}{2}\phi^2 + \frac{\lambda\sqrt{G_N}}{3}\phi^3\right). \tag{1.36}$$

If we consider higher order interactions terms, they would have been accompanied by higher powers in $\sqrt{G_N}$. Since the Einstein-Hilbert action is of order $1/G_N$, we have performed a weak-field expansion around the background solution in powers of the field fluctuations. Now, using (1.34), and (1.36), we find:

$$\langle \mathcal{O}_1(x_1)...\mathcal{O}_n(x_n)\rangle_{\text{conn}} = \frac{1}{G_N}\frac{\delta^n S_{\text{AdS}}\left[\phi[\bar{\phi}]\right]}{\delta\bar{\phi}(x_1)...\delta\bar{\phi}(x_n)}\bigg|_{\bar{\phi}=0}. \tag{1.37}$$

Therefore, to compute connected a n-point correlation function we only need to substitute in the action the classical solution for the field ϕ in terms of boundary sources $\bar{\phi}$, and take the appropriate variations. For the example (1.36), we would use the solution (1.26) with $\lambda \to \lambda\sqrt{G_N}$. We can see that the correlators are given by a generalized type of Feynman diagrams organized in powers of G_N.

The first diagram in Fig. 2.5 represents a two-point function of primary operators. It can be found from the bulk-to-boundary progragator:

$$\langle \mathcal{O}(x_1)\mathcal{O}(x_2)\rangle = \lim_{z\to\epsilon} G_{b\partial}^\Delta(z, x_1; x_2) = \epsilon^\Delta\frac{1}{(x_1 - x_2)^{2\Delta}}, \tag{1.38}$$

where $\epsilon \to 0$, and should be considered as a boundary cuttoff. The second diagram in Fig. 2.5 corresponds to a three point function, and in integral representation
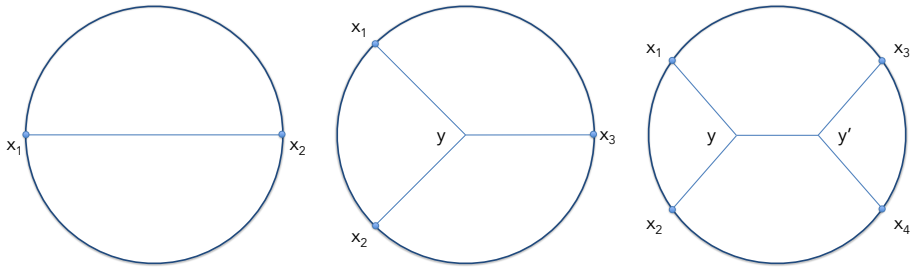
Figure 1.2: *Examples of Witten diagrams in AdS_{d+1}. The interior represents the bulk of AdS, and the circumference is its boundary, where the CFT operators $O_i(x_i)$ live. The lines represent the bulk-to-boundary and bulk-to-bulk AdS propagators defined in (1.21) and (1.27). The bulk vertexes are integrated over the bulk coordinates.*

reads:

$$\langle \mathcal{O}_1(x_1)\mathcal{O}_2(x_2)\mathcal{O}_3(x_3)\rangle = \lambda\sqrt{G_N}\int dy^{d+1}\sqrt{g}\, G_{b\partial}^{\Delta_1}(y,x_1)G_{b\partial}^{\Delta_2}(y,x_2)G_{b\partial}^{\Delta_3}(y,x_3)$$

$$= \lambda\sqrt{G_N}\,\frac{1}{(x_{12})^{(\Delta_1+\Delta_2-\Delta_3)/2}(x_{23})^{(\Delta_2+\Delta_3-\Delta_1)/2}(x_{13})^{(\Delta_1+\Delta_3-\Delta_2)/2}}\,,$$

$$(1.39)$$

where in the last inequality we ignored an overall normalization that depends on the conformal weights. The third diagram in Fig. 2.5 is the 4-point function when the theory has only scalar fields, and a non-derivative cubic interaction:

$$\langle \mathcal{O}_1(x_1)\mathcal{O}_2(x_2)\mathcal{O}_3(x_3)\mathcal{O}_4(x_4)\rangle =$$

$$= \lambda^2 G_N\int dy^{d+1}\int dy'^{d+1}\, G_{b\partial}^{\Delta_1}(y,x_1)G_{b\partial}^{\Delta_2}(y,x_2)G_{bb}^{\Delta_3}(y',y)G_{b\partial}^{\Delta_3}(y',x_3)G_{b\partial}^{\Delta_4}(y',x_4)\,.$$

$$(1.40)$$

Performing the previous double integral for generic d and conformal dimensions is not an easy task. Some results can be found in [20], where they manage to write (1.47) as an infinite double sum, which simplifies for some specific dimensions of the operators. In [21] they follow a more successful approach which consists on decomposing the integral (1.47) as finite sum over contact diagrams with an interaction ϕ^4, whose closed form can be obtained [22].

1/N-expansion in CFT

To compare the correlation functions obtained using bulk methods (Sec. 1.2.3), with those in the boundary (Sec. 1.2.1), we need to know what the weak-field

expansion means in the CFT. In the AdS/CFT correspondence, the degrees of freedom of the CFT, N_{dof}, are related to the gravitational constant via

$$N_{\text{dof}} = \frac{\ell^{d-1}}{G_N} \, . \tag{1.41}$$

For concreteness, in the rest of the this section we assume $N_{\text{dof}} = N^2$. This choice is widespread in the literature since it corresponds to a gauge theory with group $SU(N)$ in $d = 4$, the first and most explored example of the AdS/CFT correspondence. From (1.41) we infer that a weakly coupled gravity theory implies a large number of degrees of freedom in the dual CFT, and the expansion around $G_N \to 0$ should be translated in the CFT side as an expansion in $N \to \infty$. Therefore, for CFTs with weakly coupled gravity duals the free two-point functions do not scale with N, and the connected n-point contribute as

$$\langle \mathcal{O}_1(x_1)...\mathcal{O}_n(x_n) \rangle_{\text{conn}} \sim \frac{1}{N^{n-2}} \, . \tag{1.42}$$

where the symbol $\sim$ means that we just show the leading order in $1/N$ for each correlator, but ignore their explicit form.

There is another peculiarity of CFTs with weakly coupled gravity duals. If the their spectrum contains two primary operators $\mathcal{O}_1$ and $\mathcal{O}_2$, it necessarily contains as well *multi-trace primary operators*, which are composed by conglomerations of $\mathcal{O}_1$ and $\mathcal{O}_2$. For example, primary double-trace operators are schematically:

$$[\mathcal{O}_1\mathcal{O}_2]_{n,l} \approx \mathcal{O}_1 \partial^{2n} \partial_{\mu_1}...\partial_{\mu_l} \mathcal{O}_2 \, , \qquad \Delta_{n,l}^{12} = \Delta_1 + \Delta_2 + 2n + l \, ... \tag{1.43}$$

where the symbol $\approx$ means there is a linear combination of operators of type $\mathcal{O}_1 \partial^{2n} \partial_{\mu_1}...\partial_{\mu_l} \mathcal{O}_2$, which together result in the primary double-trace operator $[\mathcal{O}_1\mathcal{O}_2]_{n,l}$. $\Delta_{n,l}^{12}$ is its conformal dimension to first order in $1/N$ theory , and the dots ... stand for corrections in the large N limit. As a consequence, in the large N limit the OPE of two operators will contain single and multi-trace operators whose OPE coefficients should be expanded around $1/N$. For a single trace operator $\mathcal{O}$ in the OPE of $\mathcal{O}_1\mathcal{O}_2$, the scaling of the three-point function (1.42) shows that its OPE coefficient can be expanded as:

$$\lambda_{12\mathcal{O}} = \lambda_{12\mathcal{O}}^{(1)}/N + ... \, . \tag{1.44}$$
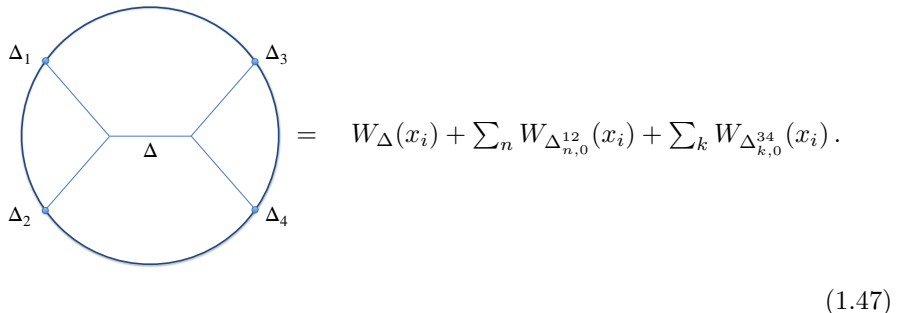
Following an analogous logic, for a generic double-trace trace operator $[\mathcal{O}_i\mathcal{O}_j]_{n,l}$, with $i, j \neq 1, 2$:

$$\lambda_{12[\mathcal{O}_i\mathcal{O}_j]_{n,l}} = \lambda_{12[\mathcal{O}_i\mathcal{O}_j]_{n,l}}^{(2)}/N^2 + ... \, . \tag{1.45}$$

For $i, j = 1, 2$, there is a contribution from the disconnected piece of $\langle \mathcal{O}_1\mathcal{O}_2[\mathcal{O}_1\mathcal{O}_2]_{n,l} \rangle$, which is of order N^0:

$$\lambda_{12[\mathcal{O}_1\mathcal{O}_2]_{n,l}} = \lambda_{12[\mathcal{O}_1\mathcal{O}_2]_{n,l}}^{(0)} + ... \, . \tag{1.46}$$

Now we are ready to compare the results of the n-point CFT correlators obtained in Sec. 1.2.1 with their holographic computation in Sec. 1.2.3. At order $1/N^0$, the CFT two-point function (1.6) is already equivalent to (1.38). For three-point function, we see that (1.7) is equivalent to (1.39). Using (1.44), we can relate the OPE coefficient to the gravity coupling constant as $\lambda = \lambda_{123}^{(1)}$. The $1/N$-expansion of the four-point functions does not have such a direct comparison on both sides of the duality. In the CFT side, we have restrictions over which operators will appear in the conformal block decomposition (1.9) at each order. Using (1.44) and (1.45), we infer that to order $1/N^2$ there are contributions to the 4-point function of conformal block of single trace operators $\mathcal{O}$, and double trace operators $[\mathcal{O}_1 \mathcal{O}_2]_{n,l}$, and $[\mathcal{O}_3 \mathcal{O}_4]_{n,l}$. We should be able to observe the same behavior on the AdS side. In [23], they use Mellin integrals to identify the following conformal block contributions in the scalar exchange Witten diagram:

$$= \quad W_\Delta(x_i) + \sum_n W_{\Delta_{n,0}^{12}}(x_i) + \sum_k W_{\Delta_{k,0}^{34}}(x_i) \,.$$

(1.47)

where the sums run over the double trace operator defined in (1.43). Double trace operators with $l \neq 0$ would appear in (1.47) when considering derivative scalar interactions in the Witten diagram. The result (1.47) can be alternatively found by imposing crossing symmetry for the CFT four-point function at order $1/N^2$ (following the program initiated by [24]).

1.3 Spinning fields and holography

In the previous section, we have introduced the holographic correspondence with a simple example: we have shown that a scalar field in AdS_{d+1} behaves as a source for a primary operator in a CFT_d, from which we can compute CFT correlation functions using Witten diagrams. However, these are two of the many entries of AdS/CFT dictionary, which we briefly reviewed in Fig. 1.1. This dictionary maps bulk to boundary quantities, and it is continuously improved and put to the test by the community. In this thesis, we focus on theories containing *spinning fields*

in AdS as a framework to analyze different entries of the AdS/CFT dictionary. In this section, we will first present the symmetric traceless tensors which will represent the *massive* spin fields. Then, we will see that the arguments we gave in Sec. 1.2.2 for the scalar field is easily generalizable for fields carrying spin. This will set up the context for the research carried out in Chapter 2. In Sec. 1.3.3, we will briefly comment about holography for *massless* spin fields. The relevance of theories of higher spin massless fields will be reviewed in Sec. 1.5.2, where we focus on three-dimensions, and they will be center of Chapter 4.

1.3.1 Primary operators and AdS fields with spin

In Section 1.2, we explained how a scalar field $\phi(y)$ in AdS_{d+1} is related to a primary operator $\mathcal{O}(x)$ in a CFT_d. However, we can consider more generic theories containing different types of fields. We consider the tensorial generalization of the primary operator in (1.5):

$$\mathcal{O}'_{i_1\ldots i_s}(x') = \left|\frac{\partial x'}{\partial x}\right|^{-\Delta/d} \frac{\partial x^{j_1}}{\partial x'^{i_1}} \cdots \frac{\partial x^{j_s}}{\partial x'^{i_s}} \mathcal{O}_{j_1\ldots j_s}(x)\,. \tag{1.48}$$

where $i_a, j_a = 1, ..., d$, are boundary indexes. We can rewrite (1.48) in terms of $SO(d)$ transformations, $R^j{}_i = \left|\frac{\partial x'}{\partial x}\right|^{-1/d} \frac{dx^j}{dx'^i}$. We can then rewrite:

$$\mathcal{O}'_{i_1\ldots i_s}(x') = \left|\frac{\partial x'}{\partial x}\right|^{-\frac{\Delta+s}{d}} R^{j_1}{}_{i_1} \ldots R^{j_s}{}_{i_s}\ \mathcal{O}_{j_1\ldots j_s}(x)\,, \tag{1.49}$$

Therefore i_a, j_a transform $SO(d)$ indices (plus a scaling) under $SO(d+1,1)$. The generators of $SO(d)$ allow for unitary, irreducible, and finite-dimensional *spin* representations labelled by s and Δ

AdS$_{d+1}$ spacetimes have the same $SO(d+1,1)$ symmetry than conformal field theories. A natural condition for the bulk field is to be in the same representation of $SO(d+1,1)$ than its dual primary operator. In AdS, particle representations labeled by mass m and spin s, correspond to the following free field equations [25]:

$$(\nabla^2 - m^2)\phi_{\mu_1\ldots\mu_s} = 0\,, \qquad \nabla^{\mu_1}\phi_{\mu_1\ldots\mu_s} = 0\,, \qquad g^{\mu_1\mu_2}\phi_{\mu_1\ldots\mu_s} = 0\,, \tag{1.50}$$

where ∇_μ is the AdS$_{d+1}$ covariant derivative, and $\mu_a = 1, ..., d+1$ are bulk indices. The two last equations impose transversability, and tracelessness, and they are commonly known as Fierz-Pauli conditions. In this work, we will consider for simplicity representations which result in fields and operators symmetric in all their indices.

We would like to make the relation between spinning AdS fields and CFT operators more precise. The following procedure is a generalization from the scalar field case in Sec.1.2.2, and we will briefly highlight some interesting points. At the boundary, we have just to consider the tangencial components of the spin indexes μ_a This means that at $z = 0$ we have $\phi_{z...\mu_s} \to 0$, and the boundary field will carry indexes i_a. Analysing (1.50) close to the boundary, we see that its solution behaves asymptotically

$$\phi(z, x) \sim z^{\Delta_\pm - s}, \qquad \Delta_\pm = \frac{d}{2} \pm \sqrt{\frac{d^2}{4} + s + m^2}, \qquad (1.51)$$

where $\Delta_\pm$ are the positive and negative roots of $m^2 = \Delta(\Delta - d) - s$. We define $\Delta \equiv \Delta_+$, and we consider solutions with following boundary conditions:

$$\lim_{z \to 0} z^{\Delta + s - d} \phi_{\mu_1...\mu_s}(z, x) = \bar{\phi}_{i_1...i_s}(x), \qquad \Delta = \frac{d}{2} + \sqrt{\frac{d^2}{4} + s + m^2}., \quad (1.52)$$

We refer to $\bar{\phi}_{i_1...i_s}(x)$ as the boundary value of $\phi_{\mu_1...\mu_s}(y)$. Setting $s = 0$, we reproduce the result (1.20). As in (1.21), the solution to the free equations of motion (1.50) can be written using bulk-to-boundary propagator:

$$\phi_{\mu_1...\mu_s}(y) = \int d^d x' G^\Delta_{b\partial}(y, x')|^{i_1...i_s}_{\mu_1...\mu_s} \; \bar{\phi}_{i_1...i_s}(x'), \qquad (1.53)$$

where $G^\Delta_{b\partial}(y, x')|^{i_1...i_s}_{\mu_1...\mu_s}$ is the spinning bulk-to-boundary propagator which solves (1.50) for y, and carries both bulk, and boundary indexes.

So far, we considered free fields, but we can add interactions. An example of cubic interaction between two scalars and one spin-s field is
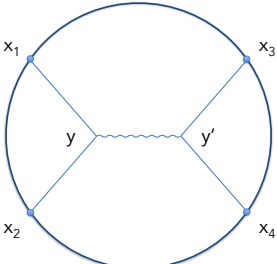
$$\phi_1 \nabla_{\mu_1}...\nabla_{\mu_s} \phi_2 \; \phi_3^{\mu_1...\mu_s}. \qquad (1.54)$$

We can consider other cubic interactions, as well with spin in all the three fields. The solution (1.53) must be modified when adding interactions, considering a bulk-to-bulk propagator, as we did for the scalar field in (1.26). The propagator is completely determined from the equations (1.50) with $m^2 = \Delta(\Delta - d) - s$, and carries bulk indexes, i.e., $G^\Delta_{bb}(y, y')|^{\nu_1...\nu_s}_{\mu_1...\mu_s}$.

1.3.2 CFT correlators and Witten diagrams with spin

We can show that $\int d^d x \, \mathcal{O}_{i_1...i_s} \bar{\phi}^{i_1...i_s}$ is invariant under conformal transformations, analogously as we did for the scalar case in (1.29). Then, the boundary field

$\bar{\phi}^{i_1 \dots i_s}(x)$ should be interpreted as a source for the operator $\mathcal{O}_{i_1 \dots i_s}(x)$ with scaling dimension Δ. The correlators of CFT primary operators can be computed holographically using Witten diagrams that take into account all relevant interactions of the theory. A simple example is the four-point function of scalar operators. Considering only cubic interactions, and leading order in $1/N$, this correlator is computed by the following sum over Witten diagrams:

$$\langle \mathcal{O}_1(x_1)\mathcal{O}_2(x_2)\mathcal{O}_3(x_3)\mathcal{O}_4(x_4) \rangle_{\text{conn}} \quad = \quad \sum_s \qquad \text{(1.55)}$$

where the wavy line represents a spin-s bulk-to-bulk propagator, which will be contracted derivatives of the scalar bulk-to-boundary propagator to reproduce the interactions of the type (1.54). Therefore, the sum s runs over all the possible interactions in the theory. The comparison of the spinning exchange Witten diagrams with the conformal block decomposition can be done as in (1.47), although the details are more complicated. It was demonstrated that the conformal blocks for the double trace operators $[\mathcal{O}_1\mathcal{O}_2]_{n,l}$, and $[\mathcal{O}_3\mathcal{O}_4]_{n,l}$ with $l = 0, \dots, s$ should appear in the decomposition of a spin-s exchange Witten diagram [24, 26–28].

The analysis becomes even more complicated for correlators with primary operators that carry spin. For example, conformal symmetry does not fix a single form for the three-point function as in the scalar case (1.7), or a single conformal block as in (1.9), but we have different possible independent *tensor structures*. In the holographic of computation, we need to consider the Witten diagrams with all the relevant *interactions*. The difficulties come into play because the number of possible tensor structures and interactions increases very fast as we increase the spin of the external operators. Our focus in Chapter 2 will be these type of spinning correlators. Specifically, in Sec. 2.2.1 we will introduce the embedding formalism, which is an indispensable tool to study tensors in AdS, and CFT. In Sec. 2.2.2, we will review the calculation of spinning three-point function in both sides of the duality, mapping the CFT tensor structures to the bulk interactions. The rest of the sections in Chapter 2 will be aimed to find an efficient way to decompose spinning 4-point Witten diagrams in terms of the spinning conformal blocks. For the latter, we will use *geodesic Witten diagrams*, which give a holographic interpretation to

the conformal partial waves.

1.3.3   Conserved currents and massless fields

Before moving on, we would like to comment about the special situation when $\Delta = s + d - 2$. In this case, the dual bulk field has mass $m^2 = (s+d-2)(s-2) - s$. This mass is related to the so-called unitarity bound:

$$m^2 \geq (s + d - 2)(s - 2) - s\,, \tag{1.56}$$

below which states with negative norm appear in the particle representation associated to (1.50). The saturation of this bound corresponds to zero norm states, and, therefore, the equations (1.50) in this limit represent *massless spin fields*. The massless spin field equations will be analysed in further detail in Sec. 1.5, but for now it is important know they admit an additional gauge symmetry:

$$\delta_\xi \phi_{\mu_1 \dots \mu_s} = \nabla_{(\mu_1} \xi_{\mu_2 \dots \mu_s)}\,. \tag{1.57}$$

where $\xi_{\mu_1 \dots \mu_s}$ is the symmetric and traceless gauge parameter. Therefore, we often refer to massless fields as *gauge fields*. The source term $\int d^d x\, \mathcal{O}_{i_1 \dots i_s} \bar{\phi}^{i_1 \dots i_s}$, should be invariant to this variation:

$$0 = \int d^d x\, \mathcal{O}_{i_1 \dots i_s} \delta \bar{\phi}^{i_1 \dots i_s} = - \int d^d x\, \partial^{i_1} \mathcal{O}_{i_1 \dots i_s}\, \xi^{i_1 \dots i_s}\,, \tag{1.58}$$

where in the second inequality we have used (1.57) at the boundary, partial integration, and the fact that $\mathcal{O}_{i_1 \dots i_s}$ is symmetric in all its indices. Equation (1.58) implies that

$$\partial^{i_1} \mathcal{O}_{i_1 \dots i_s} = 0. \tag{1.59}$$

Therefore, gauge fields in AdS backgrounds are dual to conserved currents in the CFT. This gives us evidence supporting the sixth entry our AdS/CFT dictionary in Fig. (1.1).

1.4   3d/2d holography

A part of this thesis addresses a particular situation of the holographic duality: the *AdS₃/CFT₂ correspondence*. In the bulk, the theory is very interesting mainly due

to its simplicity: gravity in 3-dimensions does not propagate degrees of freedom[2]. This feature makes it a useful framework to study aspects of quantum and classical gravity avoiding some complications we encounter in higher dimensions. Moreover, gravity theories in AdS$_3$ backgrounds are dual to conformal field theories in two dimensions. In this case, the conformal algebra becomes infinite dimensional, which results in constraints for the spectrum of the theory. These restrictions lead to a more controlled version of the holographic duality.

The real power of 3d gravity is that it still contains exciting features despite circumventing problems from higher dimensions. For example, we can construct *3-dimensional black holes* solutions when adding a negative cosmological constant. Black holes are fascinating objects which enclose essential questions associated to quantum gravity, as exemplified by (1.1). Moreover, they pose difficult puzzles for the holographic correspondence. For example, it is challenging to map bulk and boundary observables in black hole geometries as a result of their event horizons. In this thesis, we will exploit the simplicity of 3-dimensional theories to address questions about black holes geometries in the context of holography.

In this section, we explicitly review some aspects of conformal field theories in two dimensions, and Einstein-Hilbert gravity in AdS$_3$ backgrounds, highlighting the features that make them special. Moreover, we give explicit evidence of the AdS$_3$/CFT$_2$ duality, mapping their infinite-dimensional algebras, and their observables. In Sec. 1.4.2, we review the reformulation of AdS$_3$ gravity as a theory of gauge connections. This formalism makes explicit the lack of propagating degrees of freedom of 3d gravity, and the variables are easier to manipulate. For example, the information about the metric is encoded in the flat connections, and the diffeomorphisms become gauge transformations. This formalism will be very useful in Sec. 1.5, where it will allow us to easily describe in a treatable manner theories of higher spin gravity.

1.4.1   Briefest review to AdS$_3$/CFT$_2$

CFT$_2$

This is a very brief review of some aspects of CFT$_2$ which will be interesting to us. For more details, we refer the reader to the very nice review [29].

---

[2]This holds for 3-dimensional Einstein-Hilbert gravity, which consists of a massless graviton. One could consider other gravitational theories which carry propagating degrees of freedom in three dimensions, such as theories with massive gravitons.

In Sec. 1.2.1, we found that the conformal transformations for a *d*-dimensional field theory in flat space were scaling, translations, dilatations, Lorentz, and special conformal transformations (1.3). However, when the number of dimension is two, the conformal transformations are generalised to all possible analytic coordinate transformations:

$$z \to \tilde{z}(z), \qquad \bar{z} \to \bar{\tilde{z}}(\bar{z}), \qquad (1.60)$$

where we used $ds^2 = dz d\bar{z}$ in complex coordinates: $z, \bar{z} = x \pm it_E$, and t_E is the Euclidean time. This makes $d = 2$ a very interesting special case in conformal field theories. A *primary* operator in CFT$_2$ is defined by the transformation law:

$$\tilde{\mathcal{O}}(\tilde{z}, \bar{\tilde{z}}) = \left(\frac{\partial \tilde{z}}{\partial z}\right)^{-h} \left(\frac{\partial \bar{\tilde{z}}}{\partial \bar{z}}\right)^{-\bar{h}} \mathcal{O}(z, \bar{z}). \qquad (1.61)$$

where $(h, \bar{h})$ are the scaling dimensions. *Primary* operators are different form *quasi-primary* operators in (1.61). All primary fields are by definition quasi-primaries, but the opposite statement is not true.

A crucial object in our analysis will be the *stress tensor*. It is usually defined in quantum field theories through the usual Noether procedure as the conserved current associated to translations In CFT$_2$, the stress energy tensor takes a very simple form, with only two non-vanishing components:

$$T_{zz}(z) \equiv T(z), \qquad T_{\bar{z}\bar{z}}(\bar{z}) \equiv \bar{T}(\bar{z}). \qquad (1.62)$$

Consider the following infinitesimal version of the conformal transformation:

$$z \to z + \epsilon(z), \qquad \bar{z} \to \bar{z} + \bar{\epsilon}(\bar{z}). \qquad (1.63)$$

The conserved current associated to (1.63) can be written in terms of the stress tensor:

$$J(z) = \epsilon(z)T(z), \qquad \bar{J}(\bar{z}) = \bar{\epsilon}(\bar{z})\bar{T}(\bar{z}), \qquad (1.64)$$

which allows us to write the usual Ward identities for a conformal transformation as:

$$\delta_\epsilon \mathcal{O}(z, \bar{z}) = -\mathrm{Res}[\epsilon(z)T(z)\mathcal{O}(z, \bar{z})]. \qquad (1.65)$$

As a consequence of the previous formula, we can obtain the transformation properties of the operator $\mathcal{O}$ under a conformal transformation from the singular terms in the OPE of $T\mathcal{O}$. From symmetry considerations we can find the OPE of the stress tensor with itself:

$$T(z)T(\omega) = \frac{c/2}{(z-w)^4} + \frac{2}{(z-w)^4}T(\omega) + \frac{1}{z-w}\partial T(\omega) + ... \qquad (1.66)$$

where c is a theory dependent constant, and it is known as *central charge*. Therefore, the transformation of the stress tensor under conformal transformations is

$$\delta_\epsilon T(z) = \epsilon(z)\partial T(z) + 2\partial\epsilon(z)T(z) + \frac{c}{12}\partial^3\epsilon(z).$$
(1.67)

The transformation for $\bar{T}$ is analogous, and we assume $\bar{c} = c$. Now we can consider the mode expansion of the stress-energy tensor:

$$T(z) = \sum_{n\in\mathbb{Z}} z^{-n-2}L_n, \qquad\qquad \bar{T}(\bar{z}) = \sum_{n\in\mathbb{Z}} \bar{z}^{-n-2}\bar{L}_n.$$
(1.68)

These series can be inverted, and using (1.65)-(1.67) it can be shown that L_m form an infinite dimensional algebra:

$$[L_m, L_n] = (m - n)L_{m+n} + \frac{c}{12}(m^3 - m)\delta_{m+n}$$
(1.69)

and likewise for $\bar{L}_m$. This is the infinite-dimensional *algebra of conserved charges* of CFT$_2$, known as the Virasoro conformal algebra.

AdS$_3$

We will now turn our focus to gravitational theories in three dimensions. We start by considering the Einstein-Hilbert action:

$$S_{EH} = \frac{1}{16\pi G_3} \int_{\mathcal{M}} \sqrt{-g}(R - 2\Lambda),$$
(1.70)

where G_3 is the gravitational constant, Λ the cosmological constant, and the integral is performed over a generic 3-dimensional manifold $\mathcal{M}$, which we consider in Lorentzian signature. The equations of motion are

$$R_{\mu\nu} + g_{\mu\nu}R + g_{\mu\nu}\Lambda = 0.$$
(1.71)

In three dimensions the Riemann tensor, $R_{\mu\nu\rho\sigma}$, has six independent components, the same as the Ricci tensor, $R_{\mu\nu}$, and the metric. The Riemann tensor is completely determined once the metric and the cosmological constant are fixed via the equations of motion:

$$R_{\mu\nu\rho\sigma} = \Lambda (g_{\nu\rho}g_{\nu\sigma} - g_{\mu\sigma}g_{\nu\rho})$$
(1.72)

This implies that there are non-propagating degrees of freedom for gravity in three dimensions, which is an enormous simplification respect the higher-dimensional cases. All metrics that are a solution to the vacuum equations (1.71) in three dimensions are locally equivalent to each other.
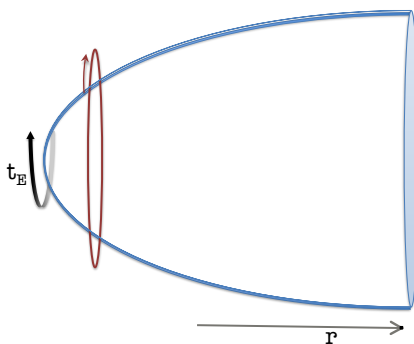
Figure 1.3: *Geometry of the Euclidean BTZ black hole where the compact direction is Euclidean time $t = it_E$. The red curve depicts the cycle along which the smoothness condition* (1.75) *is imposed. In Euclidean signature, the geometry ends at a finite value of $r = r_+$, which corresponds to the horizon.*

Despite the simplicity of the local features of three-dimensional gravity, the analysis of its global properties still leads to very interesting physics, even at the classical level. In the following we develop some examples which support this affirmation. We fix the cosmological constant as $\Lambda = -1/\ell^2$. A solution to the 3-dimensional equations in (1.71) is:

$$ds^2_{\text{AdS}} = \ell^2 \left(-\cosh^2 \rho \, dt^2 + d\rho^2 + \sinh^2 \rho \, d\phi^2 \right) .\tag{1.73}$$

with $\phi \sim \phi + 2\pi$. The metric (1.73) is known as the *global AdS$_3$* space-time. This is another parametrization for the hyperboloid metric (1.13), from which we have already studied the Poincare metric (1.16). Another solution to the vacuum Einstein equations with $\Lambda = -1/\ell^2$ is:

$$ds^2_{\text{BTZ}} = -\frac{(r^2 - r_+^2)(r^2 - r_-^2)}{r^2 \ell^2} dt^2 + \frac{\ell^2 r^2}{(r^2 - r_+^2)(r^2 - r_-^2)} dr^2 + r^2 \left(d\phi + \frac{r_+ r_-}{\ell r^2} dt \right)^2 ,\tag{1.74}$$

which is known as the *BTZ black hole*, and we consider $r_+ > r_-$. Global AdS$_3$ and BTZ spacetimes are locally equivalent to each other, and we can find a change of coordinates that relates them which evidences this fact. However, we can consider global properties that allow us to distinguish them as physically different solutions. The topology of global AdS$_3$ is a cylinder with compact direction $\phi \sim \phi + 2\pi$. Let us now analytically continue to Euclidean time with $t = it_E$, and consider the complex coordinates $z = \phi + it_E/\ell$, and $\bar{z} = \phi - it_E/\ell$. In these coordinates, the BTZ metric (1.74) requires the following *smoothness condition* to avoid a conical singularity at $r = r_+$:

$$z \sim z + i\beta_+ , \qquad \bar{z} \sim \bar{z} + i\beta_- , \qquad \beta_\pm = \frac{2\pi\ell}{r_+ \pm r_-} .\tag{1.75}$$

These conditions result in a smooth cigar-like geometry (Figure 1.3), which corresponds to a solid torus topology with contractible cycle along t_E-direction. With (1.75) we can interpret BTZ solution as a black hole with event horizon at $r = r_+$, to which we can associate thermodynamical properties. From (1.1), we can find that the BTZ entropy is

$$S = \frac{2\pi r_+}{4 G_N} \, . \tag{1.76}$$

For a review of the BTZ black hole, and its thermodynamical interpretation, see [30].

Global properties are as well the key to the holographic correspondence for AdS$_3$. In this context, they are tightly related to the choice of boundary conditions. In three dimensions, boundary conditions are specially relevant, since there are no propagating degrees of freedom in the bulk and the physics is encoded at the boundary. To explore the importance of boundary conditions, let us start by considering a set of coordinates where the metric takes Fefferman-Graham form:

$$ds^2 = \ell^2 d\rho^2 + g_{ij}(x^k, \rho) dx^i dx^j, \tag{1.77}$$

where $i, j, k = 1, 2$, and $\infty > \rho > 0$. We assume that g_{ij} has the following ρ-expansion:

$$g_{ij}(x^k, \rho) = e^{2\rho} g_{ij}^{(0)}(x^k) + g_{ij}^{(2)}(x^k) + ..., \tag{1.78}$$

where $g_{ij}^{(0)}$ acts as a boundary metric, and the dots ... stand for sub-leading terms in e^ρ. Metrics with the behaviour (1.77)-(1.78) are known as *asymptotically AdS space-times*, since these conditions are fulfilled by (1.73) when $x^i = x^+, x^-$, with , with $x^\pm = t \pm \phi$. We need to specify the boundary terms for the action, such they are consistent with (1.77)-(1.78). We consider the Gibbons-Hawking boundary term, and a counter-term:

$$S_{\text{GH}} = \frac{1}{8\pi G_3} \int_{\partial \mathcal{M}} d^2 x \sqrt{-g} \, \text{Tr}\,(K) \, , \qquad S_{\text{ct}} = -\frac{1}{8\pi G_3} \int_{\partial \mathcal{M}} d^2 x \sqrt{-g}, \tag{1.79}$$

where $K_{ij} = \partial_\rho g_{ij}/2$ is the extrinsic curvature, and $\partial \mathcal{M}$ is the boundary of the 3-dimensional manifold $\mathcal{M}$. The choice of (1.79) ensures that the action

$$S = S_{\text{EH}} + S_{\text{GH}} + S_{\text{ct}} \, , \tag{1.80}$$

has a well defined variational principal, it fulfils Einstein field equations, and its solutions are asymptotically AdS$_3$ [31]. The on-shell variation is:

$$\delta S = \frac{1}{2} \int_{\partial M} d^2 x \sqrt{-g^{(0)}} T^{ij} \delta g_{ij}^{(0)} \, , \tag{1.81}$$

with:

$$T_{ij} = \frac{1}{16\pi G_3 \ell} \left(g_{ij}^{(2)} - \text{Tr}(g^{(2)}) g_{ij}^{(0)} \right) , \tag{1.82}$$

where T_{ij} is the boundary stress tensor. Let us assume that the boundary metric is $g^{(0)} = -dx^+ dx^-$. In this case, Einstein's equations imply:

$$g_{+-}^{(2)} = g_{-+}^{(2)} = 0 , \qquad \partial_- g_{++}^{(2)} = \partial_+ g_{--}^{(2)} = 0 . \tag{1.83}$$

In this case, the stress tensor is traceless and conserved stress tensor at the boundary $g^{(0)}$, and has only two non-vanishing components:

$$T_{++} = \frac{1}{8\pi G_3 \ell} g_{++}^{(2)}(x^+) , \qquad T_{--} = \frac{1}{16\pi G_3 \ell} g_{--}^{(2)}(x^-) . \tag{1.84}$$

Using the boundary stress energy tensor we can compute conserved charges in gravity [32]. For example, global time translations are associated to the energy, and rotations to the angular momentum, and they are defined at the boundary. It is convenient now to comment about the distinction between coordinate transformations (*local* diffeomorphisms), and true isometries of the theory (*global* diffeomorphisms). The coordinate transformations relate physically equivalent solutions which only differ by a choice of gauge. However, diffeormophisms that reach the boundary change the global structure of the solution, and connect solutions which are physically distinct. The boundary conserved charges in gravity are associated to these global symmetries of the space-time.

We can observe that the AdS$_3$ boundary tensor (1.89) shares features with the CFT$_2$ stress-tensor (1.62): they are both traceless, conserved, and have a holomorphic/anti-holomophic factorization. This opens the door to the AdS$_3$/CFT$_2$ duality, for which we will give more evidence in the following. Consider the infinitesimal coordinate transformation:

$$\rho \to \rho - \frac{1}{2}(\partial_+ \epsilon^+ + \partial_- \epsilon^-) ,$$

$$x^+ \to x^+ + \epsilon^+ - \frac{\ell^2}{2} e^{-2\rho} \partial_-^2 \epsilon^- ,$$

$$x^- \to x^- + \epsilon^- - \frac{\ell^2}{2} e^{-2\rho} \partial_+^2 \epsilon^+ \tag{1.85}$$

where $\epsilon^+ \equiv \epsilon^+(x^+)$, and $\epsilon^- \equiv \epsilon^-(x^-)$ are the parameters of the transformation. Notice that (1.85) are the conformal transfomations (1.63) at the boundary ρ. This change preserves the form of the metric (1.77)-(1.78), leaving invariant $g_{ij}^{(0)}$, but modifying $g_{ij}^{(2)}$. This induces a transformations for the stress tensor (1.89):

$$\delta T_{++} = \epsilon^+ \partial_+ T_{++} + 2\partial_+ \epsilon^+ T_{++} + \frac{\ell}{8\,G_3} \partial_+^3 \epsilon^+ . \tag{1.86}$$

and similarly for T_{--}. We see that the AdS$_3$ boundary stress tensor transforms as the CFT$_2$ stress tensor under conformal transformations (1.68), and we identify $g_{ij}^{(0)}$ as the CFT$_2$ metric. This is another manifestation of the duality we observed in Sec. 1.3.3 between boundary conserved currents, and bulk gauge fields. Moreover, comparing (1.68) with (1.86) we can relate the gravitational constant to the CFT central charge

$$c = \frac{3\ell}{2G_3}\,. \tag{1.87}$$

The previous equality was first encountered by Brown and Henneaux in their article [33], which is considered one of the precursors to the holographic correspondence. In this work, they analyse the *asymptotic symmetry group of AdS$_3$*, which is found by computing the Poisson brackets of the boundary global charges. They find that the Poisson structure follows two copies of the algebra (1.69) with (1.87), when imposing asymptotically AdS$_3$ conditions. Therefore, the asymptotic symmetry group of AdS$_3$ is two copies of Virasoro, which coincides with the infinite dimensional algebra of the dual CFT$_2$.

Before moving on, we would like to introduce the following exact solution of the vacuum Einstein field equations with $\Lambda = -1/\ell^2$ [34]:

$$ds^2 = \ell^2 d\rho^2 + 8\pi G_3 \ell \left(\mathcal{L} \, (dx^+)^2 + \bar{\mathcal{L}} \, (dx^-)^2 \right) - \left(\ell^2 e^{2\rho} + (8\pi G_3)^2 \mathcal{L} \bar{\mathcal{L}} e^{-2\rho} \right) dx^+ dx^- \,, \tag{1.88}$$

where $\mathcal{L} = \mathcal{L}(x^+)$, and $\bar{\mathcal{L}} = \bar{\mathcal{L}}(x^-)$ are arbitrary functions. This metric is in Fefferman-Graham form (1.77), and it is asymptotically AdS$_3$ (1.78). Since (1.88) is an exact solution of the equations of motion, the sub-leading terms in (1.78) are zero. We can identify the boundary stress tensor (1.89) with

$$T_{++} = \mathcal{L}\,, \qquad\qquad T_{--} = \bar{\mathcal{L}}\,. \tag{1.89}$$

It is very interesting to notice that performing the change of coordinates (1.85) does not modify the form of the solution (1.88). However, the functions $\mathcal{L}$, and $\bar{\mathcal{L}}$ undergo a tranformations: $\mathcal{L} \to \mathcal{L} + \delta\mathcal{L}$, where $\delta\mathcal{L}$ is just the transformation for the stress tensor in (1.86) (and analogously for $\bar{\mathcal{L}}$). The transformation (1.85) is the *residual conformal symmetry* we find after we have fixed the set of local diffeomorphisms. It acts non-trivially on the boundary elements $\mathcal{L}(x^+)$, and $\bar{\mathcal{L}}(x^-)$, relating two different solutions which are globally distinct.

1.4.2 Chern-Simons formulation of AdS$_3$ gravity

In the previous section, we have seen that three-dimensional gravity does not have propagating degrees of freedom. There exists an alternative description in terms of

Chern-Simons (CS) gauge connections that makes the topological character of 3d gravity explicit. In this section, we briefly review this formalism, and for further details, we refer the reader to the original articles [35, 36] and more recently in, e.g., [34, 37]. Let us start by considering the Chern-Simons action:

$$S_{CS}[A] = \frac{k}{4\pi} \int_{\mathcal{M}} \text{Tr}\left(A \wedge dA + \frac{2}{3} A \wedge A \wedge A \right) , \tag{1.90}$$

where A is gauge field, the trace $\text{Tr}(...)$ is a shortcut notation for the contraction using the Killing forms of the algebra, and k is the Chern-Simons level. The gauge group is chosen to match the symmetry group of AdS$_3$, which in Lorentzian signature is $SO(2,2) \cong SL(2,\mathbb{R}) \times SL(2,\mathbb{R})$. Therefore, we consider gauge connections A, $\bar{A}$ valued in two independent copies of $sl(2,\mathbb{R})$ [3], which algebra is given by

$$[L_0, L_\pm] = \mp L_\pm , \qquad [L_1, L_{-1}] = 2L_0 , \tag{1.91}$$

To show the equivalence among both theories, we need to consider the vielbein formulation of general relativity. In this formalism, the choice of coordinates is replaced by the election of a local basis on the tangent bundle. This basis is formed by three independent vectors: $e^a = e^a_\mu dx^\mu$, with $a = 1, 2, 3$, known as vielbein. We can relate the metric of a curved manifold $g_{\mu\nu}$ to a flat (non-coordinate) metric η_{ab} using the vielbein:

$$g_{\mu\nu} e^\mu_a e^\nu_b = \eta_{ab} . \tag{1.92}$$

The Einstein-Hilbert action in 3 dimensions can be rewritten in vielbein formalism as:

$$S_{EH}[e, \omega] = \frac{1}{8\pi G_3} \int_{\mathcal{M}} e^a \wedge \left(d\omega_a + \epsilon_{abc} \omega^b \wedge \omega^c + \frac{1}{6\ell^2} \epsilon_{abc} e^b \wedge e^c \right) . \tag{1.93}$$

where ω^a is related to spin connection via $\omega^a = \epsilon^{abc} \omega_{bc}/2$, and ϵ_{abc} the Levi-Civita tensor. In our particular case, we choose the flat indices "a" to be valued in $sl(2,\mathbb{R})$. We define the gauge connections as:

$$A = (\omega^a + \frac{1}{\ell} e^a) L_a , \quad \bar{A} = (\omega^a - \frac{1}{\ell} e^a) \bar{L}_a . \tag{1.94}$$

With (1.94), one can show that the following actions are equivalent up to total derivatives:

$$S_{\text{EH}}[e, \omega] = S_{CS}[A] - S_{CS}[\bar{A}] . \tag{1.95}$$

The gravitational constant is related to the Chern-Simons level via

$$k = \frac{\ell}{4G_3} , \tag{1.96}$$

---

[3]The lower case in $sl(2,\mathbb{R})$ refers to the algebra generators, in contrast to $SL(2,\mathbb{R})$, which represents the group elements.

and the space-time metric can be recovered directly from the connections through

$$g_{\mu\nu} = 2\mathrm{tr}_f(e_\mu e_\nu) \ , \tag{1.97}$$

where we are taking the trace in the fundamental representation of $sl(2, \mathbb{R})$.

The advantage of the Chern-Simons formalism of 3d gravity is that in most situations the gauge connections are easier to manipulate than the space-time metric. For example, the Einstein field equations are reduced to the flatness condition on the gauge connection:

$$dA + A \wedge A = 0 \ , \quad d\bar{A} + \bar{A} \wedge \bar{A} = 0 \ . \tag{1.98}$$

Moreover, the diffeomorphisms and Lorentz symmetries of the Einstein-Hilbert action are just the gauge transformations:

$$A \to L(A + d)L^{-1} \qquad \bar{A} \to R^{-1}(\bar{A} + d)R \, , \tag{1.99}$$

with $L, R \in SL(2, \mathbb{R})$, which we will often call *left*, and *right* gauge groups. The transformation (1.99) is extremely useful, because with it we can conveniently reparametrise any connection. For example, the radial dependence can be gauged away, i.e. we can always find a gauge transformation that rewrites the connections as [38]:

$$A = b(\rho)^{-1} \left(a(x^+, x^-) + d \right) b(\rho) \, , \qquad \bar{A} = b(\rho) \left(\bar{a}(x^+, x^-) + d \right) b(\rho)^{-1} \, . \tag{1.100}$$

Here ρ is the holographic radial direction, and x^+, x^- are boundary coordinates. The advantage of this reparametrization is that we can isolate the boundary values of the connections, where the global charges are encoded, and interpret the radial direction as emergent from the gauge transformation. With (1.100), we can find that the following connection is a solution of (1.98)

$$a = \left(L_+ - \frac{2\pi\mathcal{L}(x^+)}{k} L_- \right) dx^+, \quad \bar{a} = -\left(L_- - \frac{2\pi\bar{\mathcal{L}}(x^-)}{k} L_+ \right) dx^-, \quad b(\rho) = e^{\rho L_0} \, . \tag{1.101}$$

Using the definitions (1.94)-(1.97), we can see that the previous connections are equivalent to the metric (1.88), with (1.96). We will extensively use (1.101) in the main text, because these connections parametrize the space of all solutions that are asymptotically AdS$_3$. We can observe this explicitly by fixing different values for $\mathcal{L}$, and $\bar{\mathcal{L}}$. For simplicity, we will set from now on the AdS radius to $\ell = 1$. For example, with $\mathcal{L} = \bar{\mathcal{L}} = 0$ we have:

$$A_{\mathrm{Poin}} = e^\rho L_+ dx^+ + L_0 d\rho \ , \tag{1.102}$$

$$\bar{A}_{\mathrm{Poin}} = -e^\rho L_- dx^- - L_0 d\rho \ . \tag{1.103}$$

The previous connections represent the Poincare metric in (1.16) after the change $z = e^{-\rho}$. For $2\pi\mathcal{L}/k = 2\pi\bar{\mathcal{L}}/k = -1/4$:

$$A_{\text{AdS}} = \left(e^{\rho}L_+ + \frac{e^{-\rho}L_-}{4} \right) dx^+ + L_0 d\rho, \tag{1.104}$$

$$\bar{A}_{\text{AdS}} = - \left(e^{\rho}L_- + \frac{e^{-\rho}L_+}{4} \right) dx^- - L_0 d\rho \,, \tag{1.105}$$

we recover global AdS$_3$ (6.66); after a rigid rotation of ρ. And when $\mathcal{L}$ and $\bar{\mathcal{L}}$ are constant and positive:

$$A_{\text{BTZ}} = \left(e^{\rho}L_+ - \frac{2\pi\mathcal{L}}{k} e^{-\rho}L_- \right) dx^+ + L_0 d\rho, \tag{1.106}$$

$$\bar{A}_{\text{BTZ}} = - \left(e^{\rho}L_- - \frac{2\pi\bar{\mathcal{L}}}{k} e^{-\rho}L_+ \right) dx^- - L_0 d\rho \,, \tag{1.107}$$

with $2\pi\mathcal{L}/k = \frac{(r_+ + r_-)^2}{4}$, and $2\pi\bar{\mathcal{L}}/k = \frac{(r_+ - r_-)^2}{4}$. In this case the connections are equivalent to the BTZ (6.65) after the change $r^2 = r_+^2 \cosh^2(\rho - \rho_*) + r_-^2 \sinh^2(\rho - \rho_*)$, with $e^{2\rho_*} = (r_+^2 - r_-^2)/4$.

We will now revisit some aspects of 3d gravity from the Chern-Simons perspective. We have already studied all the following properties in metric formulation, but rewriting them in Chern-Simons formulations will be particularly useful in the next chapter, where we consider theories with a generalized gauge group.

Asymptotically AdS$_3$: A space-time is considered asymptotically AdS$_3$ when (1.77) and (1.78) are fulfilled. We will define the analogous of these conditions in Chern-Simons formalism. By comparison with (1.104), we infer:

$$A_{x^-} = 0 \,, \qquad\qquad \bar{A}_{x^+} = 0 \,, \tag{1.108}$$

which assuming the radial gauge (1.100), implies the following boundary conditions:

$$a_{x^-} = 0 \,, \qquad\qquad \bar{a}_{x^+} = 0 \,. \tag{1.109}$$

Moreover, the radial component of the connection tends to the global solution at the boundary:

$$A - A_{\text{AdS}}\big|_{\rho\to\infty} = O(1) \,, \qquad \bar{A} - \bar{A}_{\text{AdS}}\big|_{\rho\to\infty} = O(1) \tag{1.110}$$

This condition means that the term of order one in the $\rho-$expansion of A is fixed by A_{AdS}. Conditions (1.109) and (1.110) are considered as a generalisation of asymtotically AdS$_3$ in Chern-Simons formulation, and their imposition will be crucial in the following section. It is important for these later purposes to highlight that

the form of $b(\rho)$ is not specified by the boundary conditions. The only constraint in $b(\rho)$ is that (1.110) is fulfilled.

Conformal residual symmetry: In metric formulation, we found that the global diffeomorphisms (1.85) left the metric (1.88) invariant. An analogous procedure in Chern-Simons variables is finding the gauge transformations that preserve the form of the connections (1.101). To see that explicitly we consider the infinitesimal version of the gauge transformation (1.99) on a:

$$\delta a = [a, \lambda] + d\lambda \,, \tag{1.111}$$

where $\lambda \in sl(2, \mathbb{R})$ is the infinitesimal gauge parameter, defined from with $L = e^{\lambda} = 1 + \lambda + ...$ Requiring that the form of a does not change after the previous gauge transformation, we get some constraints on the gauge parameter, which result in the same transformation behavior for $\mathcal{L}$ found in (1.86). Moreover, the analysis of the global charges can be formulated in terms of Chern-Simons variables, and, as expected, it results in two copies of Virasoro algebras as asymptotics. We will not review this here, and we refer to [34, 39, 40].

Smoothness condition: We would like to characterize black hole solutions in the Chern-Simon formalism. We have seen in the previous section that the essential feature that distinguishes the BTZ black hole from other solutions is the smoothness condition (1.75) in Euclidean signature. This condition implies a torus topology with a contractible cycle around the Euclidean thermal direction. In Chern-Simons formalism, this is equivalent to impose that the holonomy along this cycle belongs to the center of the group, i.e. it is a trivial holonomy. This ensures that the connection is single valued around the thermal cycle of the torus, and smoothly goes to zero at the horizon. It was proposed in [41] the following smoothness condition for the BTZ connections:

$$\mathcal{P} \exp \left(\oint_{\mathcal{C}_E} A_{\mathrm{BTZ}} \right) = e^{2\pi i L_0} \,, \qquad \mathcal{P} \exp \left(\oint_{\mathcal{C}_E} \bar{A}_{\mathrm{BTZ}} \right) = e^{2\pi i L_0} \,, \tag{1.112}$$

where $\mathcal{C}_E$ represents the thermal cycle $z \sim z + i\beta_+$, and $\bar{z} \sim \bar{z} + i\beta_-$, and the BTZ connections are (1.106). The holonomy is trivial because $e^{2\pi i L_0}$ belongs to the center of the group, i.e. commutes with all the other elements [4]. Considering the fundamental representation of the algebra, the holonomy conditions (1.112) are fulfilled if

$$e^{\beta_+ a_z} = e^{2\pi i L_0} \,, \qquad e^{\beta_- \bar{a}_{\bar{z}}} = e^{2\pi i L_0} \tag{1.113}$$

where a, and $\bar{a}$ are the BTZ connections in the parametrization (1.100), and $\cong$ means equal up to conjugation. Equation (1.113) boils down to a condition over

---

[4]Other choices for the center are possible, but Hol=$e^{2\pi i L_0}$ ensures that we reproduces the BTZ smoothness condition found in metric formalism (1.75).

the eigenvalues of a, and $\bar{a}$:

$$\lambda_z = 2\pi i L_0/\beta_+ \ , \qquad \lambda_{\bar{z}} = 2\pi i L_0/\beta_- \ . \tag{1.114}$$

This finally imposes $\beta_\pm = \frac{2\pi}{r_+ \pm r_-}$, and we recover the smoothness condition found in the metric formalism (1.75), with $\ell = 1$.

1.5 Higher spin gravity in 3d

Higher spin gravity theories are an extension of Einstein gravity coupled to an infinite tower of massless spinning fields in AdS backgrounds. They are an interesting topic of study in the context of quantum gravity since they can be thought as a bridge between Einstein gravity and string theory, which possesses an infinite number of massive higher spin states. Moreover, they are as well attractive for holography. For example, higher spin theories in AdS$_4$ are conjectured to be dual to rather simple CFT, such the free $O(N)$ vector model in $d = 3$ [42, 43]. Higher spin gravities can be used as a framework to study the holographic correspondence, or use holography as a tool to learn about the higher spin theories themselves.

There is a lot of potential in higher spin gravity due to the enhanced gauge symmetries they possess. However, these theories are complicated to manipulate: they have highly non-linear equations of motion, and the infinite number of fields is required to obtain consistent interactions in $d \geq 4$ [44, 45]. This situation greatly simplifies in three dimensions. Analogously to Einstein-Hilbert gravity, higher spin gauge theories do not carry propagating degrees of freedom in three dimensions, and they can be rewritten as a theory of gauge connections [38]. This formalism hides very well the complicated dynamics of the theory and makes higher spin gravity much more treatable. Moreover, in three dimensions, the theory admits a truncation, where the addition of infinitely many fields is not necessary [46]. These features make higher spin gauge theories in 3d an excellent toy-model for their higher-dimensional cousins.

In this thesis, we use higher spin gravity in AdS$_3$ as a playground for the holographic correspondence. These theories possess an enlarged number of gauge symmetries which make the metric field behave in a peculiar way, very different from what we expect from usual Einstein-Hilbert gravity. Therefore, the notion of space-time is ill-defined. However, using the holographic correspondence, we can make sense of geometrical objects such black holes in higher spin gravity, defining them from their thermal properties and their dual CFT states. How the geometry

in the gravitational theory emerges from the purely quantum degrees of freedom is one of the most fundamental questions of the holographic correspondence, and it still remains unsolved. In the context of higher spin gravity, we can tackle this problem from a different angle: since there is no notion of geometry in these theories, we can try to define it taking the degrees of freedom of the CFT as fundamental. This will be the aim of Chapter 4.

In this section, we will first explain how to reformulate AdS$_3$ higher spin gravity as a Chern-Simons gauge theory. Then, we will analyze these theories in the context of the holographic duality, and we will finish by reviewing how to construct higher-spin black hole solutions.

1.5.1 Higher spin gravity as Chern-Simons theory

We will start by considering *free massless spin fields* in AdS$_{d+1}$ background. A Lagrangian formulation of their equations of motion was first found by Fronsdal [47]:

$$\mathcal{F}_{\mu_1...\mu_s} - ((s+d-2)(s-2)+s)\,\phi_{\mu_1...\mu_s} + 2g_{(\mu_1\mu_2}\phi^{\lambda}_{\mu_3...\mu_s)\lambda} = 0\,. \qquad (1.115)$$

with

$$\mathcal{F}_{\mu_1...\mu_s} \equiv \nabla^2\phi_{\mu_1...\mu_s} - \nabla_{(\mu_1|}\nabla^{\lambda}\phi_{|\mu_2...\mu_s\lambda)} + \nabla_{(\mu_1}\nabla_{\mu_2}\phi^{\lambda}_{\mu_3...\mu_s)\lambda}\,. \qquad (1.116)$$

where ∇ is the AdS covariant derivative. This system is invariant under gauge transformations of the type:

$$\delta_\xi\phi_{\mu_1...\mu_s} = \nabla_{(\mu_1}\xi_{\mu_2...\mu_s)}\,. \qquad (1.117)$$

where $\xi_{\mu_1...\mu_s}$ is the symmetric and traceless gauge parameter. These equations are equivalent to (1.50) when fixing $m^2 = (s+d-2)(s-2) - s$. As we have explained in Sec. 1.3.3, in this case the equations (1.50) represent massless spin fields, which are dual to conserved currents in the CFT. We will explore more this duality in Sec. 1.5.2 in the context of 3d gravity.

We have now the free equations for massless spin fields, and the next step is to consider interactions. In general, this is a very complicated task, mainly because we need to do it without spoiling the gauge invariance of the equations of motion. Avoiding many difficulties, Vasiliev managed to find a consistent theory of massless interacting fields in *AdS* background for general dimensions [44, 45]. However, his construction necessarily requires an infinite number of spin fields. The analysis is

greatly simplified for the 3-dimensional case, where consistent interactions can be found without the necessity of adding an infinite tower of fields (See [46] for an example). However, it was not until [38, 48] that the study of truncated higher spin 3-dimensional gravities was placed into a more treatable framework. In these papers, they exploit the fact that the equations (1.115) in three dimensions do not have propagating degrees of freedom for $s \geq 2$. Inspired by the pure gravity case, they consider two Chen-Simons theories with the gauge group now generalized to $SL(N, \mathbb{R}) \times SL(N, \mathbb{R})$. In analogy with the pure gravity case, the gauge connections are defined as:

$$A^a = (\omega^a + e^a) \,, \quad \bar{A}^a = (\omega^a - e^a) \,, \tag{1.118}$$

where e^a, and ω^a, are a generalized version of the vielbein, and spin connection, where now the flat indexes "a" are valued in $sl(N, \mathbb{R})$. The basis we will use for the $sl(N, \mathbb{R})$ algebra is found in (6.44), and it is convenient to appreciate that contains a $sl(2, \mathbb{R})$ subgroup formed by $\{L_0, L_1, L_{-1}\}$. They propose that the following action represents a theory of *higher spin gravity*:

$$S_{\text{HS}}[e, \omega] = S_{CS}[A] - S_{CS}[\bar{A}] \,, \tag{1.119}$$

where $A, \bar{A} \in sl(N, \mathbb{R})$[5]. We can see this by substituting (1.118) in the right-hand-side of the previous equation. Then, it is found that the $sl(2, \mathbb{R})$-valued component of e^a and ω^a reproduces the Einstein-Hilbert action in vielbein formalism, and the rest of components represent massless field with higher spin, and their interactions. The field formalism is recovered via the identification:

$$\phi_{\mu_1 \ldots \mu_{s-1} \mu_s} \sim \text{Tr}\left(e_{(\mu} \ldots e_{\mu_{s-1}} e_{\mu_s)}\right) \,, \tag{1.120}$$

where the $\sim$ means that we have ignored a normalization that depends on the Lie algebra metric. As a consistency check, it can be shown that the Chern-Simons equations of motion

$$dA + A \wedge A = 0 \,, \quad d\bar{A} + \bar{A} \wedge \bar{A} = 0 \,, \tag{1.121}$$

at linerised level around the AdS connections are equivalent to the free Fronsdal equations (1.115) for a tower of $N - 1$ massless fields with spin $s = 2, \ldots N$ [38] [6].

The Chern-Simons formulation of higher spin gravity is a great tool to study these theories. As it happened for pure gravity, the topological character of the theory is made explicit, and the very complicated equations of motion can be seen

---

[5] To make contrast, we will often call *pure gravity* to the theory with $A, \bar{A} \in sl(2, \mathbb{R})$.

[6] We chose $\{L_0, L_1, L_{-1}\}$ as $sl(2, \mathbb{R})$ subgroup in $sl(N, \mathbb{R})$. Other choices of $sl(2, \mathbb{R})$ embedding are possible, and they result in a different spectrum for the theory [49]. For example, choosing the $sl(2, \mathbb{R})$ subgroup $\{\frac{1}{2}L_0, \frac{1}{4}W_{\pm 2}\}$, a $SL(3, \mathbb{R}) \times SL(3, \mathbb{R})$ Chern-Simons gauge theory is equivalent to AdS gravity coupled to spin-1, and spin-3/2 gauge fields [50].

just as flatness conditions over the gauge connection. In the following sections, we will exploit these advantages. Before doing so, we would like to highlight an interesting feature of higher spin gravity. The symmetries of the fields can be found from the gauge transformations (1.99), with $L, R \in SL(N, \mathbb{R})$. Using this, we can observe that the spin-2 metric field has an enlarged number of symmetries respect to the pure gravity case. As a consequence, the symmetries of the theory allow for changes in the causal structure and curvature of the space-time (see [51] for example). This does not fit our usual notion of geometry, which implies that higher spin theories do not have a geometrical description. This strange characteristic will be at the center of our research in Chapter 4.

1.5.2 Higher spin holography in 3d

We want to find the connections $A, \bar{A} \in sl(N, \mathbb{R})$ which are solutions to the flat equations of motion (1.98). As proposed in [38], we consider solutions that follow the conditions for asymptotically AdS as defined in (1.109)-(1.110). The previous conditions ensure that the associated background field $g_{\mu\nu}$ asymptotes to global AdS at the boundary. In the following, we will explain how these requirements lead to a generalized version of the $3d/2d$ holographic correspondence as the one formulated for pure gravity in the previous sections. In [38], they find the most general solution fulfilling the conditions for asymptotically AdS$_3$. Assuming (1.100), this is:

$$a_{x^+} = L_1 + \sum_{s=2}^{N} J_{(s)}(x^+) W^{(s)}_{-s+1} \,, \quad \bar{a}_{x^-} = -L_{-1} + \sum_{s=2}^{N} \bar{J}_{(s)}(x^-) W^{(s)}_{s-1} \,, \quad (1.122)$$

where $J_{(s)}(x^+)$, and $\bar{J}_{(s)}(x^-)$ are any arbitrary function, and $a_{x^-} = \bar{a}_{x^+} = 0$. Here $\{L_0, L_{\pm 1}\}$ are the generators of the $sl(2, \mathbb{R})$ subalgebra in $sl(N, \mathbb{R})$, and $W^{(s)}_j$ are the spin-s generators with $j = -(s-1), ...(s-1)$, which follow the algebra in (6.44).

In Sec. 1.4.2, we discussed the global residual symmetries for asymptotically AdS$_3$ space-times in the Chern-Simons formalism. Let use the same procedure for higher spin gravity. We would like to find if there is any gauge transformation that does not change the form of the connections (1.122). Using (1.111), it can be shown that this transformation exists, and it comes associated with a change:

$$J_{(s)} \to J_{(s)} + \delta J_{(s)} \,, \qquad \bar{J}_{(s)} \to \bar{J}_{(s)} + \delta \bar{J}_{(s)} \,, \qquad (1.123)$$

where $\delta J_{(s)}$, $\delta \bar{J}_{(s)}$ can be found explicitly, but we will not repeat them here (for more details see [38]). The transformation properties found for $J_{(s)}$ and $\bar{J}_{(s)}$ show

that they behave as CFT conserved currents of conformal dimension s, where $J_{(2)}$ acts as the stress-energy tensor. In [38], they find the charges in Chern-Simons formalism that correspond to the global transformations. Their Poisson structure corresponds to two copies of the $\mathcal{W}_N$ algebra. These algebras are an extension of Virasoro, where the case $\mathcal{W}_2$ explicitly corresponds to (1.69). This is a generalization of the Brown-Henneaux procedure for computing the asymptotical symmetries in 3d gravity: imposing the generalised asymptotically AdS$_3$ boundary conditions (1.122) implies that the asymptotic algebra is $\mathcal{W}_N \times \mathcal{W}_N$.

1.5.3 Black holes in higher spin gravity

We have seen above that higher spin gravity can be very easily analysed in its Chern-Simons formulation, which is a straightforward generalization of the pure gravity case. Moreover, the asymptotic symmetries are two copies of $\mathcal{W}_N$ algebra, a generalization of Virasoro. An interesting solution in the pure case is the BTZ black hole, whose charges are associated to the Virasoro zero modes. Therefore, the natural question to ask is if there exists a generalization of the 3-dimensional BTZ black hole which carries the charges related to the $\mathcal{W}_\mathcal{N}$ algebras. Since higher spin gravity does not admit a geometrical description, this generalized black hole is defined through its thermal properties, and considering a dual thermal CFT. Therefore, the following analysis is centered in the Euclidean aspects of the solution, which is posteriorly continued to Lorentzian. There is extensive literature that studies higher spin black holes, and here we will briefly review their main features, and write two explicit solutions in $SL(3, \mathbb{R}) \times SL(3, \mathbb{R})$. For a more complete view we refer the reader to the original works [37, 41, 51–54].

We start the analysis by considering source terms for the spin-s currents $J_{(s)}$, and $\bar{J}_{(s)}$. We will consider two types of deformations, some modifying the CFT Lagrangian, and others the Hamiltonian:

$$S = S_{\text{CFT}} + \int dz \sum_s J_{(s)} \mu_{(s)} + \int d\bar{z} \sum_s \bar{J}_{(s)} \bar{\mu}_{(s)} \,,$$

$$H = H_{\text{CFT}} + \int d\phi \sum_s J_{(s)} \mu_{(s)} + \int d\phi \sum_s \bar{J}_{(s)} \bar{\mu}_{(s)} \,, \qquad (1.124)$$

where $\mu_{(s)}$, and $\bar{\mu}_{(s)}$ are the spin-s sources, and the sum runs over $s = 3, ..., N$. In [54], they extensively study how the two deformations affect differently the CFT properties: they lead to distinct Ward identities, and partition functions. Now, the interesting question is how these deformations are translated into the bulk dual theories. The first thing to notice is that the boundary condition (1.109) should

be relaxed to take into account the presence of deformations. To exemplify this, let us focus in the focus in the $SL(3, \mathbb{R}) \times SL(3, \mathbb{R})$. Assuming (1.100), we define:

$$
\begin{aligned}
a_+ &= L_1 - \frac{2\pi\mathcal{L}}{k}L_{-1} - \frac{\pi\mathcal{W}}{2k}W_{-2}\,, \\
a_- &= \mu\left(W_2 + \frac{4\pi\mathcal{W}}{k}L_{-1} + \left(\frac{2\pi\mathcal{L}}{k}\right)^2 W_{-2} - \frac{4\pi\mathcal{L}}{k}W_0\right)\,, \\
\bar{a}_- &= -\left(L_{-1} - \frac{2\pi\bar{\mathcal{L}}}{k}L_1 - \frac{\pi\bar{\mathcal{W}}}{2k}W_2\right)\,, \\
\bar{a}_+ &= \bar{\mu}\left(W_{-2} + \frac{4\pi\bar{\mathcal{W}}}{k}L_1 + \left(\frac{2\pi\bar{\mathcal{L}}}{k}\right)^2 W_2 - \frac{4\pi\bar{\mathcal{L}}}{k}W_0\right)\,.
\end{aligned}
\tag{1.125}
$$

where $\mathcal{L}$ and $\bar{\mathcal{L}}$ are related to stress tensor, $\mathcal{W}$, and $\bar{\mathcal{W}}$ to the spin-3 current, and μ is the spin-3 source, and we consider the previous parameters constant. The component a_- and $\bar{a}_+$ are determined using $[a_+, a_-] = [\bar{a}_-, \bar{a}_+] = 0$. This ensures that differents linear combinations of (1.125) satisfy the equation of motion. It was shown in [41] that for Lagrangrian deformations, the currents are encoded in a_{x^+} and the sources in a_{x^-}, and vice-versa for $\bar{a}$ as:

$$
a_h = a_+ dx^+ + a_- dx^-\,, \qquad \bar{a}_h = \bar{a}_+ dx^+ + \bar{a}_- dx^-\,,
\tag{1.126}
$$

These boundary conditions are called *holomorphic*. See [41] for an explicit proof how this solution recovers the Ward identities expected from a Lagrangian deformation of the CFT For the Hamiltonian deformations, the components $(a_\phi, \bar{a}_\phi)$ carry the information about the currents [55–58].

$$
a_c = a_+ d\phi + (a_+ + a_-)dt, \qquad \bar{a}_c = -\bar{a}_- d\phi + (\bar{a}_+ + \bar{a}_-)dt\,.
\tag{1.127}
$$

This is called the *canonical* prescription. The canonical boundary conditions are more natural from the gravitational perspective, while the holomorphic resonate with the CFT.

Now we will analyze the thermal properties of the solutions (1.126) and (1.127), to relate them to stationary Euclidean black holes. We start by assuming a torus topology, and sources and currents that do not depend on the coordinates. In pure gravity, the feature that distinguishes the BTZ black hole from other solutions is the trivial holonomy (1.113), so it is natural to assume a similar condition for higher spin black holes [41].

$$
\mathcal{P}\exp\left(\oint_{\mathcal{C}_E} A\right) = e^{2\pi i L_0}\,, \qquad \mathcal{P}\exp\left(\oint_{\bar{\mathcal{C}}_E} \bar{A}\right) = e^{2\pi i L_0}\,,
\tag{1.128}
$$

where L_0 denotes the Cartan element of the $sl(2, \mathbb{R})$ subgroup in $sl(N, \mathbb{R})$. The choice of the center in the right hand side of (1.128) ensures that the solution is

smoothly connected to the BTZ when we turn off the higher spin sources[7]. For simplicity, we turn off rotation, i.e. $\beta_+ = \beta_- \equiv \beta$, $\mathcal{L} = \bar{\mathcal{L}}$ and $\mathcal{W} = -\bar{\mathcal{W}}$, and $\mu = -\bar{\mu}$. Using the parametrization (1.100), the previous condition reduces to:

$$e^{\beta a_{t_E}} = e^{2\pi i L_0} , \qquad e^{\beta \bar{a}_{t_E}} = e^{2\pi i L_0} , \qquad (1.129)$$

which reduces to a condition over the eigenvalues of a_t, and $\bar{a}_t$

$$\lambda_t = 2\pi L_0/\beta , \qquad \bar{\lambda}_t = 2\pi L_0/\beta . \qquad (1.130)$$

where t is the Lorentzian time $t = it_E$. Since a_c and a_h have the same time component a_t, demanding the holonomy condition in the non-rotating case is equivalent for both solutions (1.126), and (1.127). Equation (1.130) imposes relations among the parameters $\mathcal{L}$, $\mathcal{W}$, μ, and β, which are fulfilled when [41, 51]:

$$\mathcal{W} = \frac{4(C-1)\mathcal{L}}{C^{3/2}}\sqrt{\frac{2\pi\mathcal{L}}{k}} , \qquad \mu = \frac{3\sqrt{C}}{4(2C-3)}\sqrt{\frac{k}{2\pi\mathcal{L}}} , \qquad \frac{\mu}{\beta} = \frac{3}{4\pi}\frac{(C-3)\sqrt{4C-3}}{(3-2C)^2} . \qquad (1.131)$$

where $C \geq 3$ is a dimensionless parameter which helps us to solve the contraints. The limit $C \to \infty$ makes the higher spin charges vanish, and we recover the BTZ case. It can be deduced from the constraints (1.131) that:

$$\frac{\partial \mathcal{L}}{\partial \mu} = \frac{\partial \mathcal{W}}{\partial \beta} \qquad (1.132)$$

This is the integrability condition corresponding to the existence of the first law for a higher spin black hole, where β and μ are chemical potentials associated to the charges $\mathcal{L}$, and $\mathcal{W}$, respectively. We can, therefore, associate an entropy to the solutions (1.126)-(1.127) . In [52, 54], they do this by computing the free energy related to the different deformations (1.124). Assuming the smoothness condition, the higher spin black hole entropy in both cases is:

$$S = 2\pi k \operatorname{Tr}\left[(\lambda_\phi - \bar{\lambda}_\phi)L_0\right] , \qquad (1.133)$$

where λ_ϕ and $\bar{\lambda}_\phi$ are the matrix of the eigenvalues of a_ϕ, and $\bar{a}_\phi$. We observe that the smoothness condition is a robust and successful definition of Euclidean black holes. It reproduces in an elegant manner many of the properties we expect in solutions with a thermodynamical interpretation. Therefore, when the constraints (1.131) are fulfilled, we define the connections (1.126) as the *holomorphic higher spin black hole*, and (1.127) as the *canonical higher spin black hole*. It is important to comment that even though in the literature $b(\rho)$ is commonly chosen in analogy to the pure gravity case (1.101), we are free to pick any as long as it fulfils (1.110). This will be crucial in Chapter 4.

---

[7]The choice of center in the right hand side of (1.113) is not unique [50]. The interpretations of other choices are discussed in [59–61].

2 SPINNING GEODESIC WITTEN DIAGRAMS

OR HOW TO RELATE GRAVITATIONAL INTERACTIONS & OPE STRUCTURES USING GEODESIC WITTEN DIAGRAMS

In Sec. 1.2, we have introduced Witten diagrams which are used to compute boundary correlation functions holographically. In a similar fashion, *geodesic Witten diagrams* were recently proposed as dual objects of the CFT conformal partial waves [62]. Geodesic Witten Diagrams give holographic meaning to the conformal block decomposition of four-point Witten diagrams. This chapter is based on [1], and focuses on these objects. While the original proposal of geodesic Witten diagrams was formulated for only external scalar fields, here we extend it to spinning fields. We find a systematic way to evaluate geodesic Witten diagrams for external fields of arbitrary spin. Using this procedure we discuss how to draw a line between the tensor structures in the CFT and cubic interactions in AdS. We contrast this map to known results using three-point Witten diagrams: the maps obtained via volume versus geodesic integrals differ. Despite these differences, we show how to decompose four-point exchange Witten diagrams in terms of geodesic diagrams

2.1 Introduction

Conformal field theories (CFTs) have a unique position within quantum field theory. They are central to the ambitious questions that drive many theorists: the quest of classifying all possible fixed points of the renormalization group equations, and unveiling the theorems that accompany the classification. And in modern

times, they are also at the center of the holographic principle, as we have seen in Chapter 1. Therefore, conformal field theories are key to unveil novel features about quantum gravity in AdS.

In a CFT, symmetries play a crucial role. The exploitation of the conformal group gives an efficient organizational principle for the observables in the theory. An example of such a principle is the conformal block decomposition of four point correlation functions. As we have seen in Sec.1.2.1, 4-point functions can be decomposed into portions that are purely determined by symmetries (conformal partial waves) and the theory dependent data (OPE coefficients). Having analytic and numerical control over this decomposition has been key in recent developments. This includes the impressive revival of the conformal bootstrap program [63–65], and we refer to [66–68] for an overview on this area.

Our aim here is to apply the efficiency of the conformal block decomposition to holography: can we organize observables in AdS gravity as we do in a CFT? This question has been at the heart of holography since its conception [19, 69, 70], with perhaps the most influential result the prescription to evaluate CFT correlation functions via Witten diagrams, as we reviewed in Section 1.2.3. However, there is an obvious question that remained unanswered until very recently: what is the holographic dual of the conformal blocks? The idea placed forward in [62] was to consider *geodesic Witten diagram* in AdS_{d+1} as the counterpart of a CFT_d conformal partial wave. An example of geodesic Witten diagram is

$$\mathcal{W}_{\Delta|0}(x_1, x_2, x_3, x_4) = \int_{\gamma_{12}} d\lambda \int_{\gamma_{34}} d\lambda' G_{b\partial}^{\Delta_1|0}(y(\lambda), x_1) G_{b\partial}^{\Delta_2|0}(y(\lambda), x_2)$$

$$\times G_{bb}^{\Delta|0}(y(\lambda), y'(\lambda')) G_{b\partial}^{\Delta_3|0}(y'(\lambda'), x_3) G_{b\partial}^{\Delta_4|0}(y'(\lambda'), x_4)$$

(2.1)
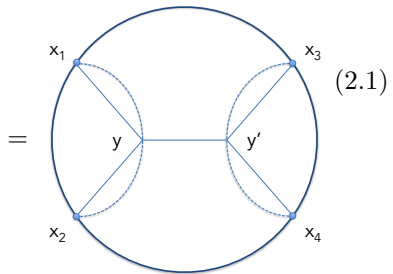
where γ_{ij} is a geodesic that connects the boundary points (x_i, x_j), which are represented by the dotted lines; λ is an affine parameter for γ_{12} and λ' for γ_{34}. Like the conventional Witten diagrams (Fig. 2.5), this one involves bulk–to–boundary and bulk–to–bulk propagators in AdS, with the important difference that the contact terms of the fields are projected over geodesics rather than integrated

over the entire volume of AdS. In [62], it was shown that the scalar geodesic Witten diagram in (2.1) was equivalent to the scalar conformal partial wave [1], i.e.,

$$\mathcal{W}_{\Delta|l}(x_1, x_2, x_3, x_4) = W_{\Delta|l}(x_1, x_2, x_3, x_4)\,, \qquad (2.2)$$

where $\mathcal{W}_{\Delta|l}$ is the geodesic Witten diagram (2.1) generalized to include a spin-l exchange, and $W_{\Delta|l}$ is the conformal block in (1.9). Moreover, they set up a procedure to decompose the scalar Witten diagram in terms of geodesic Witten diagrams, and, therefore, in terms of conformal blocks

In this chapter, we will study geodesic Witten diagrams when with spinning external legs. Our goal is two-fold: to give a method to evaluate a spinning conformal partial wave using holography, and to show how Witten diagrams decompose in terms of these building blocks. The first step towards this direction was given [71], where only one external leg had non-trivial spin. Here we expand that discussion to include spin on all possible positions of the diagram, and our current limitation is that we are only considering symmetric and traceless fields in the external and exchange positions. Our strategy is to cast the CFT construction of conformal partial waves in [72] along the lines of the AdS proposal in [62]. In particular, we will show how to decode the tensor structures (i.e. OPE structures) appearing in three point functions and conformal partial waves in terms of bulk differential operators acting on geodesic diagrams.

Witten diagrams with more than three legs, and beyond tree-level are infamous for how difficult are to evaluate. The integrals involved become quite cumbersome as the specie of the field changes, and even more intricate if internal lines are involved. The first explicit results are those in [20, 22, 23, 73–77],and more recently the subject has been addressed by using a Mellin representation of the diagrams (see e.g. [26, 78–83]). Specially, this formalism simplifies the complicated task of decomposing Witten diagram in terms of conformal partial waves of multi-trace operators. Having a clean and efficient decomposition of a Witten diagram in terms of geodesic diagrams is a computational tool that allow us to tackle these problems in a novel manner. Our method to decode the tensor structures provides a step forward in this direction which optimises the evaluation of correlations functions in AdS/CFT.

This chapter is organized as follows. Sec. 2.2.1 is a review on the embedding space formalism to describe CFT_d and AdS_{d+1} quantities. In section 2.2.2, we review CFT three-point functions for spinning fields, and their holographic

---

[1]We use the term *scalar* conformal partial wave to denote that the external fields are scalar operators; the exchanged field can be a symmetric traceless tensor. A *spinning* conformal partial wave is when at least one external fields is a symmetric traceless tensor.

computation via Witten diagrams, which maps OPE tensor structures to bulk interactions. In Sec. 2.2.3 we will review how to obtain the OPE tensor structures via suitable differential operators. Our main result is in Sec. 2.3 where we give an AdS counterpart of the differential operators found Sec. 2.2.3. This shows how one can obtain any spinning conformal partial wave via an appropriate geodesic Witten diagram with perfect agreement with the CFT. In Sec. 2.4 we discuss certain features of this method by focusing mostly on low spin examples. We first discuss the relation among gravitational interactions and OPE structures using geodesic diagrams, and contrast it with the reconstruction done using Witten diagrams, which we reviewed as well in 2.2.2. Even though there are non-trivial cancellations in the geodesic diagrams (which do not occur with volume integrals), in Sec. 2.5 we show how to decompose four point exchange Witten diagrams in terms of geodesic diagrams. We end with a discussion of our results and future directions in Sec. 2.6.

2.2 Practicalities for spinning correlators

This section is a compilation of previous results from the literature that will be useful in this chapter.

2.2.1 Embedding space formalism

The analysis of objects carrying indices in CFT_d and AdS_{d+1} is simplified using embedding space formalism. In this section, we will review its basics, and use it during the rest of this chapter. This formalism was recently revisited and exploited in [27, 84, 85], and we mainly follow their presentation. All of our discussion will be in Euclidean signature, in which the symmetry group of CFT_d and AdS_{d+1} is $SO(d+1,1)$.

CFT side of embedding

A natural description of $SO(d+1,1)$ is in the embedding space $\mathbb{M}^{d+2}$: this makes conformal symmetry constraints simple Lorentz symmetry conditions (which are more easily implemented). In this section we will show how to uplift the CFT_d fields on $\mathbb{R}^d$ to $\mathbb{M}^{d+2}$, and write correlation functions in this language.

We start defining the dot product in $\mathbb{M}^{d+2}$ as

$$P_1 \cdot P_2 \equiv P_1^A P_2^B \eta_{AB} = -\frac{1}{2} P_1^+ P_2^- - \frac{1}{2} P_1^- P_2^+ + \delta_{ab} P_1^a P_2^b \ , \qquad (2.3)$$

where we are using light cone coordinates

$$P^A = (P^+, P^-, P^a) \ . \qquad (2.4)$$

A point $x^a \in \mathbb{R}^d$ is embedded in $\mathbb{M}^{d+2}$ by null stereographic map of the coordinates

$$x^a \ \rightarrow \ P^A = (1, x^2, x^a) \ , \qquad a = 1, \ldots, d \ . \qquad (2.5)$$

This implies that the CFT$_d$ coordinates live in the projective light cone

$$P^2 = 0 \ , \quad P \equiv \lambda P \ , \quad \lambda \in \mathbb{R} \ . \qquad (2.6)$$

In the embedding formalism there is a very economical way of manipulating $\mathbb{R}^d$ symmetric and traceless tensors. This is discussed extensively in [84], and the bottom line is to encode the tensorial properties in a polynomial. One defines an auxiliary vector Z^A, and considers the contraction

$$T(P, Z) \equiv Z^{A_1} \cdots Z^{A_n} T_{A_1 \cdots A_n}(P) \ , \qquad (2.7)$$

with the following restrictions and properties:

1. $Z^2 = 0$ encodes the traceless condition.

2. $T(P, Z + \alpha P) = T(P, Z)$ makes the tensor tangent to the light cone $P^2 = 0$.

3. Homogeneity defines the conformal weight Δ and spin l as $T(\lambda P, \alpha Z) = \lambda^{-\Delta} \alpha^l T(P, Z)$.

All of these condition are conformally invariant which makes $T_{A_1 \cdots A_n}(P)$ an $SO(d+1, 1)$ symmetric traceless tensor. From here, a symmetric traceless tensor field on $\mathbb{R}^d$ is given by

$$t_{a_1 \cdots a_n} = \frac{\partial P^{A_1}}{\partial x^{a_1}} \cdots \frac{\partial P^{A_n}}{\partial x^{a_n}} T_{A_1 \cdots A_n}(P) \ , \qquad (2.8)$$

with P^A given by (2.5). It is important to note that any tensor $T_{A_1 \cdots A_n}(P)$ proportional to P^A projects to zero: such tensor will be *pure gauge*. And hence, without loss of generality we can require the orthogonality condition

$$Z \cdot P = 0 \ . \qquad (2.9)$$

We can as well extract $t_{a_1 \cdots a_n}$ from the polynomial directly. First, the polynomial in $(d+2)$-dimensions can be brought into d-dimensional variables via the relation

$$T(P, Z) = t(x, z) , \quad \text{with} \quad Z^A = (0, 2x \cdot z, z) , \quad P^A = (1, x^2, x^a) . \qquad (2.10)$$

Then the components of the tensor in $\mathbb{R}^d$ are

$$t_{a_1 \cdots a_n} = \frac{1}{n!(d/2-1)_n} D_{a_1} \ldots D_{a_n} t(x, z) , \qquad (2.11)$$

where $(d)_l = \Gamma(d+l)/\Gamma(d)$ and D_a are differential operators that do the job of projecting the polynomial to symmetric traceless tensors:

$$D_a = \left(\frac{d}{2} - 1 + z \cdot \frac{\partial}{\partial z} \right) \frac{\partial}{\partial z^a} - \frac{1}{2} z^a \frac{\partial^2}{\partial z \cdot \partial z} . \qquad (2.12)$$

This operator is also convenient for other purposes. For example, we can do full contractions via the polynomial directly: given two symmetric traceless tensors in $\mathbb{R}^d$, their contraction is

$$f_{a_1 \cdots a_n} g^{a_1 \cdots a_n} = \frac{1}{n!(d/2-1)_n} f(x, D) g(x, z) . \qquad (2.13)$$

In the $(d+2)$-dimensional variables we have

$$f_{a_1 \cdots a_n} g^{a_1 \cdots a_n} = \frac{1}{n!(d/2-1)_n} F(P, D) G(P, Z) , \qquad (2.14)$$

where

$$D_A = \left(\frac{d}{2} - 1 + Z \cdot \frac{\partial}{\partial Z} \right) \frac{\partial}{\partial Z^A} - \frac{1}{2} Z_A \frac{\partial^2}{\partial Z \cdot \partial Z} . \qquad (2.15)$$

AdS side of embedding

The embedding formalism is as well useful to encode tensorial structures in AdS. Here we will follow [27, 86], and we highlight [28, 85, 87, 88] for its recent use in the context of higher spin gravity. We consider euclidean AdS_{d+1} in Poincare coordinates:

$$ds^2 = \frac{1}{z^2} \left(dz^2 + dx^a dx_a \right) . \qquad (2.16)$$

where we are taking the AdS radius to be one, and $a = 1, \ldots d$. We have seen in Sec. 1.2.2 that AdS_{d+1} spaces can be embedded in the $(d+2)$-dimensional hyperboloid (1.13). In this Chapter we consider instead the light-cone embedding

coordinates, defined as $Y^{\pm} = Y^0 \pm Y^{d+1}$. In this case, we recover Poincare with the change:

$$y^{\mu} = (z, x^a) \;\rightarrow\; Y^A = \frac{1}{z}(1, z^2 + x^2, x^a) \; . \tag{2.17}$$

where the index A is defined as in (2.3), and (2.4). The AdS boundary points are obtained by sending $Y \to \infty$, and in this limit we approach the light cone (2.6). The induced AdS metric is

$$G_{AB} = \eta_{AB} + Y_A Y_B \; , \tag{2.18}$$

which plays a role as a projector.

Following the CFT discussion, we can as well describe symmetric and traceless tensor in AdS_{d+1} as polynomials [27]. Adapting the conditions in (2.7) to AdS gives

$$\mathcal{T}(Y; W) \equiv W^{A_1} \cdots W^{A_n} \mathcal{T}_{A_1 \cdots A_n}(Y) \; , \tag{2.19}$$

where we introduce now a auxiliary tensor W^A. The restrictions and properties are

1. $W^2 = 0$ encodes the traceless condition.

2. $W \cdot Y = 0$ imposes an orthogonality condition.

3. Requiring that $\mathcal{T}(Y, W + \alpha Y) = \mathcal{T}(Y, W)$ makes the tensor transverse to the surface $Y^2 = -1$.

4. Homogeneity $(Y \cdot \partial_Y + W \cdot \partial_W + \mu)\mathcal{T}(Y, W) = 0$ for some given value of μ.[2]

The components of the tensor can be easily recovered by introducing a projector. Given

$$K_A = \frac{d-1}{2}\left(\frac{\partial}{\partial W^A} + Y_A Y \cdot \frac{\partial}{\partial W}\right) + W \cdot \frac{\partial}{\partial W}\frac{\partial}{\partial W^A} \tag{2.20}$$

$$+ Y_A\left(W \cdot \frac{\partial}{\partial W}\right)\left(Y \cdot \frac{\partial}{\partial W}\right) - \frac{1}{2}W_A\left(\frac{\partial^2}{\partial W \cdot \partial W} + Y \cdot \frac{\partial}{\partial W}Y \cdot \frac{\partial}{\partial W}\right),$$

we obtain symmetric and traceless tensor in AdS via

$$\mathcal{T}_{A_1 \cdots A_n}(Y) = \frac{1}{n!\left(\frac{d-1}{2}\right)_n} K_{A_1} \cdots K_{A_n} \mathcal{T}(Y, W) \; . \tag{2.21}$$

---

[2]For a bulk massive spin-J field in AdS_{d+1}, we have $\mu = \Delta + J$ with $M^2 = \Delta(\Delta - d) - J$.

And the component in AdS_{d+1} space is

$$t_{\mu_1 \cdots \mu_n} = \frac{\partial Y^{A_1}}{\partial y^{\mu_1}} \cdots \frac{\partial Y^{A_n}}{\partial y^{\mu_n}} \mathcal{T}_{A_1 \cdots A_n}(Y) \ , \tag{2.22}$$

If a tensor is of the type $\mathcal{T}_{A_1 \cdots A_n}(Y) = Y_{(A_1} \mathcal{T}_{A_2 \cdots A_n)}(Y)$ it is unphysical, i.e. it has a vanishing projection to AdS_{d+1}.

A covariant derivative in AdS is defined in the ambient space $\mathbb{M}^{d+2}$ as

$$\nabla_A = \frac{\partial}{\partial Y^A} + Y_A \left(Y \cdot \frac{\partial}{\partial Y} \right) + W_A \left(Y \cdot \frac{\partial}{\partial W} \right) \ . \tag{2.23}$$

When acting on an transverse tensor we have

$$\nabla_B \mathcal{T}_{A_1 \cdots A_n}(Y) = G_B^{B_1} G_{A_1}^{C_1} \cdots G_{A_n}^{C_n} \frac{\partial}{\partial Y^{B_1}} \mathcal{T}_{C_1 \cdots C_n}(Y) \ , \tag{2.24}$$

where G_{AB} is the induced AdS metric. Using the polynomial notation, we can write the divergence of a tensor as

$$\nabla \cdot (K \mathcal{T}(Y, W)) \ , \tag{2.25}$$

which after projecting to AdS_{d+1} would give $\nabla^\mu t_{\mu\mu_2 \cdots \mu_n}$. And we can as well write

$$t_{\mu_1 \cdots \mu_n} \nabla^{\mu_1} \cdots \nabla^{\mu_n} \phi = \frac{1}{n! \left(\frac{d-1}{2} \right)_n} \mathcal{T}(Y, K)(W \cdot \nabla)^n \Phi(Y) \ ,$$

$$t_{\mu_1 \cdots \mu_n} f^{\mu_1 \cdots \mu_n} = \frac{1}{n! \left(\frac{d-1}{2} \right)_n} \mathcal{T}(Y, K)\mathcal{F}(Y, W) \ . \tag{2.26}$$

where t and f are symmetric and traceless tensors. Note that for transverse polynomials, we have

$$\nabla \cdot K = K \cdot \nabla \ , \tag{2.27}$$

It is useful to notice that for polynomials of the form (2.19) where the tensor is already symmetric, traceless and transverse, the projector reduces to $K = \left(\frac{d-1}{2} + n - 1 \right) \partial_W$. Since this will be the case in all our calculations, we will simply use ∂_W to contract indices.

2.2.2 Spinning three-point functions

In Chapter 1, we have reviewed that CFT correlation function can be alternatively computed using Witten diagrams in AdS. We focused on correlation functions for scalar operators, and in this chapter will consider external symmetric spinning

operators. In this section, we will review the calculation of 3-point functions for operators with generic spin in both sides of the duality. This analysis will prove to be useful later in this chapter since a 4-point function can be roughly thought as two 3-points functions. This section is mostly a summary of some the results in [84, 85].

OPE tensor structures

The main appeal of the embedding formalism is that one can conveniently describe n-point functions for symmetric tensors which automatically satisfy the constraints of $SO(d+1,1)$. Here, we will focus on 3-point functions. We will find them by identifying polynomials in (P_i, Z_j) of the correct homogeneity modulo terms of order Z_i^2 and $Z_i \cdot P_i$.

As a warm up, consider the two point function of a spin l primary of conformal dimension Δ, which we call $G_{A_1 \dots A_l B_1 \dots B_l}(P_1, P_2)$ in embedding space. This correlation function is a $2l$ tensor which we encode in a polynomial as

$$G_{\Delta|l}(P_1, Z_1; P_2, Z_2) \equiv Z_1^{A_1} \dots Z_1^{A_l} Z_2^{B_1} \dots Z_2^{B_l} G_{A_1 \dots A_l B_1 \dots B_l}(P_1, P_2) , \qquad (2.28)$$

and projecting further to $\mathbb{R}^d$ is done via (2.8) or (2.11). Up to a constant, the appropriate polynomial is

$$G_{\Delta|l}(P_1, Z_1; P_2, Z_2) = \frac{(H_{12})^l}{(P_{12})^\Delta} , \qquad (2.29)$$

where we have introduced

$$P_{12} \equiv -2P_1 \cdot P_2 , \qquad H_{12}(Z_1, Z_2) \equiv Z_1 \cdot Z_2 + 2\frac{(Z_1 \cdot P_2)(Z_2 \cdot P_1)}{P_{12}} . \qquad (2.30)$$

The numerator in (2.29) assures that we have a polynomial of degree l (encoding the tensorial features), while the denominator contains the homogeneity property we expect from conformal invariance. One can check as well that all other properties listed below (2.7) are satisfied, and the solution is unique up to pure gauge terms.

Three point functions of symmetric traceless operators have an elegant description in this language as well. Consider three primaries of conformal dimension Δ_i and spin l_i: the three point function is expected to take the form

$$G_{\Delta_1, \Delta_2, \Delta_3 | l_1, l_2, l_3}(P_i, Z_i) = \frac{Q_3(P_i, Z_i)}{(P_{12})^{(\Delta_1 + \Delta_2 - \Delta_3)/2}(P_{23})^{(\Delta_2 + \Delta_3 - \Delta_1)/2}(P_{13})^{(\Delta_1 + \Delta_3 - \Delta_2)/2}} . \tag{2.31}$$

The denominator is chosen such that the homogeneity with respect to P_i is explicit. The numerator Q_3 should be a transverse polynomial of degree l_i for each Z_i, and homogenous of degree zero for each P_i. Given these properties, we can cast the desired polynomial in terms of 6 building blocks [84]:[3]

$$V_{1,23} \ , \quad V_{2,31} \ , \quad V_{3,21} \ ,$$
$$H_{12} \ , \quad H_{13} \ , \quad H_{23} \ , \tag{2.32}$$

where

$$V_{i,jk} = \frac{(Z_i \cdot P_j)P_{ik} - (Z_i \cdot P_k)P_{ij}}{\sqrt{P_{ij}P_{ik}P_{jk}}} \ ,$$
$$H_{ij} = Z_i \cdot Z_j + 2\frac{(Z_j \cdot P_i)(Z_i \cdot P_j)}{P_{ij}} \ . \tag{2.33}$$

Different *tensor structures* built from contribute to the three-point function. Generally, Q_3 then takes the form

$$Q_3(P_i, Z_i) = \sum_{n_i \geq 0} C_{n_1,n_2,n_3}(V_{1,23})^{l_1 - n_2 - n_3}(V_{2,31})^{l_2 - n_3 - n_1}(V_{3,21})^{l_3 - n_1 - n_2}H_{12}^{n_1}H_{13}^{n_3}H_{23}^{n_2} \ ,$$
$$\tag{2.34}$$

giving us the expected homogeneity and transverse properties. Here C_{n_1,n_2,n_3} are constant (theory dependent) coefficients. Note that each of the powers of $V_{i,jk}$ in (2.34) have to be positive, and this restricts the number of possible combinations. For fixed l_i the number of tensorial structures is

$$N(l_1, l_2, l_3) = \frac{1}{6}(l_1 + 1)(l_1 + 2)(3l_2 - l_1 + 3) - \frac{1}{24}p(p + 2)(2p + 5) - \frac{1}{16}(1 - (-1)^p) \ ,$$
$$\tag{2.35}$$

with $l_1 \leq l_2 \leq l_3$ and $p \equiv \max(0, l_1 + l_2 - l_3)$.

Spinning Interactions

In Sec. 1.3, we have seen that symmetric spinning operators in CFT are dual fields carrying spin in AdS backgrounds. We will consider symmetric-traceless fields $\phi_{\mu_1 \ldots \mu_{J_i}}$ of spin J_i and mass m_i $(i = 1, 2, 3)$, with free equations of motion:

$$(\nabla^2 - m_i^2)\phi_{\mu_1 \ldots \mu_{J_i}} = 0 \,, \qquad \nabla^{\mu_1}\phi_{\mu_1 \ldots \mu_{J_i}} = 0 \,, \qquad g^{\mu_1 \mu_2}\phi_{\mu_1 \ldots \mu_{J_i}} = 0 \,. \tag{2.36}$$

To reproduce the boundary CFT spinning three-point correlator using Witten diagrams in AdS, we need to consider all the relevant interactions among the

---

[3]Our conventions for $V_{i,jk}$ and H_{ij} are very similar to those in [89], which differ slightly from those in [84]. Note that our definition of $V_{i,jk}$ differs to that of [89] by a minus sign.

symmetric-traceless fields $\phi_{\mu_1 \ldots \mu_{J_i}}$. In [90, 91], they take advantage of the embedding formalism to find the most general vertex of cubic interactions (modulo field re-parametrization and total derivatives)

$$V_3 = \sum_{n_i=0}^{J_i} g(n_i) I_{J_1,J_2,J_3}^{n_1,n_2,n_3}(Y_i)|_{Y_i=Y} \ , \tag{2.37}$$

where $g(n_i)$ are arbitrary coupling constants, and

$$
\begin{aligned}
I_{J_1,J_2,J_3}^{n_1,n_2,n_3}(Y_i) = \ & \mathcal{Y}_1^{J_1-n_2-n_3} \mathcal{Y}_2^{J_2-n_3-n_1} \mathcal{Y}_3^{J_3-n_1-n_2} \\
& \times \mathcal{H}_1^{n_1} \mathcal{H}_2^{n_2} \mathcal{H}_3^{n_3} \, \mathcal{T}_{J_1}(Y_1,W_1)\mathcal{T}_{J_2}(Y_2,W_2)\mathcal{T}_{J_3}(Y_3,W_3) \ . \tag{2.38}
\end{aligned}
$$

Here $\mathcal{T}_{J_i}(Y_i, W_i)$ are polynomials in the embedding formalism that contain the components of the symmetric traceless tensor field in AdS. This cubic interaction is built out of six basic contractions which are defined as[4]

$$
\begin{aligned}
\mathcal{Y}_1 = \partial_{W_1} \cdot \partial_{Y_2} \ , & \quad \mathcal{Y}_2 = \partial_{W_2} \cdot \partial_{Y_3} \ , & \quad \mathcal{Y}_3 = \partial_{W_3} \cdot \partial_{Y_1} \ , \\
\mathcal{H}_1 = \partial_{W_2} \cdot \partial_{W_3} \ , & \quad \mathcal{H}_2 = \partial_{W_1} \cdot \partial_{W_3} \ , & \quad \mathcal{H}_3 = \partial_{W_1} \cdot \partial_{W_2} \ . \tag{2.39}
\end{aligned}
$$

For more details on the construction of this vertex we refer to [86]. It is important to highlight that the number of terms in the interaction vertex (2.37) is also the number (2.35) that counts the independent tensor structures.

The spinning CFT 3-point function in (2.31) can be computed holographically using the Witten diagram associated to the vertex V_3 [85]:

$$G_{\Delta_1,\Delta_2,\Delta_3|J_1,J_2,J_3}(P_i,Z_i) \quad = \quad$$ $$\tag{2.40}$$

The explicit computation of this Witten diagram involves an integral over spinning bulk-to-boundary propagators, which are found in Appendix 6.1 using the advantages of the embedding formalism. The spinning propagators will be contracted accordingly to reproduce the different interactions in V_3. As an example, in Appendix 6.3 we perform the integrals for some of the simplest interactions in V_3.

---

[4]All derivatives here are partial, but by using the homogeneity of $\mathcal{T}_{J_i}(Y_i, W_i)$ one can relate them to covariant derivatives.

As expected, the results are some combination of tensor structures that appear in (2.34). The general result for all interactions in V_3 can be found appendix A of [85], and it is a lengthy expression we will not reproduce here. However, it is interesting to notice that since the number of independent interactions in (2.37) is exactly the same as the number of independent structures the CFT three point function (2.35), there is a one-to-one relation between the coupling constants of gravity interactions and the OPE coefficients C_{n_1,n_2,n_3} in (2.34).

2.2.3 Spinning 4-point functions from CFT differential operators

In Sec. 2.2.2 we have seen that three-point function of spining primary operators can be rewritten in terms of the 6-basic tensor structures.

$$V_{1,23} , \quad V_{2,31} , \quad V_{3,21} ,$$
$$H_{12} , \quad H_{13} , \quad H_{23} . \tag{2.41}$$

For operational purposes, and later on to evaluate conformal partial waves, it is more convenient to generate the tensorial structures in (2.34) via differential operators. This was originally done in [72], and the basic idea is as follows. Say we look at the OPE of two operators which carry spin:

$$\mathcal{O}_1^{l_1}(x_1)\mathcal{O}_2^{l_2}(x_2) = \sum_{\mathcal{O}} \lambda_{12\mathcal{O}} C(x_{12}, \partial_2)^{l_1,l_2,l} \, \mathcal{O}^l(x_2) . \tag{2.42}$$

The OPE structures now carry the tensorial properties of the external operators, relative to cases where the left hand side operators are scalar primaries. The point made in [72] is to view these more complicated objects as derivatives of the basic scalar OPE we analysed in Sec. 1.2.1. More explicitly, if the OPE between two scalar primaries is

$$\mathcal{O}_1(x_1)\mathcal{O}_2(x_2) = \sum_{\mathcal{O}} \lambda_{12\mathcal{O}} C(x_{12}, \partial_2)^l \, \mathcal{O}^l(x_2) , \tag{2.43}$$

then

$$C(x_{12}, \partial_2)^{l_1,l_2,l} = D_{x_1,x_2}^{l_1,l_2} C(x_{12}, \partial_2)^l , \tag{2.44}$$

where $D_{x_1,x_2}^{l_1,l_2}$ is a differential operator that creates the tensorial structure for l_1 and l_2. Taking this relation for granted, it would then imply that the three point functions would be related as

$$\langle \mathcal{O}_1^{l_1}(x_1)\mathcal{O}_2^{l_2}(x_2)\mathcal{O}_3^{l_3}(x_3)\rangle = D_{x_1,x_2}^{l_1,l_2}\langle \mathcal{O}_1(x_1)\mathcal{O}_2(x_2)\mathcal{O}_3^{l_3}(x_3)\rangle . \tag{2.45}$$

The idea is that we can represent any three point function of symmetric traceless structures as derivatives of a scalar-scalar-spin correlation function.

One can cast as well (2.45) as a polynomial relation in embedding space: given a function $G_{\Delta_1,\Delta_2,\Delta_3|l_1,l_2,l_3}(P_i, Z_i)$ of certain degree in Z_i, we would like to relate it to a polynomial of lower degree via suitable differential operators, i.e.

$$G_{\Delta_1,\Delta_2,\Delta_3|l_1,l_2,l_3} = D\left(P_i, Z_i, \frac{\partial}{\partial P_i}, \frac{\partial}{\partial Z_i}\right) G_{\Delta_1',\Delta_2',\Delta_3|0,0,l_3} + O(Z_i^2, P_i^2, Z_i \cdot P_i) ,$$
(2.46)

with $i = 1, 2$. The differential operators have to satisfy certain basic properties:

1. D must raise the degree in Z_1 up to l_1 and Z_2 up to l_2.

2. D must take terms $O(Z_n^2, P_n^2, Z_n \cdot P_n)$ to terms of the same kind: keep pure gauge terms as pure gauge.

3. D must map transverse functions to themselves.

A basis of operators that will satisfy these requirements are

$$D_{1\,ij} \equiv -\frac{1}{2}P_{ij}\left(Z_i \cdot \frac{\partial}{\partial P_j}\right) - (Z_i \cdot P_j)\left(P_i \cdot \frac{\partial}{\partial P_j}\right) - (Z_i \cdot Z_j)\left(P_i \cdot \frac{\partial}{\partial Z_j}\right) \quad (2.47)$$
$$+ (Z_j \cdot P_i)\left(Z_i \cdot \frac{\partial}{\partial Z_j}\right) ,$$
$$D_{2\,ij} \equiv -\frac{1}{2}P_{ij}\left(Z_i \cdot \frac{\partial}{\partial P_i}\right) - (Z_i \cdot P_j)\left(P_i \cdot \frac{\partial}{\partial P_i}\right) + (Z_i \cdot P_j)\left(Z_i \cdot \frac{\partial}{\partial Z_i}\right) ,$$
(2.48)

in addition to H_{ij} in (2.33). The operator $D_{1\,ij}$ increases the spin at position i by one and decreases the dimension by one at position i; $D_{2\,ij}$ increases the spin at position i by one and decreases the dimension by one at position j. H_{ij} increases the spin by one at both i and j and leaves the conformal dimensions unchanged. The commutation relation between these operators are

$$[D_{1\,12}, D_{1\,21}] = \frac{1}{2}P_{12}H_{12}\left(Z_1 \cdot \partial_{Z_1} - Z_2 \cdot \partial_{Z_2} + P_1 \cdot \partial_{P_1} - P_2 \cdot \partial_{P_2}\right) , \quad (2.49)$$

$$[D_{2\,12}, D_{2\,21}] = \frac{1}{2}P_{12}H_{12}\left(Z_1 \cdot \partial_{Z_1} - Z_2 \cdot \partial_{Z_2} - P_1 \cdot \partial_{P_1} + P_2 \cdot \partial_{P_2}\right) , \quad (2.50)$$

and all other pairings are zero, including $[D_{k\,ij}, H_{i'j'}] = 0$.

To see how this works, it is useful to just state the map for a few examples.

Defining the three point function of three scalar primaries as

$$T(\Delta_1, \Delta_2, \Delta_3) \equiv \frac{1}{(P_{12})^{(\Delta_1+\Delta_2-\Delta_3)/2}(P_{23})^{(\Delta_2+\Delta_3-\Delta_1)/2}(P_{13})^{(\Delta_1+\Delta_3-\Delta_2)/2}} \tag{2.51}$$

we have that increasing the spin by one at position $i = 1$ is achieved by

$$\begin{aligned} G_{\Delta_1,\Delta_2,\Delta_3|1,0,0} &= V_{1,23}T(\Delta_1, \Delta_2, \Delta_3) \\ &= \frac{2}{\Delta_3 + \Delta_2 - \Delta_1 - 1}D_{1\,12}T(\Delta_1 + 1, \Delta_2, \Delta_3) \\ &= \frac{2}{\Delta_3 - \Delta_2 + \Delta_1 - 1}D_{2\,12}T(\Delta_1, \Delta_2 + 1, \Delta_3) \,. \end{aligned} \tag{2.52}$$

In the first line we wrote it as in (2.31)-(2.34), and in the last two lines we casted the same answer in terms of differential operators acting on the scalar correlation function. The three point function of two vectors and a scalar is the superposition of two tensorial structures:

$$G_{\Delta_1,\Delta_2,\Delta_3|1,1,0} = C_1 V_{1,23}V_{2,13}T(\Delta_1, \Delta_2, \Delta_3) + C_2 H_{12}T(\Delta_1, \Delta_2, \Delta_3) \,. \tag{2.53}$$

The first term can be written in terms of derivatives as

$$\begin{aligned} V_{1,23}V_{2,13}T(\Delta_1, \Delta_2, \Delta_3) &= \frac{4}{\Delta_3^2 - (\Delta_1 - \Delta_2)^2}D_{1\,12}D_{1\,21}T(\Delta_1 + 1, \Delta_2 + 1, \Delta_3) \\ &\quad + \frac{H_{12}}{\Delta_3 + \Delta_2 - \Delta_1}T(\Delta_1, \Delta_2, \Delta_3) \,. \end{aligned} \tag{2.54}$$

How to map the polynomials $V_{i,jk}$'s to $D_{i\,jk}$'s is not one-to-one, as reflected explicitly in (2.52) among other cases. Nevertheless, one can always go from the basis of $V_{i,jk}$'s to $D_{i\,jk}$'s, and this transformation can be implemented systematically as discussed in [72]. In appendix 6.2 we give further examples and discuss briefly the conditions on Q_3 imposed by conservation.

The interesting application of these differential operators is to evaluate spinning conformal partial waves as done in [72]. Analogously as done for the scalar case in (1.9), we can find the conformal partial wave expansion of the spinning 4-point functions using the OPE (2.42):

$$\langle \mathcal{O}_1^{l_1}(x_1)\mathcal{O}_2^{l_2}(x_2)\mathcal{O}_3^{l_3}(x_3)\mathcal{O}_4^{l_4}(x_4) \rangle = \sum_{\mathcal{O}} \lambda_{12\mathcal{O}}\lambda_{34\mathcal{O}}W_{\Delta|l}^{l_1,l_2,l_3,l_4}(x_1, x_2, x_3, x_4) \,, \tag{2.55}$$

To find the spinning conformal partial wave $W_{\Delta|l}^{l_1,l_2,l_3,l_4}(x_1, x_2, x_3, x_4)$ is a more complicated task than to find its scalar version $W_{\Delta|l}(x_1, x_2, x_3, x_4)$. This is mainly due to the fact that in the spinning case there are many different invariant structures that can be fixed by conformal symmetry. Then, it is useful to write the

spinning partial waves as simply derivatives acting on the known scalar partial wave using (2.44) or (2.45):

$$W_{\Delta|l}^{l_1,l_2,l_3,l_4}(x_1,x_2,x_3,x_4) = D_{x_1,x_2}^{l_1,l_2} D_{x_3,x_4}^{l_3,l_4} W_{\Delta|l}(x_1,x_2,x_3,x_4) \ . \tag{2.56}$$

And in the embedding space formalism, the conformal partial wave is a suitable polynomial with the basis of differential operators that generate the tensor structures are given by (2.47) and H_{ij}. More explicitly

$$W_{\Delta|l}^{l_1,l_2,l_3,l_4}(P_i;Z_i) = D_{\text{left}} D_{\text{right}} W_{\Delta|l}(P_1,P_2,P_3,P_4) \ , \tag{2.57}$$

with D_{left} is a chain of powers of D_{ijk} and H_{ij} operators acting on (P_1,P_2), and similarly for D_{right} acting on (P_3,P_4). The exchange field $\mathcal{O}$ is neccesarly a traceless symmetric tensor.

2.3 Spinning geodesic Witten diagrams

As explained in Sec. 2.1, the AdS_{d+1} object dual to a scalar conformal partial wave $W_{\Delta|0}(x_1,x_2,x_3,x_4)$ is the following geodesic Witten diagram [62]:

$$\mathcal{W}_{\Delta|0}(x_1,x_2,x_3,x_4) = \int_{\gamma_{12}} d\lambda \int_{\gamma_{34}} d\lambda' G_{b\partial}^{\Delta_1|0}(y(\lambda),x_1) G_{b\partial}^{\Delta_2|0}(y(\lambda),x_2)$$
$$\times G_{bb}^{\Delta|0}(y(\lambda),y'(\lambda')) G_{b\partial}^{\Delta_3|0}(y'(\lambda'),x_3) G_{b\partial}^{\Delta_4|0}(y'(\lambda'),x_4) \tag{2.58}$$

The geodesic that connects the boundary points (x_i,x_j) is γ_{ij}, and λ is an affine parameter for γ_{12} and λ' for γ_{34}. This integral involves bulk–to–boundary and bulk–to–bulk propagators in AdS projected along geodesics connecting the endpoints, as depicted in Fig. 2.1. Geodesic Witten diagrams will be the center of the rest of this chapter.

Our interest here is to explore cases where the external and internal lines have non-trivial spin. In this section we will give a prescription on how to obtain $W_{\Delta|l}^{l_1,l_2,l_3,l_4}(x_1,x_2,x_3,x_4)$ by using a basis of AdS_{d+1} differential operators which will act on (2.58). This should be viewed as the gravitational version of the relations in (1.9), where suitable tensor structures are built a by a set derivatives acting on x_i. We stress that we will not use local cubic interactions to capture the conformal partial wave in this section. We postpone to section 2.4 the interpretation of this construction in terms of cubic interactions in the bulk.
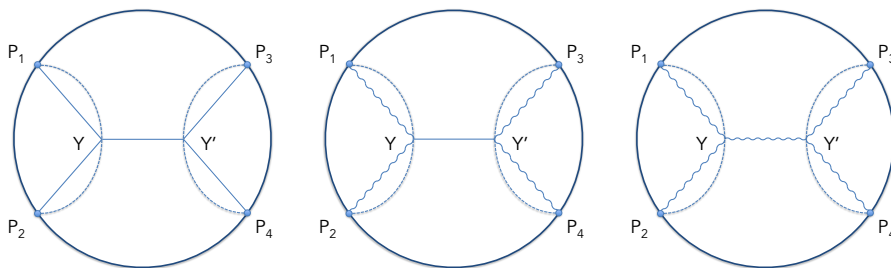
Figure 2.1: *Examples of geodesic Witten diagrams in AdS_{d+1}. The doted line indicates that we are projecting the propagators over a geodesic that connects the endpoints. Straight lines correspond to scalar fields, while wavy lines are symmetric traceless tensors of spin J. The first diagram corresponds to the scalar block in* (2.58)*. The middle diagram (with scalar propagator in the exchange) will be the focus of section 2.3.1 and the last diagram (with a spin-J field exchanged) is the focus of section 2.3.2.*

2.3.1 Construction of bulk differential operators: scalar exchanges

To start we want to give an AdS analog of the CFT operators that generate tensor structures in spinning conformal partial waves. We recall that there are two class of operators

$$D_{ijk} , \qquad \text{and} \qquad H_{ij} . \tag{2.59}$$

The operators D_{ijk}, defined in (2.47), are differential operators that basically raise spin at position j; these operators we will map to differential operators acting on bulk coordinates. H_{ij}, defined in (2.33), raises the spin at position i and j; it is not a differential operator, so its action will remain unchanged. H_{ij} does induce a cubic interaction and we will discuss its effect in section 2.4.

The action of a single operator in (2.59) on a conformal partial wave $W_{\Delta|l}(P_i)$ will affect either the pair (P_1, P_2) or (P_3, P_4), but not all points simultaneously. So let's consider the components in the integral (2.58) that only depends on γ_{12} which connects (P_1, P_2):

$$\int_{\gamma_{12}} d\lambda \, G_{b\partial}^{\Delta_1|0}(Y_\lambda, P_1) G_{b\partial}^{\Delta_2|0}(Y_\lambda, P_2) G_{bb}^{\Delta|0}(Y_\lambda, Y') . \tag{2.60}$$

We casted the propagators in embedding space, and their explicit form is found in Appendix 6.1[5] .Fig. 2.2 depicts diagrammatically the content in (2.60), and

---

[5]We recall our notation: Y^A denotes AdS points and W^A are the auxiliary vectors that soak up bulk spin. The analogous CFT quantities are P^A and Z^A, respectively.
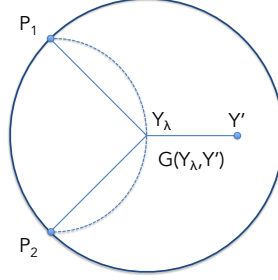
Figure 2.2: *A precursor diagram where two legs are in the boundary and one in the bulk. This type of object appears at intermediate steps when evaluating conformal blocks.*

we note that Y' is not necessarily projected over γ_{34}. Here $G_{b\partial}^{\Delta_1|0}(Y, P_1) \equiv G_{b\partial}^{\Delta_1|0}(Y, P_1; 0, 0)$ given in (6.2); in general we will omit dependence on variables that are not crucial for the equation in hand.

Using Poincare coordinates, a geodesic that connects x_i with x_j is

$$\gamma_{ij}: \quad y^\mu(\lambda) = (r(\lambda), x^a(\lambda)) = \left(\frac{(x_{ij}^2)^{\frac{1}{2}}}{2\cosh(\lambda)}, \frac{x_i^a + x_j^a}{2} + \frac{(x_{ij})^a}{2}\tanh(\lambda) \right) , \quad (2.61)$$

with $x_{ij} \equiv x_i - x_j$. Passing this information to the embedding formalism, we have

$$\gamma_{ij}: \qquad Y_\lambda^A \equiv \frac{e^{-\lambda}P_i^A + e^\lambda P_j^A}{\sqrt{P_{ij}}} , \quad P_{ij} = -2P_i \cdot P_j , \qquad (2.62)$$

where we used (2.5) and (2.17). Evaluating (2.60) along γ_{12} gives

$$\frac{1}{(P_{12})^{(\Delta_1+\Delta_2)/2}} \int_{-\infty}^{\infty} d\lambda \, e^{-\Delta_{12}\lambda} \, G_{bb}^{\Delta|0}(Y_\lambda, Y') , \qquad \Delta_{12} = \Delta_1 - \Delta_2 . \qquad (2.63)$$

To increase the spin at P_1 and/or P_2 we would act on (2.63) with a combination of the differential operators in (2.47). By inspection of the integral in (2.63), $D_{i\,jk}$ has only a non-trivial action over the bulk–to–bulk propagators: $G_{b\partial}$ plays no role in building the OPE structures. Another way of staying this is to note that

$$D_{k\,ij} G_{b\partial}^{\Delta_n|0}(Y_\lambda, P_n) = 0 , \qquad n = 1, 2 . \qquad (2.64)$$

Hence, the task ahead is to build a bulk differential operator that acts on the third leg of the diagram: $G_{bb}^{\Delta|0}(Y_\lambda, Y')$.

Let's consider then a general function $G(Y_\lambda \cdot Y')$ that doesn't depend explicitly on P_i (only through the geodesics in Y_λ), and further more with no W dependence.

We want to find differential operators $\mathcal{D}$ such that

$$D_{k\,ij} G\left(Y_\lambda \cdot Y'\right) = \mathcal{D}_{k\,ij} G\left(Y_\lambda \cdot Y'\right) \ , \tag{2.65}$$

where $\mathcal{D}_{k\,ij}$ has derivatives with respect to Y' only. This equality implies that $\mathcal{D}$ has to satisfy the same basic properties those in D, listed in section 2.2.3. The set of differential operators that satisfy our requirements is

$$\mathcal{D}_{1\,ij} = Z_i \cdot Y' \, P_i \cdot \partial_{Y'} + \frac{1}{2} \Psi_{iY'} \, Z_i \cdot \partial_{Y'} \ ,$$

$$\mathcal{D}_{2\,ij} = H_{ij}(Z_i, Y') P_j \cdot \partial_{Y'} + \frac{1}{2} \Psi_{jY'} H_{ij}(Z_i, \partial_{Y'}) \ . \tag{2.66}$$

where Ψ_{ij} is given in (6.3) and $H_{ij}(Z_i, Z_j)$ is defined in (2.33). The key property to constrain (2.66) is to demand transversality of the operators (i.e. that it commutes with $P_i \cdot \partial_{Z_i}$), and the rest follows from demanding (2.65). Note that these operators do not scale under $Y' \to \alpha Y'$, which leaves the homogeneity properties of the third field intact. $\mathcal{D}_{1\,ij}$ is increasing the spin by one and decreasing the dimension by one at position i, while $\mathcal{D}_{2\,ij}$ increases the spin at position i by one and decreases the dimension by one at position j. The extra subscript $(1,2)$ in (2.66) is to keep the notation in the same line as in (2.47).

To verify that $\mathcal{D}$ has exactly the same effect as D, it is instructive to go through some identities. One can show the following relation by direct calculation

$$[D_{k\,ij}, \mathcal{D}_{k'\,i'j'}]f(Y') = [\mathcal{D}_{k\,ij}, \mathcal{D}_{k'\,i'j'}]f(Y') \ . \tag{2.67}$$

Let's call D_1, D_2 two generic operators of the form $D_{k\,ij}$, then

$$\begin{aligned}
D_1 D_2(Y_\lambda \cdot Y') &= (D_1 Y_\lambda) \cdot (\mathcal{D}_2 Y') + Y_\lambda \cdot (D_1 \mathcal{D}_2 Y') \\
&= Y_\lambda \cdot (\mathcal{D}_2 \mathcal{D}_1 Y') + Y_\lambda \cdot ([D_1, \mathcal{D}_2] Y') \\
&= Y_\lambda \cdot (\mathcal{D}_1 \mathcal{D}_2 Y') = \mathcal{D}_1 \mathcal{D}_2 (Y_\lambda \cdot Y')
\end{aligned} \tag{2.68}$$

where in the third line we used (2.67). Then for the product of an arbitrary number of operators,

$$\begin{aligned}
D_1 D_2 \cdots D_n Y_\lambda \cdot Y' &= Y_\lambda \cdot (\mathcal{D}_2 \cdots \mathcal{D}_n \mathcal{D}_1 Y') + Y_\lambda \cdot (D_1 \mathcal{D}_2 \cdots \mathcal{D}_n Y') \\
&= Y_\lambda \cdot (\mathcal{D}_1 \mathcal{D}_2 \cdots \mathcal{D}_n Y') = \mathcal{D}_1 \mathcal{D}_2 \cdots \mathcal{D}_n Y_\lambda \cdot Y'
\end{aligned} \tag{2.69}$$

where in the first line we used the induction hypothesis for $n-1$ operators and in the second line we pushed D_1 through and used (2.67) to put everything in terms of $\mathcal{D}$. The conclusion is that boundary derivatives on geodesic integrals can be replaced by bulk derivatives:

$$\begin{aligned}
H_{12}^{n_{12}}(\mathcal{D}_{2,12}^{n_1} \mathcal{D}_{2,21}^{n_2} \mathcal{D}_{1,12}^{m_1} \mathcal{D}_{1,21}^{m_2} &- D_{2,12}^{n_1} D_{2,21}^{n_2} D_{1,12}^{m_1} D_{1,21}^{m_2}) \\
&\times \int_{\gamma_{12}} d\lambda \, G_{b\partial}^{\Delta_1|0}(Y_\lambda, P_1) G_{b\partial}^{\Delta_2|0}(Y_\lambda, P_2) G_{bb}^{\Delta|0}(Y_\lambda, Y') = 0 \ . \tag{2.70}
\end{aligned}$$

We just found that the dual of D are derivatives with respect to Y'. However, the generic form of this differential operators is $\mathcal{D}(Y') = Y'^A Z_i^B S_{ABC} \partial_{Y'}^C$, where S is antisymmetric under $A \leftrightarrow C$ due to (2.66). Hence

$$Y'^A Z_i^B S_{ABC} \partial_{Y'}^C Y_\lambda \cdot Y' = -Y_\lambda^A Z_i^B S_{ABC} \partial_{Y_\lambda}^C Y_\lambda \cdot Y'$$
$$\Rightarrow \quad \mathcal{D}_{k\,ij}(Y') Y_\lambda \cdot Y' = -\mathcal{D}_{k\,ij}(Y_\lambda) Y_\lambda \cdot Y' \ . \tag{2.71}$$

Using (2.71) it is easy to show that for more derivatives,

$$\mathcal{D}_{k_1\,i_1 j_1}(Y') \cdots \mathcal{D}_{k_n\,i_n j_n}(Y') Y_\lambda \cdot Y' = (-1)^n \mathcal{D}_{k_n\,i_n j_n}(Y_\lambda) \cdots \mathcal{D}_{k_1\,i_1 j_1}(Y_\lambda) Y_\lambda \cdot Y' \ . \tag{2.72}$$

This of course also holds when the derivatives act on $G(Y_\lambda \cdot Y')$. It is interesting to note that the action of $\mathcal{D}(Y_\lambda)$ on bulk–to–boundary operators is trivial, i.e.

$$\mathcal{D}_{k\,ij}(Y_\lambda) G_{b\partial}^{\Delta_{1,2}|0}(Y_\lambda, P_{1,2}) = 0 \ . \tag{2.73}$$

However,

$$\mathcal{D}_{k'\,i'j'} \cdots \mathcal{D}_{k\,ij}(Y_\lambda) G_{b\partial}^{\Delta_{1,2}|0}(Y_\lambda, P_{1,2}) \neq 0 \ , \tag{2.74}$$

because (2.73) relies on properties of the geodesic γ_{12}, and in (2.74) the operation of taking derivatives with respect to Y does not commute with projecting on γ_{12}[6]. Hence, as we generate tensorial structures using $\mathcal{D}(Y_\lambda)$, it only acts on G_{bb}, i.e.

$$(-1)^N \int_{\gamma_{12}} d\lambda\, G_{b\partial}^{\Delta_1|0}(Y_\lambda, P_1) G_{b\partial}^{\Delta_2|0}(Y_\lambda, P_2) \mathcal{D}_{1,21}^{m_2} \mathcal{D}_{1,12}^{m_1} \mathcal{D}_{2,21}^{n_2} \mathcal{D}_{2,12}^{n_1} G_{bb}^{\Delta_3|0}(Y_\lambda, Y') =$$
$$D_{2,12}^{n_1} D_{2,21}^{n_2} D_{1,12}^{m_1} D_{1,21}^{m_2} \int_{\gamma_{12}} d\lambda\, G_{b\partial}^{\Delta_1|0}(Y_\lambda, P_1) G_{b\partial}^{\Delta_2|0}(Y_\lambda, P_2) G_{bb}^{\Delta_3|0}(Y_\lambda, Y') \ , \tag{2.75}$$

where $N \equiv m_1 + m_2 + n_1 + n_2$.

From here we see how to cast conformal partial waves where the exchanged field is a scalar field (dual to a scalar primary $\mathcal{O}$ of conformal dimension Δ): the version of (1.9) in gravitational language is

$$W_{\Delta|0}^{l_1, l_2, l_3, l_4}(P_i; Z_i) = \mathcal{W}_{\Delta|0}[\mathcal{D}_{\text{left}}(Y_\lambda), \mathcal{D}_{\text{right}}(Y'_{\lambda'})] \ , \tag{2.76}$$

where

$$\mathcal{W}_{\Delta|0}[\mathcal{D}_{\text{left}}(Y_\lambda), \mathcal{D}_{\text{right}}(Y'_{\lambda'})] \equiv \int_{\gamma_{12}} \int_{\gamma_{34}} G_{b\partial}^{\Delta_1|0}(Y_\lambda, P_1) G_{b\partial}^{\Delta_2|0}(Y_\lambda, P_2)$$
$$\times \left[\mathcal{D}_{\text{left}}(Y_\lambda) \mathcal{D}_{\text{right}}(Y'_{\lambda'}) G_{bb}^{\Delta|0}(Y_\lambda, Y'_{\lambda'}) \right] G_{b\partial}^{\Delta_3|0}(P_3, Y'_{\lambda'}) G_{b\partial}^{\Delta_4|0}(P_4, Y'_{\lambda'}) \ . \tag{2.77}$$

---

[6]For $\mathcal{D}_{1\,21}$ and $\mathcal{D}_{2\,12}$, (2.73) is true without projecting on γ_{12}. Furthermore, (2.74) is true only if the $\mathcal{D}$'s do not commute. However, we will use (2.75) to treat all the $\mathcal{D}$'s in the same footing.

To close this discussion, we record another convenient way to re-write (2.66):

$$\mathcal{D}_{1\,ij}(Y_\lambda) = \frac{\Psi_{i\lambda}}{2}\mathcal{H}_{i\lambda}(Z_i, \partial_{Y_\lambda})\ ,$$

$$\mathcal{D}_{2\,ij}(Y_\lambda) = \frac{\Psi_{j\lambda}}{2}\left[\mathcal{H}_{i\lambda}(Z_i, \partial_{Y_\lambda}) + 2\mathcal{V}_{\partial\,i,j\lambda}(Z_i)\mathcal{V}_{b\,\lambda,ij}(\partial_{Y_\lambda})\right]\ , \qquad (2.78)$$

where $\mathcal{H}_{ij}$ is given in (6.3), and we defined

$$\mathcal{V}_{\partial\,i,jm}(Z_i) = \frac{\Psi_{im}Z_i \cdot P_j - P_{ij}Z_i \cdot Y_m}{\sqrt{\Psi_{im}\Psi_{jm}P_{ij}}}\ , \qquad (2.79)$$

$$\mathcal{V}_{b\,m,ij}(W_m) = \frac{\Psi_{jm}W_m \cdot P_i - \Psi_{im}W_m \cdot P_j}{\sqrt{\Psi_{im}\Psi_{jm}P_{ij}}}\ , \qquad (2.80)$$

which can be viewed as the analogous CFT in (2.33).

2.3.2 Construction of bulk differential operators: spin exchanges

We now generalize the discussion to include spin fields in the exchange diagram. The prescription given in [62] for spinning exchanged operators is that the bulk–to–bulk propagator for the spin J field is contracted with the velocities of Y_λ and $Y'_{\lambda'}$, i.e.

$$G_{bb}^{\Delta|J}(Y_\lambda, Y'_{\lambda'}) \equiv G_{bb}^{\Delta|J}\left(Y_\lambda, Y'_{\lambda'}; \frac{dY_\lambda}{d\lambda}, \frac{dY'_{\lambda'}}{d\lambda'}\right)\ . \qquad (2.81)$$

This corresponds to the pullback of the propagator (6.7) along both geodesics in the diagram. Hence, a geodesic diagram that evaluates the conformal partial wave with a spin exchange is

$$\mathcal{W}_{\Delta|J}(P_1, P_2, P_3, P_4) =$$
$$\int_{\gamma_{12}} \int_{\gamma_{34}} G_{b\partial}^{\Delta_1|0}(Y_\lambda, P_1)G_{b\partial}^{\Delta_2|0}(Y_\lambda, P_2)G_{bb}^{\Delta|J}(Y_\lambda, Y'_{\lambda'})G_{b\partial}^{\Delta_3|0}(Y'_{\lambda'}, P_3)G_{b\partial}^{\Delta_4|0}(Y'_{\lambda'}, P_4)\ . \tag{2.82}$$

In manipulating (2.81) to increase the spin of the external legs, we need to treat the contractions with $\frac{dY_\lambda}{d\lambda}$ with some care. First, it is important to note that $D_{k\,ij}$ commutes with $\frac{d}{d\lambda}$, and hence its action on $G_{bb}^{\Delta|J}(Y_\lambda, Y'_{\lambda'})$ in (2.82) is straightforward. However, we need to establish how $\mathcal{D}_{k\,ij}$ acts (2.81), and this

requires understanding how to cast $\frac{d}{d\lambda}$ as a covariant operation. It is easy to check by direct computation that this can be done in two ways:

$$\frac{d}{d\lambda} = -2P_{12}^{-1}\Psi_{2\lambda}P_1 \cdot \nabla_{Y_\lambda} = 2P_{12}^{-1}\Psi_{1\lambda}P_2 \cdot \nabla_{Y_\lambda} \ . \tag{2.83}$$

But the commutator of $\mathcal{D}_{k\,ij}$ with $\frac{d}{d\lambda}$ will depend on which equality we use. For example

$$D_{1\,12}\frac{dY_\lambda}{d\lambda} = -\mathcal{D}_{1\,12}(Y_\lambda)(-2P_{12}^{-1}\Psi_{2\lambda}P_1 \cdot \nabla_{Y_\lambda})Y_\lambda \ , \tag{2.84}$$

$$D_{2\,21}\frac{dY_\lambda}{d\lambda} = -\mathcal{D}_{2\,21}(Y_\lambda)(-2P_{12}^{-1}\Psi_{2\lambda}P_1 \cdot \nabla_{Y_\lambda})Y_\lambda \ , \tag{2.85}$$

which is the expected result by (2.69) and (2.72). Unfortunately, the two other D's have the wrong sign relative to (2.69) and (2.72):

$$D_{1\,21}\frac{dY_\lambda}{d\lambda} = \mathcal{D}_{1\,21}(Y_\lambda)(-2P_{12}^{-1}\Psi_{2\lambda}P_1 \cdot \nabla_{Y_\lambda})Y_\lambda \ , \tag{2.86}$$

$$D_{2\,12}\frac{dY_\lambda}{d\lambda} = \mathcal{D}_{2\,12}(Y_\lambda)(-2P_{12}^{-1}\Psi_{2\lambda}P_1 \cdot \nabla_{Y_\lambda})Y_\lambda \ . \tag{2.87}$$

Using the other implementation of $\frac{d}{d\lambda}$ alternates the signs. In order to avoid this implementation problem, we formally define

$$\left[\mathcal{D}_{k\,ij}(Y_\lambda), \frac{d}{d\lambda}\right] \equiv 0 \ . \tag{2.88}$$

This implies that as we encounter quantities that contain explicit derivatives of λ we will manipulate them by first acting with $\mathcal{D}_{k\,ij}(Y_\lambda)$ and then taking the derivative with respect to λ. For instance,

$$\begin{aligned}
D_{k\,ij}\frac{dY_\lambda}{d\lambda} \cdot \frac{dY'_{\lambda'}}{d\lambda'} &= \frac{d}{d\lambda}\frac{d}{d\lambda'}D_{k\,ij}Y_\lambda \cdot Y'_{\lambda'} \\
&= -\frac{d}{d\lambda}\frac{d}{d\lambda'}\mathcal{D}_{k\,ij}(Y_\lambda)Y_\lambda \cdot Y'_{\lambda'} \ .
\end{aligned} \tag{2.89}$$

Given this implementation of the differential operators, the partial wave in gravitational language (2.76) generalizes to spinning exchanges by using (2.81) and (2.88). This shows that for each partial wave $W_{\Delta|J}^{l_1,l_2,l_3,l_4}(P_i; Z_i)$ in the boundary CFT there is a counterpart geodesic integral in AdS $\mathcal{W}_{\Delta|J}^{l_1,l_2,l_3,l_4}(P_i; Z_i)$ that reproduces the same quantity.

2.4 Identification of gravitational interactions via geodesic diagrams

We have given in the previous section a systematic procedure to build the appropriate tensor structures $V_{i,jk}$ and H_{ij} appearing in conformal partial waves by using directly bulk differential operators $\mathcal{D}_{ijk}(Y_\lambda)$. Using this method, we would like to identify the gravitational interactions that the operators $\mathcal{D}_{ijk}(Y_\lambda)$ are capturing.

As explained in Section 2.2.2, the identification of tensor structures with gravitational interactions has been successfully carried out in [85]: all possible cubic vertices in AdS_{d+1} where mapped to the tensor structures of a CFT_d via Witten diagrams for three point functions. Here we would like to revisit this identification using instead as a building block diagrams in AdS that are projected over geodesic integrals rather than volume integrals; and as we will show below, the geodesic diagrams do suffer from some non-trivial cancellations for certain derivative interactions.

For the discussion in this section it is sufficient to consider the following object

$$\int_{\gamma_{ij}} d\lambda \, G_{b\partial}^{\Delta_1|0}(y(\lambda), x_1) G_{b\partial}^{\Delta_2|0}(y(\lambda), x_2) G_{b\partial}^{\Delta_3|0}(y(\lambda), x_3) \ . \tag{2.90}$$

Here γ_{ij} is a geodesic that connects a pair of endpoints (x_i, x_j). Rather interestingly, it was noted in [71] that this integral actually reproduces the CFT three point function for scalar primaries; this equivalence is regardless the choice of endpoints, with different choices just giving different numerical factors.[7] The type of diagrams we will be considering are depicted in Fig. 2.3, where the dotted line represents which geodesic we will integrate over. We will first attempt to rebuild interactions using these geodesic integrals, and at the end of this section we will contrast with the results in [85].

2.4.1 Sampling three point functions via geodesics diagrams

In this subsection we will go through some explicit computations of three point functions using the method developed in section 2.3.1. Our goal is not to check that our bulk results match with the CFT values (which they do); our goal is to

---

[7]The results in [92,93] as well suggested that (2.90) reproduces correlation functions of three scalar primaries.
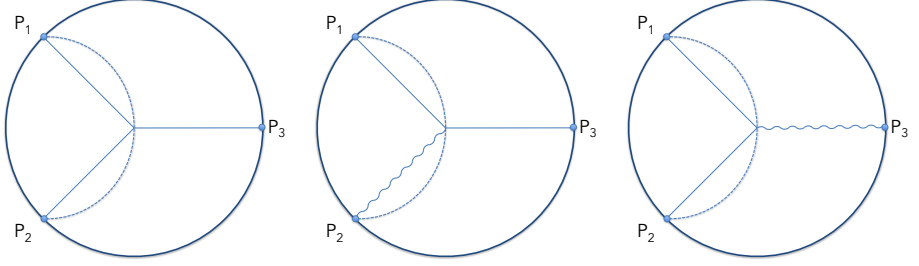
Figure 2.3: *Examples of geodesic Witten diagrams in AdS_{d+1} that capture three point functions. Straight lines correspond to scalar propagators, while wavy lines denote symmetric traceless spin-J fields; P_i is the boundary position in embedding formalism. The dotted line denotes the geodesic over which we integrate. Note that the second and third diagram only differ by the choice of geodesic.*

illustrate how these operators $\mathcal{D}_{ijk}(Y_\lambda)$, and hence $(V_{i,jk}, H_{ij})$, map up to local AdS interactions.

Our seed to all further computation is the three point function of three scalar primaries. In terms of geodesic integrals, we can write the scalar three-point function in the boundary as

$$T(\Delta_1, \Delta_2, \Delta_3) = c_{\Delta_1 \Delta_2 \Delta_3} \int_{\gamma_{12}} d\lambda \, G_{b\partial}^{\Delta_1|0}(Y_\lambda, P_1) G_{b\partial}^{\Delta_2|0}(Y_\lambda, P_2) G_{b\partial}^{\Delta_3|0}(Y_\lambda, P_3)$$

$$= \frac{1}{(P_{12})^{(\Delta_1+\Delta_2-\Delta_3)/2}(P_{23})^{(\Delta_2+\Delta_3-\Delta_1)/2}(P_{13})^{(\Delta_1+\Delta_3-\Delta_2)/2}} ,$$

$$(2.91)$$

where

$$c_{\Delta_1 \Delta_2 \Delta_3} = \frac{2\Gamma(\Delta_3)}{\Gamma\left(\frac{-\Delta_1+\Delta_2+\Delta_3}{2}\right)\Gamma\left(\frac{\Delta_1-\Delta_2+\Delta_3}{2}\right)} . \qquad (2.92)$$

Here we are ignoring the normalization of $G_{b\partial}$ in (6.2) and the gamma functions in $c_{\Delta_1 \Delta_2 \Delta_3}$ result from the integration over the geodesic γ_{12}. $G_{\Delta_1,\Delta_2,\Delta_3|0,0,0} = T(\Delta_1, \Delta_2, \Delta_3)$ is the CFT$_d$ three point function in (2.51) casted as a geodesic integral in AdS$_{d+1}$.

Example: Vector-scalar-scalar

To start, we consider the three point function of one vector and two scalar operators as built from scalar operators. Following the CFT discussion in Sec. 2.2.3, in this

case there is only one tensor structure which can be written in two ways:

$$
\begin{aligned}
G_{\Delta_1,\Delta_2,\Delta_3|1,0,0} &= V_{1,23}T(\Delta_1,\Delta_2,\Delta_3) \\
&= \frac{2D_{1\,12}}{-1-\Delta_1+\Delta_2+\Delta_3}T(\Delta_1+1,\Delta_2,\Delta_3) \\
&= \frac{2D_{2\,12}}{-1+\Delta_1-\Delta_2+\Delta_3}T(\Delta_1,\Delta_2+1,\Delta_3) \ .
\end{aligned} \tag{2.93}
$$

We would like to extract which local bulk interaction can capture the left hand side of (2.93). Let's choose the first equality for concreteness. Using (2.75), and (2.78) the bulk calculation is

$$
\begin{aligned}
&-2D_{1\,12}T(\Delta_1+1,\Delta_2,\Delta_3) \\
&= 2c_{\Delta_1+1\Delta_2\Delta_3}\int_{\gamma_{12}} d\lambda\, G_{b\partial}^{\Delta_1+1|0}(Y_\lambda,P_1)G_{b\partial}^{\Delta_2|0}(Y_\lambda,P_2)\mathcal{D}_{1,12}(Y_\lambda)G_{b\partial}^{\Delta_3|0}(Y_\lambda,P_3) \\
&= c_{\Delta_1+1\Delta_2\Delta_3}\int_{\gamma_{12}} d\lambda\, G_{b\partial}^{\Delta_1+1|0}(Y_\lambda,P_1)G_{b\partial}^{\Delta_2|0}(Y_\lambda,P_2)\Psi_{1\lambda}\mathcal{H}_{11}(Z_1,\partial_{Y_\lambda})G_{b\partial}^{\Delta_3|0}(Y_\lambda,P_3) \\
&= c_{\Delta_1+1\Delta_2\Delta_3}\int_{\gamma_{12}} d\lambda\, G_{b\partial}^{\Delta_1|1}(Y_\lambda,P_1;\partial_W,Z_1)G_{b\partial}^{\Delta_2|0}(Y_\lambda,P_2)(W\cdot\partial_{Y_\lambda})G_{b\partial}^{\Delta_3|0}(Y_\lambda,P_3) \ .
\end{aligned} \tag{2.94}
$$

The contraction appearing inside the integral can be attributed to the following local AdS interaction

$$
A_1^\mu \phi_2 \partial_\mu \phi_3 \ , \tag{2.95}
$$

where ϕ_i is a bulk scalar of mass $m_i^2 = \Delta_i(\Delta_i - d)$ and the massive vector $A_{1\mu}$ has $m_1^2 = \Delta_1(\Delta_1 - d) - 1$. It is interesting to note that from this computation alone we could not infer that there is another potential interaction: $A_1^\mu \phi_3 \partial_\mu \phi_2$. This particular interaction is absent because $A_1^\mu \partial_\mu \phi_2$ vanishes when evaluated over the geodesic γ_{12} due to (2.73). However, it would have been the natural interaction if we instead perform the integral over γ_{13} in (2.94). Hence a natural identification of the tensor structure in (2.93) with gravitational interactions is

$$
V_{1,23}: \quad A_1^\mu \phi_2 \partial_\mu \phi_3 \qquad \text{and} \qquad A_1^\mu \phi_3 \partial_\mu \phi_2 \ . \tag{2.96}
$$

If we used gauge invariance we could constraint this combination to insist that A_1 couples to a conserved current (for us, however, the vector A_1 is massive). From the perspective of the usual Witten diagrams, which involve bulk integrals, these two interactions are indistinguishable up to normalizations, since they can be related after integrating by parts. In a geodesic diagram one has to take both into account; in our opinion, it is natural to expect that all pairings of endpoints P_i have to reproduce the same tensor structure.
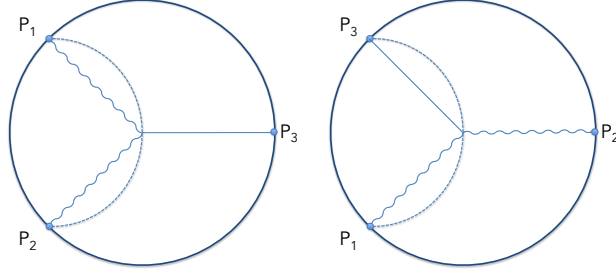
Figure 2.4: *The diagrams here differ by the choice of geodesic. Depending on this choice, a given interaction will give rise to a different tensor structure.*

Example: Vector-vector-scalar

Moving on to the next level of complexity, we now consider the geodesic integral that would reproduce the three point function of two spin-1 fields and one scalar field. There are two tensor structures involved in this correlator, and similar to the previous case, there are several combinations of derivatives that capture these structures. Choosing the combination in (2.54), we have in CFT notation that one tensor structure is

$$V_{1,23}V_{2,13}T(\Delta_1, \Delta_2, \Delta_3) =$$
$$- \frac{4D_{1\,12}D_{1\,21}T(\Delta_1 + 1, \Delta_2 + 1, \Delta_3)}{(\Delta_1 - \Delta_2)^2 - \Delta_3^2} + \frac{H_{12}T(\Delta_1, \Delta_2, \Delta_3)}{-\Delta_1 + \Delta_2 + \Delta_3} \, ,$$
$$(2.97)$$

whereas the other tensor structure is simply

$$H_{12}\, T(\Delta_1, \Delta_2, \Delta_3) \, . \tag{2.98}$$

$G_{\Delta_1, \Delta_2, \Delta_3|1,1,0}$ is the linear superposition of (2.97) and (2.98).

As it was already hinted by our previous example, the identification of the interaction will depend on the geodesic we choose to integrate over. To start, let us consider casting $T(\Delta_1, \Delta_2, \Delta_3)$ exactly as in (2.91): the geodesic is γ_{12} which connects at the positions with non-trivial spin (first diagram in Fig 2.4). For this choice of geodesic, the second tensor structure is straightforward to cast as a bulk interaction integrated over the geodesic. From the definitions (2.33) and (6.3), one can show that

$$H_{12} = \mathcal{H}_{1\lambda}(Z_1, \partial_W)\mathcal{H}_{2\lambda}(Z_2, W) \, , \tag{2.99}$$

where the right hand side is evaluated over the geodesic γ_{12}. Replacing this identity in (2.98), we find

$$H_{12}\, T(\Delta_1, \Delta_2, \Delta_3)$$
$$= c_{\Delta_1,\Delta_2,\Delta_3} \int_{\gamma_{12}} G_{b\partial}^{\Delta_1|1}(Y_\lambda, P_1; \partial_W, Z_1) G_{b\partial}^{\Delta_2|1}(Y_\lambda, P_2; W, Z_2) G_{b\partial}^{\Delta_3|0}(Y_\lambda, P_3) \ . \tag{2.100}$$

This contact term is simply in physical space the interaction

$$H_{12}: \qquad A_{1\mu} A_2^\mu \phi_3 \ . \tag{2.101}$$

This contraction will be generic every time our tensorial structure involves H_{12}. In general we will have the following relation

$$(H_{12})^n = (\mathcal{H}_{1\lambda}(Z_1, \partial_W) \mathcal{H}_{2\lambda}(Z_2, W))^n : \qquad \phi_{1\mu_1\dots\mu_n} \phi_2^{\mu_1\dots\mu_n} \phi_3 \ , \tag{2.102}$$

where $(H_{12})^n$ generates one of the tensor structure for a tensor-tensor-scalar three point function, and the natural bulk interaction is the contraction of symmetric traceless tensors coupled minimally with a scalar.

For the other tensor structure, a bit more work is required. Let's first manipulate the first term in (2.97); using (2.72) we can write

$$D_{1\,12} D_{1\,21} G_{b\partial}^{\Delta_3|0}(Y_\lambda, P_3) = \mathcal{D}_{1\,21}(Y_\lambda) \mathcal{D}_{1\,12}(Y_\lambda) G_{b\partial}^{\Delta_3|0}(Y_\lambda, P_3)$$
$$= \frac{1}{8} \Psi_{1\lambda} \Psi_{2\lambda} \mathcal{H}_{1\lambda}(Z_1, \partial_W) \mathcal{H}_{2\lambda}(Z_2, \partial_W)(W \cdot \partial_{Y_\lambda})^2 G_{b\partial}^{\Delta_3|0}(Y_\lambda, P_3)$$
$$+ \frac{1}{2} H_{12} \Psi_{2\lambda} P_1 \cdot \partial_{Y_\lambda} G_{b\partial}^{\Delta_3|0}(Y_\lambda, P_3) \ . \tag{2.103}$$

Applying this expression to (2.97) gives[8]

$$-\frac{4 D_{1\,12} D_{1\,21}}{(\Delta_1 - \Delta_2)^2 - \Delta_3^2} T(\Delta_1 + 1, \Delta_2 + 1, \Delta_3)$$
$$= -\frac{4 c_{\Delta_1+1,\Delta_2+1,\Delta_3}}{(\Delta_1 - \Delta_2)^2 - \Delta_3^2} \int_{\gamma_{12}} G_{b\partial}^{\Delta_1+1|0} G_{b\partial}^{\Delta_2+1|0} \mathcal{D}_{1,21} \mathcal{D}_{1,12} G_{b\partial}^{\Delta_3|0}$$
$$= -\frac{1}{2} \frac{c_{\Delta_1+1,\Delta_2+1,\Delta_3}}{(\Delta_1 - \Delta_2)^2 - \Delta_3^2} \int_{\gamma_{12}} G_{b\partial}^{\Delta_1|1}(\partial_W) G_{b\partial}^{\Delta_2|1}(\partial_W)(W \cdot \partial_{Y_\lambda})^2 G_{b\partial}^{\Delta_3|0}$$
$$- \frac{1}{-\Delta_1 + \Delta_2 + \Delta_3} H_{12} T(\Delta_1, \Delta_2, \Delta_3) \ . \tag{2.104}$$

---

[8]The fastest way to reproduce (2.104) from (2.103) is by using the explicit form of $G_{b\partial}^{\Delta_3|0}(Y_\lambda, P_3)$. An alternative route, which is more general, is to use (2.83): from here we can integrate by parts and rearrange the terms appropriately. This second route allows us to use (2.105) when at the third leg of the vertex we have bulk–to–bulk propagators rather than bulk–to–boundary.

Replacing (2.104) in (2.97) results in

$$V_{1,23}V_{2,13}T(\Delta_1, \Delta_2, \Delta_3)$$
$$= -\frac{c_{\Delta_1+1\Delta_2+1\Delta_3}}{2((\Delta_1-\Delta_2)^2 - \Delta_3^2)} \int_{\gamma_{12}} G_{b\partial}^{\Delta_1|1}(\partial_W) G_{b\partial}^{\Delta_2|1}(\partial_W)(W \cdot \partial_{Y_\lambda})^2 G_{b\partial}^{\Delta_3|0} \ . \quad (2.105)$$

From here we see that another natural relation arises between the OPE structures and interactions:

$$V_{1,23}V_{2,13}: \quad A_1^\mu A_2^\nu \partial_{(\mu} \partial_{\nu)} \phi_3 \quad \sim \quad A_1^\mu A_2^\nu \left(\nabla_{(\mu} \nabla_{\nu)} + \Delta_3 g_{\mu\nu} \right) \phi_3 \ . \quad (2.106)$$

where the sign $\sim$ here means that the relation is schematic: to rewrite interactions with partial derivatives as covariant derivatives, we are using homogeneity properties of fields in the embedding formalism in (2.105). In what follows we will keep most of our expressions in terms of partial derivatives.

Now let's consider building $G_{\Delta_1,\Delta_2,\Delta_3|1,1,0}$ starting from a geodesic diagram where we integrate over γ_{13} instead of γ_{12} (second diagram in Fig. 2.4). The diagram with γ_{12} already suggested as candidate interactions (2.101) and (2.106). If we integrate those interactions over γ_{13} we find[9]

$$\int_{\gamma_{13}} A_1^\mu A_2^\nu \partial_{(\mu} \partial_{\nu)} \phi_3 = 0 \ , \quad (2.107)$$

and $A_1^\mu A_{2\mu} \phi_3$ gives a linear combination of $V_{1,23}V_{2,13}$ and H_{12}. The identifications we made in (2.101) and (2.106) are obviously sensitive to the geodesic we select (there is a non-trivial kernel), and this is somewhat unsatisfactory. We can partially overcome this pathology by considering a wider set of interactions. By inspection we find that the tensor structure $V_{1,23}V_{2,13}$ is simultaneously captured by γ_{13} and γ_{12} by the interactions

$$V_{1,23}V_{2,13}: \quad \alpha_1 A_1^\nu A_2^\mu \partial_\nu \partial_\mu \phi_3 - \beta_1 \Big((\Delta_1 + \Delta_2) \phi_3 \partial_\mu A_1^\nu \partial_\mu A_1^\nu$$
$$- (1 + \Delta_1 \Delta_2) \phi_3 \partial_\nu A_1^\mu \partial_\mu A_2^\nu \Big) \ . \quad (2.108)$$

The choice of geodesic affects the overall normalization, controlled by the choice of constants α_1 and β_1. The terms multiplying β_1 when projected over γ_{12}, are proportional to the tensor structure H_{12} and their coefficients are chosen such that they cancel each other. The interaction multiplying α_1 is identically zero when integrated over γ_{13}. To capture H_{12} along both γ_{13} and γ_{12} we just need

$$H_{12}: \quad \phi_3 F_{1\mu\nu} F_2^{\mu\nu} \ . \quad (2.109)$$

---

[9]We are being schematic and brief in (2.107): it is implicit that we are using bulk–to–boundary propagators.

Here it is important to note we are not using $A_1^\mu A_{2\mu}\phi_3$ as we did in (2.101), and we still find the correct result when using γ_{12}. This is because there are many ways we can cast H_{12} as bulk quantities along γ_{12}: the relation (2.99) is not unique. For instance, one can check that

$$
G_{b\partial}^{\Delta_1|1}(Y_\lambda, P_1; \partial_W, Z_1) G_{b\partial}^{\Delta_2|1}(Y_\lambda, P_2; W, Z_2)
$$
$$
= \frac{-1}{2(\Delta_1 + \Delta_2)}(\partial_W \cdot \partial_{Y'})(\partial_{W'} \cdot \partial_Y) G_{b\partial}^{\Delta_1|1}(Y', P_1; W', Z_1) G_{b\partial}^{\Delta_2|1}(Y, P_2; W, Z_2)\big|_{Y=Y'=Y_\lambda}
$$
$$
= \frac{-1}{2(1 + \Delta_1\Delta_2)}(\partial_Y \cdot \partial_{Y'}) G_{b\partial}^{\Delta_1|1}(Y', P_1; \partial_W, Z_1) G_{b\partial}^{\Delta_2|1}(Y, P_2; W, Z_2)\big|_{Y=Y'=Y_\lambda},
$$
$$
(2.110)
$$

$$
G_{b\partial}^{\Delta_1|1}(Y_\lambda, P_1; \partial_W, Z_1) G_{b\partial}^{\Delta_2|1}(Y_\lambda, P_2; W, Z_2)
$$
$$
= -\frac{(\partial_W \cdot \partial_{Y'})(\partial_{W'} \cdot \partial_Y)}{2(\Delta_1 + \Delta_2)} G_{b\partial}^{\Delta_1|1}(Y', P_1; W', Z_1) G_{b\partial}^{\Delta_2|1}(Y, P_2; W, Z_2)\big|_{Y=Y'=Y_\lambda}
$$
$$
= -\frac{(\partial_Y \cdot \partial_{Y'})}{2(1 + \Delta_1\Delta_2)} G_{b\partial}^{\Delta_1|1}(Y', P_1; \partial_W, Z_1) G_{b\partial}^{\Delta_2|1}(Y, P_2; W, Z_2)\big|_{Y=Y'=Y_\lambda}, \quad (2.111)
$$

This type of relations are due to the projections over the geodesic, and they generate quite a bit of ambiguity as one tries to re-cast a given geodesic diagram as arising from a cubic interaction. Establishing relations such as (2.108) and (2.109) are not fundamental, and their ambiguity is not merely due to integrating by parts or using equations of motion. In appendix 6.4 we provide some further examples on how to rewrite certain tensor structures as interactions, but we have not taken into account ambiguities such as those in (2.111). Generalizing (2.108) and (2.109) for higher spin fields is somewhat cumbersome (but not impossible). We comment in the discussion what are the computational obstructions we encounter to carry this out explicit.

2.4.2 Basis of cubic interactions via Witten diagrams

In the above we made use of our bulk differential operators to identify which interactions capture the suitable tensor structures in terms of geodesic diagrams. It is time now to compare with the results in [85], where the map between cubic interactions and tensor structures was done using bulk Witten diagrams. We briefly reviewed their method in Sec. 2.2.2, and here we collect the first few terms

of their map, which will be useful for our analysis [10]:

$$I_{1,0,0}^{0,0,0} = A_1^\mu (\partial_\mu \phi_2) \phi_3 \qquad \xrightarrow[\text{bulk}]{} \qquad V_{1,23}$$

$$I_{1,1,0}^{1,0,0} = A_1^\mu A_{2\mu} \phi_3 \qquad \xrightarrow[\text{bulk}]{} \qquad \left((\Delta_1 - \Delta_2)^2 - \Delta_3^2 \right) V_{1,23} V_{2,13}$$

$$- (-2\Delta_1 \Delta_2 + \Delta_1 + \Delta_2 - \Delta_3) H_{12}$$

$$I_{1,1,0}^{0,0,0} = A_1^\mu (\partial_\mu A_2^\nu) \partial_\nu \phi_3 \qquad \xrightarrow[\text{bulk}]{} \qquad (\Delta_1 + \Delta_2 - \Delta_3 - 2) V_{1,23} V_{2,13} + H_{12} \quad (2.112)$$

In appendix 6.3 we derive specific examples to illustrate the mapping. Using this same basis of interactions and integrating them along γ_{12} gives the following map

$$I_{1,0,0}^{0,0,0} = A_1^\mu (\partial_\mu \phi_2) \phi_3 \qquad \xrightarrow[\gamma_{12}]{} \qquad 0$$

$$I_{1,1,0}^{1,0,0} = A_1^\mu A_{2\mu} \phi_3 \qquad \xrightarrow[\gamma_{12}]{} \qquad H_{12}$$

$$I_{1,1,0}^{0,0,0} = A_1^\mu (\partial_\mu A_2^\nu) \partial_\nu \phi_3 \qquad \xrightarrow[\gamma_{12}]{} \qquad H_{12} \qquad (2.113)$$

Clearly there is a tension between the tensor structures we assign to an interaction if we use a regular Witten diagram versus a geodesic diagram. The mismatch is due to the fact that certain derivatives contracted along γ_{ij} are null. This reflects upon that a geodesic diagram is sensitive to the arrangement of derivatives which, for good reasons, are discarded in (2.37).

Some agreements do occur. Let us reconsider the basis of interactions found by using geodesic interactions; from (2.109) we have (up to overall normalizations)

$$\phi_3 F_{1\mu\nu} F_2^{\mu\nu} \qquad \xrightarrow[\gamma_{ij}]{} \qquad H_{12} \qquad (2.114)$$

If we use these interactions on Witten diagrams, we obtain exactly the same map

$$\phi_3 F_{1\mu\nu} F_2^{\mu\nu} \qquad \xrightarrow[\text{bulk}]{} \qquad H_{12} \ . \qquad (2.115)$$

The details of the computations leading to (2.115) are shown in appendix 6.3. Moreover, we find that the interaction (2.108), which is $V_{1,23} V_{2,13}$ for the geodesic Witten diagram, gives the same tensor structure if we integrate over the bulk, as shown in (6.35). These relations indicate that it is possible to a have a compatible map among interactions in geodesic diagrams and Witten diagrams, even though there is disagreement at intermediate steps. However, from a bulk perspective the interaction selected in (2.115) is not in any special footing relative to those in (2.37).

---

[10]Here the notation $\xrightarrow[\text{bulk}]{}$ means that the identification between the interaction and tensor structure is done via a bulk integral, i.e. a three-point Witten diagram. Similarly, $\xrightarrow[\gamma_{ij}]{}$ denotes an analogous integral over a geodesic.

2.5 Conformal block decomposition of Witten diagrams

For a fixed cubic interaction, there is generically a mismatch among tensor structures captured by Witten diagrams versus geodesic Witten diagrams. In this section we will analyse how this affects the decomposition of four-point Witten diagrams in terms of geodesic diagrams.

Our discussion is based in the four-point exchange Witten diagram for four scalars fields, which just involves scalar fields with external legs with dimensions Δ_i, and exchanged dimension Δ. The corresponding Witten diagram is depicted in Fig. 2.5, and its integral representation is:

$$
\mathcal{A}_{0,0,0,0}^{\text{Exch}}(P_i)
$$
$$
= \int dY \int dY' G_{b\partial}^{\Delta_1|0}(Y,P_1) G_{b\partial}^{\Delta_2|0}(Y,P_2) G_{bb}^{\Delta|0}(Y,Y') G_{b\partial}^{\Delta_3|0}(Y',P_3) G_{b\partial}^{\Delta_4|0}(Y',P_4) .
$$
$$(2.116)$$

Here "dY" represents volume integrals in AdS_{d+1}. The previous diagram has been decomposed into geodesic diagrams in [62]. Here, we review this procedure. To write the volume integral (2.116) as geodesic integrals, the crucial observation the authors make is that

$$
G_{b\partial}^{\Delta_1|0}(Y,P_1) G_{b\partial}^{\Delta_2|0}(Y,P_2) = \sum_{n=0}^{\infty} a_n^{\Delta_1,\Delta_2} \varphi_n(\Delta_1,\Delta_2;Y) , \qquad (2.117)
$$

where

$$
\varphi_n(\Delta_1,\Delta_2;Y) \equiv \int_{\gamma_{12}} G_{b\partial}^{\Delta_1|0}(Y_\lambda,P_1) G_{b\partial}^{\Delta_2|0}(Y_\lambda,P_2) G_{bb}^{\Delta_n|0}(Y_\lambda,Y) . \qquad (2.118)
$$

The field $\varphi_n(Y)$ is a normalizable solution of the Klein-Gordon equation with a source concentrated at γ_{12} and mass $m_n^2 = \Delta_n(\Delta_n - d)$, and $(x)_n$ stands for the Pochhammer symbol. The equality in (2.117) holds provided one sets

$$
a_n^{\Delta_1,\Delta_2} = \frac{(-1)^n}{n!} \frac{(\Delta_1)_n(\Delta_2)_n}{\beta_n(\Delta_1 + \Delta_2 + n - d/2)_n} , \quad \Delta_n = \Delta_1 + \Delta_2 + 2n . \qquad (2.119)
$$

The constant β_n soaks the choice of normalizations used in (2.118). Replacing

(2.118) twice in (2.116) gives

$$
\mathcal{A}_{0,0,0,0}^{\text{Exch}}(P_i) = \sum_{m,k} a_n^{\Delta_1,\Delta_2} a_k^{\Delta_3,\Delta_4} \int_{\gamma_{12}} \int_{\gamma_{34}} G_{b\partial}^{\Delta_1|0}(Y_\lambda, P_1) G_{b\partial}^{\Delta_2|0}(Y_\lambda, P_2) G_{b\partial}^{\Delta_3|0}(Y'_{\lambda'}, P_3)
$$

$$
\times G_{b\partial}^{\Delta_4|0}(Y'_{\lambda'}, P_4) \int dY \int dY' G_{bb}^{\Delta_n|0}(Y_\lambda, Y) G_{bb}^{\Delta|0}(Y, Y') G_{bb}^{\Delta_k|0}(Y', Y'_{\lambda'}) .
$$

$$
(2.120)
$$

where $\Delta_k = \Delta_3 + \Delta_4 + 2k$. The integrals in the last line can be simplified by using

$$
G_{bb}^{\Delta|0}(Y, Y') = \langle Y| \frac{1}{\nabla^2 - m^2}|Y'\rangle , \qquad \int dY|Y\rangle\langle Y| = 1 , \qquad (2.121)
$$

which leads to

$$
\int dY \int dY' G_{bb}^{\Delta_n|0}(Y_\lambda, Y) G_{bb}^{\Delta|0}(Y, Y') G_{bb}^{\Delta_k|0}(Y', Y'_{\lambda'}) =
$$

$$
\frac{G_{bb}^{\Delta|0}(Y_\lambda, Y'_{\lambda'})}{(m_\Delta^2 - m_k^2)(m_\Delta^2 - m_n^2)} + \frac{G_{bb}^{\Delta_n|0}(Y_\lambda, Y'_{\lambda'})}{(m_n^2 - m_\Delta^2)(m_n^2 - m_k^2)} + \frac{G_{bb}^{\Delta_k|0}(Y_\lambda, Y'_{\lambda'})}{(m_k^2 - m_\Delta^2)(m_k^2 - m_n^2)} .
$$

$$
(2.122)
$$

And hence the four-point exchange diagram for scalars is Moreover, the scalar Witten diagram can terms or geodesic Witten diagrams $\mathcal{W}_{\Delta|0}$:

$$
\mathcal{A}_{0,0,0,0}^{\text{Exch}}(x_i) = C_\Delta \mathcal{W}_{\Delta|0}(x_i) + \sum_n C_{\Delta_n} \mathcal{W}_{\Delta_n|0}(x_i) + \sum_k C_{\Delta_k} \mathcal{W}_{\Delta_k|0}(x_i) , \quad (2.123)
$$

where we organized the expression in terms of the geodesic integral that defines $\mathcal{W}_{\Delta|0}$ in (2.58); the coefficients C_Δ basically follow from the contributions in (2.120) and (2.122). The formula (2.123) shows the decomposition of the scalar Witten diagram with scalar exchange in terms of conformal blocks, since $\mathcal{W}_{\Delta|0}(x_1, x_2, x_3, x_4) = W_{\Delta|0}(x_1, x_2, x_3, x_4)$. It is important to realise that Δ_n and Δ_k are the dimensions of scalar double trace operators of the type (1.43) with $l = 0$. This was expected from the conformal block decomposition at order $1/N^2$, as explained in sec.

2.5.1 Four-point scalar exchange with one spin-1 field

Now let's see how this decomposition will work when the external legs have spin. And the first non-trivial example is to just add a spin-1 field in one external leg
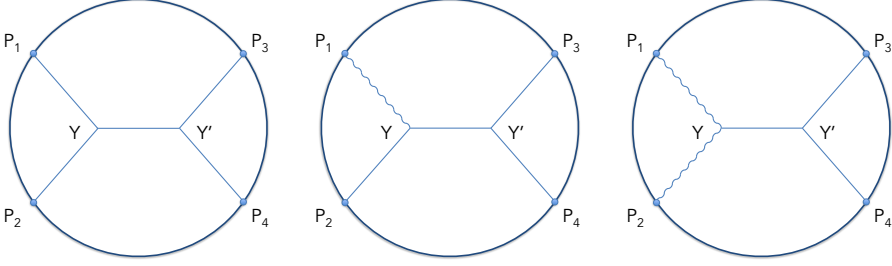
Figure 2.5: *Four-point exchange Witten diagrams in AdS_{d+1}, where the exchanged field is a scalar field of dimension Δ. The first diagram corresponds to $\mathcal{A}^{\mathrm{Exch}}_{0,0,0,0}$ in (2.116), the second diagram to $\mathcal{A}^{\mathrm{Exch}}_{1,0,0,0}$ in (2.124), and the third diagram to $\mathcal{A}^{\mathrm{Exch}}_{1,1,0,0}$ in (2.129).*

and all other fields involved are scalar. The diagram is depicted in Fig. 2.5, and the integral expression is

$$\mathcal{A}^{\mathrm{Exch}}_{1,0,0,0} = \int dY \int dY' G^{\Delta_1|1}_{b\partial}(Y, P_1, Z_1, \partial_W) \left(W \cdot \partial_Y G^{\Delta_2|0}_{b\partial}(Y, P_2) \right) G^{\Delta|0}_{bb}(Y, Y')$$
$$\times\, G^{\Delta_3|0}_{b\partial}(Y', P_3) G^{\Delta_4|0}_{b\partial}(Y', P_4) \,, \quad (2.124)$$

where we used one of the vertex interactions in (2.37). Using (6.4) and (6.6) we can rewrite this diagram in terms of the four-point scalar exchange (2.116) as

$$\mathcal{A}^{\mathrm{Exch}}_{1,0,0,0}(\Delta_1, \Delta_2, \Delta_3, \Delta_4) = \frac{2\Delta_2}{\Delta_1}\, D_{2\,12} \mathcal{A}^{\mathrm{Exch}}_{0,0,0,0}(\Delta_1, \Delta_2+1, \Delta_3, \Delta_4) \,, \qquad (2.125)$$

and $D_{2\,12}$ is defined in (2.47). And from here the path is clear: using the geodesic decomposition and trading D_{212} by $-\mathcal{D}_{2\,12}(Y_\lambda)$ we obtain

$$\mathcal{A}^{\mathrm{Exch}}_{1,0,0,0} = \tilde{C}_\Delta \mathcal{W}^{1,0,0,0}_{\Delta|0} + \sum_n \tilde{C}_{\Delta_n} \mathcal{W}^{1,0,0,0}_{\Delta_n|0} + \sum_k \tilde{C}_{\Delta_k} \mathcal{W}^{1,0,0,0}_{\Delta_k|0} \,, \qquad (2.126)$$

with suitable constants $\tilde{C}$ and

$$\mathcal{W}^{1,0,0,0}_{\Delta|0}(\Delta_1, \Delta_2, \Delta_3, \Delta_4) = D_{2\,12} \mathcal{W}_{\Delta|0}(\Delta_1, \Delta_2+1, \Delta_3, \Delta_4)$$
$$= -\frac{1}{2} \int_{\gamma_{12}} \int_{\gamma_{34}} G^{\Delta_1|1}_{b\partial}(Y_\lambda, P_1, Z_1, \partial_W) G^{\Delta_2|0}_{b\partial}(Y_\lambda, P_2)$$
$$\times\, W \cdot \partial_{Y_\lambda} G^{\Delta|0}_{bb}(Y_\lambda, Y'_{\lambda'}) G^{\Delta_3|0}_{b\partial}(Y'_{\lambda'}, P_3) G^{\Delta_4|0}_{b\partial}(Y'_{\lambda'}, P_4) \quad,$$
$$(2.127)$$

where we used (2.94). It is interesting to note how the interaction gets slightly modified due to the cancellations that occur in the geodesic integrals: in (2.124)

the derivative is acting on $G_{b\partial}^{\Delta_2|0}$, but the geodesic decomposition moves it to position of the exchanged field.

In this example it is also worth discussing the generalization of (2.117). Our decomposition of the bulk–to–boundary operators on position 1 and 2 reads

$$
\begin{aligned}
& G_{b\partial}^{\Delta_1|1}(Y, P_1, Z_1, \partial_W) W \cdot \partial_Y G_{b\partial}^{\Delta_2|0}(Y, P_2) \\
&= \frac{2\Delta_2}{\Delta_1} D_{2\,12} \left(G_{b\partial}^{\Delta_1|0}(Y, P_1) G_{b\partial}^{\Delta_2+1|0}(Y, P_2) \right) \\
&= \frac{2\Delta_2}{\Delta_1} \sum_{n=0}^{\infty} a_n^{\Delta_1, \Delta_2+1} \mathcal{D}_{2\,12}(Y) \varphi_n(\Delta_1, \Delta_2 + 1; Y) \\
&= -\frac{\Delta_2}{\Delta_1} \sum_{n=0}^{\infty} a_n^{\Delta_1, \Delta_2+1} \int_{\gamma_{12}} G_{b\partial}^{\Delta_1|1}(Y_\lambda, P_1, Z_1, \partial_W) G_{b\partial}^{\Delta_2|0}(Y_\lambda, P_2) \, W \cdot \partial_{Y_\lambda} G_{bb}^{\Delta_n|0}(Y_\lambda, Y) \ .
\end{aligned}
$$

$$(2.128)$$

It is interesting to note the different interpretations one could give to the product $A_1^\mu \partial_\mu \phi_2$ (first line) in terms of resulting bulk fields. Very crudely, from the third line one would like to say that we just have a suitable differential operator acting on the field, while from the fourth line we would say that the product induces an interaction integrated along the geodesic. This type of decompositions of bulk fields would be interesting in the context of developing further a relation between an OPE expansion in the CFT to local bulk fields as done in [92–94].

2.5.2 Four-point scalar exchange with two spin-1 fields

It is instructive as well to discuss an example with two spin-1 fields as shown in the third diagram of Fig. 2.5. For sake of simplicity we will use the cubic interaction $A_{1\mu} A_2^\mu \phi$, which is part of the basis in (2.37). The four-point exchange is

$$
\begin{aligned}
\mathcal{A}_{1,1,0,0}^{\text{Exch}} = \int dY \int dY' G_{b\partial}^{\Delta_1|1}(Y, P_1, Z_1, \partial_W) G_{b\partial}^{\Delta_2|1}(Y, P_2, Z_2, W) G_{bb}^{\Delta|0}(Y, Y') \\
\times G_{b\partial}^{\Delta_3|0}(Y', P_3) G_{b\partial}^{\Delta_4|0}(Y', P_4) \ . \quad (2.129)
\end{aligned}
$$

The new pieces are due to the presence of the spin-1 fields so we will focus on how to manipulate the propagators at position 1 and 2; the rest follows as in previous examples. Using (6.4) allows us to remove the tensorial pieces in (2.129) and recast

it in terms of tensor structures. For this case in particular we have

$$
G_{b\partial}^{\Delta_1|1}(Y, P_1, Z_1, \partial_W) G_{b\partial}^{\Delta_2|1}(Y, P_2, Z_2, W)
$$
$$
= \frac{1}{\Delta_1 \Delta_2} \mathscr{D}_{P_1}(\partial_W, Z_1) \mathscr{D}_{P_2}(W, Z_2) G_{b\partial}^{\Delta_1|0}(Y, P_1) G_{b\partial}^{\Delta_2|0}(Y, P_2)
$$
$$
= \frac{1}{\Delta_1 \Delta_2} \mathscr{D}_{P_1}(\partial_W, Z_1) \mathscr{D}_{P_2}(W, Z_2) \sum_{n=0}^{\infty} a_n^{\Delta_1, \Delta_2} \varphi_n(\Delta_1, \Delta_2; Y) \ .
$$
$$(2.130)$$

From here we can relate the combination of $\mathscr{D}_P$'s acting on φ_n to tensorial structures:

$$
\mathscr{D}_{P_1}(\partial_W, Z_1) \mathscr{D}_{P_2}(W, Z_2) \varphi_n(\Delta_1, \Delta_2; Y) =
$$
$$
- 2 D_{1\,12} D_{1\,21} \int_{\gamma_{12}} G_{b\partial}^{\Delta_1+1|0}(Y_\lambda, P_1) G_{b\partial}^{\Delta_2+1|0}(Y_\lambda, P_2) G_{bb}^{\Delta_n|0}(Y_\lambda, Y)
$$
$$
- \Delta_1(1-\Delta_2) H_{12} \int_{\gamma_{12}} G_{b\partial}^{\Delta_1|0}(Y_\lambda, P_1) G_{b\partial}^{\Delta_2|0}(Y_\lambda, P_2) G_{bb}^{\Delta_n|0}(Y_\lambda, Y) \ . \quad (2.131)
$$

This equality can be checked explicitly from the definitions of each term involved. A faster route is to infer it from the map given in [95]: from (2.112) we know the suitable structures in the interaction (which we just rewrote in terms of differential operators in (2.131)), and φ_n behaves close enough to a three point function that the map is unchanged. From here we can trade $D_{i\,jk}$ for $\mathcal{D}_{i\,jk}$, and then further use (2.104) and (2.100) to write them as smeared interactions. Without taking into account any normalizations, what we find for the contraction of two gauge fields decomposed in terms of geodesic integrals is

$$
G_{b\partial}^{\Delta_1|1}(Y, P_1, Z_1, \partial_W) G_{b\partial}^{\Delta_2|1}(Y, P_2, Z_2, W) \sim
$$
$$
\sum_n \int_{\gamma_{12}} G_{b\partial}^{\Delta_1|1}(Y_\lambda; \partial_W) G_{b\partial}^{\Delta_2|1}(Y_\lambda; \partial_W)(W \cdot \partial_{Y_\lambda})^2 G_{bb}^{\Delta_m|0}(Y_\lambda, Y)
$$
$$
+ \sum_n \int_{\gamma_{12}} G_{b\partial}^{\Delta_1|1}(Y_\lambda; \partial_W) G_{b\partial}^{\Delta_2|1}(Y_\lambda; W) G_{bb}^{\Delta_n|0}(Y_\lambda, Y) \ , \quad (2.132)
$$

where we are suppressing as well most of the variables in the propagators. This example illustrates how more interactions are needed when we decompose a Witten diagram in terms of geodesic diagrams; or in other words, how the product expansion of the bulk fields requires different interactions than those used in the direct evaluation of a three point function. But more importantly, we should highlight that casting $G_{b\partial}^{\Delta_1|1}(Y, P_1, Z_1, \partial_W) G_{b\partial}^{\Delta_2|1}(Y, P_2, Z_2, W)$ as local interactions integrated along a geodesic is ambiguous. Consider as an example the last term in (2.132). We could have written it in multiply ways due to the degeneracies shown

in (2.111): the product of two gauge fields could be casted as integrals of the interaction of $\phi A_\mu A^\mu$ or $\phi F_{\mu\nu} F^{\mu\nu}$ or similar contractions. And these interactions are not related by equations of motion nor field redefinitions. As we discussed in section 2.4.2, the identifications of gravitational interactions in a geodesic diagram is not unique and seems rather ad hoc. It would be interesting to understand if there is a more fundamental principle underlying products such as those in (2.132).

2.5.3 Generalizations for scalar exchanges

In a nutshell, this is how we are decomposing a four-point scalar exchange Witten diagram in terms of geodesics diagrams:

1. Consider a cubic interaction $I_{J_1,J_2,0}^{n_1,n_2,n_3}$ of the form (2.96), where at position 1 and 2 we place bulk–to–boundary propagators and at position 3 we have a bulk–to–bulk propagator. From (6.4) and (6.6) we will be able to strip off the tensorial part of the interaction, i.e. schematically we will have

$$I_{J_1,J_2,0}^{n_1,n_2,n_3} = \mathscr{D} \cdots \mathscr{D}\, I_{0,0,0}^{0,0,0} \; . \tag{2.133}$$

Here "$\mathscr{D} \cdots \mathscr{D}$" symbolizes a chain of contractions of operators appearing in (6.4) and (6.6), and the precise contraction depends on the interaction. The important feature is that $\mathscr{D} \cdots \mathscr{D}$ involves only derivatives with respect to Z_i or P_i (and not Y) which allows us to take this portion outside of the volume integral in a Witten diagram. Here $I_{0,0,0}^{0,0,0}$ is a cubic interaction for three scalars with the appropriate propagators used, i.e.

$$I_{0,0,0}^{0,0,0} = G_{b\partial}^{\Delta_1|0}(Y,P_1) G_{b\partial}^{\Delta_2|0}(Y,P_2) G_{bb}^{\Delta|0}(Y,Y') \; . \tag{2.134}$$

2. The map among tensor structures and cubic interactions in [95] implies that we will always be able to write the combination of $\mathscr{D}$'s in terms of CFT operators:

$$\mathscr{D} \cdots \mathscr{D} I_{0,0,0}^{0,0,0} = D \cdots D\, I_{0,0,0}^{0,0,0} \; . \tag{2.135}$$

This tells us which are the tensor structures appearing in the Witten diagram.

3. Next we can rewrite $I_{0,0,0}^{0,0,0}$ as a sum over geodesic integrals via (2.117). This allows us to trade D for our geodesic operators $\mathcal{D}(Y)$ as given in (2.70):

$$\mathscr{D} \cdots \mathscr{D} I_{0,0,0}^{0,0,0} = D \cdots D\, I_{0,0,0}^{0,0,0} = \mathcal{D} \cdots \mathcal{D} I_{0,0,0}^{0,0,0} \; . \tag{2.136}$$

4. And if desired, we can as well write the action of $\mathcal{D}$ on $I_{0,0,0}^{0,0,0}$ as an interaction via the map in (6.43). This gives a more local description of the OPE of the bulk fields in $I_{J_1,J_2,0}^{n_1,n_2,n_3}$ in terms of smeared interactions along the geodesic.

A four-point exchange Witten diagram, where the exchange particle is a scalar field, is build out of two vertices of the form $I_{J_1,J_2,0}^{n_1,n_2,n_3}$. So, keeping the loose schematic equalities, we can establish the following chain of equalities

$$
\begin{aligned}
\mathcal{A}_{J_1,J_2,J_3,J_4}^{\text{exch}} &\sim \mathscr{D}_{\text{left}}\mathscr{D}_{\text{right}}\mathcal{A}_{0,0,0,0}^{\text{exch}} \\
&\sim D_{\text{left}}D_{\text{right}}\,\mathcal{A}_{0,0,0,0}^{\text{exch}} \\
&\sim \sum_n \mathcal{W}_{\Delta_n|0}[\mathcal{D}_{\text{left}}(Y_\lambda), \mathcal{D}_{\text{right}}(Y'_{\lambda'})]\ .
\end{aligned}
\tag{2.137}
$$

where $\mathscr{D}_{\text{left}}$ corresponds to product of differential operators that recast the vertex to the left in terms boundary operators acting on position (P_1, P_2), and the analogously for $\mathscr{D}_{\text{right}}$ acting on (P_3, P_4).

2.5.4 Four-point spin exchanges

In this last portion we will address examples where the exchanged field has spin, and illustrate how the four-point exchange diagram can be decomposed in terms of the geodesic integrals. First consider the following Witten diagram

$$
\begin{aligned}
\mathcal{A}_{0,0,0,0}^{\text{Exch|spin}} = \int dY \int dY' G_{b\partial}^{\Delta_1|0}(Y,P_1)\partial_W\cdot\left(\partial_Y G_{b\partial}^{\Delta_2|0}(Y,P_2)\right) G_{bb}^{\Delta|1}(Y,Y',W,\partial_{W'}) \\
\times W'\cdot\left(\partial_{Y'} G_{b\partial}^{\Delta_3|0}(Y',P_3)\right) G_{b\partial}^{\Delta_4|0}(Y',P_4)\ .
\end{aligned}
\tag{2.138}
$$

In this diagram we are using the interaction $\phi_1\partial_\mu\phi_2 A^\mu$ on both ends, and it is depicted in Fig. 2.6. The decomposition of (2.138) in terms of geodesic integrals was done in [62] and we will not repeat it here. Next, let's consider a diagram where the field at position P_2 is a massive vector, i.e.

$$
\begin{aligned}
\mathcal{A}_{0,1,0,0}^{\text{Exch|spin}} = \int dY \int dY' G_{b\partial}^{\Delta_1|0}(Y,P_1)G^{\Delta_2|1}(Y,P_2;\partial_W,Z_2)G_{bb}^{\Delta|1}(Y,Y',W,\partial_{W'}) \\
\times W'\cdot\partial_{Y'}\left[G_{b\partial}^{\Delta_3|0}(Y',P_3)\right] G_{b\partial}^{\Delta_4|0}(Y',P_4)\ .
\end{aligned}
\tag{2.139}
$$

This would be the second diagram in Fig. 2.6, and we decided to use the interaction $\phi_1 A_2^\mu A_\mu$ for the cubic interaction on the left of the diagram. We can relate (2.139) to (2.138) by noticing the that the bulk–to–boundary operators satisfy the

following series of identities

$$G_{b\partial}^{\Delta_1|0}(Y,P_1)G_{b\partial}^{\Delta_2|1}(Y,P_2;\partial_W,Z_2) = \frac{1}{\Delta_2}\mathscr{D}_{P_2}(\partial_W,Z_2)G_{b\partial}^{\Delta_1|0}(Y,P_1)G_{b\partial}^{\Delta_2|0}(Y,P_2)$$

$$= \frac{\Delta_2-1}{\Delta_2(\Delta_1-1)}D_{1\,21}\left[\frac{1}{P_{12}}G_{b\partial}^{\Delta_1-1|0}(Y,P_1)(\partial_W\cdot\partial_Y)G_{b\partial}^{\Delta_2|0}(Y,P_2)\right]$$

$$- \frac{1}{\Delta_2-1}D_{2\,21}\left[\frac{1}{P_{12}}G_{b\partial}^{\Delta_1|0}(Y,P_1)(\partial_W\cdot\partial_Y)G_{b\partial}^{\Delta_2-1|0}(Y,P_2)\right]$$

$$(2.140)$$

Here we used (6.4), and then using the explicit polynomial dependence of $G_{b\partial}^{\Delta|0}(Y,P)$ to obtain the equality in the last line. It is interesting to note that we can now write

$$\mathcal{A}_{0,1,0,0}^{\text{Exch|spin}} = \frac{\Delta_2-1}{\Delta_2(\Delta_1-1)}D_{1\,21}\left[\frac{1}{P_{12}}\mathcal{A}_{0,0,0,0}^{\text{Exch|spin}}(\Delta_1-1,\Delta_2,\Delta_3,\Delta_4)\right]$$

$$- \frac{1}{\Delta_2-1}D_{2\,21}\left[\frac{1}{P_{12}}\mathcal{A}_{0,0,0,0}^{\text{Exch|spin}}(\Delta_1,\Delta_2-1,\Delta_3,\Delta_4)\right] \qquad (2.141)$$

And from here we can proceed by using the explicit decomposition of $\mathcal{A}_{0,0,0,0}^{\text{Exch|spin}}$ in terms of geodesic diagrams in [62] and then trading D_{ijk} by $\mathcal{D}_{ijk}$ (just as we we did in the previous examples in this section).[11]

The manipulations shown here are very explicit for the interaction we have selected, but they are robust and not specific to the example. We expect that in general we will be able to carry out a decomposition such as the one in (2.140) and have generalizations of (2.141) without much difficulty. It would be interesting to generalize this discussion and give a more systematic algorithm to decompose Witten diagrams in terms of geodesic integrals when the exchanged field has non-trivial spin.

2.6 Discussion

Our main result in this Chapter is the presentation of systematic method to evaluate conformal partial waves as geodesic integrals in AdS. From the CFT perspec-

---

[11]Note that the factor of P_{12} can be reabsorbed into bulk–to–boundary propagators projected along geodesics, i.e

$$\frac{1}{P_{12}}G_{b\partial}^{\Delta_1|0}(Y_\lambda,P_1)G_{b\partial}^{\Delta_2|0}(Y_\lambda,P_2) = G_{b\partial}^{\Delta_1+1|0}(Y_\lambda,P_1)G_{b\partial}^{\Delta_2+1|0}(Y_\lambda,P_2)\ .$$

Hence, as we cast (2.141) as a sum over geodesic integrals, all terms will have a bulk interpretation.
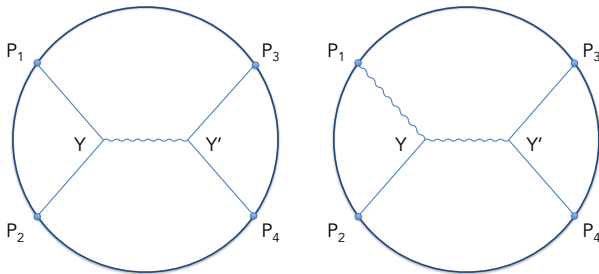
Figure 2.6: *Four-point exchange Witten diagrams in AdS_{d+1}, where the exchanged field is a symmetric tensor field of dimension Δ and spin J. In (2.138) and (2.139) we consider explicit examples where $J = 1$ for the external and exchanged field.*

tive, a spinning conformal partial wave is built from differential operators acting on the scalar conformal partial wave [72]; here we presented the analog of these differential operators in AdS and showed that they reproduce the same effect as in the CFT. More succinctly, we established

$$W^{l_1,l_2,l_3,l_4}_{\Delta|l}(P_i; Z_i) = D_{\text{left}} D_{\text{right}} W_{\Delta|l}(P_1, P_2, P_3, P_4) = \mathcal{W}_{\Delta|l}[\mathcal{D}_{\text{left}}(Y_\lambda), \mathcal{D}_{\text{right}}(Y'_{\lambda'})]\,, \tag{2.142}$$

where the last equality is a purely AdS object build out of geodesic integrals, while the left hand side are CFT quantities. Our construction of $\mathcal{D}$ and its equivalence to the CFT analog is given in section 2.3. We emphasise that this equivalence holds for any symmetric traceless field of spin J_i and conformal dimension Δ_i. We did not assume conservation of the fields, and the method works when all fields are of different species.

The immediate use of an object like $\mathcal{W}_{\Delta|l}$ is to evaluate correlation functions in holography. But relating the geodesic diagrams to regular Witten diagrams is a non-trivial task: interactions projected on geodesic integrals behave starkly different to interactions in volume integrals as we have seen explicitly throughout section 2.4. This mismatch between the two objects makes more delicate the decomposition of a Witten diagram in terms of geodesics. We carry out explicit examples in section 2.5, and discuss the general relation when the exchanged field is a scalar. The strategy we adopt for this decomposition is inspired by the identities used in [85]: one rewrites all tensorials properties of the interactions among bulk–to–boundary fields in terms of boundary operators acting on a scalar seed. This allows us to identify the CFT operators D_{ijk}, and use then our bulk operators $\mathcal{D}_{ijk}$ to write a final answer in terms of a sum of geodesic integrals. As a result, the set of cubic interactions needed to decompose a Witten diagram in terms of

geodesic diagrams is larger than the basis in (2.37). Each individual geodesic integral is, however, much easier to evaluate.

We have not discussed contact Witten diagrams here, but actually they can be treated very similarly as we did in section 2.5. The scalar case was done in [62], so the task is to manipulate the vertex along the lines of the discussion in section 2.5.3: the analog of (2.133) for a quartic interaction would allow us to identify the suitable tensor structures. Note that in a quartic interaction all propagators involved are bulk–to–boundary and hence we can strip off its tensorial features. We have not done this computation explicitly for quartic interactions, but a priori we do not expect major obstructions.

In section 2.3.2, we gave a prescription on how to evaluate conformal partial waves via geodesic diagrams when the exchanged field has non-trivial spin. And the general strategy we have adopted in this work allowed us to relate the geodesic diagrams to Witten diagrams, as we discussed in section 2.5.4. From this method it is not straightforward to infer the gravitational interaction, as we did in section 2.4, with the main obstacle being the contractions of $dY^\mu/d\lambda$ appearing in the integrand. It might be interesting to improve our prescription, to make this connection more evident. One reason it might be interesting to have this connection is to discuss conformal partial waves for anti-symmetric fields, and the differential operators that generate them. This is a case where the gravitational techniques can elucidate an organizational principle for those class of partial waves in the CFT. Until now the literature on conformal partial waves for non-symmetric structures is limited to [89, 96–102], and finding a basis of differential operators that generates them would be very interesting.

Another future direction that would be interesting to pursue is the addition of loops on the gravitational side. Very little is known about how to evaluate Witten diagrams beyond tree level, with the exception of the recent work in [103, 104]. It would be interesting to see how the geodesic diagram decomposition of a Witten diagram is affected by the presence of loops: since the geodesic diagrams are conformal partial waves, we would expect that loops only modify the OPE coefficients in the decomposition and the relation between masses in AdS and conformal dimensions in the CFT. Answering this question requires understanding also how loops alter the geodesic diagram itself and its CFT interpretation. Since conformal partial waves are dictated purely by symmetries, we expect that its holographic dual is robust against loop corrections, and its relation to loop diagrams in AdS can be made clear and straightforward. We leave this line of questions for future work.

3 GRAVITATIONAL WILSON LINES IN ADS$_3$/CFT$_2$

OR HOW TO CONSTRUCT BULK LOCAL STATES IN ADS$_3$ GRAVITY FROM CFT$_2$ ISHIBASHI STATES

This chapter is based on [2], and it focuses on gravitational Wilson lines in AdS$_3$. These objects are known to properly probe bulk physics, by coupling matter to 3-dimensional gravity in Chern-Simons formalism [105–107]. This idea was placed in the context of holography in [61, 108], where the Wilson lines are used to compute probe scalar two-point functions at the boundary of locally AdS$_3$ geometries. Their analysis was performed in the semi-classical approximation of the probe field. Here we evaluate the Wilson line beyond this limit. We provide a refined interpretation of the gravitational Wilson line in AdS$_3$ in terms of Ishibashi states in the dual CFT$_2$. This gives us a novel way to explore and reconstruct the local bulk dynamics: we can reinterpret the Wilson line as an overlap of two local bulk states. We use this to find local bulk fields dual CFT operators, even in black hole space-times.

3.1 Introduction

In this chapter we focus in 3d gravity with negative cosmological constant. As explained in Sec. 1.4, this is a topological theory with no local degrees of freedom. This fact can be made manifest by rewriting 3d gravity as a Chern-Simons theory with gauge group $SO(2,2) = SL(2,\mathbb{R}) \times SL(2,\mathbb{R})$ [35,36]. The Chern-Simons formulation has many advantages: BTZ black holes appear very naturally as topo-

logical defects around which the $sl(2, \mathbb{R})$ gauge fields have non-trivial holonomies. Diffeomorphisms may be easily understood on-shell as gauge transformations [36]. Finally, the Chern-Simons formulation is also very convenient for the extension to theories of higher spin gravity [38, 46, 48, 109, 110].

While the Chern-Simons formulation makes manifest the topological character of 3d gravity, it does so at a cost, by greatly obscuring geometric aspects. Simple geometric concepts such as proper distances or volumes are not at all transparent in the Chern-Simons formulation. The problem becomes even more acute if we consider coupling matter – e.g. a simple scalar field – to 3d gravity: this is very difficult to do in the Chern-Simons formulation, presumably because the theory is no longer purely topological. These facts make it very difficult to probe local bulk physics in the Chern-Simons formulation. This appears to be related to the fact that typical bulk observables such as (e.g.) the bulk-to-bulk propagator of a probe scalar field are not actually invariant under diffeomorphisms, and thus are difficult to formulate in a suitably gauge-invariant manner in Chern-Simons theory.

Nevertheless, in AdS$_3$ the presence of a boundary allows the formulation of suitably diffeomorphism invariant observables – the correlation functions of the dual CFT$_2$ – and thus one would expect that it would be possible to compute such objects in the Chern-Simons formulation. Some progress in this direction was made in [4, 61, 108, 111, 112], motivated largely by the computation of entanglement entropy of field theories dual to 3d bulk higher spin gravity. In this work we will develop further the approach initiated by [108], where it was argued that a Wilson line in an infinite-dimensional highest-weight representation $\mathcal{R}$ under the bulk $SL(2, \mathbb{R}) \times SL(2, \mathbb{R})$ gauge group could be used to compute boundary theory correlators, i.e.:

$$W_{\mathcal{R}}(y_i, y_f) \underset{r \to \infty}{=} \langle \Psi | \mathcal{O}(x_i) \mathcal{O}(x_f) | \Psi \rangle \ , \tag{3.1}$$

where we have picked coordinates $y^\mu = (r, x^i)$ with r an AdS holographic coordinate and x^i a CFT coordinate. Here the Wilson line $W_{\mathcal{R}}$ ends on the boundary at $r \to \infty$, and Ψ denotes the CFT$_2$ state dual to a particular configuration of Chern-Simons gauge fields that constitute the gravitational background in the interior.

The representation space $\mathcal{R}$ was generated from the Hilbert space of an auxiliary $SL(2, \mathbb{R})$-valued quantum mechanical degree of freedom $U(s)$ that lives on the Wilson line. The quadratic Casimirs of the representation $\mathcal{R}$ mapped in the usual manner to the conformal dimensions $(h, \bar{h})$ of the dual CFT operator. While this represented progress towards extracting geometric observables from the Chern-Simons formulation of 3d gravity, several issues remained obscure:

1. The relation (4.3) was understood to hold only if a particular boundary condition was used for the auxiliary field U, demanding that it approached the identity element of $SL(2,\mathbb{R})$ at the two endpoints of the Wilson line. While this is perhaps a somewhat natural choice, its precise interpretation in the CFT was not made clear.

2. All previous treatment of the $U(s)$ path integral was performed in a semi-classical limit, i.e. one in which $h \gg 1$. At a calculational level this allowed the path integral to be evaluated using its saddle-point; nevertheless this restriction seems somewhat artificial from the point of view of the dual CFT. Is it possible to go away from this limit?

3. How can one obtain other bulk observables from the Chern-Simons formulation, e.g. bulk-to-bulk propagators or one-loop determinants for scalar fields on the gravitational background?

In this work we answer these questions by providing a careful and fully quantum mechanical treatment of the Wilson line described above. In particular, we will show that the $U(s)$ worldline degree of freedom originally introduced in [108] can be understood as a particular $SL(2,\mathbb{R})$ rotation of the global part of an Ishibashi state (familiar from boundary CFT). We use this technology to develop a purely algebraic method for computing open-ended Wilson lines, and demonstrate equivalence (in the semi-classical limit) with the path-integral techniques used in [108].

The outline of this chapter is as follows. In Sec. 3.2 we review the path integral representation of $W_{\mathcal{R}}(y_i, y_f)$ proposed in [108], which will serve as a comparison to our quantum mechanical analysis. In Sec. 3.3 we turn to a detailed analysis of the quantum mechanics responsible of the geometrical features in $W_{\mathcal{R}}(y_i, y_f)$. This motivates the introduction of coherent states which we denote as *rotated Ishibashi states*. Using these states, we relate $W_{\mathcal{R}}(y_i, y_f)$ to their inner product; we rederive the path integral formulation by discretizing this inner product; and we show that $W_{\mathcal{R}}(y_i, y_f)$ is a Green's function on the group manifold $SO(2,2)$. In Sec. 3.4 we tie the quantum mechanical aspects of $W_{\mathcal{R}}(y_i, y_f)$ to its geometrical features. We show that $W_{\mathcal{R}}(y_i, y_f)$ is a Green's function on spacetime created by the Chern-Simons connections (which is a distinct statement from the properties on the group manifold). For global AdS$_3$ and the BTZ black hole, we show how to build local bulk fields by a suitable decomposition of $W_{\mathcal{R}}(y_i, y_f)$. This provides a new local probe of AdS$_3$ in the Chern-Simons formulation of 3d gravity. In Sec. 3.5 we discuss the CFT interpretation of our results. And in Sec. 3.6 we discuss future directions and related results in AdS/CFT that make use of Ishibashi states.

3.2   Path integral representation

In this section we will consider the path integral representation of a Wilson line operator in the Chern-Simons theory. As we review below, this object should be thought of as the Chern-Simons description of the worldline of a massive particle moving in the bulk. This section is a brief summary of the results in [108].

As reviewed in Sec. 1.4.2, the gauge group of the Chern-Simons theory is $SO(2,2) \simeq SL(2,\mathbb{R}) \times SL(2,\mathbb{R})$, and the bulk $sl(2,\mathbb{R})$ gauge connections are A, $\bar{A}$. The natural observables in Chern-Simons theory are Wilson loops in a certain representation $\mathcal{R}$ of the bulk gauge group; in this work we will always take $\mathcal{R}$ to be a product of two infinite-dimensional highest-weight representations in $sl(2,\mathbb{R}) \oplus sl(2,\mathbb{R})$.

We may now consider the following Wilson loop operator:

$$W_{\mathcal{R}}(C) = \mathrm{Tr}_{\mathcal{R}} \left(\mathcal{P} \exp \left(- \oint_C A \right) \mathcal{P} \exp \left(- \oint_C \bar{A} \right) \right) , \qquad (3.2)$$

and C is a closed loop in the bulk of AdS$_3$. This observable is fully gauge-invariant, and will typically be an interesting observable if the bulk loop wraps some non-trivial object in the bulk (e.g. the horizon of a BTZ black hole). Note that the trace involves a sum over the infinitely many states of the highest-weight representation.

We may also consider an open-ended Wilson *line* operator. To define this object we specify the locations of its endpoints (y_i, y_f). We must also specify boundary data in the form of two specific states $|U_i\rangle, |U_f\rangle \in \mathcal{R}$ at these endpoints. We may then define the following operator:

$$W_{\mathcal{R}}(y_i, y_f) = \langle U_f | \mathcal{P} \exp \left(- \int_\gamma A \right) \mathcal{P} \exp \left(- \int_\gamma \bar{A} \right) | U_i \rangle , \qquad (3.3)$$

where now $\gamma(s)$ is a curve with bulk endpoints (y_i, y_f) parametrized by s. $W_{\mathcal{R}}(y_i, y_f)$ is no longer fully gauge-invariant; clearly it depends in a gauge-covariant manner on the choice of boundary data $|U_i\rangle$, $|U_f\rangle$. Nevertheless, for flat connections, $W_{\mathcal{R}}(y_i, y_f)$ only depends on the topology of γ, but not on the shape of the curve.

From a geometric point of view, the Wilson line described above describes the physics of a massive point particle propagating from y_i to y_f on AdS$_3$. A point particle in the classical limit is characterized by at least one continuous parameter: the mass m. This data is stored in the choice of highest-weight representation $\mathcal{R}$ that defines the Wilson line. Further details of this representation are given in

full detail in Sec. 3.3. For now we require only that the representation is specified by two constants $(h, \bar{h})$ which determine the Casimirs of the $sl(2)$ algebra. Their identification with the mass m and orbital spin $\hat{s}$ of the particle is given by

$$m^2 = c_2 + \bar{c}_2 \ , \quad \hat{s} = \bar{h} - h \ , \tag{3.4}$$

where $c_2 = 2h(h-1)$ and $\bar{c}_2 = 2\bar{h}(\bar{h}-1)$ are the quadratic Casimirs; note that the AdS radius is set to unity.

From the point of view of AdS/CFT, the developments in $[4, 61, 108, 111, 112]$ show that if the endpoints y_i, y_f are taken to the boundary, the Wilson line operator defined in (3.3) is a bulk observable that computes correlation functions of light operators $\langle \Psi | \mathcal{O}(x_i) \mathcal{O}(x_f) | \Psi \rangle$ in the dual CFT. Here $|\Psi\rangle$ is a "heavy" state whose gravitational dual is given by the bulk connections $(A, \bar{A})$ and $\mathcal{O}(x)$ is a "light" operator whose scaling dimensions $(h, \bar{h})$ are encoded in the choice of representation $\mathcal{R}$. Here "light" denotes an operator that, as the central charge c goes to infinity, its conformal weight is fixed, while a "heavy" operator has a scaling dimension that is linear with c.

In what follows we limit the discussion to $h = \bar{h}$; see $[113, 114]$ for a discussion when $\hat{s} \neq 0$.

3.2.1 Path integral representation of the Wilson line

This particular Wilson line is somewhat more complex than those normally studied in compact gauge theories, simply due to the fact that $\mathcal{R}$ has infinitely many states in it. We now review the work of $[108]$, who constructed $\mathcal{R}$ as the Hilbert space of an auxiliary quantum mechanical system that lives on the Wilson line, replacing the trace over $\mathcal{R}$ by a path integral over a worldline field U. We pick the dynamics of U so that upon quantization the Hilbert space of the system is the desired representation $\mathcal{R}$. More concretely, we rewrite (3.2) as

$$W_{\mathcal{R}}(y_i, y_f) = \int \mathcal{D}U \, e^{-S(U, A, \bar{A})_\gamma} \ , \tag{3.5}$$

where the the auxiliary system can be described by the following action:

$$S(U, A, \bar{A})_\gamma \quad = \quad \sqrt{c_2} \int_\gamma ds \sqrt{\text{Tr}\left(U^{-1} D_s U\right)^2} \tag{3.6}$$

The variable s parametrizes the curve γ, and we pick $s \in [s_i, s_f]$. Here the trace $\text{Tr}(...)$ is a short-cut notation for the contraction using the Killing forms, i.e. if

$P \in sl(2, \mathbb{R})$

$$\text{Tr}(P^2) = \eta_{ab} P^a P^b \, , \tag{3.7}$$

where $P = P^a L_a$ and L_a is a generator of $sl(2, \mathbb{R})$. There is also a (classically) equivalent first-order formulation of this action that is more convenient for certain applications (such as the generalization to higher spin gravity). In the first order formulation it is manifest that c_2 is the Casimir of the representation, and satisfies $c_2 = 2h(h-1)$. This action requires that $h = \bar{h}$. As the entire action is multiplied by a factor of $\sqrt{c_2}$, $h \to \infty$ defines a semi-classical approximation on the path integral, and for the remainder of this section we will follow [108] and work in this limit. In subsequent sections we will relax this restriction.

This action is invariant under a local $SL(2, \mathbb{R}) \times SL(2, \mathbb{R})$ symmetry: in particular the covariant derivative is defined as

$$D_s U \equiv \frac{d}{ds} U + A_s U - U \bar{A}_s \, , \quad A_s \equiv A_\mu \frac{dy^\mu}{ds} \, , \quad \bar{A}_s \equiv \bar{A}_\mu \frac{dy^\mu}{ds} \, , \tag{3.8}$$

where $A(y)$ and $\bar{A}(y)$ are the connections that determine the background, and in the action (3.6) they are pulled back to the worldline $y^\mu(s)$. Under an $SL(2, \mathbb{R}) \times SL(2, \mathbb{R})$ gauge transformation by finite group elements $L(y)$, $R(y)$, the gauge fields transform as

$$\begin{aligned} A_\mu(y) &\to L(y)(A_\mu(y) + \partial_\mu) L^{-1}(y) \, , \\ \bar{A}_\mu(y) &\to R^{-1}(y)(\bar{A}_\mu(y) + \partial_\mu) R(y) \, . \end{aligned} \tag{3.9}$$

The worldline action is then invariant under the following transformation of the worldline field:

$$U(s) \to L(y^\mu(s)) U(s) R(y^\mu(s)) \tag{3.10}$$

Now for an open ended Wilson line as in (3.3), we must still specify boundary data on $U(s)$ at the endpoints of the curve.[1] We thus pick two $SL(2, \mathbb{R})$ elements U_i, U_f and require that $U(s = s_i) = U_i$, $U(s = s_f) = U_f$. For a semi-classical level this is sufficient, and in later sections we will explain in detail the relationship between this choice of boundary data and the quantum states $|U_i\rangle$ and $|U_f\rangle$ defined in (3.3).

We now consider the evaluation of this Wilson line on a frozen classical background defined by A and $\bar{A}$. In the semi-classical $h \to \infty$ limit, this can be done by evaluating the on-shell action (3.6) for the field $U(s)$ subject to the boundary conditions described above. This computation was explained in detail in [108]. Here

---

[1] For a closed Wilson loop as in (3.2), we simply require that the field $U(s)$ be single-valued.

we write the answer in a way that will generalize simply to our results in the next section. In particular the answer only depends on the $SL(2, \mathbb{R})$ evolution of the state from the starting point to the endpoint. If we thus consider flat connections

$$A(y) = g_L(y)dg_L(y)^{-1}, \quad \bar{A}(y) = g_R(y)^{-1}dg_R(y),$$

(3.11)

and the following group elements

$$g_L(y_f)g_L(y_i)^{-1} = \mathcal{P}\exp\left(-\int_{y_i}^{y_f} A\right), \qquad g_R^{-1}(y_f)g_R(y_i) = \mathcal{P}\exp\left(-\int_{y_i}^{y_f} \bar{A}\right),$$

(3.12)

then the on-shell action S can be written as

$$S_{\text{on-shell}} = \sqrt{\frac{c_2}{2}}\alpha, \quad V\exp(-\alpha L_0)V^{-1} \equiv g_L(y_f)g_L(y_i)^{-1}U_i g_R(y_i)^{-1}g_R(y_f)U_f^{-1},$$

(3.13)

where α labels the conjugacy class of the group element on the right-hand side of the second equation. The Wilson line (3.5) in this state is then given by

$$W_{\mathcal{R}}(y_i, y_f) = \exp\left(-\sqrt{\frac{c_2}{2}}\alpha\right).$$

(3.14)

Note that the role of the boundary data U_i, U_f in (3.13) is to tie together the two sectors, left and right; we will return to this point in what follows.

3.2.2   Geometric interpretation: proper distances

So far, our review has been very abstract, with no physical interpretation given to A and $\bar{A}$. However we know that for appropriate choices of these gauge connections, this system should represent the physics of a particle moving on AdS$_3$; we now explain how the result above is related to geometry. In particular, α defined in (3.13) turns out to be related to the proper distance from y_i to y_f.

To understand this, note that the action (3.6) can be suggestively written as

$$S = \sqrt{c_2}\int_\gamma ds\sqrt{\text{Tr}\left(\left(A_\mu - \tilde{\bar{A}}_\mu\right)\left(A_\nu - \tilde{\bar{A}}_\nu\right)\frac{dy^\mu}{ds}\frac{dx^\nu}{ds}\right)},$$

(3.15)

where the dependence on $U(s)$ in (3.19) has been hidden in the definition of $\tilde{\bar{A}}_\nu$:

$$\tilde{\bar{A}}_s \equiv U\bar{A}_s U^{-1} - \frac{d}{ds}U U^{-1}.$$

(3.16)

Note that if we now define a *generalized* vielbein[2] along the trajectory as

$$e_\mu = \frac{1}{2}\left(A_\mu - \tilde{\bar{A}}_\mu\right) \tag{3.17}$$

then we may write the action very simply in terms of the metric associated to this vielbein as $g_{\mu\nu} = 2\operatorname{Tr}_f e_\mu e_\nu$, i.e.

$$S = \sqrt{2c_2}\int_\gamma ds\sqrt{g_{\mu\nu}(y)\frac{dy^\mu}{ds}\frac{dy^\nu}{ds}}\;, \tag{3.18}$$

which is manifestly the proper distance associated to the metric $g_{\mu\nu}$. Thus the Wilson line is probing a geometry that is assembled in a particular manner from the connections $A, \bar{A}$, where the dynamics of the auxiliary field U is playing a role in tying together the two connections into a vielbein. Note that the prefactor $\sqrt{c_2}$ indicates that the value of the Casimir controls the bulk mass of the probe, as we alluded to previously.

We also consider the equations of motion obtained from varying (3.6) with respect to U:

$$\frac{d}{ds}\left((A - \tilde{\bar{A}})_\mu \frac{dy^\mu}{ds}\right) + [\tilde{\bar{A}}_\mu, A_\nu]\frac{dy^\mu}{ds}\frac{dy^\nu}{ds} = 0\;. \tag{3.19}$$

Normally one considers these as equations for $U(s)$: nevertheless, if one fixes $U(s)$ and thinks of the variable as being the choice of *path* $y^\mu(s)$, then this is precisely the geodesic equation for the metric $g_{\mu\nu}$. From here it is clear that the value of the Wilson line between any two bulk points is

$$W_\mathcal{R}(y_i, y_f) \sim \exp\left(-2h D(y_i, y_f)\right), \tag{3.20}$$

where $D(y_i, y_f) = 2\alpha$ is the length of the bulk geodesic connecting these two points. Here '$\sim$' denotes the limit of large c_2, where $c_2 = 2h(h-1) \sim 2h^2$, and hence the classical saddle point approximation is valid.

In what follows we will provide a proper quantum-mechanical treatment of this Wilson line.

3.3 Hilbert space representation

The path integral approach to evaluate (3.3) provides insight into the transformation properties for the field U: this choice is in great part responsible of the

---

[2]Technically we can only define the components of the vielbein along the trajectory; in the considerations of this section this does not matter.

geometric interpretation of $W_{\mathcal{R}}(y_i, y_f)$ in AdS$_3$ gravity. Based on this, in this section we will carefully explain the relationship between the field $U(y)$ and quantum mechanical states in the highest-weight representation. This will allow us to evaluate $W_{\mathcal{R}}(y_i, y_f)$ without the need of taking a classical limit –in contrast to (3.20)– and, in later sections, have a refined geometric and holographic interpretation of our Wilson line.

3.3.1   Highest weight representations

We first review some facts associated with highest-weight representations. Some words on notation are appropriate: when we are discussing an abstract realization of the $sl(2, \mathbb{R})$ algebra with no particular representation in mind, we will denote the generators with capital L_a. We denote the generators of $sl(2, \mathbb{R})$ acting on the highest weight state by ℓ_a. A highest-weight representation is defined with respect to a reference state $|h\rangle$ that is an eigenstate of ℓ_0 and is annihilated by ℓ_1:

$$\ell_0|h\rangle = h|h\rangle , \qquad \ell_1|h\rangle = 0 . \tag{3.21}$$

We may now define excited states by acting on $|h\rangle$ with ℓ_{-1}, and the correctly normalized states are defined by

$$\ell_{-1}|h, k\rangle = \sqrt{(k+1)(k+2h)}|h, k+1\rangle , \qquad \ell_1|h, k\rangle = \sqrt{k(k+2h-1)}|h, k-1\rangle , \tag{3.22}$$

where the state $|h, k\rangle$ has L_0 eigenvalue $(k+h)$: i.e. k counts the energy *above* the ground state, and $|h, 0\rangle = |h\rangle$. The Casimir of this representation is $2h(h-1)$:

$$\eta^{ab}\ell_a\ell_b|h, k\rangle = 2h(h-1)|h, k\rangle , \tag{3.23}$$

where η^{ab} is the Killing form.

We will be interested in states that transform in a highest-weight representation under a tensor product of two independent copies of $sl(2, \mathbb{R}) \times sl(2, \mathbb{R})$ with $h = \bar{h}$, and so we will label them as $|h, k\rangle \otimes |h, \bar{k}\rangle \equiv |h; k, \bar{k}\rangle$, where the ground state is $|h, 0, 0\rangle$. We denote the $sl(2, \mathbb{R})$ generators acting on the first k index (the "left") by ℓ_a and those acting on the $\bar{k}$ index (the "right") as $\bar{\ell}_a$. These form two independent $sl(2, \mathbb{R})$ algebras, and we have

$$[\ell_a, \bar{\ell}_a] = 0 . \tag{3.24}$$

The group action of each copy of $SL(2, \mathbb{R})$ on these states is the usual one: in particular, we have

$$G(M^{-1})\ell_a G(M) = D_a{}^{a'}(M)\ell_{a'} , \qquad \overline{G}(M^{-1})\bar{\ell}_a\overline{G}(M) = D_a{}^{a'}(M)\bar{\ell}_{a'} , \tag{3.25}$$

with the D's the representation matrices for the adjoint representation of $sl(2,\mathbb{R})$. Note that we have

$$G(M_1)G(M_2) = G(M_1 M_2) \ , \qquad D_a{}^b(M_1)D_b{}^c(M_2) = D_a{}^c(M_1 M_2) \ . \qquad (3.26)$$

3.3.2 Rotated Ishibashi states

We will now define a family of quantum states that have the same transformation as the classical field $U(y)$ in (3.10). To do so it is convenient to consider the following triplet of $sl(2,\mathbb{R})$ operators, labeled by an element $U \in SL(2,\mathbb{R})$:

$$Q_a(U) \equiv \ell_a + D_a{}^{a'}(U)\bar{\ell}_{a'} \ . \qquad (3.27)$$

This is a linear combination of the generators on the two sides, with one side rotated by U. We will denote a state that is annihilated by $Q_a(U)$ for all a as $|U\rangle$, i.e.

$$Q_a(U)|U\rangle = 0 \ . \qquad (3.28)$$

This defines a *rotated state*, each labeled by an element U of $SL(2,\mathbb{R})$. We now explore some of the properties of these states. First consider commuting $G(L)\overline{G}(R)$ through $Q_m(U)$. We find

$$G(L)\overline{G}(R^{-1})Q_a(U) = D_a{}^{a'}(L^{-1})Q_{a'}(LUR)G(L)\overline{G}(R^{-1}) \ . \qquad (3.29)$$

Acting with this relation on the state $|U\rangle$, we find that the state $G(L)\overline{G}(R^{-1})|U\rangle$ is annihilated by $Q_a(LUR)$. But by the definition of the U states, this means that

$$G(L)\overline{G}(R^{-1})|U\rangle = |LUR\rangle \ . \qquad (3.30)$$

Thus we see that acting on a U state with an element of $SL(2,\mathbb{R}) \times SL(2,\mathbb{R})$ causes it to transform inhomogenously precisely as the *classical U* field did in (3.10). We also note that every U state is left invariant under *some* diagonal subgroup of $SL(2,\mathbb{R}) \times SL(2,\mathbb{R})$, that with $L = UR^{-1}U^{-1}$.

It will be useful to have some explicit examples of $|U\rangle$ in terms of the highest weight representation discussed above. As a start let us consider the state $|U\rangle = |\Sigma_{\text{Ish}}\rangle$ whose action on the generators is

$$D_a{}^{a'}(\Sigma_{\text{Ish}})\,\bar{\ell}_{a'} = \Sigma_{\text{Ish}}\,\bar{\ell}_a\,\Sigma_{\text{Ish}}^{-1} = -\bar{\ell}_{-a} \ , \qquad (3.31)$$

and as a group element is

$$\Sigma_{\text{Ish}} \equiv \exp\left(-i\frac{\pi}{2}(L_1 - L_{-1})\right) \ . \qquad (3.32)$$

Using (3.31), (3.28) becomes

$$\left(\ell_a - \overline{\ell}_{-a}\right)|\Sigma_{\text{Ish}}\rangle = 0 \ . \tag{3.33}$$

This equation has the following unique solution,

$$|\Sigma_{\text{Ish}}\rangle = \sum_{k=0}^{\infty} |h; k, k\rangle \ , \tag{3.34}$$

which is (in its Virasoso incarnation [115]) called the "Ishibashi state." Another choice for our states is setting $|U\rangle = |\Sigma_{\text{cross}}\rangle$ whose action is

$$D_a{}^{a'}(\Sigma_{\text{cross}})\,\overline{\ell}_{a'} = \Sigma_{\text{cross}}\,\overline{\ell}_a\,\Sigma_{\text{cross}}^{-1} = -(-1)^a\overline{\ell}_{-a} \ , \tag{3.35}$$

and as a group element it reads

$$\Sigma_{\text{cross}} \equiv \exp\left(\frac{\pi}{2}(L_1 + L_{-1})\right) \ . \tag{3.36}$$

For this choice (3.28) becomes

$$\left(\ell_a - (-1)^a\overline{\ell}_{-a}\right)|\Sigma_{\text{cross}}\rangle = 0 \ , \tag{3.37}$$

and the unique solution to this equation is

$$|\Sigma_{\text{cross}}\rangle = \sum_{k=0}^{\infty}(-1)^k|h; k, k\rangle \ , \tag{3.38}$$

which is usually referred to as the "crosscap (or twisted) Ishibashi state" [115]. The state $|\Sigma_{\text{cross}}\rangle$ (rather than $|\Sigma_{\text{Ish}}\rangle$) will play an important role in section 3.4, for reasons that we will elaborate on there.

If we can construct any reference state in this family, then we can find any other state by acting on it with an appropriately chosen $G(L)$ and/or $\bar{G}(R^{-1})$.[3] And for this reason we will call the states $|U\rangle$ (in a slight abuse of notation) rotated Ishibashi states. Our rotated Ishibashi states are coherent states that live in the product of two highest weight representations and only involve the global part of the conformal group, unlike the states used for boundary CFT [115, 116].

---

[3]Note that we are allowed to rotate a $|U\rangle$ state if $G(L)$ has a well defined action on the representation. This implies that not any rotation is allowed. For example, we cannot rotate $|\Sigma_{\text{cross}}\rangle$ to the state $|U = \mathbb{1}\rangle$, which is ill defined since setting $U = \mathbb{1}$ in (3.28) has no solution in the highest weight representation. The reason is that Σ_{cross} is an outer automorphism: it has a well defined action on the group elements as signalled by (3.35), but not on the states of representation (it would flip the sign of L_0 eigenvalue). Similar statements hold for Σ_{Ish}.

3.3.3 Inner product

An important object in our analysis is the inner product of a rotated Ishibashi state. These states are not orthogonal– they form an overcomplete basis– which leads to a non-trivial expression. The relevant matrix element to evaluate any such inner product is

$$\langle \Sigma | G(L) \overline{G}(R^{-1}) | \Sigma \rangle \ , \tag{3.39}$$

where $|\Sigma\rangle$ is a reference state from our family of rotated Ishibashi states. For concreteness we will take $|\Sigma\rangle$ to be either

$$|\Sigma_{\text{Ish}}\rangle \quad \text{or} \quad |\Sigma_{\text{cross}}\rangle \ , \tag{3.40}$$

as defined in (3.34) and (3.38).

Evaluating (3.39) leads to

$$
\begin{aligned}
\langle \Sigma | G(L) \overline{G}(R^{-1}) | \Sigma \rangle &= \langle \Sigma | G(L \, \Sigma \, R \, \Sigma^{-1}) | \Sigma \rangle \\
&= \sum_{k=0}^{\infty} |a_k|^2 \langle h, k | G(L \, \Sigma \, R \, \Sigma^{-1}) | h, k \rangle \\
&= \sum_{k=0}^{\infty} \langle h, k | G(L \, \Sigma \, R \, \Sigma^{-1}) | h, k \rangle \\
&= \sum_{k=0}^{\infty} \exp(-\alpha(k+h)) = \frac{e^{-\alpha h}}{1 - e^{-\alpha}} \ .
\end{aligned}
\tag{3.41}
$$

In the first equality we used (3.30). In the second line we used (3.34) and (3.38); the coefficient a_k is equal to 1 and $(-1)^k$, respectively. In the third line we used that $|a_k|^2 = 1$, which reduces the computation to a trace of the group element inside the bracket. In the last line we decomposed the group element as

$$L \, \Sigma \, R \, \Sigma^{-1} \equiv V \exp(-\alpha L_0) V^{-1} \ , \tag{3.42}$$

where α controls the conjugacy class of the group element in question. The last equality is our final result, which is just a $sl(2, \mathbb{R})$ character of $G(L \, \Sigma \, R \, \Sigma^{-1})$. From here the role of $|\Sigma\rangle$ is becoming more evident: it controls how the right element R would act as left element relative to L and vice versa.

The result (3.41) immediately generalizes to the inner product between any two of the U-states as defined in (3.28): any rotated state continuously connected to Σ will satisfy

$$\langle U_1 | U_2 \rangle = \frac{e^{-\alpha h}}{1 - e^{-\alpha}} \ , \qquad U_1^{-1} U_2 \equiv V \exp(-\alpha L_0) V^{-1} \ . \tag{3.43}$$

In other words, the inner product between any two U-states U_1 and U_2 is a function only the "magnitude" α of the conjugacy class of the group element that relates U_1 to U_2. α can be thought of as an invariant distance between the two elements on the group manifold (and indeed we will develop its geometric interpretation in the next subsection). Note that as U_1 approaches U_2, $\alpha \to 0$ and thus the norm of any U state itself is infinite: this divergence can be seen immediately from noting that the norm of $|\Sigma\rangle$ diverges.

Finally, the U states satisfy a completeness relation. It is shown in Appendix 6.6 through explicit computation that for $2h > 1$ we have

$$\int dU |U\rangle\langle U| = \frac{(2\pi)^2}{2(2h-1)} \mathbb{1} \, , \tag{3.44}$$

where dU is the Haar measure on $SL(2, \mathbb{R})$. In pedestrian terms, this simply means that we treat $SL(2, \mathbb{R})$ as being locally AdS$_3$ and integrate over it using the usual volume measure, taking care to integrate over $SL(2, \mathbb{R})$ and not over its universal cover.

3.3.4 The Green's function on the group manifold

Here we discuss a few further properties of the inner product $\langle U_1|U_2\rangle$ computed above. In particular, the inner product (3.43) is actually a Green's function with respect to the invariant Laplacian on the $SL(2, \mathbb{R})$ group manifold.

We begin by placing coordinates σ^α on the group manifold $SL(2, \mathbb{R})$. Let us denote the usual generators of $sl(2, \mathbb{R})$ in the fundamental representation by L_a. As $SL(2, \mathbb{R})$ is a group manifold, there exist vector fields ξ_a^α and $\bar{\xi}_a^\alpha$ that generate the group action on a point in the manifold from the left and from the right, i.e.

$$\xi_a^\alpha \frac{\partial U(\sigma)}{\partial \sigma^\alpha} = L_a U(\sigma) \, , \qquad \bar{\xi}_a^\alpha \frac{\partial U(\sigma)}{\partial \sigma^\alpha} = U(\sigma) L_a \, . \tag{3.45}$$

As the U-states (3.30) transform in the same way, they satisfy:

$$\xi_a^\alpha \partial_\alpha |U(\sigma)\rangle = |L_a U(\sigma)\rangle = \ell_a |U(\sigma)\rangle \, , \tag{3.46}$$

as well as a similar relation for the barred sector. Now we act with this relation twice on the σ_2 coordinates parametrizing the inner product $\langle U(\sigma_1)|U(\sigma_2)\rangle$ with $U(\sigma_1) \neq U(\sigma_2)$. In particular, denote the Killing form on $sl(2, \mathbb{R})$ by η^{ab} and compute

$$\eta^{ab} \langle U(\sigma_1)| \xi_a^\alpha \partial_\alpha \left(\xi_b^\beta \partial_\beta |U(\sigma_2)\rangle \right)\rangle = \eta^{ab} \langle U(\sigma_1)| \ell_b \ell_a |U(\sigma_2)\rangle = 2h(h-1)\langle U(\sigma_1)|U(\sigma_2)\rangle \, , \tag{3.47}$$

where in the last equality we have used the Casimir relation (3.95). It is straightforward to verify that the second-order differential operator on the left-hand side of (3.47) is (up to a factor of $\frac{1}{2}$) the invariant Laplacian on $SL(2,\mathbb{R})$, which we denote by $\Box_U$. As our analysis holds only for non-coincident U_1, U_2, we conclude that

$$\left(\frac{1}{2}\Box_{U_2} - 2h(h-1)\right)\langle U_1|U_2\rangle = \frac{1}{8\pi}\delta(U_1, U_2) \; . \tag{3.48}$$

Here $\delta(U_1, U_2)$ is a delta function on the group manifold that is nonzero only if $U_1 = U_2$, and which is normalized to satisfy $\int dU\delta(U_0, U) = 1$ with dU the Haar measure on $SL(2,\mathbb{R})$ and U_0 a reference group element. This can of course also be checked by explicitly verifying that (3.43) satisfies the appropriate Laplacian; this is also the fastest way to verify the existence of the delta function on the right-hand side.

3.3.5 Relationship to path integral

In this section we will demonstrate that the in the large-h limit, the inner product defined above can be computed from a path integral over a classical field $U(s)$, as used in [108] and reviewed in Sec. 3.2. Essentially we will perform the analogue of the usual construction of the path integral for quantum mechanical systems, where the non-compact nature of the representation, and therefore of the U states, provide some extra wrinkles.

Consider computing an inner product of the form

$$\langle U_f|G(L)\bar{G}(R^{-1})|U_i\rangle \; . \tag{3.49}$$

To give this a quantum-mechanical interpretation, we will represent the group elements L and R as path-ordered exponentials of gauge fields $A(s)$ and $\bar{A}(s)$, where s should be thought of as "time", i.e.

$$L = \mathcal{P}\exp\left(-\int_{s_i}^{s_f} A_s ds\right) \; , \qquad R^{-1} = \mathcal{P}\exp\left(-\int_{s_i}^{s_f} \bar{A}_s ds\right) \; . \tag{3.50}$$

To make contact with conventional quantum mechanics, one can imagine that A and $\bar{A}$ define a Hamiltonian for the system defining time-evolution along s. We will now derive a path integral expression for the inner product (3.49). We follow the normal algorithm of dividing the path from s_i to s_f into many small intervals of size ϵ, discretizing the path as $s_i, s_{i+1}, s_{i+2}\cdots s_{f-1}, s_f$, where the time step is $s_j - s_{j-1} = \epsilon$.

We may then break up each path-ordered exponential:

$$\mathcal{P} \exp\left(-\int_{s_i}^{s_f} A_s ds\right) = e^{-\epsilon A_s(s_f)} e^{-\epsilon A_s(s_{f-1})} \cdots e^{-\epsilon A_s(s_i)} = \prod_j e^{-\epsilon A_s(s_j)} \ , \quad (3.51)$$

and similarly for the right sector. The inner product takes the form

$$\langle U_f | G(L)\bar{G}(R^{-1}) | U_i \rangle = \langle U_f | \prod_j \left[G\left(e^{-\epsilon A_s(s_j)}\right) \overline{G}\left(e^{-\epsilon \bar{A}_s(s_j)}\right) \right] | U_i \rangle \ . \quad (3.52)$$

We now use (3.44) to insert a complete set of U states at each time step. We find

$$\langle U_f | G(L)\bar{G}(R^{-1}) | U_i \rangle = $$
$$\mathcal{N} \langle U_f | \prod_j \left[G\left(e^{-\epsilon A_s(s_j)}\right) \overline{G}\left(e^{-\epsilon \bar{A}_s(s_j)}\right) \int dU | U(s_j)\rangle\langle U(s_j)| \right] | U_i \rangle \ ,$$
$$(3.53)$$

where we have introduced an overall prefactor $\mathcal{N}$ to absorb factors of the form $(2h-1)^\infty$ into the usual ambiguities in the measure of the path integral. We see that we must evaluate many inner products of the form

$$\langle U(s_{j+1}) | G\left(e^{-\epsilon A_s(s_j)}\right) \overline{G}\left(e^{-\epsilon \bar{A}_s(s_j)}\right) | U(s_j)\rangle \ . \quad (3.54)$$

To evaluate this inner product, we make the usual assumption that most contributions to the path integral come from reasonably smoothly varying $U(s)$, so that we may assume that $U(s_{j+1}) = U(s_j) + \epsilon \frac{dU(s_j)}{ds} + \mathcal{O}(\epsilon^2)$. Thus to lowest order in ϵ we are evaluating

$$\left\langle U(s_j)\left(\mathbb{1} + U(s_j)^{-1}\epsilon\frac{dU(s_j)}{ds}\right) \middle| G\left(e^{-\epsilon A_s(s_j)}\right) \overline{G}\left(e^{-\epsilon \bar{A}_s(s_j)}\right) \middle| U(s_j)\right\rangle \ . \quad (3.55)$$

We use the transformation property of the U states (3.30) to move all of the group elements to the ket on the right to obtain

$$\left\langle U(s_j)\middle| e^{-\epsilon A_s(s_j)}U(s_j)e^{-\epsilon \bar{A}_s(s_j)}\left(\mathbb{1} - U(s_j)^{-1}\epsilon\frac{dU}{ds}(s_j)\right) \right\rangle \ . \quad (3.56)$$

Next, we use the general form for the inner product (3.43) to conclude that

$$\langle U(s_{j+1}) | G\left(e^{-\epsilon A_s(s_j)}\right) \overline{G}\left(e^{-\epsilon \bar{A}_s(s_j)}\right) | U(s_j)\rangle = \frac{e^{-\alpha(s_j)h}}{1 - e^{-\alpha(s_j)}} \ , \quad (3.57)$$

where $\alpha(s_j)$ is given by the conjugacy class of the $SL(2,\mathbb{R})$ element

$$M(s_j) \equiv e^{-\epsilon\left(U^{-1}\frac{dU}{ds} + U^{-1}A_s U - \bar{A}_s\right)}\bigg|_{s=s_j} \ , \quad M(s_j) = V^{-1}\exp(-\alpha(s_j)L_0)V \ , \quad (3.58)$$

where to obtain this expression we expanded all terms up to order ϵ, and then re-exponentiated the resulting expression. It should be understood that this expression is correct only up to order ϵ. We have encountered a version of (3.58) in (3.42) and (3.43), and we will encounter again in subsequent sections. The a simple way to read off $\alpha(s_j)$ is by noticing that (3.58) –and its counsins (3.42) and (3.43)– are independent of the $sl(2)$ representation. With these freedom, we choose to solve this equation in the fundamental representation of $sl(2)$, described by the 2×2 traceless matrices, where α is given by a trace:

$$\alpha(s_j) = 2\epsilon\sqrt{\mathrm{Tr}_f\left(U^{-1}D_sU\right)^2}\Bigg|_{s=s_j} .\tag{3.59}$$

Here the gauge-covariant derivative D_sU is that defined in (3.8), and our conventions for the fundamental representation are given in appendix 6.5.

We have thus computed the contribution of one infinitesimal piece of the path. Assembling all of these pieces by taking the product, we see that the full inner product (3.49) is given by

$$\langle U_f|G(L)\bar{G}(R^{-1})|U_i\rangle = \mathcal{N}\prod_j\left(\int dU(s_j)\frac{e^{-\alpha(s_j)h}}{1-e^{-\alpha(s_j)}}\right)\Bigg|_{U(s_i)=U_i,U(s_f)=U_f} .\tag{3.60}$$

We now consider taking the continuum limit $\epsilon \to 0$; the product of integrals $dU(s_j)$ over each group element at each point on the path becomes a path integral $[\mathcal{D}U]$ over a continuous worldline field $U(s)$. We first consider the numerator of the above expression: this naturally becomes an integral over a smooth action:

$$\prod_j\exp\left(-h\alpha(s_j)\right) \to \exp\left(-2h\int_{s_i}^{s_f}ds\sqrt{\mathrm{Tr}_f\left(U^{-1}D_sU\right)^2}\right) ,\tag{3.61}$$

i.e. precisely the exponential of the action $S[U]$ postulated on physics grounds in [108].

We now turn to the denominator $1 - e^{-\alpha(s_j)}$. In the limit $\epsilon \to 0$, each $\alpha(s_j)$ is infinitesimal, and thus we may write:

$$\prod_j(1-e^{-\alpha(s_j)})^{-1} \approx \prod_j(\alpha(s_j))^{-1} = \prod_j\sqrt{\frac{\epsilon}{2\pi}}\int d\sigma(s_j)\exp\left(-\frac{\epsilon}{2}\sigma(s_j)^2\alpha(s_j)^2\right) ,\tag{3.62}$$

where we have introduced a new auxiliary field $\sigma(s_j)$ at each point on the worldline; integrating out this field generates the denominator (up to an overall ill-defined prefactor that depends on the discretization). The full path integral is thus

$$\int_{U(s_i)=U_i}^{U(s_f)=U_f}[\mathcal{D}U]\exp\left(-S[U,\sigma]\right) .\tag{3.63}$$

where the full continuum action is

$$S[U, \sigma] = \int_{s_i}^{s_f} ds \left(2h \sqrt{\mathrm{Tr}_f \left(U^{-1} D_s U \right)^2} + \frac{1}{2} \sigma(s)^2 \, \mathrm{Tr}_f \left(U^{-1} D_s U \right)^2 \right) . \quad (3.64)$$

In the $h \to \infty$ limit, we may ignore the second term in the action: this is then precisely the path integral (3.5)-(3.6) which was proposed on symmetry grounds in [108].

We can now see that at finite h, the path integral proposed in [108] must be corrected by additional "quantum" terms arising from the measure of the path integral when integrating over U states. This additional term –the wrinkle we alluded to at the start of this subsection– arises from the fact that the inner product of two nearby U states is divergent, which is itself a direct consequence of the non-compactness of $SL(2, \mathbb{R})$ and the resulting infinite tower of highest weight states. It would be interesting to understand better the physical significance of this term; however in this chapter we will not attempt to treat the path integral (3.5) at finite h, and will instead simply directly compute matrix elements from the algebraic approach developed above.

3.4   Wilson lines: Local Fields and Geometry

Our goal in this section is to give a geometric interpretation to the algebraic construction in Sec. 3.3. We will start in Sec. 3.4.1, by going through the simple exercise of casting our gravitational Wilson line in (3.3) along the lines of the discussion in Sec. 3.3.3. In Sec. 3.4.2 we will argue that for invertible connections $(A, \bar{A})$, we can interpret the transformation properties of the group elements in the Wilson line as moving the endpoints of the operator in AdS$_3$. This justifies the geometric interpretation of the algebraic object. And finally, in Sec. 3.4.3 we will show how to build a local bulk field from our rotated Ishibashi states; these constructions will be explicitly done for global AdS and the static BTZ black hole.

3.4.1   Gravitational Wilson line as an overlap of two states

The results in Sec. 3.3 gives a prescription to evaluate overlap of states in the highest weight representation. In this section we would like to implement those

results to a gravitational Wilson line. More concretely, we would like to analyse

$$W_{\mathcal{R}}(y_f, y_i) = \langle \Sigma | \, G \left(\mathcal{P} e^{- \int_{y_i}^{y_f} A} \right) \, \bar{G} \left(\mathcal{P} e^{- \int_{y_i}^{y_f} \bar{A}} \right) | \Sigma \rangle \,, \qquad (3.65)$$

as an overlap of a suitable initial and final $|U\rangle$ state. We keep the reference state $|\Sigma\rangle$ generic so far, and we will discuss the different choices Σ_{Ish}, and Σ_{cross} in Sec. 3.4.3. As in Sec. 3.2, $\gamma(s)$ is a curve with bulk endpoints (y_i, y_f); we use the affine parameter $s \in [s_i, s_f]$ where $y(s = s_i) = y_i$ and $y(s = s_f) = y_f$.

To recast (3.65) as an inner product, it is useful to rewrite the flat connections as

$$A(y) = g_L(y) dg_L(y)^{-1} \,, \quad \bar{A}(y) = g_R(y)^{-1} dg_R(y) \,, \qquad (3.66)$$

Using the transformation of the path ordered exponential under (3.66):

$$\mathcal{P} \, e^{- \int_\gamma A} = g_L(y_f) g_L(y_i)^{-1} \,, \qquad \mathcal{P} \, e^{- \int_\gamma \bar{A}} = g_R^{-1}(y_f) g_R(y_i) \,, \qquad (3.67)$$

and therefore

$$\langle \Sigma | G \left(\mathcal{P} \, e^{- \int_\gamma A} \right) \bar{G} \left(\mathcal{P} \, e^{- \int_\gamma \bar{A}} \right) | \Sigma \rangle = \langle \Sigma | G \left(g_L(y_f) g_L(y_i)^{-1} \right) \bar{G} \left(g_R^{-1}(y_f) g_R(y_i) \right) | \Sigma \rangle \,, \qquad (3.68)$$

To write this expression as an overlap between to states, we define

$$|U(y)\rangle \equiv G \left(g_L(y)^{-1} \right) \bar{G} \left(g_R(y) \right) | \Sigma \rangle \,. \qquad (3.69)$$

and with this, we can rewrite the previous amplitude as

$$\langle \Sigma | G \left(\mathcal{P} \, e^{- \int_\gamma A} \right) \bar{G} \left(\mathcal{P} \, e^{- \int_\gamma \bar{A}} \right) | \Sigma \rangle = \langle U(y_f) | U(y_i) \rangle \,. \qquad (3.70)$$

It is important to note that in this expression we have implicitly assumed that the group element g_L obeys

$$g_L^{-1} = g_L^\dagger \,,$$

and similarly for g_R. All of our manipulations will use group elements that are unitary. And we should stress that $|U(y)\rangle$ is not gauge invariant. In its definition in (3.69) we implicitly made a choice: we are splitting the path from y_i to y_f to a mid point where $g_L = g_R = \mathbb{1}$, and without any further specification of the connections, we have not motivated nor justified this choice. This bug does not affect (3.70), and we will ignore it for now. We will return to this point in Sec. 3.4.3 when we directly analyse $|U(y)\rangle$.

Having casted the gravitational Wilson line as an inner product in (3.70), we can now use the same logic that leads to (3.41) and (3.42). In particular we find

that

$$\langle \Sigma | G \left(\mathcal{P} \, e^{-\int_\gamma A} \right) \bar{G} \left(\mathcal{P} \, e^{-\int_\gamma \bar{A}} \right) | \Sigma \rangle = \frac{e^{-\alpha(y_i, y_f) h}}{1 - e^{-\alpha(y_i, y_f)}} \tag{3.71}$$

where, following (3.42) for this case, $\alpha(y_i, y_f)$ is given by the solution to

$$g_L(y_f) g_L(y_i)^{-1} \tilde{g}_R(y_i)^{-1} \tilde{g}_R(y_f) = V \exp(-\alpha(y_i, y_f) L_0) V^{-1} \,. \tag{3.72}$$

and we define

$$\tilde{g}_R \equiv \Sigma^{-1} g_R \Sigma \,, \qquad \tilde{\bar{A}} \equiv \Sigma^{-1} \bar{A} \Sigma \,. \tag{3.73}$$

Note that while, by definition, A and $\bar{A}$ act on different spaces, the role of Σ is to tie together these two sectors; $\tilde{\bar{A}}$ can be thought of as the 'left' version of the 'right' connection. To solve for $\alpha(y_i, y_f)$ in (3.72), it is useful to note that this equation is independent of the $sl(2, \mathbb{R})$ representation, and hence we can simply use a finite dimensional representation.[4] Using the fundamental representation of $sl(2, \mathbb{R})$, and after taking the trace both sides of (3.72), gives

$$\cosh \left(\frac{\alpha(y_i, y_f)}{2} \right) = \left(\frac{1}{2} \text{Tr}_f \left(g_L(y_f) g_L(y_i)^{-1} \tilde{g}_R(y_i)^{-1} \tilde{g}_R(y_f) \right) \right) \,. \tag{3.74}$$

where Tr_f is the trace in the fundamental representation. Using (3.66) together with (6.61) and (6.62), we find that $\alpha(s_i, s_f) = 2D(s_i, s_f)$ is the geodesic length of an effective metric given by

$$g_{\mu\nu} = \frac{1}{2} \text{Tr}(A_\mu - \tilde{\bar{A}}_\mu)(A_\nu - \tilde{\bar{A}}_\nu) \,. \tag{3.75}$$

The relevant metric for global AdS and BTZ is given in (6.63). It is worth to comment that the conventions for the AdS and BTZ connections used in this Chapter are different to those used in Chapter 1. The formulation in the highest weight representation used here requires unitary group elements (6.61), which was not fulfilled by the connections (1.101). For more details, see Appendix 6.7. Finally, the inner product is

$$\langle \Sigma | G \left(\mathcal{P} \, e^{-\int_\gamma A} \right) \bar{G} \left(\mathcal{P} \, e^{-\int_\gamma \bar{A}} \right) | \Sigma \rangle = \frac{e^{-2hD(y_i, y_f)}}{1 - e^{-2D(y_i, y_f)}} \,. \tag{3.76}$$

This is the familiar bulk-to-bulk propagator of a minimally coupled scalar field in a locally AdS$_3$ background [117, 118]. In the semi-classical limit, where the numerator is negligible and h is large, the saddle point approximation of the path integral in (3.76) precisely agrees with (3.20). The background metric (3.75) is in agreement with (3.18), and (3.72) is equivalent to (3.13).

---

[4]There is an ambiguity in the sign in front of α when (3.72) is considered in a finite dimensional representation. However, $\alpha > 0$ as required by the convergence of (3.41).

At the level of evaluating (3.76), the detailed nature of $|\Sigma\rangle$ can be overlooked: provided the endpoint states satisfies

$$G(L)G(R^{-1})|\Sigma\rangle = |L\Sigma R\rangle \ , \tag{3.77}$$

we will obtain (3.76), and interpret it as the bulk-to-bulk propagator of a scalar field with background metric (3.75). With this perspective, if the input is $g_{\mu\nu}$, we could just infer the values of $(A, \tilde{A})$ and use them in (3.76), without making explicit reference to the difference between $\bar{A}$ and $\tilde{A}$, and hence neglect the role of $|\Sigma\rangle$. However, $|U(y)\rangle$ is an object sensitive to $|\Sigma\rangle$, and as we will discuss in section 3.4.3, this will disentangle the different features that $|\Sigma\rangle$ captures as we build local probes in AdS₃.

3.4.2 Algebra meets geometry

An expression such as (3.76) makes rather evident that the Wilson line is a propagator, and hence its ties to geometry. The drawback however is the brut aspect of the observation: it relied on evaluating explicitly the observable on AdS₃ and the BTZ background. In this section we will do better. We will show that the object

$$W_{\mathcal{R}}(y_f, y_i) = \langle\Sigma| G\left(\mathcal{P}e^{-\int_{y_i}^{y_f} A}\right) \overline{G}\left(\mathcal{P}e^{-\int_{y_i}^{y_f} \bar{A}}\right) |\Sigma\rangle \tag{3.78}$$

can be understood as a bulk-to-bulk propagator with respect to the bulk spacetime metric associated with the flat connections $A, \bar{A}$. The important improvement here relative to our prior observations is that here we treat the Wilson line quantum mechanically, and as such it will capture the geometry as perceived by a *bulk field* of an arbitrary mass.

We begin by assuming that the bulk spacetime is simply connected (e.g. for pure AdS₃). In this case all paths from y_i to y_f are topologically equivalent, and (3.78) is a well-defined function of the two endpoints.

We first recall that in (3.48) it was shown that the object $\langle U_1|U_2\rangle$ was a Green's function on the group manifold $SL(2,\mathbb{R})$. This is logically distinct from showing that the matrix element (3.78) is a Green's function on the bulk metric defined by $A, \bar{A}$.

To make a connection between these two objects, we first need to establish how the matrix elements in (3.78) change if we move, for instance, the point y_f. The

dependence on endpoints y_i and y_f enters in (3.78) as follows: using (3.66)-(3.67), the matrix element reads

$$W_{\mathcal{R}}(y_f, y_i) = \langle \Sigma | G(g_L(y_f) g_L(y_i)^{-1}) \bar{G}(g_R(y_f)^{-1} g_R(y_i)) | \Sigma \rangle$$
$$= \langle \Sigma | G(g_L(y_f) g_L(y_i)^{-1} \tilde{g}_R(y_i)^{-1} \tilde{g}_R(y_f)) | \Sigma \rangle \ . \tag{3.79}$$

In the second line we made use of the transformation properties of our reference states (3.30), and used the definition $\tilde{g}_R \equiv \Sigma^{-1} g_R \Sigma$. We note that this is where the choice of $|U\rangle$ to be rotated states is crucial: the state combines both sectors, which will lead to a geometric interpretation of $W_{\mathcal{R}}(y_f, y_i)$ in the subsequent steps. From (3.79), the full dependence on y_i and y_f enters through the following group element

$$\mathcal{G}(y_f, y_i) \equiv g_L(y_f) g_L(y_i)^{-1} \tilde{g}_R(y_f)^{-1} \tilde{g}_R(y_i) \ . \tag{3.80}$$

Taking an y_f derivative of this group element, we have

$$\frac{\partial}{\partial y_f^\mu} \mathcal{G}(y_f, y_i) = -A_\mu(y_f) \mathcal{G}(y_i, y_f) + \mathcal{G}(y_i, y_f) \tilde{\bar{A}}_\mu(y_f) \ . \tag{3.81}$$

Recall now that (3.48) was shown by exploiting the fact that the left and right action of the group generated a set of vector fields on the group manifold (3.45). We would now like to extend this idea to the geometric bulk, i.e. we seek a set of vector fields $\zeta_a^\mu, \bar{\zeta}_a^\mu$ defined on AdS$_3$ such that

$$\zeta_a^\mu \frac{\partial}{\partial y_f^\mu} \mathcal{G}(y_f, y_i) = L_a \mathcal{G}(y_f, y_i) \ , \qquad \bar{\zeta}_a^\mu \frac{\partial}{\partial y_f^\mu} \mathcal{G}(y_f, y_i) = \mathcal{G}(y_f, y_i) L_a \ . \tag{3.82}$$

Multiplying both sides of these equations by L_b and taking a trace, we see that the defining relations become

$$\zeta_a^\mu \, \mathrm{tr}_f \left(\left(-A_\mu + \mathcal{G} \tilde{\bar{A}}_\mu \mathcal{G}^{-1} \right) L_b \right) = \eta_{ab} \ , \qquad \bar{\zeta}_a^\mu \, \mathrm{tr}_f \left(\left(-\mathcal{G}^{-1} A_\mu \mathcal{G} + \tilde{\bar{A}}_\mu \right) L_b \right) = \eta_{ab} \ . \tag{3.83}$$

These equations will have solutions for $\zeta, \bar{\zeta}$ if the 3×3 matrices (with rows labaled by μ and columns by b) multiplying them from the right are invertible. However from (1.94), we see that these matrices are closely related to the usual vielbein $e \sim A - \tilde{\bar{A}}$ in the metric formulation of 3d gravity, with one side rotated by the $SL(2, \mathbb{R})$ transformation defined by $\mathcal{G}(y_f, y_i)$. The condition that the generalized vielbeins above be invertible appears to be required for a simple geometric interpretation of the bulk spacetime.

If the generalized vielbeins shown above are invertible, then the $\zeta, \bar{\zeta}$ exist, and we have shown that movement in bulk spacetime is equivalent to movement on the group manifold. Furthermore the condition (3.82) guarantees that they satisfy the

$sl(2, \mathbb{R}) \times sl(2, \mathbb{R})$ algebra as Killing vectors on the bulk spacetime. Thus following through the same steps as in (3.48), we conclude that

$$\left(\frac{1}{2} \Box_{y_f} - 2h(h-1) \right) W_{\mathcal{R}}(y_f, y_i) = \frac{1}{8\pi} \frac{\delta(y_f, y_i)}{\sqrt{-g}} \tag{3.84}$$

where now $\Box_{y_f}$ is the Laplacian on the bulk AdS₃ spacetime. The construction of $\zeta, \bar{\zeta}$ will be carried out explicitly in Sec. 3.4.3.

We now consider the case where the bulk spacetime is not simply connected, e.g. the BTZ black hole. For a black hole the bulk connections have a nontrivial holonomy around the black hole horizon. In this case the definition of the open-ended Wilson line $W_{\mathcal{R}}(y_f, y_i)$ in (3.78) is incomplete: as there are multiple inequivalent bulk paths that connect y_i and y_f, we must specify a path, and different choices of path will result in different answers.

In this case, if we would like to obtain an unambiguous answer that depends only on the endpoints, one prescription is to sum over all inequivalent paths, i.e., we define a path-summed Wilson line as

$$W_{\mathcal{R}}(y_f, y_i) = \sum_{C(y_f, y_i)} W_{\mathcal{R}}(C(y_f, y_i)) \tag{3.85}$$

where the sum is over all topologically inequivalent paths $C(y_f, y_i)$ that connect y_f to y_i. An example of such situation is nicely capture by the BTZ black hole. In this case the inequivalent paths correspond to geodesics winding around the horizon multiple times, and the resulting propagator is a sum over these windings. For the static black hole, the resulting propagator is

$$W_{\mathcal{R}}(y_f, y_i)_{\text{BTZ}} = \sum_{n \in \mathbb{Z}} \frac{e^{-2hD_n(y_i, y_f)}}{1 - e^{-2D_n(y_i, y_f)}} \ , \tag{3.86}$$

with

$$D_n(y_i, y_f) = \frac{1}{r_+^2} \left(r_f r_i \cosh(r_+ \Delta\phi + 2\pi r_+ n) - \sqrt{(r_f^2 - r_+^2)(r_i^2 - r_+^2)} \cosh(r_+ \Delta t) \right) \ . \tag{3.87}$$

Here we are using the geodesic length in (6.68), and n controls the number of times the path encloses the horizon. In the metric formulation this sum can be understood as the sum over images that gives the propagator the correct periodicity condition (see e.g. [119]), which in complete agreement with our expression.

3.4.3 Local fields

In the last portion of this section we will evaluate and interpret $|U(y)\rangle$ as defined in (3.69). As mentioned there, this definition is gauge dependent. A definition of $|U(y)\rangle$ that reinstates this dependence is

$$|U(y)\rangle = G\left(g_L(y_0)g_L(y)^{-1}\right)\bar{G}\left(g_R^{-1}(y_0)g_R(y)\right)|\Sigma\rangle\,. \tag{3.88}$$

where y_0^μ is a bulk reference point where $|U(y_0)\rangle = |\Sigma\rangle$. In other words, the point y_0^μ defines where in the bulk we should locate the state $|\Sigma\rangle$. Once this choice is made, $|U(y)\rangle$ is a prescription on how to move through the bulk the state $|\Sigma\rangle$ from y_0^μ to a point y^μ.

We will decompose the state (3.88) as a sum over local functions in the infinite-dimensional representation

$$|U(y)\rangle = \sum_{k,\bar{k}=0}^{\infty} \Phi_{k,\bar{k}}^*(y)|h,k,\bar{k}\rangle\,, \tag{3.89}$$

and evaluate $\Phi_{k,\bar{k}}(y)$. Alternatively, the function $\Phi_{k,\bar{k}}(y)$ is

$$\Phi_{k,\bar{k}}(y) = \langle U(y)|h,k,\bar{k}\rangle = \langle h,k,\bar{k}|U(y)\rangle^\dagger\,. \tag{3.90}$$

This function is the object that will provide local bulk information in the Chern-Simons formulation of 3d gravity.

The explicit calculation of this $\Phi_{k,\bar{k}}(y)$ can be a complicated task. A way to proceed is by using the technique in Appendix A of [120]. The aim there is to find a differential operators $\mathcal{L}_a(y)$ whose action in the inner product (3.90) is

$$\langle U(y)|\ell_a|h,k,\bar{k}\rangle = \mathcal{L}_a(y)\,\langle U(y)|h,k,\bar{k}\rangle\,. \tag{3.91}$$

where ℓ_a is the infinite-dimensional generator that acts as in (3.22), and $\mathcal{L}_a(y)$ is a differential operator acting on the y variables, whose explicit form depends on the state $|U(y)\rangle$. Analogous formulas can be found for the barred sector. These operators are precisely the vector fields introduced in (3.82), i.e. we have

$$\mathcal{L}_a(y) = \zeta_a^\mu \frac{\partial}{\partial y^\mu}\,, \qquad \bar{\mathcal{L}}_a(y) = \bar{\zeta}_a^\mu \frac{\partial}{\partial y^\mu}\,. \tag{3.92}$$

Equation (4.22), together with (3.22), implies that

$$\mathcal{L}_{-1}\Phi_{k,\bar{k}}(y) = \sqrt{(k+1)(k+2h)}\Phi_{k+1,\bar{k}}(y)\,,$$
$$\bar{\mathcal{L}}_{-1}\Phi_{k,\bar{k}}(y) = \sqrt{(\bar{k}+1)(\bar{k}+2h)}\Phi_{k,\bar{k}+1}(y)\,. \tag{3.93}$$

$\Phi_{0,0}(y)$ can be fully determined by solving following differential equations

$$\mathcal{L}_0(y)\Phi_{0,0}(y) = h\Phi_{0,0}(y)\,, \qquad \mathcal{L}_1(y)\Phi_{0,0}(y) = 0\,, \tag{3.94}$$

together with its barred version. Therefore, we will be able to infer the form of $\Phi_{k,\bar{k}}(y)$, by successively applying $\mathcal{L}_{-1}(y)$, and $\bar{\mathcal{L}}_{-1}(y)$ to the seed $\Phi_{0,0}(y)$. From here it follows that $\Phi_{k,\bar{k}}(y)$ obeys the Casimir equation

$$\left(\mathcal{L}^2(y) + \bar{\mathcal{L}}^2(y)\right)\Phi_{k,\bar{k}}(y) = 4h(h-1)\Phi_{k,\bar{k}}(y)\,, \tag{3.95}$$

where $\mathcal{L}^2 = -(\mathcal{L}_{-1}\mathcal{L}_1 + \mathcal{L}_1\mathcal{L}_{-1}) + 2\mathcal{L}_0^2$. In other words, $\Phi_{k,\bar{k}}(y)$ is a local bulk field of mass $m^2 = 4h(h-1)$ and whose boundary conditions are given by the highest weight conditions (3.93)-(3.94).

Finally, once we have the explicit expression of the functions $\Phi_{k,\bar{k}}(y)$, we will compute the inner products of two states (3.89) as

$$\langle U(y_f)|U(y_i)\rangle = \sum_{k,\bar{k}}^{\infty} \Phi_{k,\bar{k}}(y_f)\Phi_{k,\bar{k}}^*(y_i)\,. \tag{3.96}$$

Note that when we evaluate (3.96) we will not make use of (3.41), and hence the derivations in this portion give an alternative and more direct derivation of (3.76). In the following, we will carry out this procedure for two explicit backgrounds. Sec. 3.4.3 is devoted to global AdS$_3$, which agrees completely with the results in [120], and Sec. 3.4.3 focuses on the static BTZ black hole.

Global *AdS$_3$*

Let us consider the state $|U\rangle$ for global AdS$_3$ and build explicitly $\Phi_{k,\bar{k}}(y)$ for this background. To start we will first infer the group elements from the standard metric for AdS$_3$, i.e.

$$ds^2 = -\cosh^2\rho\,dt^2 + d\rho^2 + \sinh^2\rho\,d\phi^2\,. \tag{3.97}$$

Using (3.75), it is straight forward to read from (3.97) unitary group elements g_L and $\tilde{g}_R$. Details are presented in App. 6.7, and the resulting elements are

$$g_L(y) = e^{(\ell_1-\ell_{-1})\rho/2}e^{-i\ell_0 x^+}\,, \qquad \tilde{g}_R(y) = e^{-i\ell_0 x^-}e^{(\ell_1-\ell_{-1})\rho/2}\,, \tag{3.98}$$

where $x^\pm = t \pm \phi$. We will use the definition (3.88) with $g_L(y_0) = \mathbb{1} = g_R(y_0)$; this places $|\Sigma\rangle$ at the origin of AdS in accordance with the results in [120–122]. This gives

$$\begin{aligned} |U(y)\rangle_{\text{AdS}} &= G\left(g_L(y)^{-1}\right)\bar{G}\left(g_R(y)\right)|\Sigma\rangle \\ &= G\left(g_L(y)^{-1}\tilde{g}_R(y)^{-1}\right)|\Sigma\rangle \\ &= e^{ix^+\ell_0}e^{-\rho(\ell_1-\ell_{-1})}e^{ix^-\ell_0}|\Sigma\rangle\,, \end{aligned} \tag{3.99}$$

where we used (3.30) and (3.98). For most of the following derivations we will drop the subscript "AdS" and restore it when needed.

The next step is to find the differential operators $\mathcal{L}_a(y)$ in (4.22) for global AdS$_3$. For that we use the inner product as

$$\Phi_{k,\bar{k}}(y) = \langle U(y)|h,k,\bar{k}\rangle = \langle\Sigma|e^{-ix^-\ell_0}e^{\rho(\ell_1-\ell_{-1})}e^{-ix^+\ell_0}|h,k,\bar{k}\rangle\,, \qquad (3.100)$$

Taking derivatives with respect to the global coordinates gives

$$\partial_{x^+}\langle U(y)|h,k,\bar{k}\rangle = -i\langle\Sigma|e^{-ix^-\ell_0}e^{\rho(\ell_1-\ell_{-1})}e^{-ix^+\ell_0}\ell_0|h,k,\bar{k}\rangle\,,$$
$$\partial_\rho\langle U(y)|h,k,\bar{k}\rangle = \langle\Sigma|e^{-ix^-\ell_0}e^{\rho(\ell_1-\ell_{-1})}(\ell_1-\ell_{-1})e^{-ix^+\ell_0}|h,k,\bar{k}\rangle\,,$$
$$\partial_{x^-}\langle U(y)|h,k,\bar{k}\rangle = -i\langle\Sigma|e^{-ix^-\ell_0}\ell_0 e^{\rho(\ell_1-\ell_{-1})}e^{-ix^+\ell_0}|h,k,\bar{k}\rangle\,, \qquad (3.101)$$

and using commutation relations, we can move the generators that are not in the exponents to the right, to get

$$\partial_{x^+}\langle U(y)|h,k,\bar{k}\rangle = -i\langle U(y)|\ell_0|h,k,\bar{k}\rangle\,,$$
$$\partial_\rho\langle U(y)|h,k,\bar{k}\rangle = \langle U(y)|(e^{-ix^+}\ell_1 - e^{ix^+}\ell_{-1})|h,k,\bar{k}\rangle\,,$$
$$\partial_{x^-}\langle U(y)|h,k,\bar{k}\rangle = -i\langle U(y)|\cosh 2\rho\,\ell_0 + \frac{\sinh 2\rho}{2}(e^{-ix^+}\ell_1 + e^{ix^+}\ell_{-1})|h,k,\bar{k}\rangle\,. \tag{3.102}$$

Now, it is straight forward to obtain the differential operators that follow (4.22) for global AdS$_3$; these read

$$\mathcal{L}_0 = i\partial_{x^+}\,,$$
$$\mathcal{L}_{\pm 1} = ie^{\pm ix^+}\left[\frac{\cosh 2\rho}{\sinh 2\rho}\partial_{x^+} - \frac{1}{\sinh 2\rho}\partial_{x^-} \mp \frac{i}{2}\partial_\rho\right]\,. \qquad (3.103)$$

It is important to remark that these differential operators were built without making direct reference to $|\Sigma\rangle$.

To find the barred differential operators we follow a procedure analogous to what we did in (3.101)-(3.102), but using the following inner product:

$$\Phi_{k,\bar{k}}(y) = \langle U(y)|h,k,\bar{k}\rangle = \langle\Sigma|\Sigma^{-1}e^{ix^+\bar{\ell}_0}e^{-\rho(\bar{\ell}_1-\bar{\ell}_{-1})}e^{ix^-\bar{\ell}_0}\Sigma|h,k,\bar{k}\rangle\,, \qquad (3.104)$$

where we are rewriting the action of the left group elements as an action via the right, i.e.

$$|U(y)\rangle_{\text{AdS}} = G\left(g_L(y)^{-1}\right)\bar{G}\left(g_R(y)\right)|\Sigma\rangle$$
$$= \bar{G}\left(\Sigma^{-1}\tilde{g}_R(y)g_L(y)\Sigma\right)|\Sigma\rangle\,. \qquad (3.105)$$

113

While in (3.100) we could ignore Σ, we are now forced to understand how Σ acts on the states to infer the differential operators $\bar{\mathcal{L}}_a$. A sensible choice is to require that $\bar{\mathcal{L}}_a$ are related to $\mathcal{L}_a$ by replacing $x^+ \leftrightarrow x^-$, i.e.

$$\bar{\mathcal{L}}_0 = i\partial_{x^-} , \tag{3.106}$$

$$\bar{\mathcal{L}}_{\pm 1} = ie^{\pm ix^-}\left[\frac{\cosh 2\rho}{\sinh 2\tilde{\rho}}\partial_{x^-} - \frac{1}{\sinh 2\rho}\partial_{x^+} \mp \frac{i}{2}\partial_\rho\right] .$$

This is the familiar assignment of Killing vectors in AdS$_3$; the interesting twist here is that not any choice of probe Σ will achieve this assignment. A choice of $|\Sigma\rangle$ that delivers (3.106) for the group element (3.104) is the crosscap state in (3.38):

$$|\Sigma\rangle = |\Sigma_{\text{cross}}\rangle .$$

The Ishisbashi state $|\Sigma_{\text{Ish}}\rangle$ has a different effect. Using (3.31) in (3.104) would lead to operators $\bar{\mathcal{L}}_a$ that are related to $\mathcal{L}_a$ through $x^+ \leftrightarrow -x^-$, and $\rho \to -\rho$. It is not clear if this choice has a natural interpretation in the geometrical description of fields in AdS$_3$, and it might be interesting to investigate this in the future.

Our starting point in this subsection was the metric for AdS$_3$ in (3.97). Another starting point is to use the fact that global AdS$_3$ is maximally symmetric, and the group elements that label rotations and translations in this space is

$$|U(y)\rangle_{\text{AdS}} = e^{i\ell_0 x^+} e^{i\bar{\ell}_0 x^-} e^{-\frac{\rho}{2}(\ell_1 - \ell_{-1} + \bar{\ell}_1 - \bar{\ell}_{-1})}|\Sigma_{\text{cross}}\rangle , \tag{3.107}$$

as it was done in [120, 122]. For the crosscap state, using (3.107) is in complete agreement with (3.98) and leads to favourable features, while the choice $|\Sigma_{\text{Ish}}\rangle$ would not lead to the usual notion of a local field in AdS$_3$.

The differential operators (3.103), and (3.106) are Killing vectors of global AdS$_3$, as advocated in Sec. 3.4.2. Moreover, $\left(\mathcal{L}^2(y) + \bar{\mathcal{L}}^2(y)\right)$ in (3.95) is the usual d'Alembertian for AdS$_3$. Therefore, $\Phi_{k,\bar{k}}(s)$ is a scalar field with mass $m^2 = 4h(h-1)$ in a global AdS background. Now, we can solve (3.94) using the previous differential operators, as done in [123]; the highest weight state is

$$\Phi_{0,0}(y) = \langle U(y)|h, 0, 0\rangle = \frac{e^{-2iht}}{(\cosh \rho)^{2h}} . \tag{3.108}$$

To find $\Phi_{k,\bar{k}}(y)$ we simply need to identify the solutions to (3.95) and organize them as $\mathcal{L}_{-1}(y)$, and $\bar{\mathcal{L}}_{-1}(y)$ acting on (3.108). This leads to

$$\Phi_{k,\bar{k}}(y) = C_{k,\bar{k}}\, e^{-ih(x^+ + x^-)}e^{-i(kx^+ + \bar{k}x^-)}(\tanh \rho)^{\bar{k}-k}(\cosh \rho)^{-2h}P_k^{(\bar{k}-k,\, 2h-1)}(\chi) , \tag{3.109}$$

where we define $\chi \equiv 1 - 2\tanh^2\rho$, the function $P_n^{(a,\,b)}(\chi)$ is a Jacobi polynomial, and $C_{k,\bar{k}} = (-1)^k \sqrt{\frac{k!(2h+\bar{k}-1)!}{\bar{k}!(2h+k-1)!}}$ is a constant that has been chosen to match the normalizations in (3.93). Therefore, we found the state (3.89) in a global AdS background. This is in complete agreement with the known results of normalizable wavefunction in AdS$_3$ as in, e.g., [124].

We are ready to compute the overlap of two states at different positions in the bulk. Using (3.96) with (3.109) gives

$$
\begin{aligned}
\langle U(y_f)|U(y_i)\rangle = \sum_{k,\bar{k}=0}^{\infty} & \, e^{-ih(\Delta x^+ + \Delta x^-)} e^{-i(k\Delta x^+ + \bar{k}\Delta x^-)} \frac{k!(2h+\bar{k}-1)!}{\bar{k}!(2h+k-1)!} \\
& \times (\tanh\rho_f \tanh\rho_i)^{\bar{k}-k}(\cosh\rho_f \cosh\rho_i)^{-2h} P_k^{(\bar{k}-k,\,2h-1)}(\chi_f) P_k^{(\bar{k}-k,\,2h-1)}(\chi_i)\,.
\end{aligned}
$$
(3.110)

The previous sum is performed in the Appendix 6.8. If we choose $x = \tanh^2\rho_i$, $y = \tanh^2\rho_f$, $r = e^{-i\Delta x^-}$, and $s = e^{-i\Delta x^+}$, the left hand side of (6.75) is equal to (3.110). Applying (6.75), we find

$$
\langle U(y_f)|U(y_i)\rangle = \frac{\left(\sigma(y_i,y_f) + \sqrt{\sigma^2(y_i,y_f) - 1}\right)^{-(2h-1)}}{2\sqrt{\sigma^2(y_i,y_f) - 1}} = \frac{e^{-2hD(y_i,y_f)}}{1 - e^{-2D(y_i,y_f)}}\,.
$$
(3.111)

where $D(y_i,y_f)$ is the geodesic length of global AdS, given in (6.67) with $C = -1/4$. This in complete agreement with the result in (3.76).

BTZ

As we did for global AdS$_3$, we will now find the local functions $\Phi_{k,\bar{k}}(y)$ for the static BTZ background. Our starting point is to build the group elements $(g_L, \tilde{g}_R)$ from the metric, which for the black hole reads

$$
ds^2 = -(r^2 - r_+^2)dt^2 + \frac{dr^2}{r^2 - r_+^2} + r^2 d\phi^2\,.
$$
(3.112)

In Appendix 6.7 we build the appropriate connections for the black hole are (6.62) that are compatible with (3.112) and unitary in the highest weight representation.

The resulting BTZ state is[5]

$$|U(y)\rangle_{\text{BTZ}} = G\left(g_L(y)^{-1}\tilde{g}_R(y)^{-1}\right)|\Sigma\rangle = e^{-\frac{i}{4}((8C-2)\ell_0-(4C+1)(\ell_1+\ell_{-1}))x^+}e^{-\rho(\ell_1-\ell_{-1})}$$
$$\times\, e^{-\frac{i}{4}((8C-2)\ell_0+(4C+1)(\ell_1+\ell_{-1}))x^-}|\Sigma\rangle\,,$$
(3.113)

where we casted all the elements as acting on the left, and we introduced

$$r = r_+\cosh^2(\rho-\rho_*)\,,\qquad 4C = e^{2\rho_*} = r_+^2\,,\qquad x^\pm = t\pm\phi\,.$$
(3.114)

Following the same procedure as in Sec. 3.4.3, we can find differential operators defined as (4.22) for the BTZ state. Using[6]

$$\Phi_{k,\bar{k}}(y) = \langle U(y)|h,k,\bar{k}\rangle = \langle\Sigma|e^{\frac{i}{4}((8C-2)\ell_0+(4C+1)(\ell_1+\ell_{-1}))x^-}e^{\rho(\ell_1-\ell_{-1})}$$
$$\times\, e^{\frac{i}{4}((8C-2)\ell_0-(4C+1)(\ell_1+\ell_{-1}))x^+}|h,k,\bar{k}\rangle\,,$$
(3.115)

we find the non-barred differential operators

$$\mathcal{L}_0 = -2\alpha_+\sqrt{C}\sinh\left(2\sqrt{C}x^+\right)\partial_\rho + \left(\alpha_- + \frac{1+f(\rho)^2}{2f(\rho)}\alpha_+\cosh\left(2\sqrt{C}x^+\right)\right)\partial_{x^+}$$
$$+ \frac{1-f(\rho)^2}{2f(\rho)}\alpha_+\cosh\left(2\sqrt{C}x^+\right)\partial_{x^-}\,,$$
$$\mathcal{L}_{\pm1} = \left(\pm\frac{1}{2}\cosh\left(2\sqrt{C}x^+\right) - 2\alpha_-\sqrt{C}\sinh\left(2\sqrt{C}x^+\right)\right)\partial_\rho$$
$$+ \left(\alpha_+ + \frac{1+f(\rho)^2}{8\sqrt{C}f(\rho)}\left(\alpha_-4\sqrt{C}\cosh\left(2\sqrt{C}x^+\right) \mp \sinh\left(2\sqrt{C}x^+\right)\right)\right)\partial_{x^+}$$
$$+ \left(\alpha_+ + \frac{1-f(\rho)^2}{8\sqrt{C}f(\rho)}\left(\alpha_-4\sqrt{C}\cosh\left(2\sqrt{C}x^+\right) \mp \sinh\left(2\sqrt{C}x^+\right)\right)\right)\partial_{x^-}\,.$$
(3.116)

with

$$f(\rho) \equiv \frac{e^{2\rho}-4C}{4C+e^{2\rho}}\,,\qquad \alpha_\pm \equiv \frac{i(4C\pm1)}{16C}\,.$$
(3.117)

In order to obtain the barred generators, we proceed as done for global AdS$_3$ in (3.104)-(3.105), i.e. we rewrite the state $|U(y)\rangle_{\text{BTZ}}$ as having an action only via

---

[5]Following the discussion around (3.88) and (3.98), we have chosen here $g_L(y_0) = \mathbb{1} = \tilde{g}_R(y_0)$. In contrast to global AdS$_3$, there is no physical motivation to make this choice for BTZ: it simply makes some of the subsequent manipulations easier. It would be interesting to investigate what is a physically sound choice of y_0^μ in future work.

[6]For simplicity, we will omit the subscript 'BTZ' in most of this section, and restore it when needed.

right group elements. This gives

$$\Phi_{k,\bar{k}}(y) = \langle U(y)|h,k,\bar{k}\rangle = \langle\Sigma|\Sigma^{-1}e^{\frac{i}{4}\left(-(8C-2)\bar{\ell}_0+(4C+1)(\bar{\ell}_1+\bar{\ell}_{-1})\right)x^+}$$
$$\times e^{\rho(\bar{\ell}_1-\bar{\ell}_{-1})}e^{\frac{i}{4}\left(-(8C-2)\bar{\ell}_0-(4C+1)(\bar{\ell}_1+\bar{\ell}_{-1})\right)x^-}\Sigma|h,k,\bar{k}\rangle\,.$$
$$(3.118)$$

As before, we will fix Σ such that the barred differential operators, $\bar{\mathcal{L}}_a$, are equal to the non-barred operators with $x^+ \leftrightarrow x^-$, as it is natural in the metric formulation. A quick inspection singles out $|\Sigma_{\text{cross}}\rangle$ as the appropriate choice rather than $|\Sigma_{\text{Ish}}\rangle$. Using $|\Sigma\rangle = |\Sigma_{\text{cross}}\rangle$ in (3.118) we find

$$\bar{\mathcal{L}}_0 = -2\alpha_+\sqrt{C}\sinh\left(2\sqrt{C}x^-\right)\partial_\rho + \left(\alpha_- + \frac{1+f(\rho)^2}{2f(\rho)}\alpha_+\cosh\left(2\sqrt{C}x^-\right)\right)\partial_{x^-}$$
$$+ \frac{1-f(\rho)^2}{2f(\rho)}\alpha_+\cosh\left(2\sqrt{C}x^-\right)\partial_{x^+}\,,$$
$$\bar{\mathcal{L}}_{\pm 1} = \left(\pm\frac{1}{2}\cosh\left(2\sqrt{C}x^-\right) - 2\alpha_-\sqrt{C}\sinh\left(2\sqrt{C}x^-\right)\right)\partial_\rho$$
$$+ \left(\alpha_+ + \frac{1+f(\rho)^2}{8\sqrt{C}f(\rho)}\left(\alpha_-4\sqrt{C}\cosh\left(2\sqrt{C}x^-\right)\mp\sinh\left(2\sqrt{C}x^-\right)\right)\right)\partial_{x^-}$$
$$+ \left(\alpha_+ + \frac{1-f(\rho)^2}{8\sqrt{C}f(\rho)}\left(\alpha_-4\sqrt{C}\cosh\left(2\sqrt{C}x^-\right)\mp\sinh\left(2\sqrt{C}x^-\right)\right)\right)\partial_{x^+}\,.$$
$$(3.119)$$

The differential operators (3.116) and (3.119) might not look like the standard basis for the local Killing vectors on BTZ. Nevertheless, they locally satisfy the Killing equation for (3.112) and the expected $sl(2,\mathbb{R})_L \times sl(2,\mathbb{R})_R$ algebra.

Having evidence that the state $|\Sigma_{\text{cross}}\rangle$ is a natural probe (with usual geometric properties we associate to BTZ), we can infer from (3.113) that

$$|U(y)\rangle_{\text{BTZ}} = e^{-\frac{i}{4}((8C-2)\ell_0-(1+4C)(\ell_1+\ell_{-1}))x^+}$$
$$\times e^{-\frac{i}{4}\left((8C-2)\bar{\ell}_0-(1+4C)(\bar{\ell}_1+\bar{\ell}_{-1})\right)x^-}e^{-\frac{\rho}{2}(\ell_1-\ell_{-1}+\bar{\ell}_1-\bar{\ell}_{-1})}|\Sigma_{\text{cross}}\rangle\,.$$
$$(3.120)$$

One can obtain $|U(y)\rangle_{\text{BTZ}}$ from the gauge transformation that relates global AdS$_3$ and BTZ, and using (3.107). We found, however, instructive to take a perspective where the metric is the first input and from there build (3.120).

It is very satisfactory that the same state, $|\Sigma_{\text{cross}}\rangle$, leads to a geometrical interpretation of $(\mathcal{L}_a, \bar{\mathcal{L}}_a)$ for both BTZ and global AdS$_3$. In contrast, the Ishibashi state $|\Sigma_{\text{Ish}}\rangle$ acting on (3.118) leads to some tension: $\mathcal{L}_a$ and $\bar{\mathcal{L}}_a$ for BTZ are not related via $x^+ \leftrightarrow -x^-$, and $\rho \to -\rho$, as we found for global AdS$_3$.

We now return to building $\Phi_{k,\bar{k}}(y)$. To start consider (3.94): given (3.116), it is clear that $\Phi_{0,0}(y)$ is non-separable in any of its variables, which makes (3.94) very difficult to solve. In order to simplify (3.94), we will make a change of variables; using (6.69) we now have

$$
\begin{aligned}
\mathcal{L}_0 = -\frac{1}{4r_+}&\Big(i\left(r_+^2+1\right)Z^2\partial_{X^+}+Z\left(r_+^2(X^-+1)+X^--1\right)\partial_Z\\
&+\left(r_+^2(X^-+1)^2+(X^--1)^2\right)\partial_{X^-}\Big),\\
\mathcal{L}_{\pm1} = -\frac{1}{4r_+}&\Big(i(r_+\mp i)^2Z^2\partial_{X^+}+((r_+\mp i)X^-+r_+\pm i)(r_+\mp i)Z\partial_Z\\
&+\left((r_+\mp i)X^-+r_+\pm i\right)^2\partial_{X^-}\Big),
\end{aligned}
\tag{3.121}
$$

The barred operators are defined analogously with $X^+\leftrightarrow X^-$. The advantage of (3.121), relative to (3.116), is that the differential operators just involve powers on the coordinates, and hence we can find a suitable polynomial solution to (3.94). The unique solution to (3.94) reads

$$
\Phi_{0,0}(y)=Z^{-2h}\left(-1+\frac{\left(X^-+\frac{r_++i}{r_+-i}\right)\left(X^++\frac{r_++i}{r_+-i}\right)}{Z^2}\right)^{-2h}
\tag{3.122}
$$

$$
=\left(2r\left(r_+^2+1\right)\cosh(r_+\phi)+\sqrt{r^2-r_+^2}\left((r_+-i)^2e^{-r_+t}+(r_++i)^2e^{r_+t}\right)\right)^{-2h}
$$

where in the second line we have changed to BTZ coordinates in (6.65). And as expected the solution (3.122) not separable in this coordinate system. Acting with $\mathcal{L}_{-1}(y)$, and $\bar{\mathcal{L}}_{-1}(y)$ in (3.122), and inspired by the the Jacobi polynomial form of the global case (3.109), the general expression for a descendant of (3.122) reads

$$
\begin{aligned}
\Phi_{k,\bar{k}}(y)=&C_{k,\bar{k}}\left(\frac{Z}{(X^-+a)(X^++a)-Z^2}\right)^{2h}\left(a\frac{(X^-+a)(X^++\frac{1}{a})-Z^2}{(X^-+a)(X^++a)-Z^2}\right)^{\bar{k}}\\
&\times\left(a\frac{(X^-+\frac{1}{a})(X^++\frac{1}{a})-Z^2}{(X^-+a)(X^++\frac{1}{a})-Z^2}\right)^{k}\left(a^2-1\right)^{2h}P_k^{(\bar{k}-k,\,2h-1)}(\kappa),
\end{aligned}
\tag{3.123}
$$

where

$$
\kappa=1-2\frac{(X^-+a)(X^++\frac{1}{a})-Z^2}{(X^-+a)(X^++a)-Z^2}\cdot\frac{(X^-+\frac{1}{a})(X^++a)-Z^2}{(X^-+\frac{1}{a})(X^++\frac{1}{a})-Z^2},\qquad a\equiv\frac{i+r_+}{-i+r_+},
\tag{3.124}
$$

and $C_{k,\bar{k}}$ is same factor as in (3.109). It is straight forward to verify that $\Phi_{k,\bar{k}}(y)$ in (3.123) satisfies the d'Alembertian equation on the static BTZ background.

Having an explicit expression for $\Phi_{k,\bar{k}}(y)$, we can compute the overlap of two states (3.89) for the BTZ black hole. Using (3.123), we see that he sum we need to perform in (3.96) is exactly equal to (6.75), where

$$X = \frac{|\tau_i|}{|\gamma_i|} \,, \qquad Y = \frac{|\tau_f|}{|\gamma_f|} \,, \qquad r = |a|^2 \sqrt{\frac{\tau_f \gamma_f^*}{\tau_f^* \gamma_f} \frac{\tau_i^* \gamma_i}{\tau_i \gamma_i^*}} \,, \qquad s = |a|^2 \sqrt{\frac{\tau_f^* \gamma_f^*}{\tau_f \gamma_f} \frac{\tau_i \gamma_i}{\tau_i^* \gamma_i^*}} \,, \tag{3.125}$$

and

$$\gamma_{i,f} \equiv (X_{f,i}^- + a)(X_{f,i}^+ + a) - Z_{f,i}^2 \,, \qquad \tau_{i,f} \equiv (X_{f,i}^- + \frac{1}{a})(X_{f,i}^+ + a) - Z_{f,i}^2 \,. \tag{3.126}$$

Using the result for the sum (6.75), with the previous definition for X, Y, r, and s, we find the the overlap of the two states in the BTZ black hole:

$$\langle U(y_f)|U(y_i)\rangle = \frac{\left(\sigma(y_i, y_f) + \sqrt{\sigma^2(y_i, y_f) - 1}\right)^{-(2h-1)}}{2\sqrt{\sigma^2(y_i, y_f) - 1}} \,, \tag{3.127}$$

where $\sigma(y_i, y_f)$ is the geodesic distance for Poincare (6.71), which can be rewritten as the geodesic length in BTZ (6.68) using (6.72). With no surprises, this is in complete agreement with (3.76).

It is interesting to analyse the behaviour of the field (3.123) in the BTZ coordinates. Looking at (6.72), we see that the BTZ boundary $r \to \infty$ is located at $Z \to 0$, and in this limit we have $\Phi_{k,\bar{k}} \to 0$. The horizon $r = r_+$ is at the Poincare boundary $(X^+, X^-, Z) \to \infty$, where $\Phi_{k,\bar{k}}$ as well vanishes. This behaviour, together with the fact that solves the BTZ wave equation, shows that (3.123) behaves as a *quasi-normal mode* for the black hole. However, it is not a traditional BTZ quasi-normal mode as those built in, e.g., [125–128]. There are a few discrepancies, and a few similarities, with this literature that are worth highlighting.

1. *Highest weight condition.* As it was observed in [129, 130], imposing the highest weight conditions (3.93)-(3.94) leads to eigenfunctions that obey the quasinormal modes conditions. This is a first indication that $\Phi_{k,\bar{k}}(y)$ should have been regular throughout, as they certainly are.

2. *Separability of eigenfunctions.* The most canonical way to find solutions to the Casimir equation (3.95) is by casting the basis of solutions in a Fourier decomposition in (t, ϕ), which are the natural directions for the Killing symmetries of the black hole. This leads a eigenfunctions that are separable functions in the coordinate system (r, t, ϕ), in strike contrast to (3.123). The construction of the operators $\mathcal{L}_a$ in [129], which is used to build a basis for

quasinormal modes, is as well compatible with the separability ansatz. From a technical point of view, our lack of separability could be attributed to the unitary condition we enforce in (3.120): this leads to a group elements that are simply different to those used in prior work.[7]

3. *Periodicity conditions.* By design, the connections $(A, \bar{A})$ that character-ize BTZ in the Chern-Simons formulation have the following feature [41, 131]: they are single valued along the thermal cycle in Euclidean signa-ture (smoothness of the Euclidean cigar geometry), and carry a non-trivial holonomy around the spatial cycle (an indication that the connection has a finite size horizon). This is reflected in (3.123) by the fact that our eigen-functions are not periodic as we take $\phi \sim \phi + 2\pi$, but are periodic under $t \sim t + i2\pi/r_+$. This is clearly not a feature of the modes built in [125–128], which are decomposed in periodic Fourier modes along the ϕ direction.

4. *Inner Product.* Despite the two differences above, it is interesting to note that if we evaluated the overlap (3.96) using the quasinormal modes in [126], it would lead to (3.127). The derivations are shown in appendix 6.9. This indicates that the bulk-to-bulk correlation functions are not sensitive to how we represent $\Phi_{k,\bar{k}}(y)$.

3.5   CFT interpretation

Here we discuss the CFT interpretation of the results above. In particular, consider computing a Wilson line in AdS$_3$, ending at the AdS boundary at the two boundary points z_1, z_2 at radial coordinate ρ_1, ρ_2 with generic boundary conditions U_1, U_2 at each endpoint. What, precisely, is this object in the CFT?

The considerations of the previous section should make it clear that the result-ing object is a suitably smeared two-point function, and here we simply provide a purely boundary interpretation of this smearing procedure. The kinematics of these procedure are very familiar from the language of the the HKLL construc-tion [132,133] and this section may be understood as a translation of some of those results into the language of Chern-Simons gravity.

Let us first consider what data we have; at each endpoint z_i in the CFT we are

---

[7]We could have parametrized the group elements in (3.120) so that we obtain the same basis for $\mathcal{L}_a$ in [129] that leads to separability. However, with this choice the state is not unitary and hence $\langle U| \neq (|U\rangle)^\dagger$.

supplied with a length scale $e^{-\rho_i}$ arising from the cutoff and an $SL(2,\mathbb{R})$ element arising from the boundary conditions on the Wilson line. There is a natural way to associate this data with the global descendants of a boundary operator $\mathcal{O}$: first, act on the Ishibashi crosscap state $|\Sigma_{\text{cross}}\rangle$ with the $SL(2,\mathbb{R})$ elements U_i as explained in detail in Section 3.3 to construct a state $|U_i\rangle$, where the states in the highest weight representation are understood as conformal descendants of $\mathcal{O}$. Next, remove two discs from the CFT, each centered at z_i with radius $e^{-\rho_i}$; on each of these discs place the boundary data appropriate to $|U_i\rangle$. This is the CFT dual to the open-ended Wilson line with boundary condition U_i.

Mathematically this is essentially the same construction as [120–122]. There are two main differences: in all of these works the specification of the $SL(2,\mathbb{R})$ element was interpreted to specify a point in AdS$_3$ rather than a boundary condition on a Wilson line. Furthermore in [121, 134, 135] the full Virasoro group was considered rather than just its global subgroup. The former is just a matter of interpretation, and we will touch briefly on the latter in the conclusion.

3.5.1 Example: CFT on the plane

We now present some elementary computations to explain how this works in the basic case of Poincaré AdS$_3$ in coordinates:

$$ds^2 = d\rho^2 + e^{2\rho}dzd\bar{z} \ , \tag{3.128}$$

dual to the CFT on the plane with complex coordinates $z, \bar{z}$. Rather than working with boundary data on the edge of an excised disc at each endpoint, it is more convenient to perform the state-operator correspondence to map each descendant on the edge to a local operator at the center of the disc. As there are an infinite number of states in the sum, this is a very non-local operator which we denote by $\mathcal{O}_{U_i}(z_i, \bar{z}_i)$. We will use a variant of the HKLL construction to compute the two-point function

$$\langle \mathcal{O}_{U_1}(z_1, \bar{z}_1)\mathcal{O}_{U_2}(z_2, \bar{z}_2)\rangle \ , \tag{3.129}$$

and then reproduce this answer from a Wilson line computation.

Focus on the first endpoint at $(z_1, \bar{z}_1)$. We first consider the case where the boundary state U_1 is the crosscap Ishibashi state $|\Sigma_{\text{cross}}\rangle$ itself. Consider the disc centered at z_1 in the CFT, with radius $e^{-\rho}$; we would like to place the boundary data corresponding to the crosscap Ishibashi state:

$$|\Sigma_{\text{cross}}\rangle = \sum_m (-1)^m |m, m\rangle = \sum_m (-1)^m c_m^2 \ell_{-1}^m \bar{\ell}_{-1}^m |h, h\rangle \ , \tag{3.130}$$

where the normalization constant in each sector is $c_m = \sqrt{\frac{\Gamma(2h)}{\Gamma(m+1)\Gamma(m+2h)}}$. We now use the state-operator correspondence to replace each state on the disc $\ell_{-1}^m \bar{\ell}_{-1}^m |0\rangle$ with the operator $\partial^m \bar{\partial}^m \mathcal{O}(z_1)$ at the center. However, we should note that the evolution from the center of the disc to the edge will cause each state's amplitude to be multiplied by a factor of $e^{+\rho(2h+2m)}$. Compensating for this, the operator that creates the crosscap state on a disc of radius $e^{-\rho_1}$ is

$$|\Sigma_{\text{cross}}\rangle \to \mathcal{O}_\Sigma^{(\rho_1)}(z_1, \bar{z}_1) = \sum_m c_m^2 (-1)^m e^{-\rho_1(2h+2m)} \partial^m \bar{\partial}^m \mathcal{O}(z_1, \bar{z}_1) \ . \qquad (3.131)$$

The sum over derivatives of the local operator $\mathcal{O}$ can be written as an integral over the following kernel [136, 137]

$$\mathcal{O}_\Sigma^{(\rho_1)}(z_1, \bar{z}_1) = \frac{2h-1}{\pi} \int dz d\bar{z} \left(\frac{e^{-2\rho_1} - (z-z_1)(\bar{z} - \bar{z}_1)}{e^{-\rho_1}} \right)^{2h-2} \mathcal{O}(iz, i\bar{z})$$
$$\equiv K(\rho_1, z_1, \bar{z}_1)[\mathcal{O}] \ , \qquad (3.132)$$

where in the last line we have introduced some new notation. We note that this is nothing but the usual HKLL smearing kernel in Euclidean signature, though our interpretation is somewhat different.

We now consider deforming away from the crosscap state to a more general U-state. The $SL(2,\mathbb{R})$ generators have a simple geometric action on the plane, and this geometric action results in a transformation of the parameters in kernel K. In particular, if we parametrize the $SL(2,\mathbb{R})$ element U_1 in a convenient way as

$$U_1 = e^{-w_1 \frac{i}{2}(-2L_0 - L_1 - L_{-1})} e^{\sigma_1(L_{-1} - L_1)} e^{\bar{w}_1 \frac{i}{2}(-2L_0 + (L_1 + L_{-1}))} \ , \qquad (3.133)$$

then it is shown in Appendix 6.10 that the appropriate smeared operator is

$$\mathcal{O}_{U_1}^{(\rho_1)}(z_1, \bar{z}_1) = K(\rho_1 + \sigma_1, z_1 + e^{-\rho_1} w, \bar{z}_1 + e^{-\rho_1} \bar{w}_1)[\mathcal{O}] \ . \qquad (3.134)$$

We now pause to interpret this result from the point of view of HKLL. Recall that the smearing function (3.134) corresponds to the HKLL representation of a bulk field in Poincaré coordinates (3.128), where the precise coordinate values of the bulk reconstructed field are

$$(\rho_a, z_a, \bar{z}_a) = (\rho_1 + \sigma, z_1 + e^{\rho_1} w, \bar{z}_1 + e^{-\rho_1} \bar{w}_1) \ , \qquad (3.135)$$

In particular, the proper distance D within AdS$_3$ between two points with coordinate values $(\rho_a, z_a, \bar{z}_a)$ and $(\rho_b, z_b, \bar{z}_b)$ satisfies $\cosh D = \sigma$ where

$$\sigma = \frac{e^{-2\rho_a} + e^{-2\rho_b} + (z_a - z_b)(\bar{z}_a - \bar{z}_b)}{2e^{-\rho_a - \rho_b}} \ . \qquad (3.136)$$

Let us now consider computing the two-point function (3.129) of two U states inserted at distinct points on the boundary z_1, z_2. This is a well-posed CFT computation involving integrals over two K kernels. Rather than repeat it here, we simply note that it is a standard HKLL computation, and by construction the result is the usual bulk-to-bulk AdS$_3$ propagator between points with Poincare coordinate values given by (3.135) (and a corresponding relation relating $(\rho_a, z_a, \bar{z}_a)$ to $(\rho_2, z_2, \bar{z}_2)$), i.e.

$$\langle \mathcal{O}_{U_1}^{(\rho_1)}(z_1, \bar{z}_1) \mathcal{O}_{U_2}^{(\rho_2)}(z_1, \bar{z}_1) \rangle = \frac{e^{-2h\sigma}}{1 - e^{-2\sigma}} \, . \tag{3.137}$$

Such expressions are by now very familiar.

We will now reproduce this CFT result from a Chern-Simons computation. In particular, we consider the following gauge connections for Poincaré AdS$_3$ in Euclidean signature:

$$a = \frac{i}{2} \left(-2L_0 + L_1 + L_{-1} \right) dz \, , \quad \bar{a} = -\frac{i}{2} \left(-2L_0 + L_1 + L_{-1} \right) d\bar{z} \, , \quad b = e^{(L_{-1} - L_1)\frac{\rho}{2}} \, . \tag{3.138}$$

As usual the full connections are related to the objects recorded here by $A = b^{-1} (a + d) b$, $\bar{A} = b(\bar{a} + d)b^{-1}$. Full conventions are in Appendix 6.7; in particular these connections are equivalent to those in (6.62) with $C \to 0$, together with the usual Euclidean continuation $x^+ \to z, x^- \to -\bar{z}$ and a rescaling of the field-theory directions by a factor of 2; the last step is convenient so that the resulting coordinate system is precisely equivalent to (3.128).

The prescription above states that the two point-function (3.129) is calculated in the Chern-Simosn representation by the following matrix element:

$$\langle \mathcal{O}_{U_1}^{(\rho_1)}(z_1, \bar{z}_1) \mathcal{O}_{U_2}^{(\rho_2)}(z_1, \bar{z}_1) \rangle = \langle U_2 | G \left(\mathcal{P} \, e^{-\int_\gamma A} \right) \bar{G} \left(\mathcal{P} \, e^{-\int_\gamma \bar{A}} \right) |U_1\rangle \, . \tag{3.139}$$

We may easily verify this relation. (3.43) now tells us that the right-hand side of this expression is equal to this matrix element is equal to

$$\langle U_2 | G \left(\mathcal{P} \, e^{-\int_\gamma A} \right) \bar{G} \left(\mathcal{P} \, e^{-\int_\gamma \bar{A}} \right) |U_1\rangle = \frac{e^{-h\alpha}}{1 - e^{-\alpha}} \, , \tag{3.140}$$

where as usual α is defined as the L_0 conjugacy class of the following group element:

$$V e^{-\alpha L_0} V^{-1} = \tilde{g}_R(y_2) U_2^{-1} g_L(y_2) g_L(y_1)^{-1} U_1 \tilde{g}_R(y_1)^{-1} \, , \tag{3.141}$$

with

$$\tilde{g}_R(y) = e^{\rho \frac{L_1 - L_{-1}}{2}} e^{-a_z z} \qquad g_L(y) = e^{\bar{a}_z \bar{z}} e^{\rho \frac{L_1 - L_{-1}}{2}} \, . \tag{3.142}$$

Computing α from here and the explicit representation of $U_{1,2}$ as in (3.133), we find that it is precisely equal to σ as defined in (3.136); thus we find that the Chern-Simons computation agrees with the CFT result, confirming (3.139).

Note that everything in this computation is fixed by kinematics, and we have simply shown how the $SL(2,\mathbb{R})$ parameters characterizing the boundary conditions combines with the geometric data to give the familiar HKLL result.

3.6   Discussion

We provided a full quantum mechanical description treatment of worldline degree of freedom of a Wilson line in $SO(2,2)$ Chern-Simons theory. This degree of freedom allowed us to build a local probe in the Chern-Simons description of AdS$_3$ gravity. There are a few striking features of this probe which we highlight.

1. We designed states in the worldline quantum mechanics such that they would couple to both $(A, \bar{A})$. This condition naturally introduced the notion of *rotated Ishibashi states*, which we denote as $|U\rangle$, and their coupling to the connections creates a background spacetime metric

$$g_{\mu\nu} = \frac{1}{2}\text{Tr}(A_\mu - \tilde{\bar{A}}_\mu)(A_\nu - \tilde{\bar{A}}_\nu) \, , \qquad (3.143)$$

   where $\tilde{\bar{A}} = U^{-1}\bar{A}U$. These rotated Ishibashi states are at the core of giving a geometric, and hence local, interpretation to $W_{\mathcal{R}}(y_f, y_i)$. In particular, we showed that $W_{\mathcal{R}}(y_f, y_i)$ is the bulk-to-bulk propagator of a scalar field propagating on (3.143). The most natural choice of rotated state that leads to regular background metrics is the crosscap state (3.38), i.e. $|U\rangle = |\Sigma_{\text{cross}}\rangle$.

2. Using purely the Chern-Simons formulation, we can build local bulk fields that probe the background geometry (3.143). These local probes are defined in (3.90) and we investigated some their properties for global AdS$_3$ and the static BTZ black hole.

It is very satisfactory that our choice $|U\rangle = |\Sigma_{\text{cross}}\rangle$ is compatible with the proposals in [120–122], and we also reproduce the smearing functions of the HKLL [132,133] proposal for vacuum solutions. This is expected since the symmetries of AdS$_3$ constrain heavily the resulting bulk field, leaving little room for disagreement at this level of discussion. Perhaps the interesting difference of our approach is that our construction leaves room to consider other probes $|U\rangle$, and highlights

some of the gauge dependence in the construction of the local field $\Phi_{k,\bar{k}}(y)$, which we emphasised around (3.88). For black holes the situation is more delicate: for instance, it would be interesting to compare and complement the proposals in [136, 138–141] with our derivations in Sec. 3.4.3. Along these lines it would be interesting to carry out our derivations for the rotating BTZ black holes, and other backgrounds in 3D gravity we have not explored.

We comment very briefly on one other aspect; as we have been able to reproduce bulk-to-bulk propagators from the Chern-Simons description of 3d gravity, it is worth wondering whether all of the aspects of the quantum field theory of a scalar field on a gravitational background can be obtained from the Chern-Simons computation, e.g. can we obtain a one-loop scalar field determinant on a BTZ black hole background? As this is essentially the same information as the bulk-to-bulk propagator, we might think so. Indeed we expect the logarithm of the one-loop determinant $\mathcal{W}$ to be the sum over connected Feynman diagrams, which in our context is the sum of Wilson lines that each wrap the horizon n times on topologically distinct paths C_n. We find:

$$\mathcal{W} = 2 \sum_{n=1}^{\infty} \frac{1}{n} \operatorname*{Tr}_{\mathcal{R}} \left[\mathcal{P} \exp\left(-\oint_{C_n} A \right) \mathcal{P} \exp\left(-\oint_{C_n} \bar{A} \right) \right] = 2 \sum_n \frac{1}{n} \left(\frac{e^{-hn\alpha}}{1 - e^{-n\alpha}} \right)^2,$$
(3.144)

Here we have assumed that the topologically trivial path does not contribute; the factor of 2 arises from positive and negative n. The combinatoric factor $\frac{1}{n}$ is a symmetry factor[8] and as usual α is the conjugacy class of the holonomy of A (or $\bar{A}$) around the black hole; on the BTZ background it evaluates to $\alpha = 2\pi r_+$. The result above is then precisely the logarithm of the usual one-loop scalar determinant on a black-hole background; see e.g. [142] for details and a repackaging of this result in CFT language.

An important issue that we have not addressed is quantum corrections due to fluctuations of the background connections. This would capture $1/c$ corrections, i.e. corrections controlled by the AdS radius in Planck units, or equivalently subleading terms controlled by the level of the Chern-Simons theory. Work in this direction has been done for $SL(2)$ Chern-Simons theory, where Virasoro conformal blocks are known to be tied to appropriate Wilson line in Chern-Simons [105, 143, 144]. Recent developments for this holomorphic theory include [145–149]. It would be interesting to evaluate $1/c$ corrections of our worldline quantum mechanics; in this case we expect that the intertwining of the two copies of $sl(2)$

---

[8]To understand this symmetry factor, consider having n objects which must be connected into closed paths; there are $(n-1)!$ distinct cycles (and not $n!$) as the starting point of the cycle is arbitrary. Compensating for this overcounting results in this factor of n.

will produce interesting features. For example, we should be able to probe if the global conditions in (3.37) are enhanced to the Virasoro conditions on the Ishibashi state [134,135], or something completely different, such as the conditions proposed in [137]. We leave these questions for future work.

Another natural direction forward is to use our construction to build probes in $SL(N) \times SL(N)$ Chern-Simons theory. This would provide a unique way to build local probes in higher spin gravity. The construction of Wilson line probes for higher spin backgrounds is reviewed in the following Chapter, and a discussion of Ishibashi states for $\mathcal{W}_3$ algebra was done in [150]. This is a natural starting point for future investigations.

4

ETERNAL HIGHER SPIN
BLACK HOLES

OR HOW TO CREATE A NOTION OF CAUSALITY FOR HIGHER SPIN GRAVITY
USING GRAVITATIONAL WILSON LINES

In the AdS/CFT correspondence, it is still unclear how the notion of classical spacetime is emergent from the degrees of freedom of the quantum field theory. A good framework to tackle this problem are higher spin gauge theories in AdS$_3$. These theories have an enlarged number of symmetries that causes that the notion of geometry becomes ill-defined. However, the Wilson lines studied in Chapter 3 can be extended to higher spin gravity theories, and can be thought as a higher-spin generalisation of the proper distance. In this chapter, based in [3], we exploit this fact. We use these Wilson lines to explicitly provide a notion of causality in higher spin gravity, which allows us to associate a Penrose diagram to higher spin black holes. We also provide new conditions for a higher spin black holes that assure its thermo-field double interpretation. Therefore, we introduce a notion of 'geometry' for higher spin gravity which is based on the degrees of freedom of the dual theory.

4.1   Introduction

Higher spin gauge theories of gravity provide toy models where one can examine ideas of stringy geometry in a controlled setting. In this chapter we consider these type of theories in three dimensions, and truncate of the number of spin fields

to $N - 1$. In Sec. 1.5, we reviewed the Chern-Simons formalism of higher spin gravity, as well as the construction of higher spin black hole solutions. Much of the literature about higher spin black holes deals with static properties and thermodynamics, and so can largely be thought of as studies of the black hole in its Euclidean section. In this chapter we study instead the Lorentzian structure of eternal higher spin black holes. In particular, as we review below, it is well-understood in AdS/CFT that an eternal black hole is dual to the thermo-field state in a doubled tensor product of the dual field theory Hilbert space. In what follows, we will discuss the interpretation of eternal higher spin black holes from this point of view.

In particular, the standard identification of the two-sided black hole with the thermofield state is tied to the causal structure of an eternal black hole. The fact that the two copies of the CFT are decoupled but entangled is roughly dual to the fact that the two boundaries of the eternal black hole are connected – but not causally so – by an Einstein-Rosen bridge. To fully flesh out this interpretation in the higher spin case, it would be helpful to give an operational meaning to the "causal structure" of an eternal higher spin black hole. As explained in Sec. 1.5, this is a nontrivial endeavour: in higher spin theories, conventional notions of geometry are not even gauge-invariant, and we will require different tools to organize our thinking.

These theories do not admit a conventional geometric understanding; however they do admit interesting higher-spin-invariant probes such the Wilson line operator. These objects are a generalization of gravitational AdS$_3$ Wilson studied in Chapter 3. In this case, we will see that they should be thought of as the higher-spin analogue of a bulk proper distance, and, therefore, they provide us with a sensitive probe of bulk higher spin geometries. Interestingly, we find that the study of Wilson lines on the eternal black hole background requires a refined understanding of regularity properties on the bulk gauge connections. One of our main results is the description of a particular bulk gauge choice – which we call *Kruskal gauge* – that is in many ways the Chern-Simons analogue of the Kruskal choice of coordinates that permit passage through the event horizon to the full maximally extended spacetime. This gauge choice simply amounts to demanding that the connections be *smooth* when evaluated at the Euclidean origin: while this may sound like a very benign condition, it involves an interplay between the bulk radial coordinate and Euclidean time, and so is novel from the point of view of Chern-Simons theory. In particular, it is stronger than the familiar "holonomy conditions" of Euclidean regularity that are normally used to define black hole connections: however, given a black hole that satisfies the holonomy condition, there is an algorithm that can be followed to place it into Kruskal gauge. Some

128

work that also implements this stronger notion of regularity is in [151].

With an understanding of this bulk gauge choice we then proceed to study the properties of eternal higher spin black holes. In this chapter, we present computations in several gauges to illustrate potential pitfalls, and verify that in Kruskal gauge, all correlators behave as expected for a thermofield state. We also study some of the resulting physics: in particular, we demonstrate that the interior of a two-sided eternal black hole "grows" with time (as measured by the action of a bulk Wilson line). We also highlight some interesting features of purely one-sided correlators, studying in particular the behavior of the extremal limit and providing evidence for the emergence of an infrared AdS$_2$.

The organization of this chapter is as follows. We begin in Sec. 4.2 by briefly reviewing generalization of the gravitation Wilson line in theories of higher spin gravity in AdS$_3$. In Sec. 4.3 motivating a more refined notion of regularity adequate for Lorentzian eternal black holes, defining two forms of the Kruskal gauge mentioned above and explaining their relation. In Section 4.4 we apply this formalism to the familiar BTZ black hole and discuss the maximally extended spacetime in the Chern-Simons formalism. In Section 4.5 we turn finally to the higher spin black hole, where we present computations in several gauges that have appeared in the literature previously as well as in Kruskal gauge. In Section 4.6 we discuss some simple applications, including a determination of the entanglement velocity chracterizing the speed of entanglement growth for the higher-spin black hole. We conclude in Section 4.7 with a brief discussion and some directions for future research.

4.2 Wilson lines in Higher spin gravity

This section is a summary of the results found in [4, 108, 111]. In these papers, they show that the gravitational Wilson line in AdS$_3$ higher spin gravity reproduces boundary two-point functions, and entanglement entropy in the dual CFTs. We will explain that this observable is the closest object that resembles a geodesic for higher spin gravities.

We consider again the Wilson line operator introduced in Sec. 3.2 in the context of AdS$_3$ gravity:

$$W_{\mathcal{R}}(y_i, y_f) = \langle U_f | \mathcal{P} \exp\left(-\int_\gamma A\right) \mathcal{P} \exp\left(-\int_\gamma \bar{A}\right) |U_i\rangle , \qquad (4.1)$$

where $\mathcal{R}$ is the representation, $\gamma(s)$ is a curve with bulk endpoints (y_i, y_f) parametrized by s, and $|U_i\rangle, |U_f\rangle \in \mathcal{R}$ are two states located at these endpoints. We are now interested in interpreting these Wilson lines as observables in AdS$_3$ higher spin gravity. In Sec. 1.5, we have seen that the Chern-Simon gauge connections should be chosen as $A, \bar{A} \in sl(N, \mathbb{R})$. In order for the Wilson line to carry the quantum numbers corresponding to a particle in the bulk, we choose $\mathcal{R}$ as the highest weight infinite-dimensional representation of $sl(N, \mathbb{R}) \oplus sl(N, \mathbb{R})$. The highest weight representation is defined respect to the reference state $|\mathrm{hw}\rangle = |h, h_3, ..., h_N\rangle$:

$$
\begin{aligned}
\ell_0 |\mathrm{hw}\rangle &= h |\mathrm{hw}\rangle \,, & \ell_1 |\mathrm{hw}\rangle &= 0 \,, \\
w_0^{(s)} |\mathrm{hw}\rangle &= h_s |\mathrm{hw}\rangle \,, & w_j^{(s)} |\mathrm{hw}\rangle &= 0 \,, \qquad j = 1, ... s-1 \,.
\end{aligned}
\tag{4.2}
$$

where $s = 2, ..., N$, and the elements ℓ_0, ℓ_{-1}, $w_0^{(s)}$, $w_j^{(s)}$ follow the $sl(N, \mathbb{R})$ algebra in (6.44). The use of lowercase means we are considering the generators in the infinite dimensional representation, in consistency with the notation in Sec. 3.3. An equivalent requirement to (4.2) is imposed for the barred sector of the algebra, and for simplicity we consider $(h, h_s) = (\bar{h}, \bar{h}_s)$. .

The Wilson line is evaluated as a path integral over an auxiliary field $U(s)$, whose dynamics are chosen such that it carries the information about the representation. This is analogous to what we did for pure gravity in Sec. 3.2, but in this case we need to consider a slightly generalized version of the probe action (3.6), and $U \in SL(N, \mathbb{R})$. For more details see [4]. In the $SL(N, \mathbb{R}) \times SL(N, \mathbb{R})$ case, the Wilson still computes boundary two-point functions [61]:

$$
W_{\mathcal{R}}(y_i, y_f) \underset{r \to \infty}{=} \langle \Psi | \mathcal{O}(x_i) \mathcal{O}(x_f) | \Psi \rangle \,.
\tag{4.3}
$$

where the heavy state $|\Psi\rangle$ carries higher spin charges, and backreacts to create a higher spin background, such as those studied in Sec. 1.5, with connections $(A, \bar{A})$. The parameters of the representation (h, h_s) are the dimensions of the light operator $\mathcal{O}(x)$[1]. To reproduce (4.3), the boundary values of the auxiliary field need to be fixed to $U_i = U_f = \mathbb{1}$, which ensures that the answer is Lorentz invariant. In Appendix 6.11, we review the explicit computation of these Wilson lines, which is controlled by traces of the following matrix

$$
M(y_i, y_f) = g_R(y_i) g_L(y_i) g_L^{-1}(y_f) g_R^{-1}(y_f) \,,
\tag{4.4}
$$

which assumes that the connections are flat, i.e.

$$
A = g_L dg_L^{-1} \,, \quad \bar{A} = g_R^{-1} dg_R \,.
\tag{4.5}
$$

---

[1] By analogy with the pure gravity case, light here denotes an operator whose eigenvalues are fixed as the central charge c goes to infinity. The heavy operator will have scaling dimensions that are linear with c.

It is important to remark that equation (4.3) is only valid in the semi-classical limit of the probe field, i.e. $c \gg h$, $h_s \gg 1$. In this case, the result for Wilson line is just given by the saddle-point approximation in the path integral. In this chapter we will only work with a semi-classical probe, in contrast with Chapter 3, where the goal was to evaluate AdS$_3$ Wilson line beyond this limit.

The Wilson line (4.3) was originally proposed in [108] to compute *holographic entanglement entropy* in higher spin gravity. In this paper, they fix the parameters of highest weight representation as:

$$ h_s = \bar{h}_s = 0\,, \qquad h = \bar{h}\,, \tag{4.6} $$

and the value of h is chosen such that it creates a conical deficit in the bulk à la [152]. In this situation, the Wilson line reproduces results for the entanglement entropy in the dual CFTs [153]. Moreover, it undergoes some other non-trivial checks. For example, the Wilson line with a closed path around the horizon of a higher spin black hole appropriately computes its entropy [52]. The proposal in [108] can be thought of as a generalization of the holographic entanglement entropy of Ryu and Takayanagi [154]. They showed that the entanglement entropy of a CFT region is equivalent to the length of a geodesic that connects its endpoints through the bulk. By extension, the Wilson line with (4.6) is considered as the closest object to the geodesic length for higher spin gravity theories. In the rest of this chapter, we will further develop this idea.

4.3 Eternal black holes

In general relativity, a Lorentzian eternal black hole can be maximally extended to possess two asymptotic regions that are connected through an Einstein-Rosen bridge. In the context of (ordinary, spin-2) AdS/CFT this is well-understood [119, 155]: the two asymptotic regions correspond to two copies of the dual field theory, and the black hole defines a thermofield state in the doubled field theory:

$$ |\psi\rangle = \frac{1}{\sqrt{Z}} \sum_n e^{-\frac{\beta}{2}(E_n + \mu Q_n)} |\mathcal{U}n\rangle_L \otimes |n\rangle_R \,. \tag{4.7} $$

We included in the definition of $|\psi\rangle$ a chemical potential μ that couples to a conserved charge Q that commutes with H. Here $|n\rangle$ runs over a full basis of energy eigenstates of the CFT, E_n and Q_n labels their energies and charges, and $\mathcal{U}$ is the anti-unitary operator that implements CPT. The full Hilbert space is composed by two copies of the original CFT Hilbert space: $\mathcal{H} = \mathcal{H}_L \otimes \mathcal{H}_R$.

We briefly review a Euclidean path integral "explanation" of this fact [119]. Consider performing the field theory Euclidean path integral on a manifold that is the product of the spatial direction(s) and an interval of Euclidean time with length $\frac{\beta}{2}$. It is necessary to specify field-theoretical boundary data on the two endpoints of the interval; the dependence of the path integral on the boundary data defines a state in the doubled copy of the field theory. This state is precisely (4.7). The suppression by $\exp\left(-\frac{\beta H}{2}\right)$ arises from the evolution through $\frac{\beta}{2}$ of Euclidean time.

Now consider implementing this procedure holographically. The path-integral over a full cycle of Euclidean time β with periodic boundary conditions corresponds to studying the usual Euclidean black hole described in Section 1.5. We may however cut open this path integral after evolution through Euclidean time $\frac{\beta}{2}$ and analytically continue to Lorentzian time. The resulting Lorentzian manifold is the eternal maximally extended black hole, and the arguments above indicate that the resulting field-theory state is the thermofield state (4.7).

Thus we expect that regular Euclidean gauge connections should (upon analytic continuation) map in a straightforward manner to the dual field theory in a thermofield state. This has consequences: as we review in Appendix 6.12, 2-point functions on this state satisfy very specific periodicity conditions. Consider a charged scalar operator $\mathcal{O}$, and we denote $\mathcal{O}_L$ as an operator acting on $\mathcal{H}_L$ and similarly for $\mathcal{O}_R$. Two point functions that involve $\mathcal{O}_{L,R}$ satisfy

$$
\begin{aligned}
\langle\psi|\mathcal{O}_R(t_f)\mathcal{O}_R(t_i)|\psi\rangle &= \langle\psi|\mathcal{O}_R(t_f)\mathcal{O}_R(t_i - i\beta)|\psi\rangle \\
&= \langle\psi|\mathcal{O}_L(-t_f)\mathcal{O}_L(-t_i)|\psi\rangle \\
&= \langle\psi|\mathcal{O}_L(-t_f - i\beta/2)\mathcal{O}_R(t_i)|\psi\rangle \\
&= \langle\psi|\mathcal{O}_R(t_f)\mathcal{O}_L(-t_i - i\beta/2)|\psi\rangle .
\end{aligned} \tag{4.8}
$$

In a mild notational abuse, we will refer to these all as Kubo-Martin-Schwinger or KMS conditions (even though technically only the first is "the" KMS condition).

We may now ask whether relations such as (4.8) are satisfied for eternal black holes in higher spin gravity. One immediate technical obstruction is that it is difficult to couple matter to these theories: a procedure as simple as probing the bulk with, for example, a scalar operator is cumbersome. This was one reason why in [156] the question of the thermofield state was phrased in Vasiliev's higher spin gravity which includes a massive scalar field.

However, this is an obstruction that we can now overcome, using the Wilson line (3.3), with its higher spin generalization explained in section 4.2. The key property is that as we take the endpoints to the boundary, the Wilson line computes two-
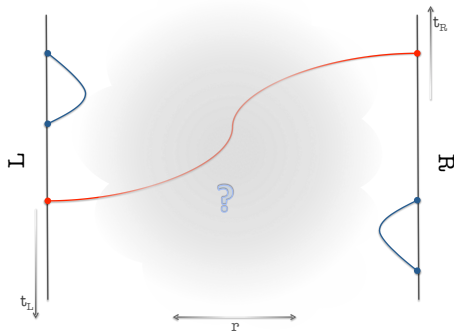
Figure 4.1: *Topology of the eternal black hole, which contains at least two boundaries: the right (R) boundary at $r \to \infty$ and left (L) boundary at $r \to -\infty$. At this stage the interior is undetermined (and hence the question mark). The different lines correspond to various Wilsons lines we will study: blue lines correspond to $W_{\mathcal{R}}(t_{i|R}, t_{f|R})$ or $W_{\mathcal{R}}(t_{i|L}, t_{f|L})$, and red to $W_{\mathcal{R}}(t_{i|R}, t_{f|L})$.*

point functions of CFT operators as shown in (4.3). As explained in Section 4.2, this fact still holds when we extend the definition to higher spin gravity [61]. We will often be interested in the particular case when the state $|\Psi\rangle$ in (4.3) is the thermofield state (4.7): in that case we access operators in the left or the right tensor factor of the Hilbert space by taking the bulk points y_i to the appropriate boundary. We will omit explicit mention of a radial coordinate and use a subscript notation to indicate on which side the corresponding boundary coordinate is located. For example, for a correlator between the right and left boundary we have

$$W_{\mathcal{R}}(x_{i|R}, x_{f|L}) = \langle \psi | \mathcal{O}_R(x_i) \mathcal{O}_L(x_f) | \psi \rangle \ , \tag{4.9}$$

with $|\psi\rangle$ the thermofield state. A schematic depiction of the configutations we will study are shown in Figure 4.1.

The Wilson line gives us a fairly sensitive probe of higher spin geometry, allowing us to directly evaluate correlation functions such as those appearing in (4.8). As we will see, establishing the validity of relations such as (4.8) in a two-sided black hole in the Chern-Simons formulation of gravity will require a more careful definition of Euclidean regularity than the holonomy condition (1.113).

4.3.1 Refined notions of Euclidean regularity

Here we describe the conditions required for a thermofield interpretation. Consider first choosing a radial coordinate r so that we can form the Cartesian complex coordinates

$$w = r \exp\left(\frac{2\pi i \tau}{\beta}\right) \ , \qquad \bar{w} = r \exp\left(-\frac{2\pi i \tau}{\beta}\right) \ . \tag{4.10}$$

We now claim that entirely regular physics on the Lorentzian section of a Euclidean black hole background – i.e. the interpretation of in terms of a thermofield state – requires *that the spacetime-dependent gauge parameters $g_L(y)$, $g_R(y)$ be smooth functions of $w, \bar{w}$ near the Euclidean origin.* In particular, we will allow only non-negative integer powers of $w, \bar{w}$ in a Taylor expansion about the origin:

$$g_L, \, g_R(w, \bar{w} \to 0) \sim \sum_{m,n \in \mathbb{Z}^+} c_{mn} w^m \bar{w}^n \ . \tag{4.11}$$

This is just the usual condition for smoothness of a scalar function at the origin of a disc D^2: nevertheless, interpreted from the Chern-Simons point of view, it is a stronger constraint on the bulk gauge connections than those normally considered in the literature. In particular, it is stronger than the holonomy condition (1.113) in that it involves radial dependence as well as the Euclidean time direction. This same important observation was made recently in [151]. The difference in the following will be the implementation of this more refined notion of regularity: the authors in [151] considered directly the metric-like fields and our implementation uses solely the Chern-Simons connections.

We will say that a connection satisfying (4.11) is in *strong Kruksal gauge*: as we explain, it is the gauge-theoretical analog of the Kruskal coordinate system that permits passage through the horizon. Note that in this gauge we have

$$A_\tau(r=0) = g_L \partial_\tau g_L^{-1}\big|_{r=0} = r \left(\frac{2\pi i}{\beta} g_L \left(e^{\frac{2\pi i \tau}{\beta}} \partial_w - e^{-\frac{2\pi i \tau}{\beta}} \partial_{\bar{w}}\right) g_L^{-1}\right)\bigg|_{r=0} = 0 \ , \tag{4.12}$$

where the the smoothness condition (4.11) ensures that the derivatives are regular at the origin, establishing the last equality. The time components of all gauge fields are zero at the horizon. This is a very natural condition for gauge fields propagating on black hole background (and indeed is extensively used in the usual understanding of the thermodynamics of charged black holes –see e.g. [157, 158]). It is thus interesting to note that the BTZ black hole written in the usual choice of gauge –despite (1.100) being widely accepted as being "regular"– actually does not satisfy it.

There is, however a weaker gauge condition that one can impose. We see from (4.4) that the Wilson lines studied in this paper depend only on the combination $g_R(y)g_L(y)$. Thus if we only care about such Wilson lines we might demand only that the composite field $g_R(y)g_L(y)$ be smooth as a function of $w, \bar{w}$, and not the individual functions $g_R(y)$ and $g_L(y)$ themselves. We will call this *weak Kruskal gauge*. In weak Kruskal gauge we find only that $A_\tau - \bar{A}_\tau = 0$ at the horizon, and the usual BTZ black hole turns out to already be in weak Kruskal gauge. We note that while the Wilson lines discussed in this paper cannot tell the difference between strong and weak Kruskal gauges, other probes that couple less symmetrically to the left and right connections – such as e.g. a particle with spin[2] – will be sensitive to the difference, and we expect such probes to display regular behavior only in strong Kruskal gauge. Importantly, the higher spin black hole as written in (1.125) is *not* in either Kruskal gauge.

The need for such conditions is most easily understood with a toy model of a flat $U(1)$ gauge field B in two dimensions. As a proxy for the near-horizon region, consider Euclidean $\mathbb{R}^2$:

$$ds^2 = dr^2 + r^2 d\tau^2 = dw d\bar{w} \ , \tag{4.13}$$

with $w = re^{i\tau}$ as usual. As B is flat, it can be written in terms of a group element $g(w, \bar{w}) \in U(1)$:

$$B = g^{-1} dg \ , \tag{4.14}$$

This is the $U(1)$ analog of (4.5). The $U(1)$ analog of the holonomy condition (1.113) merely states that g should be single-valued around the τ circle, i.e

$$g(r, \tau + 2\pi) = g(r, \tau) \ . \tag{4.15}$$

Importantly, it makes no reference to the radial direction. In particular, consider e.g.

$$g_0(r, \tau) = e^{i\tau} = \sqrt{\frac{w}{\bar{w}}} \ , \tag{4.16}$$

which respects this holonomy condition. Consider now a particle with $U(1)$ charge q moving on this Euclidean background: its action contains a term $iq \int_C B$ integrated along its worldline C, and there are no obvious pathologies associated with it.

Now we analytically continue Euclidean $\mathbb{R}^2$ to Rindler space $\mathbb{R}^{1,1}$ in the usual way via

$$w = -v \qquad \bar{w} = u. \tag{4.17}$$

---

[2]See [113, 159] for work towards constructing a Wilson line to describe such a particle.
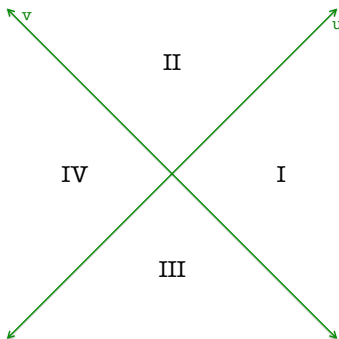
Figure 4.2: *Four quadrants covered by the coordinates (u, v) on $\mathbb{R}^{1,1}$. In quadrant **I**: $u > 0$, $v < 0$; in quadrant **IV**: $v > 0$, $u < 0$.*

The Lorentzian metric is simply $ds^2 = -dudv$ and is well defined for all u, v in all quadrants in Figure 4.2. However we now find that the analytic continuation of the $U(1)$ group element is

$$g_0(u, v) = \sqrt{-\frac{u}{v}} \ . \tag{4.18}$$

This has a branch cut along the horizons $uv = 0$: in other words, without specifying more information, the phase acquired by a charged particle moving on the Lorentzian section is ill-defined as we cross the quadrants in Figure 4.2. Thus the innocuous-seeming Euclidean group element (4.16) does not result in well-defined Lorentzian physics. The $SL(N, \mathbb{R})$ analog of this pathology will manifest itself later on when we attempt to compute two-sided correlators in the eternal black hole and demonstrate consistency with the properties of the thermofield state.

Precisely to avoid such ambiguities when performing the analytic continuation (4.17), the Kruskal gauge condition demands that $g(x)$ – or rather its $SL(N, \mathbb{R})$ analogs $g_L(y)$ and $g_R(y)$ – be smooth functions of $w, \bar{w}$, and thus also of u, v after analytic continuation.

We now show that the relations (4.8) follow from weak Kruskal gauge. We now show that the relations (4.8) follow from weak Kruskal gauge. As described in (4.4), boundary theory correlation functions are controlled through the Wilson line by the object

$$M(y_i, y_f) = g_R(y_i)g_L(y_i)g_L^{-1}(y_f)g_R^{-1}(y_f) \ , \tag{4.19}$$

where the points are at one of the two boundaries. We need to understand how

to go from Euclidean to Lorentzian time: as is conventional, the mapping is

$$w = f(r)e^{\frac{2\pi i}{\beta}\tau} \to -v \ , \qquad \bar{w} = f(r)e^{-\frac{2\pi i}{\beta}\tau} \to u \ , \qquad (4.20)$$

where $f(r)$ is an *odd* function that vanishes linearly at the black hole horizon and diverges at the AdS boundary. In quadrant **I** we have $u > 0$ and $v < 0$, which we parametrize in terms of a Lorentzian time coordinate t_R as

$$u = f(r)e^{\frac{2\pi}{\beta}t_R} \ , \qquad v = -f(r)e^{-\frac{2\pi}{\beta}t_R} \ . \qquad (4.21)$$

In quadrant **IV** we have $u < 0$ and $v > 0$, which we parametrize as

$$u = -f(r)e^{-\frac{2\pi}{\beta}t_L} \ , \qquad v = f(r)e^{\frac{2\pi}{\beta}t_L} \ . \qquad (4.22)$$

This identification uniquely fixes M in the entire maximally extended spacetime. We may now verify the validity of the relations (4.8), which require that the two-point function $\langle\psi|\mathcal{O}_R(t_f)\mathcal{O}_R(t_i)|\psi\rangle$ is equal to all of the following:

1. $\langle\psi|\mathcal{O}_R(t_f)\mathcal{O}_R(t_i-i\beta)|\psi\rangle$. A shift in τ by a full period β has no action on u, v, $u \to e^{2\pi i}u$, and M is single-valued as a function of u, v. This property (and only this property) actually follows from the holonomy condition (1.113) alone and does not require a Kruskal gauge.

2. $\langle\psi|\mathcal{O}_L(-t_f-i\beta/2)\mathcal{O}_R(t_i)|\psi\rangle$. From the global coordinates (4.22) and (4.21) we see that the point labeled by $(r = r_\Lambda, t_R = t_f)$ in the right quadrant is the *same* as the point labeled by $\left(r = r_\Lambda, t_L = -t_f \pm i\frac{\beta}{2}\right)$ in the left quadrant. Taking $r_\Lambda \to \infty$ now relates M to the appropriate correlation function. The equality with $\langle\psi|\mathcal{O}_L(-t_f - i\beta/2)\mathcal{O}_R(t_i)|\psi\rangle$ follows in the same way.

3. $\langle\psi|\mathcal{O}_L(-t_f)\mathcal{O}_L(-t_i)|\psi\rangle$. This equality is most easily understood by moving each point from the right quadrant to the left using the manipulation above, and then translating both arguments in Euclidean time by $\frac{i\beta}{2}$.

These relations may seem like kinematic trivialities: however it is important to note that if we do not pick the bulk gauge connections to satisfy (4.11), then branch cuts in the u, v plane mean that the relations above do not hold – for example the second relation was not satisfied by the scalar field correlators computed in [156]. We believe that (4.11) are, however, crucial for a complete interpretation of the black hole as a thermofield state.

4.3.2 Parametrizing black hole connections in Kruskal gauge

Having established the desirable properties of these gauges, we now turn to their explicit construction. As it turns out, any black hole can be placed in (either strong or weak) Kruskal gauge. Recall from (1.125) that the standard parametrization of black hole solutions to Chern-Simons gravity involves two constant flat connections $a, \bar{a}$ that point only in the field theory directions, in terms of which (4.5) becomes

$$g_L(y) = b(r)^{-1} e^{-a_i x^i} , \quad g_R(y) = e^{\bar{a}_i x^i} b(r)^{-1} . \tag{4.23}$$

From here we find that $A_\tau(r) = b^{-1}(r) a_\tau b(r)$ and thus is never zero for any value of r. This presentation of the black hole is then not in strong Kruskal gauge. To put it into strong Kruksal gauge, we will need to "unwrap" the effect of moving in τ. Note that (1.113) tells us that a_τ and $\bar{a}_\tau$ are conjugate to L_0

$$a_\tau = V \left(\frac{2\pi i L_0}{\beta} \right) V^{-1} , \qquad \bar{a}_\tau = \bar{V} \left(\frac{2\pi i L_0}{\beta} \right) \bar{V}^{-1} . \tag{4.24}$$

Consider now the following gauge transformation:

$$g_L^{(K)} = \Lambda_L g_L , \qquad g_R^{(K)} = g_R \Lambda_R , \qquad \Lambda_L = \Lambda_R^{-1} = \exp \left(\frac{2\pi i L_0}{\beta} \tau \right) G . \tag{4.25}$$

Here G is a constant (arbitrary) element of the group. The gauge transformed connections can be written

$$A^{(K)} = B(r, \tau)^{-1} \left(a_{(\phi)} + d \right) B(r, \tau) , \qquad \bar{A}^{(K)} = \overline{B}(r, \tau) \left(\bar{a}_{(\phi)} + d \right) \overline{B}^{-1}(r, \tau) . \tag{4.26}$$

Here the notation indicates that $a_{(\phi)}$ is a connection whose ϕ component is equal to that of the original a but whose τ component is zero. We have

$$B(r, \tau) = e^{a_\tau \tau} b(r) G^{-1} e^{-i L_0 \frac{2\pi \tau}{\beta}} , \qquad \overline{B}(r, \tau) = e^{i L_0 \frac{2\pi \tau}{\beta}} G \bar{b}(r) e^{-\bar{a}_\tau \tau} . \tag{4.27}$$

The gauge transformation (4.25) is far from unique. There are two crucial features of our choice. First, it is important that it winds once around $SL(2, \mathbb{R})$ as we traverse the time cycle. Second, it is a Lorentz transformation: this assures that the gauge transformation does not affect (4.4) which evaluates CFT correlators.

In the gauge (4.26) we can now impose the strong Kruskal gauge condition (4.11). Focusing for now on the unbarred connection, we see that this new parametrization treats r and τ together in the new object $B(r, \tau)$. It is convenient to use (4.24) to rewrite

$$B(r, \tau) = V e^{\frac{2\pi i \tau}{\beta} L_0} V^{-1} b(r) G^{-1} e^{-i \frac{2\pi \tau}{\beta} L_0} . \tag{4.28}$$

The full τ dependence now enters in the conjugation of $V^{-1}b(r)G^{-1}$ by $e^{i\frac{2\pi\tau}{\beta}L_0}$. The smoothness condition (4.11) tells us that in the expansion of B around the origin we can only have terms of the form $r^n e^{\pm\frac{2\pi i n\tau}{\beta}}$ with n integer, thus tying together the r and τ dependence. This is a constraint on $b(r)$: given a choice of a, we can now explicitly solve for $b(r)$. Typically we demand that $b(r)$ approach the standard choice at infinity so that our connections satisfy asymptotically AdS boundary conditions.[3] We note that there is still considerable freedom in the choice of $b(r)$: its behavior at infinity and at the horizon is fixed, but the topological nature of the theory means that it is essentially utterly unconstrained in the interior. In Appendix 6.14 we demonstrate an algorithm to find a suitable $b(r)$ explicitly for the higher spin black hole.

We turn now to weak Kruskal gauge. Here there is no need for an "unwrapping" procedure: instead, we may start from the original (4.23) and using the explicit diagonalization (4.24) we find

$$g_R(y)g_L(y) = \bar{V}\exp\left(\frac{2\pi iL_0\tau}{\beta}\right)\bar{V}^{-1}\left(\bar{b}(r)^{-1}b(r)^{-1}\right)V\exp\left(-\frac{2\pi iL_0\tau}{\beta}\right)V^{-1},$$

(4.29)

where we have omitted the ϕ dependence. We see that it is now the object $\bar{V}^{-1}\left(\bar{b}(r)^{-1}b(r)^{-1}\right)V$ that is conjugated by $e^{i\frac{2\pi\tau}{\beta}L_0}$: thus the analyticity condition applied to $g_R(y)g_L(y)$ can be viewed as a weaker condition on the product $b(r)\bar{b}(r)$.

To summarize: to put a black hole into weak Kruskal gauge we only need to judiciously choose the *product* $b\bar{b}$. To put it into strong Kruskal gauge we must unwrap the τ dependence via a Lorentz transformation and then judiciously choose $b(r), \bar{b}(r)$.

4.4 Eternal BTZ in Chern-Simons formulation

In this section we warm up by studying the familiar BTZ black hole in the Chern-Simons formulation of $SL(2,\mathbb{R})$ gravity. We will demonstrate that the definitions above permit access to all regions of the maximally extended spacetime. The results here can be compared with those obtained from the usual metric description of the BTZ black hole; see e.g. [119, 160, 161].

---

[3]It is very important that $b(r)$ and $\bar{b}(r)$ asymptote e^{rL_0} as $r \to \infty$. Relations such as (4.3) rely on this profile at infinity, and we do not want to tamper with it.

As we rewieved in Sec. 1.4.2, the connections corresponding to non-rotating BTZ can be written using:

$$A = b(r)^{-1} \left(a(x^+, x^-) + d \right) b(r) , \qquad \bar{A} = \bar{b}(r) \left(\bar{a}(x^+, x^-) + d \right) \bar{b}(r)^{-1} . \quad (4.30)$$

with

$$a = \left(L_1 - 2\pi\mathcal{L}L_{-1} \right) dx^+ , \qquad \bar{a} = - \left(L_{-1} - 2\pi\mathcal{L}L_1 \right) dx^- . \quad (4.31)$$

The black hole temperature can be determined by imposing the holonomy condition (1.113) and is $\beta = \sqrt{\frac{\pi}{2\mathcal{L}}}$. In the literature there is a standard choice for the radial functions $b(r)$, $\bar{b}(r)$, which we considered in (1.101). However, in this section we will instead *derive* them by demanding Euclidean regularity in the sense described in the previous section. The gauge connections (4.31) can be diagonalized as in (4.24). The definition of the similarity matrices $V, \bar{V}$ leaves unfixed the normalizations of each of the eigenvectors. By adjusting these normalizations $V, \bar{V}$ can be made to have unit determinant and also satisfy the following relations:

$$V(L_1 - L_{-1})V^{-1} = -2L_0 , \qquad \bar{V}(L_1 - L_{-1})\bar{V}^{-1} = -2L_0 , \quad (4.32)$$

as well as be related to each other via

$$V\bar{V}^{-1} = \exp(2\rho_0 L_0) , \quad \rho_0 \equiv \frac{1}{2} \log \left(2\pi\mathcal{L} \right) . \quad (4.33)$$

The relations among V and $\bar{V}$ – which are unique to $sl(2)$ and do not have a simple analog in the higher spin case – permit simple computations to be performed in the BTZ case. ρ_0 has been presciently named, but at this moment has no geometric significance.

4.4.1 Strong Kruskal gauge

We would first like to put the connections (4.31) in strong Kruskal gauge. We perform a time-dependent Lorentz transformation of the form described in (4.25):

$$\Lambda_L = \Lambda_R^{-1} = \exp \left(\frac{2\pi i L_0}{\beta} \tau \right) V^{-1} e^{\rho_0 L_0} . \quad (4.34)$$

With the benefit of hindsight, we have chosen $G = V^{-1} e^{\rho_0 L_0}$. Using (4.33) this is equivalent to

$$\Lambda_L = \Lambda_R^{-1} = \exp \left(\frac{2\pi i L_0}{\beta} \tau \right) \bar{V}^{-1} e^{-\rho_0 L_0} . \quad (4.35)$$

We now find that the gauge-transformed connection in the unbarred sector takes the form (4.26) with

$$B^{-1}(r,\tau) = e^{\frac{2\pi i L_0}{\beta}\tau} V^{-1} e^{\rho_0 L_0} b^{-1}(r) V e^{-\frac{2\pi i L_0}{\beta}\tau} V^{-1}, \qquad (4.36)$$

Consider now the Euclidean coordinates:

$$w \equiv \tanh\left(\frac{r}{2}\right) e^{\frac{2\pi i}{\beta}\tau} , \qquad \bar{w} = \tanh\left(\frac{r}{2}\right) e^{-\frac{2\pi i}{\beta}\tau} . \qquad (4.37)$$

Here (again with the benefit of hindsight) we have picked a specific radial function $\tanh\left(\frac{r}{2}\right)$ of r: in order for this change of coordinates to be well-defined this function must be odd and have a smooth Taylor expansion in odd powers of r (starting with the linear term in r) near $r = 0$. We now demand that $B(r,\tau)$ be a smooth function of $w, \bar{w}$. This is conveniently viewed as a constraint on the function $V^{-1} e^{\rho_0 L_0} b^{-1}(r) V$.

We briefly digress from this specific example to discuss the general case: consider expanding

$$V^{-1} e^{\rho_0 L_0} b^{-1}(r) V = \exp\left(\sum_a F_a(r) T^a\right) , \qquad (4.38)$$

with the $F_a(r)$ a set of mode functions and the T^a running over the generators of the algebra. The conjugation by $e^{\frac{2\pi i L_0}{\beta}\tau}$ attaches a power of $e^{-\frac{2\pi i h_a}{\beta}\tau}$ to each term in the sum, where $h(a)$ is the weight of the generator T^a under L_0. The analyticity condition then requires that $F_a(r \to 0) \sim r^{|h(a)|}$, so that the full radial and time dependence can be expressed as a product of integer powers of w and $\bar{w}$. In the higher spin case this system of constraints must be systematically solved, as explained in Appendix 6.14.

However for the purposes of the BTZ black hole it is sufficient to make a rather simple and consistent choice for F_a; we can take

$$V^{-1} e^{\rho_0 L_0} b^{-1}(r) V = \exp\left(\frac{r}{2}(L_1 - L_{-1})\right) . \qquad (4.39)$$

This choice satisfies the condition above, as $L_{\pm 1}$ have weight ± 1. Using (4.32) we then find

$$b(r) = \exp((r + \rho_0)L_0) . \qquad (4.40)$$

We can follow precisely the same procedure for the barred sector (using now the form of the gauge transformation in (4.35)) to derive an expression for $\bar{b}(r)$ and conclude that $\bar{b}(r) = b(r)$.

Finally, to put this into a more familiar form we can define a new coordinate $\rho \equiv r + \rho_0$, in terms of which we have

$$b(\rho) = \bar{b}(\rho) = e^{\rho L_0} \qquad (4.41)$$

This is of course the usual choice of radial gauge function used in (1.101) for the $SL(2, \mathbb{R})$ gravity, which we have now derived. Note that the horizon – which has physical significance as the fixed point of translations in Euclidean time, and the place where the time components of the Kruskal connections vanish – is at $r = 0$, which maps to the usual $\rho = \rho_0$. In this approach ρ_0 appeared purely algebraically from the original relation (4.33).

4.4.2 Maximally extended connections

From above we can now explicitly compute the spacetime-dependent gauge parameters $g_L(y)$ and $g_R(y)$ on the Euclidean section in the strong Kruskal gauge that we have constructed: in terms of $w, \bar{w}$ in (4.37) we find

$$
\begin{aligned}
g_L(y) &= \frac{1}{\sqrt{2\pi\beta(1 - w\bar{w})}} \begin{pmatrix} e^{-\frac{\pi\phi}{\beta}} \left(e^{\frac{2\pi\phi}{\beta}} - w\right)\beta & e^{-\frac{\pi\phi}{\beta}} \left(w + e^{\frac{2\pi\phi}{\beta}}\right)\pi \\ e^{-\frac{\pi\phi}{\beta}} \left(\bar{w}e^{\frac{2\pi\phi}{\beta}} - 1\right)\beta & e^{-\frac{\pi\phi}{\beta}} \left(e^{\frac{2\pi\phi}{\beta}}\bar{w} + 1\right)\pi \end{pmatrix}, \\
g_R(y) &= \frac{1}{\sqrt{2\pi\beta(1 - w\bar{w})}} \begin{pmatrix} e^{-\frac{\pi\phi}{\beta}} \left(e^{\frac{2\pi\phi}{\beta}} - \bar{w}\right)\beta & e^{-\frac{\pi\phi}{\beta}} \left(e^{\frac{2\pi\phi}{\beta}}w - 1\right)\beta \\ e^{-\frac{\pi\phi}{\beta}} \left(\bar{w} + e^{\frac{2\pi\phi}{\beta}}\right)\pi & e^{-\frac{\pi\phi}{\beta}} \left(e^{\frac{2\pi\phi}{\beta}}w + 1\right)\pi \end{pmatrix}.
\end{aligned}
\qquad (4.42)
$$

They are analytic and smooth functions of $w, \bar{w}$ near the origin. There is a singularity at $w\bar{w} = 1$: from (4.37) we see that this is the AdS boundary.

We can now analytically continue to the real-time coordinates u and v via (4.20) to obtain gauge parameters that are well defined on the entire maximally extended spacetime. Though we do not need it, we may also compute the metric following from these connections:

$$ds^2 = -\frac{4}{(1 + uv)^2} du\, dv + \left(\frac{2\pi}{\beta}\right)^2 \left(\frac{uv - 1}{uv + 1}\right)^2 d\phi^2 . \qquad (4.43)$$

This is the usual BTZ metric in Kruskal coordinates, and the associated Penrose diagram is depicted in Figure 4.3. It is important to note that this is nothing but the coordinate transformation of the original BTZ metric (6.65): the gauge transformation that we performed on the gauge connections to put it into strong
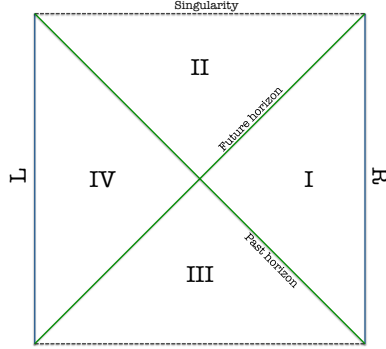
Figure 4.3: *Penrose diagram for static BTZ solution.*

Kruskal gauge is in the Lorentz subgroup of $SL(2, \mathbb{R}) \times SL(2, \mathbb{R})$, and so does not affect the metric.

From the form of $g_L(y)$ and $g_R(y)$ written above it is now straightforward to compute the Wilson line. Using (4.4) we compute between the trace of M between any two points (u_i, v_i) and (u_f, v_f) (we set the spatial separation to 0); this gives

$$\text{Tr}(M(y_i, y_f)) = \frac{2}{(1 + u_f v_f)(1 + u_i v_i)} \left((1 - u_i v_i)(1 - u_f v_f) + 2(u_f v_i + u_i v_f) \right) .$$
(4.44)

In the pure gravity case, the Wilson line between two points is related to this object via . Now by taking these points to the appropriate boundaries we may compute boundary correlators. It is instructive to map back to boundary time using the appropriate version of (4.21) and (4.22): on quadrant **I** with $u > 0$ and $v < 0$ we have

$$u = \tanh\left(\frac{r}{2}\right) e^{\frac{2\pi t_R}{\beta}} , \qquad v = -\tanh\left(\frac{r}{2}\right) e^{-\frac{2\pi t_R}{\beta}} ,$$
(4.45)

and on quadrant **IV** we have $u < 0$ and $v > 0$, leading to

$$u = -\tanh\left(\frac{r}{2}\right) e^{-\frac{2\pi t_L}{\beta}} , \qquad v = \tanh\left(\frac{r}{2}\right) e^{\frac{2\pi t_L}{\beta}} .$$
(4.46)

Note that the globally defined Killing vector corresponding to time translations is $u\partial_u - v\partial_v$, which is ∂_{t_R} on the right side and $-\partial_{t_L}$ on the left side.

Computing now the correlator between two points at the R boundary and keeping track only of the universal information, we find

$$\log W_{\mathcal{R}}(t_{i|R}, t_{f|R}) = -2h \log\left(-\frac{1}{\epsilon^2} \sinh^2\left(\frac{\pi}{\beta}(t_f - t_i)\right) \right) ,$$
(4.47)

where we have introduced a UV cutoff ϵ that vanishes at $r \to \infty$. On the other hand, we may also compute a correlator between an initial point on the right boundary and a final point on the left boundary. We then find

$$\log W_{\mathcal{R}}(t_{i|R}, t_{f|L}) = -2h \log\left(\frac{1}{\epsilon^2}\cosh^2\left(\frac{\pi}{\beta}(t_f + t_i)\right)\right) . \qquad (4.48)$$

These are of course just the usual results for geodesic distance on the BTZ black hole background. Note in particular that the two-sided correlator is related to the one-sided correlator by the KMS relation (4.8).

4.5   Eternal higher spin black holes

In this section we study the Lorentzian properties of higher spin black holes solutions. In particular, we will consider three different gauges which differ only by the radial parametrization of the connection:

Wormhole gauge: This corresponds to the choice of radial parametrization as $b(r) = \bar{b}(r) = e^{rL_0}$. The metric and connections are smooth for the entire range of r, with no horizon: hence it is a 'wormhole'. This gauge does not satisfy neither the weak or strong Kruskal condition. However, it does asymptote to AdS in the conventional sense at the R boundary, i.e. $r \to \infty$ in Figure 4.1, and hence reproduces CFT correlators.

Horizon gauge: This gauge is designed to give a horizon in the metric of the higher spin black hole. An explicit constructions is given in [51]: this solution does satisfy the weak Kruskal condition, however it does not asymptote to AdS on either side of Figure 4.1.

Strong Kruskal gauge: An explicit construction of connections that satisfies (4.11) and reproduces correctly the dual CFT correlators.

In higher spin gravity we lack the hindsight of BTZ due to the alternative metric formulation in the spin-2 case. Our way to probe and test our definitions will be to use the Wilson line (3.3) on the three Lorentzian backgrounds listed above. As mentioned around (4.3), $W_{\mathcal{R}}(C_{ij})$ captures boundary (CFT) correlators which allows us to test the KMS relations (4.8) for arbitrary probes. More importantly, $W_{\mathcal{R}}(C_{ij})$ is the object that describes the dynamics of massive (charged or not) particles in Chern-Simons theory: this gives a robust definition of causality and connectedness of the geometry which we can easily implement and exploit.

For concreteness, we will focus on higher spin black holes in $sl(3) \times sl(3)$ Chern-Simons theory. As showed in Appendix 6.11, for this theory we can compute the Wilson line in the saddle point approximation using:

$$- \log W_{\mathcal{R}}(C_{ij}) = \text{Tr}(\log(M)P_0) \ , \quad P_0 = \frac{h}{2}L_0 + w_3 W_0 \ , \qquad (4.49)$$

where P_0 governs the two quantum numbers of the representation $\mathcal{R}$: h which is the mass (or conformal dimension) and h_3 corresponding to the spin-3 charge of the probe. For $h \neq 0$ and $h_3 = 0$, equation (4.49) is the most natural definition of 'geodesic' in higher spin gravity; in particular, we will use the sign of $\log W_{\mathcal{R}}(C_{ij})$ to signal if endpoints are either spacelike, timelike or null separated. This is the key to associating a Penrose diagram to a given solution, and justify why our definition of Kruskal gauge actually gives rise to the desired definition of eternal black hole.

4.5.1 Failures and successes of the wormhole gauge

The wormhole gauge corresponds to black hole connections of the form (1.100) with boundary components given by (1.125)-(1.127) and radial functions $b(r) = \bar{b}(r) = e^{rL_0}$. This is the most commonly used parametrization of the connections in the literature.

To probe the geometry we will evaluate $W_{\mathcal{R}}(y_i, y_f)$ for the configurations shown in Figure 4.1. To start, we consider a Wilson line with no time separation $\Delta t = 0$, and with both endpoints in the asymptotic region R: for both holomorphic (1.126) and canonical (1.127) solutions, the result is

$$- \log W_{\mathcal{R}}(x_{i|R}, x_{f|R}) = h \log \left(\frac{\beta \sinh\left(\frac{\pi \Delta \phi}{\beta}\right)}{\pi \epsilon} \right)^4 + \frac{12h\mu^2}{\beta^2} \left[\frac{32\pi^2}{9} \left(\frac{\sigma \pi \Delta \phi}{\beta} \right) \coth \left(\frac{\pi \Delta \phi}{\beta} \right) \right.$$

$$\left. - \frac{20\pi^2}{9} - \frac{4\pi^2}{3} \operatorname{cosech}^2 \left(\frac{\pi \Delta \phi}{\beta} \right) \left\{ \left(\frac{\sigma \pi \Delta \phi}{\beta} \coth \left(\frac{\pi \Delta \phi}{\beta} \right) - 1 \right)^2 + \left(\frac{\sigma \pi \Delta \phi}{\beta} \right)^2 \right\} \right] + O(\mu^4) \ ,$$

$$(4.50)$$

where we used (6.101) with $h_3 = 0$ and expanded around $\mu \to 0$. Recall that in this notation $x_{i|R}$ denotes that the endpoint is placed at $r \to \infty$ (while $x_{i|L}$ used below will refer to $r \to -\infty$). The symbol σ has been introduced to differentiate between the two types of black holes

$$\sigma = 2 : \text{holomorphic black hole} \ ,$$

$$\sigma = 1 : \text{canonical black hole} . \tag{4.51}$$

These are the results originally reported in [108, 111].

The Wilson line has different features depending on whether the holomorphic and canonical solution is used. When expanded to first order in μ, the Wilson line (4.50) for the canonical black hole matches a perturbative CFT result found in [153] when $h = c/12(n-1)$: this corresponds to the dimension of the twist field that evaluates entanglement entropy as $n \to 1$. When interpreted as entanglement entropy, strong subadditivity inequalities imply that the Wilson line must be non-decreasing and concave down as a function of $\Delta\phi$ [162]. Direct examination of the function above shows that this is true for the canonical black hole [4, 163], but is not true for the holomorphic black hole [108, 111].

Another key requirement for the entanglement entropy is that when evaluated for large intervals in a mixed state, it should saturate to a linearly growing result $S_{EE}(\Delta\phi) \sim s\Delta\phi$ where s is the ordinary thermal entropy density associated to the mixed state. For most values of C this is true for both kinds of black hole, but for the holomorphic black hole there is an eigenvalue crossing at $C_0 = 3(9 + \sqrt{33})/8 \simeq 5.53$, and for $C < C_0$ the asymptotic limit of the holomorphic black hole entanglement entropy is then *not* consistent with its own thermal entropy density. While we present computations in both kind of black hole for completeness, we will restrict attention to the better-behaved canonical black hole when discussing the physical implications of our results.

The above result is only probing physics at the R boundary in Figure 4.1, but we can easily explore the properties of the geometry by moving the endpoints of the Wilson line. To start we set $\Delta\phi = 0$ and explore the dependence on the (r, t) plane. The Wilson lines for various configurations in Figure 4.1 reads

$$-\log W_{\mathcal{R}}(t_{i|R}, t_{f|R}) = h \log \left[\frac{C^2 \sinh^2\left(\frac{\pi\Delta t}{\beta}\right)\left(4(C-3)\sinh^2\left(\frac{\pi\Delta t}{\beta}\right) - 9\right)}{4\pi^2 \mathcal{L}^2 (C-3)^2(4C-3)\epsilon^4} \right] ,$$

$$\tag{4.52}$$

$$-\log W_{\mathcal{R}}(t_{i|L}, t_{f|L}) = h \log \left[\frac{4\pi^2 \mathcal{L}^2 \sinh^2\left(\frac{\pi\Delta t}{\beta}\right)}{C^2(C-3)^2(4C-3)\epsilon^4} \right]$$

$$+ h \log \left[(4(C-3)((C-6)C+4)^2 \sinh^2\left(\frac{\pi\Delta t}{\beta}\right) - (5(C-4)C+12)^2 \right] ,$$

$$\tag{4.53}$$

$$-\log W_{\mathcal{R}}(t_{i|R}, t_{f|L}) = h \log \left[\frac{4(C-3)((C-6)C+4)\cosh^4\left(\frac{\pi\Delta t}{\beta}\right)}{(C-3)^2(4C-3)\epsilon^4} \right.$$

$$\left. + \frac{(C(9C-38)+24)\cosh^2\left(\frac{\pi\Delta t}{\beta}\right) + 4C - 3}{(C-3)^2(4C-3)\epsilon^4} \right],$$
(4.54)

where C is given in (1.131), and we used (6.102). When both endpoints are at the R (or L) boundary we have $\Delta t = t_i - t_f$; when the endpoints are at different boundaries we have instead $\Delta t = t_i + t_f$. We should note that this reversal of the time coordinate on the left side may seem artificial, as in this gauge there is no notion of the bulk degeneration of the Killing direction; we perform it here largely for consistency with later sections, where it follows naturally. These expressions are valid for finite (μ, β) (or alternative finite charges $(\mathcal{L}, \mathcal{W})$).

From (4.52)-(4.54) we can draw many conclusions about the causal properties of the wormhole gauge. First, the solution is not symmetric with respect to the two boundaries R and L:[4] $W_{\mathcal{R}}(t_{i|R}, t_{f|R}) \neq W_{\mathcal{R}}(-t_{i|L}, -t_{f|L})$. This already violates one of the equalities listed in (4.8). Second, it is evident as well that $W_{\mathcal{R}}(t_{i|R}, t_{f|R}) \neq W_{\mathcal{R}}(-t_{i|R} - i\beta/2, t_{f|L})$: the wormhole gauge does *not* satisfy the last equality in (4.8). This solution cannot be interpreted as thermofield state.

Related to the two above properties, a third feature is as follows: the argument in the logarithm of (4.54) has a zero at

$$\cosh^2\left(\frac{\pi\Delta t}{\beta}\right) = \frac{-24 + C\left(38 - 9C - \sqrt{C(17C-60)+36}\right)}{8(C-3)((C-6)C+4)},$$
(4.55)

which has a real solution for Δt when $\sqrt{5} + 3 > C > 3$. This illustrates that a two-sided correlator will change sign depending on the time separation for this range of C; see Figure 4.4. If we interpret (4.54) as a geodesic distance between the two boundaries, it means that the separation between g_L and g_R can be either timelike, null or spacelike depending on Δt. Hence we can send timelike signals between the two sides in the wormhole gauge, which obviously does not fit the causal properties we would attribute to an eternal black hole.

It is instructive to compare our analysis with the one performed in [156]. There they evaluated two-sided correlators in a first order expansion about $\mu \to 0$ for

---

[4]This asymmetry is not an artefact of the position of the boundaries: the answers cannot be made symmetric by a rescaling of the cutoff ϵ at each boundary.

the scalar field in Vasiliev theory. This field has a non-zero spin-3 charge: we may mimic their analysis by considering a Wilson line with non-vanishing h_3 to find

$$W_{\mathcal{R}}(x_{i|R}, x_{f|R}) = \frac{4h_3\pi\mu}{3\beta} \frac{-3\sinh\left(\frac{2\pi(\Delta\phi+\Delta t)}{\beta}\right) + \frac{2\sigma\pi\Delta\phi}{\beta}\left(\cosh\left(\frac{2\pi(\Delta\phi+\Delta t)}{\beta}\right) + 2\right)}{\sinh^2\left(\frac{\pi(\Delta\phi+\Delta t)}{\beta}\right)}$$

$$+ (\Delta t \leftrightarrow -\Delta t) + \dots, \tag{4.56}$$

$$W_{\mathcal{R}}(x_{i|R}, x_{f|L}) = \frac{4h_3\pi\mu}{3\beta} \frac{\sinh\left(\frac{2\pi(\Delta\phi+\Delta t)}{\beta}\right) + \frac{2\sigma\pi\Delta\phi}{\beta}\left(\cosh\left(\frac{2\pi(\Delta\phi+\Delta t)}{\beta}\right) - 2\right)}{\cosh^2\left(\frac{\pi(\Delta\phi+\Delta t)}{\beta}\right)}$$

$$+ (\Delta t \leftrightarrow -\Delta t) + \dots, \tag{4.57}$$

where we are only displaying the linear term in μ-expansion of the Wilson line. The result above is in perfect agreement with the expression in [156,164]. The first order correction (4.57) does not have a singularity, and this suggests that the two boundaries are causally disconnected as argued in [156]. However, as illustrated by (4.55), this apparent regularity is an artifact of the μ expansion: over a finite range of C the correlator allows for timelike geodesics.

Based on this analysis, we would attribute to the wormhole gauge a Penrose diagram with a rectangular shape where signals can cross from one boundary to another. Even though this solution has no thermofield double interpretation, we should keep in mind that the result for the R side correlators are compatible with CFT computations. This agreement with the dual theory is an important feature to preserve as we build the connections associated with the thermofield state.

4.5.2 Failures and successes of the horizon gauge

We could attribute the failure of the wormwhole gauge to the lack of a preferred point in the geometry that we can associate with a horizon. The first attempt to fix this feature was discussed in [51]. They considered connections for which the radial function in (1.100) is modified as follows

$$A(r) = b(r)^{-1}(a+d)\,b(r)\,, \qquad b(r) = e^{(r+\rho_0)L_0}g(r)\,, \tag{4.58}$$
$$\bar{A}(r) = \bar{b}(r)\,(\bar{a}+d)\bar{b}(r)^{-1}\,, \qquad \bar{b}(r) = g(r)e^{(r+\rho_0)L_0}\,.$$

At this stage ρ_0 is a free parameter, which in [51] is set to be equal to the BTZ value(4.33). The group element $g(r)$ is fixed by demanding that the connections
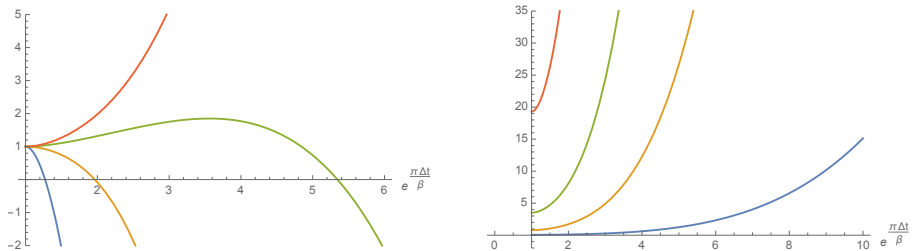
Figure 4.4: *Plot for the universal part of $W_{\mathcal{R}}^{-1}(t_{i|R}, t_{f|L})$ in the wormhole gauge (left), and horizon gauge (right). We set $h = \mathcal{L} = 1$ and the cutoffs are set to one (i.e. only the universal piece is plotted). The different curves correspond to different values of C: $C = 3.3$ (blue), $C = 4$ (yellow), $C = 5$ (green), and $C = 7.5$ (red). We see that for the wormhole gauge the correlator can change sign, while for the horizon gauge it is always positive.*

satisfy

$$A_t(-r) = h^{-1}(r)\bar{A}_t(r)h(r)\,, \tag{4.59}$$

$$A_\phi(-r) = -h^{-1}(r)\bar{A}_\phi(r)h(r)\,, \tag{4.60}$$

with $h(r) \in SL(3, \mathbb{R})$ and arbitrary modulo the condition $h(0) = \mathbb{1}$. In [51], one explicit combination of $h(r)$ and $g(r)$ is found that fulfils the above conditions. These results are reviewed in the Appendix 6.13. This construction provides a smooth horizon for the static holomorphic and canonical black hole. The motivation is quite natural: it is a generalization of the condition that the time component of the generalized vielbein $A_t(r) - \bar{A}_t(r)$ vanishes at a point. Their construction assures smoothness of the metric and spin-3 field around the horizon at $r = 0$, and for this reason we denote this construction as *horizon gauge*.

The horizon gauge is compatible with weak Kruskal gauge defined in Section 4.3.1. Both conditions imply the vanishing of $A_t(r) - \bar{A}_t(r)$ at the origin, and moreover we have verified that the combination $g_R(y)g_L(y)$ is a smooth function at the origin of the Euclidean disc. The real difference lies not at the horizon but at infinity: essentially the relations imposed above between A and $\bar{A}$ at all values of r seem to fix the behavior of $b(r), \bar{b}(r)$ everywhere. In particular, they do not approach the usual asymptotically AdS choice $b(r) \sim e^{rL_0}$ at infinity: this means that the CFT interpretation of this gauge choice is obscure, and has implications for correlation functions as computed using the Wilson line.

As in the wormhole case, we would like to analyze the features of the Wilson line for the horizon gauge. We consider first the case $\Delta\phi = 0$, and we compute the leading order of the Wilson line in the cutoff, which is denoted by ε in this case.

Using the results in sections 6.13 and 6.11, we obtain

$$-\log W_{\mathcal{R}}(t_{i|R}, t_{f|R}) = -\log W_{\mathcal{R}}(t_{i|L}, t_{f|L}) = h \log \left(\frac{3\beta \sinh\left(\frac{\pi \Delta t}{\beta}\right)}{8\pi\mu\varepsilon} \right)^4$$

$$-\frac{16h\pi^2\mu^2 \left(31 + \operatorname{csch}^2\left(\frac{\pi\Delta t}{\beta}\right)\right)}{9\beta^2} + O(\mu^4),$$

$$(4.61)$$

$$-\log W_{\mathcal{R}}(t_{i|R}, t_{f|L}) = h \log \left(\frac{3\beta \cosh\left(\frac{\pi \Delta t}{\beta}\right)}{8\pi\mu\varepsilon} \right)^4$$

$$-\frac{16h\pi^2\mu^2 \left(31 - \operatorname{sech}^2\left(\frac{\pi\Delta t}{\beta}\right)\right)}{9\beta^2} + O(\mu^4).$$

$$(4.62)$$

The full expression for the time correlators in the black hole gauge is less gentle to the eye than for the wormhole, and for this reason we only show the two first terms in the expansion around $\mu \to 0$. We see from (4.61)-(4.62) that at leading order in μ the KMS conditions in (4.8) hold; this persists at all orders in the μ-expansion. Therefore, the correlation functions of the black hole gauge do have the features of a thermofield double state.

To analyze if the two sides are connected or disconnected, analogously as we did in 4.5.1, we should consider all terms in the μ-expansion of $W_{\mathcal{R}}(t_{i|R}, t_{f|L})$. Since the expression is more cumbersome for finite μ, we plotted $W_{\mathcal{R}}(t_{i|R}, t_{f|L})$ for a wide range of values C, and found that it is always positive (see Fig. 4.4). This is in complete agreement that the horizon gauge has two causally disconnected sides, as it should.

However, there are some problems when we compare these answers with the results from wormhole gauge (which itself agrees with the CFT, as described earlier). For instance, if we expand the wormhole solution (4.52) around $\mu \to 0$ the result is

$$-\log W_{\mathcal{R}}(t_{i|R}, t_{f|R}) = h \log \left(\frac{\beta^4 \sinh^4\left(\frac{\pi \Delta t}{\beta}\right)}{\pi^4 \epsilon^4} \right)$$

$$-\frac{16h\mu^2\pi^2 \left(3 \operatorname{csch}^2\left(\frac{\pi\Delta t}{\beta}\right) + 5\right)}{3\beta^2} + O(\mu^4).$$

$$(4.63)$$

It is evident that (4.61) is not equal to (4.63) even if we try to adjust the cutoff ϵ and ε. A similar problem occurs if we consider spatial separations. Thus the

horizon gauge does not reproduce the known results of two point functions for spin-3 operators in a CFT with $\mathcal{W}_3$ symmetry.

4.5.3 A successful gauge

In this last portion we report on the values of the Wilson line for the strong Kruskal gauge. As discussed in section 4.3, this gauge is defined by demanding that $g_L(y)$ and $g_R(y)$ are smooth functions near the Euclidean origin. This imposes restrictions on the radial functions $b(r)$ and $\bar{b}(r)$; in Appendix 6.14 we demonstrate how to build a solution to these regularity conditions while preserving the asymptotic behavior. Note that once we know that a solution exists, we do not actually need to use its explicit form to calculate correlators: since we are imposing AdS asymptotics at the R boundary, one-sided correlators will agree with those computed from the wormhole gauge above. Furthermore by design of the strong Kruskal gauge, the Wilson line that interpolates between L and R is related to the single-sided correlator via the expected half-shift in β.

Thus for equal space separation the values of $W_{\mathcal{R}}(C_{ij})$ are

$$\log W_{\mathcal{R}}(t_{i|R}, t_{f|R}) = \log W_{\mathcal{R}}(t_{i|L}, t_{f|L})$$
$$= -h \log \frac{C^2 \sinh^2\left(\frac{\pi \Delta t}{\beta}\right)\left(4(C-3)\sinh^2\left(\frac{\pi \Delta t}{\beta}\right) - 9\right)}{4\pi^2 \mathcal{L}^2 (C-3)^2(4C-3)\epsilon^4} , \quad (4.64)$$

$$\log W_{\mathcal{R}}(t_{i|R}, t_{f|L}) = -h \log \frac{C^2 \cosh^2\left(\frac{\pi \Delta t}{\beta}\right)\left(4(C-3)\cosh^2\left(\frac{\pi \Delta t}{\beta}\right) + 9\right)}{4\pi^2 \mathcal{L}^2 (C-3)^2(4C-3)\epsilon^4} . \quad (4.65)$$

Recall that these expressions hold for both holomorphic and canonical black holes since the time component of $(A, \bar{A})$ is the same. Since $C \geq 3$, the argument of logarithm of (4.65) is always positive: at zero spatial separation the two sides are causally disconnected for all ranges of Δt. This gauge is so far compatible with the expected properties of an eternal higher spin black hole, and it reproduces correctly the known results in the CFT (which involve setting $\Delta t = 0$ and a fix charge configuration without chemical potentials).

It is also useful to record the values of the Wilson lines for $\Delta t = 0$. If the probe

is not charged, i.e. $h_3 = 0$, we have

$$
\log W_{\mathcal{R}}(x_{i|R}, x_{f|R}) = -h \log \left[\frac{\left(1 + \frac{3}{\sqrt{4C-3}}\right) e^{\lambda_1 \Delta\phi} - 2\, e^{\lambda_2 \Delta\phi} + \left(1 - \frac{3}{\sqrt{4C-3}}\right) e^{\lambda_3 \Delta\phi}}{8\pi\mathcal{L}(C-3)C^{-1}\epsilon^2} \right.
$$
$$
\left. \times\ \frac{\left(1 + \frac{3}{\sqrt{4C-3}}\right) e^{-\lambda_1 \Delta\phi} - 2\, e^{-\lambda_2 \Delta\phi} + \left(1 - \frac{3}{\sqrt{4C-3}}\right) e^{-\lambda_3 \Delta\phi}}{8\pi\mathcal{L}(C-3)C^{-1}\epsilon^2} \right],
$$
$$
\log W_{\mathcal{R}}(x_{i|R}, x_{f|L}) = -h \log \left[\frac{\left(1 + \frac{3}{\sqrt{4C-3}}\right) e^{\lambda_1 \Delta\phi} + 2\, e^{\lambda_2 \Delta\phi} + \left(1 - \frac{3}{\sqrt{4C-3}}\right) e^{\lambda_3 \Delta\phi}}{8\pi\mathcal{L}(C-3)C^{-1}\epsilon^2} \right.
$$
$$
\left. \times\ \frac{\left(1 + \frac{3}{\sqrt{4C-3}}\right) e^{-\lambda_1 \Delta\phi} + 2\, e^{-\lambda_2 \Delta\phi} + \left(1 - \frac{3}{\sqrt{4C-3}}\right) e^{-\lambda_3 \Delta\phi}}{8\pi\mathcal{L}(C-3)C^{-1}\epsilon^2} \right].
$$
$$
(4.66)
$$

These functions are plotted in Figure 4.5. Here λ_i are the eigenvalues of a_ϕ component of the connection which read

$$
(\lambda_1, \lambda_2, \lambda_3)
$$
$$
= \sqrt{\frac{2\pi\mathcal{L}}{C}} \left(-\sigma + \sqrt{4C-3}\,\frac{2C + 3(\sigma - 2)}{2C - 3},\ 2\sigma,\ -\sigma - \sqrt{4C-3}\,\frac{2C + 3(\sigma - 2)}{2C - 3} \right)
$$
$$
(4.67)
$$

and σ controls if the solution is holomorphic or canonical as defined in (4.51).

It is also interesting to evaluate the Wilson line with $h = 0$ and $h_3 \neq 0$: this would correspond to a probe that only carries higher spin charge. In Figure 4.6 we plot the behavior of such a Wilson line between two spatially separated points on the two boundaries. It is interesting that there is a reflection symmetry associated with flipping the sign of the spatial direction together with the higher spin charge of the probe: $W_{\mathcal{R}}(x_{i|R}, x_{f|L})\big|_{h_3} = W_{\mathcal{R}}(-x_{i|R}, -x_{f|L})\big|_{-h_3}$. The behavior shown here may be interpreted as a potential well felt by the charged probe arising from its coupling to the background spin-3 field. It would be interesting to explore further the implications of such non-monotonic behavior.

4.6 Applications

In this section we explore various properties of the thermofield state in higher spin gravity as accessed by the two-sided black hole in Kruksal gauge. We perform our
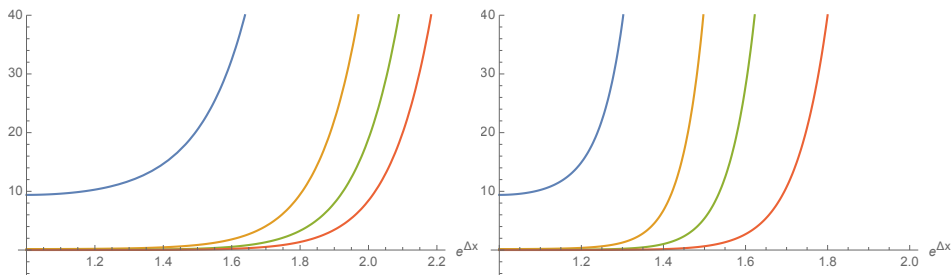
Figure 4.5: *Plot of the universal part of $W_{\mathcal{R}}^{-1}(x_{i|R}, x_{f|L})$ when $h = 2$, $h_3 = 0$ for canonical (left), and holomorphic black hole (right). Here $\mathcal{L} = 1$ and we removed the cutoff. The different curves correspond to different values of C: $C = 3.3$ (blue), $C = 4$ (yellow), $C = 5$ (green), and $C = 7.5$ (red). We see that for both black holes the correlator is always positive.*
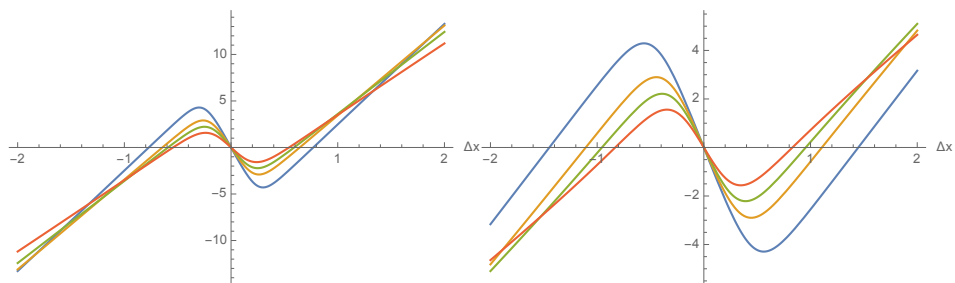

Figure 4.6: *Plot of $-\log W_{\mathcal{R}}(x_{i|R}, x_{f|L})$ when $h = 0$, $h_3 = 1$ for in the canonical (left), and holomorphic black hole (right). The different curves correspond to different values of C: $C = 3.3$ (blue), $C = 4$ (yellow), $C = 5$ (green), and $C = 7.5$ (red).*

computations in the canonical black hole: for the most part, the results for the holomorphic black hole are very similar, except where the complications in the holomorphic black hole discussed around (4.51) manifest themselves.

4.6.1 Higher spin black hole interiors and entanglement velocities

It is well-known that the interior of a ordinary (spin-2) eternal black hole grows as one moves "upwards" in time (i.e. in the time direction $\partial_{t_L} + \partial_{t_R}$ that is orthogonal to the Killing direction). It was demonstrated in [165] that this growth can be given a simple field-theoretical interpretation in terms of the time-dependence of entanglement entropy.

We briefly review the setup: recall from (4.7) that the thermofield state is given by

$$|\psi\rangle = \frac{1}{\sqrt{Z}} \sum_n e^{-\frac{\beta}{2} H} |\mathcal{U}n\rangle_L \otimes |n\rangle_R \,, \qquad H|n\rangle = (E_n + \mu Q_n)|n\rangle \,, \qquad (4.68)$$

where we have included the deformation by the chemical potential in the Hamiltonian. One can now define a one-parameter family of states by acting on this state with the sum of the left and right Hamiltonians:

$$|\psi(t_\star)\rangle \equiv e^{i(H_L + H_R)t_\star}|\psi\rangle \,. \qquad (4.69)$$

This action moves us "upwards" in time (note that the orthogonal action of $H_L - H_R$ leaves $|\psi\rangle$ invariant, and corresponds in the bulk to the Killing direction). Consider now the entanglement entropy in the state $|\psi(t_\star)\rangle$ of a region given by the union of two intervals, one in the left CFT and one in the right, both of length $\Delta\phi$. This may be computed holographically by considering the geometry shown in Figure 4.7, where the endpoints on each side are separated by a distance $\Delta\phi$ and are located at $t_L = t_R = t_\star$, where $t_\star$ increases as we move upwards.

In our setup, there are two configurations of Wilson lines that contribute: one set of Wilson lines joins each endpoint of an interval with its partner in the other CFT by crossing through the black hole interior. Its contribution can be found from (4.64) with $\Delta t = t_L + t_R = 2t_\star$ to be

$$S_{conn} = -2 \log W_{\mathcal{R}}(t_{i|R}, t_{f|L}) \quad \sim \quad 2h \log \frac{C^2 e^{\frac{8\pi t_\star}{\beta}}}{16\pi^2 \mathcal{L}^2 (C-3)(4C-3)\epsilon^4}$$
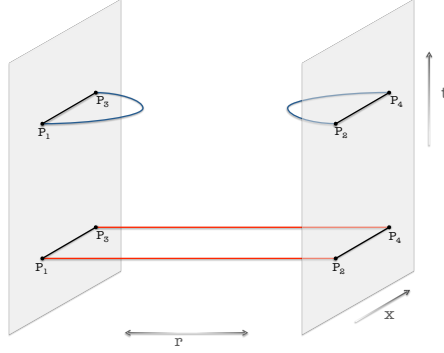
Figure 4.7: *Configurations for time evolution of entanglement entropy in the thermofield state. From the bulk perspective it is a competition between the connected configuration (red lines), which gives* (4.70), *and the disconnected contribution (blue lines) in* (4.71).

$$= \frac{16h\pi t_\star}{\beta} + S_{div} \ , \tag{4.70}$$

where we have specialized to times $t_\star \gg \beta$ and where

$$S_{div} \equiv 2h \log \left[\frac{C^2}{16\pi^2 \mathcal{L}^2 (C-3)(4C-3)\epsilon^4} \right] \ . \tag{4.71}$$

The second configuration contains two Wilson lines that each remain outside the black hole horizon. In this case, the result will be given by twice the one-sided Wilson line in (4.66) with $\Delta t = 0$. We will consider the limit $\Delta\phi \gg \beta$: extracting the dominant long-distance contribution we find

$$
\begin{aligned}
S_{disc} = -2 \log W_\mathcal{R}(x_{i|R}, x_{f|R}) \quad &\sim \quad 2h \log \frac{C^2 e^{(\lambda_1 - \lambda_3)\Delta\phi}}{4(C-3)(4C-3)\epsilon^4} \\
&= \quad 4h \sqrt{\frac{2\pi\mathcal{L}(4C-3)}{C}} \Delta\phi + S_{div} \ . \tag{4.72}
\end{aligned}
$$

Up till now we have focused on Wilson lines as computing two-point functions of light operators. However, as was argued in [108, 111], these Wilson lines also compute entanglement entropy if one evaluates them at the precise dimension $h \to \frac{c}{12}$. It is convenient to write the above results in terms of the entropy density in units of the inverse temperature:

$$s = \frac{c}{6} \left(\frac{\pi}{\beta} \frac{2C-3}{C-3} \right) \ . \tag{4.73}$$

We now normalize the results with this entropy density to find:

$$S_{conn} = 4svt_\star + S_{div} \ , \qquad S_{disc} = 2s\Delta\phi + S_{div} \ , \tag{4.74}$$

155

where for the time-dependent configuration we have defined an entanglement velocity

$$v \equiv \frac{C-3}{C-\frac{3}{2}} \, , \tag{4.75}$$

which interpolates from $v \to 1$ at zero higher spin charge to $v \to 0$ as we approach the extremal higher spin black hole. We see that at small times the answer is dominated by the connected configuration; however as time goes on the inside of the black hole grows linearly in size, and the connected configuration becomes energetically more and more expensive. Eventually there is a phase transition to the disconnected configuration at $t_\star = \frac{\Delta\phi}{2v}$, after which the entanglement entropy saturates at its thermal value.

The interpretation of these results is standard [165, 166]. The time evolution of entanglement entropy in $1+1$ dimensional systems may be viewed in terms of a quasi-particle picture: if the initial state is excited but has essentially only short-range entanglement, then upon time evolution the entanglement entropy grows as entangled pairs of particles stream across the endpoints of the interval, entangling the interior with the outside. The two-sided time evolution in (4.69) fits into this picture with the slight modification that we now consider entanglement across the two CFTs [165]. The entanglement velocity v defined above then quantifies how quickly these quasiparticles move: apparently as we approach extremality the entangling particles slow down to zero speed, perhaps due to scattering off of the large density of higher spin charge present. A similar result for the entangling velocity as a function of chemical potential has been derived in the context of Reissner-Nordstrom black holes in higher dimensions [167, 168]. It would be interesting to further understand the dependence of the velocity on the background charge density from a field-theoretical point of view.

To summarize: as probed by the entanglement entropy, the interior of a two-sided higher spin black hole grows with time, as expected from basic field theoretical notions of the time evolution of entanglement entropy. There are other time dependent observables worth understanding on Lorentzian higher spin backgrounds, in particular those recently reported in [169–171].

We could also probe the two-sided higher spin black hole with the "spin-3 entanglement entropy" $S^{(3)}$ of [60]. In this context this corresponds to a probe with $h = 0$, and $h_3 \neq 0$ in (4.49), and taking again the arrangement of intervals in Figure 4.7. Interestingly, however, now the configuration that interpolates between the two boundaries is trivial: $S^{(3)}_{conn} = 0$. As explained in Appendix 6.11, this is a simple consequence of the algebraic properties of the Wilson line for $\Delta\phi = 0$. More generally, there is no exponential in time behavior of two point functions of

this class of higher spin correlators.

In the limit $\Delta\phi \gg \beta$ the contribution of the blue Wilson lines in Figure 4.7 is

$$
\begin{aligned}
S_{disc}^{(3)} = -2\log W_{\mathcal{R}}(x_{i|R}, x_{f|R}) \quad &\sim \quad 2h_3 \log \frac{\left(\sqrt{4C-3}+3\right)e^{(\lambda_1+\lambda_3)\Delta\phi}}{\sqrt{4C-3}-3} \\
&= \quad -4h_3\sqrt{\frac{2\pi\mathcal{L}}{C}}\Delta\phi + S_{div}^{(3)} \ .
\end{aligned}
\tag{4.76}
$$

and we define

$$
S_{div}^{(3)} \equiv 2h_3 \log \frac{\sqrt{4C-3}+3}{\sqrt{4C-3}-3} \ .
\tag{4.77}
$$

where there is no short range "entanglement": $S^{(3)}$ has no UV divergent pieces. Note that in the regime of interest $\Delta\phi \gg \beta$ this one-sided contribution might be expected to never dominate the answer, as the two-sided contribution does not grow with time as it did in the conventional entanglement calculation above. It would be interesting to have a better interpretation of these higher-spin correlation functions on the thermofield state.

4.6.2 Extremal black holes and an emergent AdS$_2$

We now turn to the zero temperature limit of the higher spin black hole. It is well-known that charged black holes in higher dimensions generally develop an AdS$_2$ factor when cooled down to zero temperature. The AdS$_2$ indicates an emergent conformal symmetry at low energies that acts only on the time coordinate: this manifests itself in field-theory correlation functions, which now exhibit power-law correlations in time but have a finite correlation length in space [172–174].

It is not clear whether an AdS$_2$ factor appears in the extremal limit for higher spin gravity. However, it is rather straight forward to take the zero-temperature limit of the correlation functions computed above. From (1.131) we take $\frac{\beta}{\mu} \to \infty$, while holding μ fixed, by sending $C \to 3$ and holding $\mathcal{L}$ fixed. Thus from (4.52) we may simply reduce $\sinh\left(\frac{\Delta t}{\beta}\right) \to \frac{\Delta t}{\beta}$ to find:

$$
W_{\mathcal{R}}(t_{i|R}, t_{f|R}) \sim \left(\frac{\Delta t}{\mu}\right)^{-2h} \ ,
\tag{4.78}
$$

up to a overall constant. This implies an emergent scale-invariance in the time direction, where the IR scaling dimension is equal to the UV dimension (i.e. h). Actually this power law behavior is guaranteed from the definition of extremality

in [175]: in a nutshell, an extremal black hole is characterized by a_ϕ being non-diagonalizable. Using the fact that a_t and a_ϕ commute and that a_t is of the form (4.24) even in the extremal limit, it is straightforward to show that at extremality a_t is actually a nilpotent matrix. This means that that the exponentials of the form $e^{a_t \Delta t}$ appearing in M (as defined in (4.4)) truncate after only a few terms, and thus that the correlators have only polynomial (and not exponential) dependence on Δt.

On the other hand, the spatial correlation function remains non-trivial as the temperature vanishes; at large spatial separations we find

$$W_{\mathcal{R}}(x_{i|R}, x_{f|R}) \sim \exp\left(-\frac{h\sqrt{3}}{2} \frac{\Delta\phi}{\mu} \right), \tag{4.79}$$

indicating a nonzero spatial correlation length scaling with μ. This is precisely the behavior mentioned above: interpreted geometrically, it suggests an $\mathrm{AdS}_2 \times \mathbb{R}$ factorization of the higher spin geometry [172]. We also note that the two-sided correlation function across the two sides (4.65) vanishes as $\left(\frac{\beta}{\mu}\right)^{-2h}$ we take the $\frac{\beta}{\mu} \to \infty$ limit, as one would expect from the infinite "geodesic" distance down an AdS_2 throat.

It would be very interesting to understand if there is indeed an emergent $SL(2, \mathbb{R})$ acting on the bulk gauge connections in the extremal limit, perhaps following the algebraic approach of [175]. For this one would need a notion of 'near horizon geometry' in Chern-Simons theory, and within this region to argue that there is an enhancement of the symmetries of the extremal solution.

4.7   Discussion and outlook

In this chapter we motivated and implemented a definition of eternal black holes in the Chern-Simons formulation of higher spin gravity. Our definition introduces the concept of *strong (weak) Kruskal gauge* as explained in Section 4.3. A key ingredient to test our definition was the evaluation of the Wilson line defined in [108, 111]. This object was used as a probe of causality of a given Lorentzian background: it is the natural replacement of geodesic distances in higher spin gravity. The basic configurations we considered are presented in Figure 4.1.

Our proposal was tested in a variety of ways with the two most salient points being
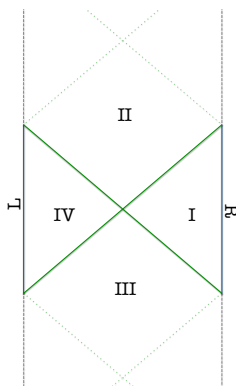
Figure 4.8: *Penrose Diagram for an sl(3) black hole. The green line correspond to the past and future outer horizon. The dotted and dashed line would tentatively be the locations of inner horizons and singularities.*

1. In the Chern-Simons formulation of $SL(2, \mathbb{R})$ gravity, we showed how our prescription permits access to the entire maximally extended spacetime for static (non-rotating) configurations. This illustrates explicitly that our refined definition of regularity agrees with the Lorentzian definitions in metric like formulation of gravity.

2. On general grounds, it is expected that an eternal black hole behaves in the dual theory as the thermofield state. Two point functions on this state satisfy KMS conditions (4.8). Our definition exactly reproduces these conditions.

Using this definition we built explicitly the strong Kruskal gauge for a higher spin black hole in $sl(3)$ gravity. The tentative Penrose diagram that we would attribute to this solution is shown in Figure 4.8. What our analysis clearly establishes are the existence of regions **I** and **IV** in the Penrose diagram. However there are some further properties of this diagram that remain puzzling. In particular, some concepts that are not addressed here include

1. *Singularity:* Due to the topological nature of the three dimensional gravitational theories we are studying, there are no curvature singularities. The line denoted "singularity" in the Penrose diagram for BTZ (see Figure 4.3) refers to a pathology of the quotient: after the dotted line there are closed timelike curves [160]. It is not clear to us what is the description of this singularity in Chern-Simons formulation, and hence its generalization to higher spin gravity remains an open question.

2. *Inner horizons:* The $sl(3)$ black hole we studied here has two free parameters: its mass $\mathcal{L}$ and spin-3 charge $\mathcal{W}$. Hence it is natural to speculate that its global properties should mimic those of a Reissner-Nordstrom solution in four dimensions. In particular, since the $sl(3)$ black hole has a non-trivial extremal limit, there should be a notion of inner horizon and the extremal case would correspond to the confluence of these horizons. However, this is another definition that is not clear how to capture in Chern-Simons theory. One reason this is puzzling is the following: what is the size of the inner horizon of a black hole in Chern-Simons theory? There is no need to consider higher spin gravity, since this question can be phrased for the rotating BTZ black hole. By design, the holonomy of the connections along ϕ encode the data of the outer horizon (a Wilson loop along ϕ evaluates the entropy of the outer horizon), and it is unclear how to modify that computation to give the "size" of an inner horizon since Wilson loops are independent of the radial position. This would be a very interesting puzzle to solve!

In addition, there are many other interesting future directions to explore which we discussed in section 4.6.

5

CONCLUSION AND OUTLOOK

OR ABOUT GEODESIC WITTEN DIAGRAMS AND GRAVITATIONAL WILSON LINES

In this thesis we have made steps towards a better understanding of the holographic correspondence. Our strategy was to exploit the control we have over correlation functions in CFTs to define meaningful objects in the gravity side: *spinning geodesic Witten diagrams*, and *gravitational Wilson lines*. Then, we use the newly acquired holographic tools to explore aspects of the gravitational theory. In the following, we will summarize our results.
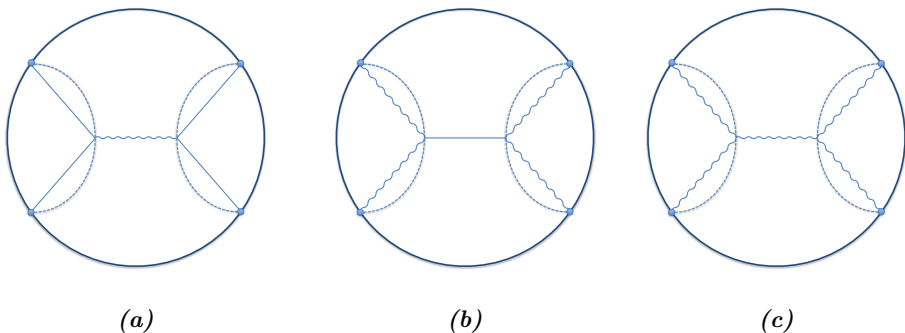

(a)   (b)   (c)

Figure 5.1: *Examples of geodesic Witten diagrams in AdS_{d+1}. The doted line indicates that we are projecting the propagators over a geodesic that connects the endpoints. Straight lines correspond to scalar fields, while wavy lines are spinning fields.*

In Chapter 2, the center of our analysis is the geodesic Witten diagrams represented in Fig. 5.1. It was proposed in [62] that the diagram 5.1a is dual to a conformal block with four external scalar operators. Our focus is the diagrams in Fig. 5.1b and Fig. 5.1c, which involve spinning fields: we find a systematical way to evaluate them, and relate them to the different CFT spinning conformal blocks. Moreover, we show how to decompose *bulk* Witten diagrams in terms of *geodesic* ones, when having spinning external fields. An interesting observation is that this decomposition is not unique, which signs that the geodesic Witten diagrams do not treat bulk interactions as fundamental.
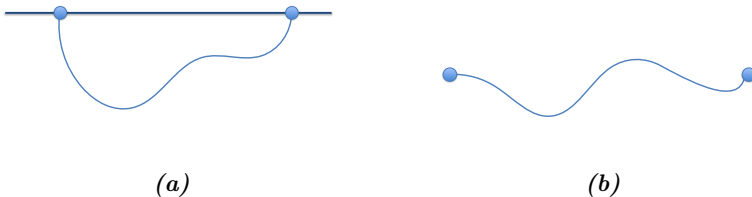

(a)   *(b)*

Figure 5.2: *Gravitational Wilson lines in AdS$_3$, where the representation carries the quantum numbers of probe scalar ($h = \bar{h}$). The Wilson line (a) hangs from the boundary, while (b) has its endpoints in the bulk of AdS$_3$*

In Chapter 3, and 4, we study gravitational Wilson lines in AdS$_3$/CFT$_2$. The Wilson line represented in Fig. 5.2a. can be used to compute probe scalar two-point functions at the boundary of locally AdS$_3$ geometries [61]. The background must be thought as generated by a *heavy* operator with dimensions $H = \bar{H}$, and the probe scalar as dual to a *light* operator with $h = \bar{h}$. This was proved in [61] for the regime $c \to \infty$, with the dimensions of the operators scaling as:

$$\frac{H}{c}\,,\ \frac{\bar{H}}{c}\,,\ h\,,\ \bar{h} = \mathcal{O}(c^0)\,, \tag{5.1}$$

and a semiclassical limit for the probe $h \gg 1$ [1]. In Chapter 3, we relax the condition $h \gg 1$ and show that when we move the end-points of the Wilson line into the bulk (Fig. 5.2b), it is equivalent to a bulk-to-bulk propagator in the locally AdS$_3$ geometry. Using this, we are able to propose an expression for local bulk states in global AdS$_3$, and BTZ backgrounds. In Chapter 4, we consider the boundary-anchored Wilson line in Fig. 5.2a in the context of AdS$_3$ higher spin gravities. We use the Wilson line to propose a notion of causality for these theories

---

[1]The dimension of the light operator is $h \gg 1$, but still has to be smaller than the one of the heavy operator. Therefore, $c \gg h \gg 1$.

based on the boundary degrees of freedom. This allows us to define *eternal higher spin black holes* from their thermo-field double dual states.

It is interesting to draw a line between the two objects analyzed in this thesis. In Chapter 2, we have considered geodesic Witten diagrams in generic $d+1$ dimensions, which are dual to CFT conformal blocks. In $d = 2$, the global conformal algebra has a Virasoro central extension as explained in Sec. 1.4. In this case, the relevant structures are the *Virasoro conformal blocks*. These are richer objects, which tend to the global conformal blocks when $c \to \infty$, and the dimensions of the operators are kept fixed. The holographic computation of Virasoro blocks was addressed using geodesic Witten diagrams in [146]. They explicitly show that the geodesic Witten diagram in Fig. 5.3 computes the holomorphic part of the Virasoro block in the $c \to \infty$ limit, and with

$$\frac{h_3}{c}\,,\ \frac{h_4}{c}\,,\ h_1\,,\ h_2\,,\ h_{\mathrm{exch}}\ =\ \mathcal{O}(c^0)\,. \tag{5.2}$$

The anti-holomorphic part is computed by the same diagram with the barred scaling dimensions[2]. If we consider the so-called *Virasoro vacuum block* with:

$$h_{\mathrm{exch}} = \bar{h}_{\mathrm{exch}} = 0\,, \qquad h_1 = h_2 = \bar{h}_1 = \bar{h}_2 \equiv h\,, \qquad h_3 = h_4 = \bar{h}_3 = \bar{h}_4 \equiv H\,, \tag{5.3}$$

we obtain the same probe two-point function than using the Wilson line in Fig. 5.2a, as expected from the results in [176]. This argument nicely relates the two central objects of this thesis. Moreover, Wilson lines have been very fruitful objects in the quest for a holographic interpretation of the conformal blocks (the main purpose of the geodesic Witten diagrams). It has been already known for some years that Wilson lines in three dimensions are related to the global and Virasoro conformal blocks [105, 143, 144], with the recent developments in the context of holography, which as well include $\mathcal{W}_\mathcal{N}$ blocks [148, 149, 177]. In addition, in [178, 179] they use a generalized version of the Wilson line to compute scalar conformal blocks in d-dimensions.

---

[2]The Virasoro blocks factorize in a holomorphic part, which depends only on the CFT$_2$ coordinate z, and an anti-holomorphic part, depending just on $\bar{z}$. Two geodesic Witten diagrams such as the one in Fig. 5.3 are needed to reproduce the full Virasoro block.
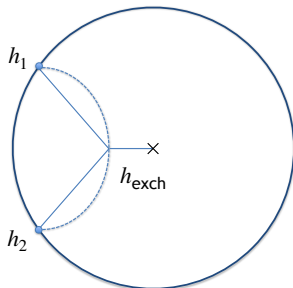
Figure 5.3: *Geodesic Witten diagram in a 3-dimensional background created by the back-reaction of two heavy operators ($h_3, h_4 \sim c$). The background has a conical defect, represented at the center of the diagram by the cross ($\times$).*

In this thesis, we have refined the roles of geodesic Witten diagrams and Wilson lines in the AdS/CFT correspondence, and their importance in the reconstruction of bulk physics from the boundary degrees of freedom. We have considered this objects in $G_N \to 0$, and we used them to solve problems in gravitational theories in their semiclassical limit[3]. For example, we learned how to decompose tree level spinning Witten diagram into simpler objects such geodesic Witten diagrams; to couple matter in the Chen-Simons formalism of 3d gravity; and to interpret Lorentzian higher spin black holes. However, our ultimate goal is to use the holographic correspondence to learn about quantum gravity. As a future direction, we would like to consider corrections due to the expansion in G_N for both the Wilson lines and the geodesic Witten diagrams. More specifically:

– In Chapter 3, we have used Wilson lines to construct bulk *local* fields. However, non-localities are expected to appear when considering $1/c$ corrections. This is due to the diffeomorphism invariance of gravity, which allows the fields to interact in a non-local way. This behavior is manifested explicitly as non-local singularities in the correlation functions. Therefore, generalizing our proposal to include $1/c$ corrections can shed some light on the understanding of the emergence of bulk physics, and the breakdown of locality. Different proposals for the reconstruction of bulk fields beyond the semiclassical level have already been considered recently in [134, 135], and [137]. Adding $1/c$-corrections to our Wilson line will make possible the comparison among these different programs.

---

[3]In the context of 3-dimensional gravity, this limit is commonly referred as $c \to \infty$ due to (1.87).

– In relation to geodesic Witten diagram, the next step is to use them to compute loops corrections to the bulk Witten diagram. The study of loops is important for several purposes, such as understanding if there is an underlying principle that organizes AdS amplitudes, or constraining the spectrum of CFTs that have holographic gravity duals. However, loop corrections to Witten diagram are very challenging at a technical level, and not so much it is known about them, except the recent results in [103, 104]. Decomposing Witten diagrams in terms geodesic of geodesic ones might avoid some of the technical difficulties: since the geodesic Witten diagrams are dual to conformal blocks, and including corrections will just modify OPE coefficients and operators dimensions. It is important to understand what this means in the bulk language since corrections drastically change the anatomy of the geodesic Witten diagram (at least naively). Moreover, computing corrections might shed some light over why geodesic Witten diagrams do not lead to a one-to-one map of the conformal blocks and the bulk interactions.

6

APPENDIXES

6.1 Spinning AdS$_{d+1}$ propagators in embedding formalim

Here we follow [27] and review some results of [180]; propagators in the AdS coordinates can be found in e.g. [181, 182] among many other references. We are interested in describing the propagator of a spin-J field. In Sec. 1.3.1, we have seen that in AdS coordinates this field is a symmetric tensor that satisfies the Fierz conditions

$$\nabla^2 \phi_{\mu_1...\mu_J} = m^2 \phi_{\mu_1...\mu_J} \ , \quad \nabla^{\mu_1} \phi_{\mu_1...\mu_J} = 0 \ , \quad \phi^\mu{}_{\mu\mu_3...\mu_J} = 0 \ . \tag{6.1}$$

These equations fully determine the AdS propagators, and the explicit answer are nicely casted in the embedding formalism. The bulk–to–boundary propagator of a symmetric traceless field of rank J can be written in a suggestive form

$$G_{b\partial}^{\Delta|J}(Y_j, P_i; W_j, Z_i) = \mathcal{C}_{\Delta,J} \frac{\mathcal{H}_{ij}(Z_i, W_j)^J}{\Psi_{ij}^\Delta} \ , \tag{6.2}$$

where $\mathcal{C}_{\Delta,J}$ is a normalization (which we will ignore), and

$$\Psi_{ij} \equiv -2P_i \cdot Y_j \ , \quad \mathcal{H}_{ij}(Z_i, W_j) \equiv Z_i \cdot W_j + 2 \frac{(W_j \cdot P_i)(Z_i \cdot Y_j)}{\Psi_{ij}} \ . \tag{6.3}$$

The mass squared is related to the conformal weight Δ of the dual operator as $m^2 = \Delta(\Delta - d) - J$. This is the analogue of the CFT two point function (2.29).

It will be also useful to rewrite the bulk–to–boundary propagator as [180]

$$G_{b\partial}^{\Delta|J}(Y, P; W, Z) = \frac{1}{(\Delta)_J}(\mathscr{D}_P(W, Z))^J G_{b\partial}^{\Delta|0}(Y, P) \,, \qquad (6.4)$$

where

$$\mathscr{D}_P(W, Z) = (Z \cdot W)\left(Z \cdot \frac{\partial}{\partial Z} - P \cdot \frac{\partial}{\partial P}\right) + (P \cdot W)\left(Z \cdot \frac{\partial}{\partial P}\right) \,. \qquad (6.5)$$

And it will also be convenient to cast the n-th derivative of $G_{b\partial}^{\Delta|J}$ in terms of scalar propagators:

$$(W' \cdot \partial_Y)^n G_{b\partial}^{\Delta|J}(Y, P; W, Z) = 2^n \Gamma(\Delta + n) \sum_{i=0}^{J} \sum_{k=0}^{i} \binom{J}{i}\binom{i}{k}\frac{(n-k+1)_k}{\Gamma(\Delta+i)} \qquad (6.6)$$

$$\times (W \cdot P)^i (W \cdot Z)^{J-i}(W' \cdot Z)^k (W' \cdot P)^{n-k}(Z \cdot \partial_P)^{i-k} G_{b\partial}^{\Delta+n|0}(Y, P) \,.$$

The bulk–to–bulk propagator of a spin-J fields can be written as[1]

$$G_{bb}^{\Delta|J}(Y_i, Y_j; W_i, W_j) = \sum_{k=0}^{J}(W_i \cdot W_j)^{J-k}(W_i \cdot Y_j W_j \cdot Y_i)^k g_k(u) \,, \qquad (6.7)$$

where $u = -1 + Y_{ij}/2$ and $Y_{ij} \equiv -2Y_i \cdot Y_j$. The functions g_k can be written in terms of hypergeometric functions via

$$g_k(u) = \sum_{i=k}^{J}(-1)^{i+k}\left(\frac{i!}{j!}\right)^2 \frac{h_i^{(k)}(u)}{(i-k)!} \,, \qquad (6.8)$$

where the recursion relation for h_i is

$$h_k = c_k\Big((d - 2k + 2J - 1)\left[(d + J - 2)h_{k-1} + (1 + u)h'_{k-1}\right] + (2 - k + J)h_{k-2}\Big) \,, \qquad (6.9)$$

where

$$c_k = -\frac{1 + J - k}{k(d + 2J - k - 2)(\Delta + J - k - 1)(d - \Delta + J - k - 1)} \,, \qquad (6.10)$$

and

$$h_0(u) = \frac{\Gamma(\Delta)}{2\pi^h\Gamma(\Delta + 1 - h)}(2u)^{-\Delta}{}_2F_1\left(\Delta, \Delta - h + \frac{1}{2}, 2\Delta - 2h + 1, -\frac{2}{u}\right) \,. \qquad (6.11)$$

---

[1]Note that (6.7) is not a homogeneous function of Y. In solving for the bulk-to-bulk operator the constrain $Y^2 = -1$ is used, which breaks the homogeneity property of the polynomials in embedding space.

6.2 More on CFT three point functions

Following the summary in section 3.5, in this appendix we give some more explicit information about the tensor structures appearing in the correlation functions.

In the main part of the text we have considered primaries operators with arbitrary conformal dimensions. Unitarity CFTs have restrictions on the possible dimensions, and is it well known the unitarity bound is

$$\Delta \geq l + d - 2 \,, \qquad l \geq 1 \,. \tag{6.12}$$

The bound is saturated by conserved currents. The presence of a current implies as well further restrictions on the correlation functions, which can be implemented in the index-free framework of [84]. Conservation of a symmetric traceless tensor requires that its divergence is zero; this implies that the entries of

$$R(P, Z) = \frac{1}{l(d/2 + l - 2)} (\partial \cdot D) T(Z, P) + O(Z^2, Z \cdot P) \,, \qquad \partial \cdot D \equiv \frac{\partial}{\partial P^A} D_A \,, \tag{6.13}$$

are zero modulo pure gauge terms. Here the operator D_A is the projector introduced in (2.15).

To see how conservation affects a three point function, consider the following two spin-2 fields and one scalar. This correlation function is the combination of three tensor structures:

$$G_{\Delta_1, \Delta_2, \Delta_3 | 2, 2, 0} = \left(\alpha H_{12}^2 + \beta H_{12} V_{1,23} V_{2,31} + \gamma V_{1,23}^2 V_{2,31}^2 \right) T(\Delta_1, \Delta_2, \Delta_3) \,, \tag{6.14}$$

where

$$H_{12} V_{1,23} V_{2,31} T(\Delta_1, \Delta_2, \Delta_3) =$$
$$\frac{-4 H_{12} D_{1\,12} D_{1\,21} T(\Delta_1 + 1, \Delta_2 + 1, \Delta_2)}{(\Delta_{12} - \Delta_3)(\Delta_{12} + \Delta_3)} - \frac{H_{12}^2 T(\Delta_1, \Delta_2, \Delta_2)}{(\Delta_{12} - \Delta_3)} \tag{6.15}$$

$$V_{1,23}^2 V_{2,31}^2 T(\Delta_1, \Delta_2, \Delta_3) = \frac{16 H_{12} D_{1\,12}^2 D_{1\,21}^2 T(\Delta_1 + 2, \Delta_2 + 2, \Delta_2)}{(\Delta_{12} - \Delta_3)(\Delta_{12} + \Delta_3)(2 + \Delta_{12} + \Delta_3)(-2 + \Delta_{12} - \Delta_3)}$$
$$+ \frac{16 H_{12} D_{1\,12} D_{1\,21} T(\Delta_1 + 1, \Delta_2 + 1, \Delta_2)}{(\Delta_{12} - \Delta_3)(\Delta_{12} + \Delta_3)(-2 + \Delta_{12} - \Delta_3)} + \frac{2 H_{12}^2 T(\Delta_1, \Delta_2, \Delta_2)}{(\Delta_{12} - \Delta_3)(-2 + \Delta_{12} - \Delta_3)} \tag{6.16}$$

Conservation implies $\Delta_1 = \Delta_2 = d$ and

$$\alpha = \frac{4h(h - 1)(2h + 1) - 4\Delta_3 h(2h - 1) + \Delta_3^2 (2h - 1)}{2\Delta_3 (\Delta_3 + 2)(h - 1)} \gamma \,, \tag{6.17}$$

$$\beta = -\frac{2 + 4h^2 + \Delta_3 - 2h(\Delta_3 + 1)}{(h - 1)(\Delta_3 + 2)}\gamma \ , \tag{6.18}$$

where $h = d/2$. Further recent developments on properties of correlation functions for conserved currents can be found in [95, 183] and references within.

6.3   Tensor structures in Witten diagrams

In this appendix we will evaluate three point Witten diagrams explicitly to illustrate how the tensor structures appear in the final answer. We will focus on the following interactions:

$$A_1^\mu \, \partial_\mu\partial_\nu\phi_2 \, A_3^\nu \ , \quad \partial_\mu A_1^\nu \, \phi_2 \, \partial_\mu A_3^\nu \ , \quad \partial_\mu A_1^\nu \, \phi_2 \, \partial_\nu A_3^\mu \ . \tag{6.19}$$

We will do this by using the techniques in [85, 180], where they write the J spinning bulk to boundary propagator and its derivatives in terms of the scalar propagators. This allows us to express the three point function of our interest in terms of scalar three point functions. In our case, we will just need the following identities for the spin-1 case, which follow from (6.4) and (6.6):

$$\Delta \, G_{b\partial}^{\Delta|1}(Y, P; W, Z) = \mathscr{D}_P(W, Z) \, G_{b\partial}^{\Delta|0}(Y, P) \ , \tag{6.20}$$

$$(W' \cdot \partial_Y)G_{b\partial}^{\Delta|1}(Y, P; W, Z) = \mathscr{D}'_P(W', W, Z) \, G_{b\partial}^{\Delta+1|0}(Y, P) \ , \tag{6.21}$$

where $\mathscr{D}_P$ are differential operators defined as

$$\mathscr{D}_P(W, Z) = (Z \cdot W)\left(Z \cdot \frac{\partial}{\partial Z} - P \cdot \frac{\partial}{\partial P}\right) + (P \cdot W)\left(Z \cdot \frac{\partial}{\partial P}\right) \ , \tag{6.22}$$

$$\mathscr{D}'_P(W', W, Z) = 2\Bigg((Z \cdot W')(P \cdot W) + \Delta(P \cdot W')(Z \cdot W) \tag{6.23}$$

$$+ (P \cdot W')(P \cdot W)\left(Z \cdot \frac{\partial}{\partial P}\right)\Bigg). \tag{6.24}$$

These operators should not be confused with the $D_{1,2}$ CFT operators in (2.47) or with the bulk diferential operators $\mathcal{D}_{1,2}$ in (2.66).

We start by evaluating a Witten diagram using the interaction $A_1^\mu \, \partial_\mu\partial_\nu\phi_2 \, A_3^\nu$. We have

$$\int dY \, G_{b\partial}^{\Delta_1|1}(Y, P_1; \partial_{W_1}, Z_1)G_{b\partial}^{\Delta_3|1}(Y, P_3; \partial_{W_3}, Z_3)(W_1 \cdot \partial_Y)(W_3 \cdot \partial_Y) \, G_{b\partial}^{\Delta_2|0}(Y, P_2) \ . \tag{6.25}$$

Here dY denotes an integral over the volume of AdS. Using (6.2) and (6.24) gives

$$\frac{4\Delta_2(\Delta_2+1)}{\Delta_1\Delta_3} \int dY\, \mathscr{D}_{P_1}(\partial_{W_1}, Z_1) G_{b\partial}^{\Delta_1|0}(Y, P_1) \mathscr{D}_{P_3}(\partial_{W_3}, Z_3) G_{b\partial}^{\Delta_3|0}(Y, P_3)$$

$$\times (W_1 \cdot P_2)(W_3 \cdot P_2)\, G_{b\partial}^{\Delta_2+2|0}(Y, P_2)$$

$$= \frac{4\Delta_2(\Delta_2+1)}{\Delta_1\Delta_3} \mathscr{D}_{P_1}(P_2, Z_1)\mathscr{D}_{P_3}(P_2, Z_3) \int G_{b\partial}^{\Delta_1|0}(Y, P_1) G_{b\partial}^{\Delta_3|0}(Y, P_3)\, G_{b\partial}^{\Delta_2+2|0}(Y, P_2)$$

$$= \frac{4\Delta_2(\Delta_2+1)\mathsf{C}_{\Delta_1,\Delta_2+2,\Delta_3}}{\Delta_1\Delta_3} \mathscr{D}_{P_1}(P_2, Z_1)\mathscr{D}_{P_3}(P_2, Z_3) T(\Delta_1, \Delta_2+2, \Delta_3)\,,$$

$$(6.26)$$

where

$$\mathsf{C}_{\Delta_1,\Delta_2,\Delta_3}$$

$$= g\frac{\pi^h}{2}\Gamma\left(\frac{\Delta_1+\Delta_2+\Delta_3-2h}{2}\right) \frac{\Gamma\left(\frac{\Delta_1+\Delta_2-\Delta_3}{2}\right)\Gamma\left(\frac{\Delta_1+\Delta_3-\Delta_2}{2}\right)\Gamma\left(\frac{\Delta_2+\Delta_3-\Delta_1}{2}\right)}{\Gamma(\Delta_1)\Gamma(\Delta_2)\Gamma(\Delta_3)}\,.$$

$$(6.27)$$

Notice that $\mathscr{D}_{P_1}(P_2, Z_1) = D_{2,12}$, and $\mathscr{D}_{P_3}(P_2, Z_3) = D_{2,32}$. Now, applying the differential operators to the scalar 3-point function we find that tensor structure corresponding to the previous diagram is the following linear combination:

$$A_1^\mu\, \partial_\mu\partial_\nu\phi_2\, A_3^\nu\ :$$

$$\frac{\Delta_2(\Delta_2+1)(\Delta_1-\Delta_2+\Delta_3-2)\mathsf{C}_{\Delta_1,\Delta_2+2,\Delta_3}\, (H_{13} + (\Delta_1-\Delta_2+\Delta_3-2)\, V_{1,23}V_{3,21})}{\Delta_1\Delta_3}\,.$$

$$(6.28)$$

For the interaction $\partial_\mu A_1^\nu\, \phi_2\, \partial_\mu A_3^\nu$ we have

$$\int dY\, (\partial_{W'} \cdot \partial_Y)\, G_{b\partial}^{\Delta_1|1}(Y, P_1; \partial_W, Z_1)(W' \cdot \partial_Y) G_{b\partial}^{\Delta_3|1}(Y, P_3; W, Z_3)\, G_{b\partial}^{\Delta_2|0}(Y, P_2)\,,$$

$$(6.29)$$

which using (6.21) is equivalent to

$$\mathscr{D}'_{P_1}(\partial_{W'}, \partial_W, Z_1)\mathscr{D}'_{P_3}(W', W, Z_3) \int dY\, G_{b\partial}^{\Delta_1+1|0}(Y, P_1) G_{b\partial}^{\Delta_3+1|0}(Y, P_3)\, G_{b\partial}^{\Delta_2|0}(Y, P_2)$$

$$= \mathsf{C}_{\Delta_1+1,\Delta_2,\Delta_3+1}\mathscr{D}'_{P_1}(\partial_{W'}, \partial_W, Z_1)\mathscr{D}'_{P_3}(W', W, Z_3)\, T(\Delta_1+1, \Delta_2, \Delta_3+1)\,.$$

$$(6.30)$$

Contracting the W's in the differential operators gives

$$\mathscr{D}'_{P_1}(\partial_{W'},\partial_W,Z_1)\mathscr{D}'_{P_3}(W',W,Z_3) =$$
$$(\Delta_1+\Delta_3)(Z_1 \cdot P_3)(Z_3 \cdot P_1) + (P_1 \cdot P_3)\Big(\Delta_1\Delta_3(Z_1 \cdot Z_3) + (Z_1 \cdot \partial_{P_1})(Z_3 \cdot \partial_{P_3})$$
$$+ (1 + \Delta_3)(P_1 \cdot Z_3)(Z_1 \cdot \partial_{P_1}) + (1 + \Delta_1)(P_3 \cdot Z_1)(Z_3 \cdot \partial_{P_3})\Big),$$
$$(6.31)$$

which leads to the following identification

$$\partial_\mu A_1^\nu \, \phi_2 \, \partial_\mu A_3^\nu : \qquad \mathsf{C}_{\Delta_1+1,\Delta_2,\Delta_3+1}\Big((\Delta_1 - \Delta_2 + \Delta_3 - 2\Delta_1\Delta_3)H_{13}$$
$$- (\Delta_1 - \Delta_2 - \Delta_3)(\Delta_1 + \Delta_2 - \Delta_3) \, V_{1,23}V_{3,21}\Big). \qquad (6.32)$$

The interaction $\partial_\mu A_1^\nu \, \phi_2 \, \partial_\nu A_3^\mu$ is computed analogously as the previous, but with different W contractions

$$\int dY \, (\partial_{W'} \cdot \partial_Y) \, G_{b\partial}^{\Delta_1|1}(Y, P_1; \partial_W, Z_1)(W \cdot \partial_Y)G_{b\partial}^{\Delta_3|1}(Y, P_3; W', Z_3) \, G_{b\partial}^{\Delta_2|0}(Y, P_2)$$
$$= \mathsf{C}_{\Delta_1+1,\Delta_2,\Delta_3+1}\mathscr{D}'_{P_1}(\partial_{W'},\partial_W,Z_1)\mathscr{D}'_{P_3}(W,W',Z_3) \, T(\Delta_1 + 1, \Delta_2, \Delta_3 + 1).$$
$$(6.33)$$

This contraction of the differential operators gives

$$\mathscr{D}'_{P_1}(\partial_{W'},\partial_W,Z_1)\mathscr{D}'_{P_3}(W',W,Z_3)$$
$$= \Delta_1\Delta_3(Z_1 \cdot P_3)(Z_3 \cdot P_1) + (P_1 \cdot P_3)\Big((\Delta_1 + \Delta_3)(Z_1 \cdot Z_3) + (Z_1 \cdot \partial_{P_1})(Z_3 \cdot \partial_{P_3})$$
$$+ (1 + \Delta_3)(P_1 \cdot Z_3)(Z_1 \cdot \partial_{P_1}) + (1 + \Delta_1)(P_3 \cdot Z_1)(Z_3 \cdot \partial_{P_3})\Big),$$

which applying it to the scalar three point function gives

$$\partial_\mu A_1^\nu \, \phi_2 \, \partial_\nu A_3^\mu : \qquad \mathsf{C}_{\Delta_1+1,\Delta_2,\Delta_3+1}\big(-(\Delta_1 + \Delta_2 + \Delta_3 - 2)H_{13}$$
$$- (\Delta_1 - \Delta_2 - \Delta_3)(\Delta_1 + \Delta_2 - \Delta_3) \, V_{1,23}V_{3,21}\big). \qquad (6.34)$$

Based on these three interactions, we can make the following map

$$H_{13} : \qquad \partial_\mu A_1^\nu \, \phi_2 \, \partial_\mu A_3^\nu - \partial_\mu A_1^\nu \, \phi_2 \, \partial_\nu A_3^\mu \,,$$
$$V_{1,23}V_{3,21} : \quad \alpha \, A_1^\mu \, \partial_\mu \partial_\nu \phi_2 \, A_3^\nu - (\Delta_1 + \Delta_3)\partial_\mu A_1^\nu \, \phi_2 \, \partial_\mu A_3^\nu$$
$$+ (1 + \Delta_1\Delta_3)\partial_\mu A_1^\nu \, \phi_2 \, \partial_\nu A_3^\mu \,, \qquad (6.35)$$

where

$$\alpha = \frac{(\Delta_1 - 1)(\Delta_3 - 1)(\Delta_1 - \Delta_2 + \Delta_3)(2 + \Delta_1 - \Delta_2 + \Delta_3)}{(\Delta_1 + \Delta_2 - \Delta_3)(\Delta_1 - \Delta_2 - \Delta_3)} \,. \qquad (6.36)$$

Modulo normalizations, this identification is compatible with the identification using geodesic diagrams (2.108) and (2.109).

6.4 Tensor-tensor-scalar structures via geodesic diagrams

Based on the two examples in sections 2.4.1 and 2.4.1, we can make a general identification between tensorial structures and a minimal set of gravitational interactions that will capture them for a fixed choice of the geodesic given by the first diagram in Fig. 2.4. We saw that the simplest way to identify H_{12} in the bulk is by an interaction that contracts indices among symmetric tensors at position 1 and 2, and the V's added derivatives on position 3 with suitable contractions on legs 1 and 2. Hence, it seems like each tensor structure $H_{12}^p V_{1,23}^q V_{2,13}^r T(\Delta_1, \Delta_2, \Delta_3)$ is reproduced by a geodesic integral of the form

$$\int_{\gamma_{12}} d\lambda \frac{\mathcal{H}_{1\lambda}(Z_1, \partial_W)^q \mathcal{H}_{1\lambda}(Z_1, \partial_{W'})^p}{\Psi_{1\lambda}^{\Delta_1}} \frac{\mathcal{H}_{2\lambda}(Z_2, \partial_W)^r \mathcal{H}_{2\lambda}(Z_2, W')^p}{\Psi_{2\lambda}^{\Delta_2}} (W \cdot \partial_{Y_\lambda})^{q+r} \Psi_{3\lambda}^{-\Delta_3} .$$

(6.37)

This is a claim we can prove. The proof requires the following identities which are easily obtained by induction:

$$(W \cdot \partial_{Y_\lambda})^n \Psi_{3\lambda}^{-\Delta_3} = (-2)^n (-\Delta_3 - n + 1)_n (W \cdot P_3)^n \Psi_{3\lambda}^{-\Delta_3 - n} ,$$

$$(\mathcal{H}_{i\lambda}(Z_i, \partial_W))^n (W \cdot P_3)^l = (l - n + 1)_n (W \cdot P_3)^{l-n} \left(\sqrt{\frac{P_{i3}\Psi_{3\lambda}}{\Psi_{i\lambda}}} \mathcal{V}_{\partial\, i,3\lambda}(Z_i) \right)^n ,$$

$$\mathcal{H}_{1\lambda}(Z_1, \partial_{W'})^p \mathcal{H}_{2\lambda}(Z_2, W')^p |_{\gamma_{12}} = p! H_{12}^p .$$

(6.38)

Applying these to the integral gives

$$2^{q+r} p! q! (-\Delta_3 - q - r + 1)_{q+r} (q+1)_r \left(\frac{P_{13}P_{23}}{P_{12}} \right)^{\frac{q+r}{2}} H_{12}^p V_{1,23}^q V_{2,13}^r$$

$$\times \int_{\gamma_{12}} \Psi_{1\lambda}^{-\Delta_1} \Psi_{2\lambda}^{-\Delta_2} \Psi_{3\lambda}^{-\Delta_3 - q - r} , \quad (6.39)$$

where we used

$$\sqrt{\frac{P_{i3}\Psi_{31}}{\Psi_{i1}}} \mathcal{V}_{\partial\, i,31}(Z_i) = -\sqrt{\frac{P_{13}P_{23}}{P_{12}}} \begin{cases} V_{1,23} & \text{if } i = 1 \\ V_{2,13} & \text{if } i = 2 \end{cases} \quad (6.40)$$

The remaining integral evaluates to

$$\int_{\gamma_{12}} \Psi_{1\lambda}^{-\Delta_1} \Psi_{2\lambda}^{-\Delta_2} \Psi_{3\lambda}^{-\Delta_3 - q - r} = \frac{T(\Delta_1, \Delta_2, \Delta_3 + q + r)}{c_{\Delta_1 \Delta_2 \Delta_3 + q + r}} , \quad (6.41)$$

173

by (2.91). Therefore (6.37) results in

$$\frac{2^{q+r}p!q!(-\Delta_3 - q - r + 1)_{q+r}(q+1)_r}{c_{\Delta_1\Delta_2\Delta_3+q+r}} H_{12}^p V_{1,23}^q V_{2,13}^r T(\Delta_1, \Delta_2, \Delta_3) \,, \qquad (6.42)$$

which completes the proof. Hence, from the analysis of the integrals over the geodesic γ_{12} (which connects the fields with spin), we find the following identification

$$H_{12}^p V_{1,23}^q V_{2,13}^r: \quad \phi_{1\mu_1\cdots\mu_p}{}^{\alpha_1\cdots\alpha_q}\phi_2{}^{\mu_1\cdots\mu_p\beta_1\cdots\beta_r}\partial_{\alpha_1}\cdots\partial_{\alpha_q}\partial_{\beta_1}\cdots\partial_{\beta_r}\phi_3 \,. \qquad (6.43)$$

As we have noticed in section 2.4.1 this identification is not unique. It is sensitive to the choice of geodesic, and moreover to redundancies that appear as derivatives are contracted along γ_{12} (i.e. generalizations of (2.111)).

6.5 $sl(N, \mathbb{R})$ conventions

A convenient basis for the $sl(N, \mathbb{R})$ algebra is represented by $\{L_0, L_{\pm 1}\}$, the generators in the $sl(2, \mathbb{R})$ subalgebra, and $W_j^{(s)}$, the higher spin generators with $j = -(s-1), \ldots (s-1)$. Their commutation relations are:

$$\begin{aligned}
[L_i, L_{i'}] &= (i - i')L_{i+i'} \,, \\
[L_i, W_j^{(s)}] &= (i(s-1) - j)W_{i+j}^{(s)} \,.
\end{aligned} \qquad (6.44)$$

In this notation, L_0 and $W_0^{(s)}$ are elements of the Cartan subalgebra. These commutation relations represent the principal embedding of $sl(N, \mathbb{R})$. We can construct $N - 1$ symmetric tensors which are regarded as the Killing forms of the algebra. The m-th order tensor is:

$$\eta_{a_1\ldots a_m} = \mathrm{tr}_f(T_{(a_1}\ldots T_{a_m)}) \,, \qquad (6.45)$$

where $m = 2, \ldots, N$, and T_a are all the generators of the algebra. Explicitly, the Lie algebra for $sl(2, \mathbb{R})$ is given by

$$[L_0, L_\pm] = \mp L_\pm \,, \qquad [L_1, L_{-1}] = 2L_0 \,, \qquad (6.46)$$

Our conventions for the fundamental representation of $sl(2, \mathbb{R})$ is

$$L_0 = \begin{pmatrix} 1/2 & 0 \\ 0 & -1/2 \end{pmatrix}, \quad L_1 = \begin{pmatrix} 0 & 0 \\ -1 & 0 \end{pmatrix}, \quad L_{-1} = \begin{pmatrix} 0 & 1 \\ 0 & 0 \end{pmatrix}. \qquad (6.47)$$

With these conventions, the Lie algebra metric reads

$$\eta_{00} = \frac{1}{2} \,, \qquad \eta_{+-} = \eta_{-+} = -1 \,. \qquad (6.48)$$

When working in $sl(3, \mathbb{R})$, we explicitly label the generators as $\{L_i, W_m\}$ with $i = -1, 0, 1$ and $m = -2, \ldots, 2$. Their algebra reads

$$
\begin{aligned}
[L_i, L_j] &= (i - j)L_{i+j} \ , \\
[L_i, W_m] &= (2i - m)W_{i+m} \ , \\
[W_m, W_n] &= -\frac{1}{3}(m - n)(2m^2 + 2n^2 - mn - 8)L_{m+n} \ .
\end{aligned}
\tag{6.49}
$$

We work with the following matrices in the fundamental representation

$$
L_1 = \begin{pmatrix} 0 & 0 & 0 \\ 1 & 0 & 0 \\ 0 & 1 & 0 \end{pmatrix} , \quad
L_0 = \begin{pmatrix} 1 & 0 & 0 \\ 0 & 0 & 0 \\ 0 & 0 & -1 \end{pmatrix} , \quad
L_{-1} = \begin{pmatrix} 0 & -2 & 0 \\ 0 & 0 & -2 \\ 0 & 0 & 0 \end{pmatrix} ,
$$

$$
W_2 = 2 \begin{pmatrix} 0 & 0 & 0 \\ 0 & 0 & 0 \\ 1 & 0 & 0 \end{pmatrix} , \quad
W_1 = \begin{pmatrix} 0 & 0 & 0 \\ 1 & 0 & 0 \\ 0 & -1 & 0 \end{pmatrix} , \quad
W_0 = \frac{2}{3} \begin{pmatrix} 1 & 0 & 0 \\ 0 & -2 & 0 \\ 0 & 0 & 1 \end{pmatrix} ,
$$

$$
W_{-1} = \begin{pmatrix} 0 & -2 & 0 \\ 0 & 0 & 2 \\ 0 & 0 & 0 \end{pmatrix} , \quad
W_{-2} = 2 \begin{pmatrix} 0 & 0 & 4 \\ 0 & 0 & 0 \\ 0 & 0 & 0 \end{pmatrix} .
\tag{6.50}
$$

The quadratic traces are

$$
\begin{aligned}
\text{tr}_f(L_0 L_0) &= 2 \ , \quad \text{tr}_f(L_1 L_{-1}) = -4 \ , \\
\text{tr}_f(W_0 W_0) &= \frac{8}{3} \ , \quad \text{tr}_f(W_1 W_{-1}) = -4 \ , \quad \text{tr}_f(W_2 W_{-2}) = 16 \ .
\end{aligned}
\tag{6.51}
$$

6.6 Completeness of rotated Ishibashi states

Here we establish a completeness relation for the $|U\rangle$ states:

$$
\int dU |U\rangle\langle U| = \frac{(2\pi)^2}{2(2h - 1)} \mathbb{1} \ .
\tag{6.52}
$$

We note that if the right-hand side exists, it must be equal to a multiple of the identity by $SL(2, \mathbb{R})$ invariance; thus the only question is whether or not the integral converges, and what the normalization factor is if it does. As the group is non-compact the convergence is not (to our knowledge) actually guaranteed. Thus we perform an explicit computation in coordinates. In particular we view the $SL(2, \mathbb{R})$ group manifold as global AdS$_3$ and place on it the usual global coordinates (ρ, t, ϕ). It is important to note that we work here not $SL(2, \mathbb{R})$ and not with its universal cover, and thus *both* coordinates t and ϕ are periodic with period 2π.

The explicit matrix elements between the $|U(\rho, t, \phi)\rangle$ states and the discrete highest-weight states $|h, k, \bar{k}\rangle$ can be constructed via the usual methods of finding the highest-weight state and systematically acting with the raising operators. The result is precisely that given in a (slightly) different context in Chapter 3: (3.109):

$$
\begin{aligned}
&\langle U(\rho, t, \phi)|h; k, \bar{k}\rangle \\
&= C_{k,\bar{k}}\, e^{-2iht} e^{-it(k+\bar{k})-i\phi(k-\bar{k})} (\tanh \rho)^{\bar{k}-k} (\cosh \rho)^{-2h} P_k^{(\bar{k}-k,\, 2h-1)} (1 - 2\tanh^2 \rho) ,
\end{aligned}
\tag{6.53}
$$

where $P_n^{(a,\, b)}$ are Jacobi polynomials, and $C_{k,\bar{k}} \equiv (-1)^k \sqrt{\frac{k!(2h+\bar{k}-1)!}{\bar{k}!(2h+k-1)!}}$. Note also that in these coordinates on the group manifold the Haar measure is just the usual volume element on AdS_3, i.e.

$$
\int dU = \int d\rho\, dt\, d\phi \sinh \rho \cosh \rho \ .
\tag{6.54}
$$

With this in hand, we simply directly compute the following matrix elements:

$$
I_{m,\bar{m};k,\bar{k}} \equiv \int dU \langle h; m, \bar{m}|U\rangle\langle U|h; k, \bar{k}\rangle \ .
\tag{6.55}
$$

From the matrix elements above, we see that this integral is proportional to $e^{-it(k+\bar{k}-m-\bar{m})} e^{-i\phi(k-\bar{k}-m+\bar{m})}$; thus the integrals over t and ϕ result in a vanishing matrix element unless $k = m$ and $\bar{m} = \bar{k}$. We conclude then that

$$
I_{m,\bar{m};k,\bar{k}} = \delta_{m,k}\delta_{\bar{m},\bar{k}} N_{k,\bar{k}} \ .
\tag{6.56}
$$

The normalization factor is given by

$$
N_{k,\bar{k}} = (2\pi)^2 \int d\rho \sinh \rho \cosh \rho \left((\tanh \rho)^{\bar{k}-k} (\cosh \rho)^{-2h} P_k^{(\bar{k}-k,\, 2h-1)} (1 - 2\tanh^2 \rho) \right)^2 ,
\tag{6.57}
$$

This is difficult to evaluate for generic k. However by $SL(2, \mathbb{R})$ invariance it must be independent of $k, \bar{k}$ (a fact we have also checked directly by numerical evaluation of the integral), allowing the integral to be performed for $k = \bar{k} = 0$, resulting in

$$
N_{k,\bar{k}} = N_{0,0} = \frac{(2\pi)^2}{2(2h - 1)} \ .
\tag{6.58}
$$

Assembling the pieces we find

$$
I_{m,\bar{m};k,\bar{k}} = \frac{(2\pi)^2}{2(2h - 1)} \delta_{m,k}\delta_{\bar{m},\bar{k}} \ ,
\tag{6.59}
$$

which is precisely the completeness relation (6.52) that we set out to show.

6.7 Metrics, connections, and geodesic distances

In this appendix we gather various properties used for global AdS and the BTZ background. We present the relevant information in Chern-Simons formulation, and the metric formulation. For the later, we gather the different coordinate systems used and the relevant geodesic distances.

In Chern-Simons formulation, we write the pair of $sl(2,\mathbb{R}) \times sl(2,\mathbb{R})$ as

$$A(y) = g_L(y)dg_L(y)^{-1}, \quad \tilde{A}(y) = \tilde{g}_R(y)^{-1}d\tilde{g}_R(y), \tag{6.60}$$

In this section we add the tilde in the right sector, for consistency with the conventions used in the main text. When the connections are constant in boundary coordinates, we can cast the group elements as

$$g_L(y) = b(\rho)^{-1}e^{-a_\mu y^\mu}, \quad \tilde{g}_R(y) = e^{\bar{a}_\mu y^\mu}b(\rho)^{-1} \quad y^\mu = (t, \phi), \tag{6.61}$$

where $b(\rho)$ parametrizes the choice of radial variable, and a_μ, and $\bar{a}_\mu$ are constant elements of the $sl(2)$ algebra. In Chapter 3, we use the following conventions to express the BTZ and global AdS metric, with[2]

$$a = -\frac{i}{4}\left((8C-2)L_0 - (1+4C)(L_1+L_{-1})\right)dx^+, \quad b(\rho) = e^{-(L_1-L_{-1})\rho/2},$$

$$\bar{a} = \frac{i}{4}\left((8C-2)L_0 + (1+4C)(L_1+L_{-1})\right)dx^-. \tag{6.62}$$

Here ρ is the radial direction and $x^\pm = t \pm \phi$ with $\phi \sim \phi + 2\pi$. Via (3.75), these connections (6.62) correspond to the metric:

$$ds^2 = d\rho^2 - \frac{1}{4}(e^\rho - 4Ce^{-\rho})^2dt^2 + \frac{1}{4}(e^\rho + 4Ce^{-\rho})^2d\phi^2. \tag{6.63}$$

For $C > 0$, it is useful to define

$$r = r_+ \cosh^2(\rho - \rho_*), \quad 4C = e^{2\rho_*} = r_+^2, \tag{6.64}$$

---

[2]We chose these explicit form of the connections because they result into unitary group elements (6.61) when we consider the highest weight representation with $(\ell_n)^\dagger = \ell_{-n}$. This is required by the purposes of Chapter 3. It is comforting to know that (6.62) is related to the more familiar form of the (non-rotating) BTZ connections used in Chapters 1, and 4

$$a = \left(L_+^e - C\,L_-^e\right)dx^+, \quad \bar{a} = -\left(L_-^e - C\,L_+^e\right)dx^-, \quad b(\rho) = \exp(\rho L_0^e).$$

via the following automorphisms:

$L:\quad L_1^e = i(2L_0 + L_1 + L_{-1})/4, \quad L_{-1}^e = 2iL_0 - iL_1 - iL_{-1}, \quad L_0^e = -(L_1 - L_{-1})/2,$

$R:\quad L_1^e = 2iL_0 + iL_1 + iL_{-1}, \quad L_{-1}^e = i(2L_0 - L_1 - L_{-1})/4, \quad L_0^e = -(L_1 - L_{-1})/2,$

and $C = 2\pi\mathcal{L}$. The automorphism labelled by R is performed in the right sector, and analogously for the left sector.

which brings (6.63) to the more familiar version of the (non-rotating) BTZ black hole:

$$ds^2 = -(r^2 - r_+^2)dt^2 + \frac{dr^2}{r^2 - r_+^2} + r^2 d\phi^2 \,, \tag{6.65}$$

For $C < 0$ the background (6.63) corresponds generically to a conical deficit. Setting $C = -1/4$, we recover from (6.63) the global AdS$_3$ spacetime:

$$ds^2 = -\cosh^2 \rho \, dt^2 + d\rho^2 + \sinh^2 \rho \, d\phi^2 \,. \tag{6.66}$$

In the next sections, we will need as well that the geodesic distance between two spacelike separated points in the bulk (y_f, y_i). For the metric in (6.63), the geodesic distance is $D(y_f, y_i) = \text{arcosh}\,\sigma(y_f, y_i)$, with

$$\sigma(y_f, y_i) = \cosh(\rho_f - \rho_i) \cosh\left(\sqrt{C}(\Delta t + \Delta\phi)\right) \cosh\left(\sqrt{C}(\Delta t - \Delta\phi)\right)$$
$$- \frac{1}{2}\left(4C\, e^{-(\rho_f + \rho_i)} + \frac{e^{\rho_f + \rho_i}}{4C}\right) \sinh\left(\sqrt{C}(\Delta t + \Delta\phi)\right) \sinh\left(\sqrt{C}(\Delta t - \Delta\phi)\right) \,. \tag{6.67}$$

which in the coordinates in (6.65) is :

$$\sigma(y_f, y_i) = \frac{1}{r_+^2}\left(r_f r_i \cosh(r_+ \Delta\phi) - \sqrt{(r_f^2 - r_+^2)(r_i^2 - r_+^2)}\cosh(r_+ \Delta t)\right) \,. \tag{6.68}$$

Moreover, the BTZ metric is locally isomorphic to *AdS*$_3$ Poincare. Using the following coordinate change

$$\frac{R^2 - T^2 + X^2 + Z^2}{2Z} = \frac{\sqrt{r^2 - r_+^2}\,\sinh(r_+ t)}{r_+} \,, \quad \frac{RT}{Z} = \frac{r \cosh(r_+ \phi)}{r_+} \,, \tag{6.69}$$

$$\frac{R^2 + T^2 - X^2 - Z^2}{2Z} = \frac{\sqrt{r^2 - r_+^2}\,\cosh(r_+ t)}{r_+} \,, \quad \frac{RX}{Z} = \frac{r \sinh(r_+ \phi)}{r_+} \,,$$

the metric (6.65) becomes

$$ds^2 = \frac{1}{Z^2}(-dT^2 + dX^2 + dZ^2) \,, \tag{6.70}$$

Null coordinates in this system are defined as $X^+ = X + T$, and $X^+ = X - T$. The geodesic distance is

$$\sigma(y_f, y_i) = \frac{(T_f - T_i)^2 + (X_f - X_i)^2 + Z_f^2 + Z_i^2}{2Z_i Z_f} \,. \tag{6.71}$$

A solution of (6.69), in the quadrant where $X, T, Z > 0\,, 1 \geq T^2 - X^2 - Z^2 > 0\,$, and $T > X$ is:

$$Z = \frac{r_+ e^{-r_+ t}}{\sqrt{r^2 - r_+^2}} \,, \qquad T = \frac{r\, e^{-r_+ t} \cosh(r_+ \phi)}{\sqrt{r^2 - r_+^2}} \,, \qquad X = \frac{r\, e^{-r_+ t} \sinh(r_+ \phi)}{\sqrt{r^2 - r_+^2}} \,. \tag{6.72}$$

6.8 Generating function of Jacobi polynomials

In this Appendix we will perform a double sum of multiplication of two Jacobi polynomials which is used in the main text. For that, we use the review on generating functions in [184]; formula (62) in Sec. 2.3 of [184] reads

$$\sum_n^\infty \frac{n!(-\alpha-\beta)!}{(-\alpha-\beta+n)!}(x-1)^n(y-1)^n t^n P_n^{(\alpha-n,\beta-n)}\left(\frac{x+1}{x-1}\right) P_n^{(\beta-n,\alpha-n)}\left(\frac{y+1}{y-1}\right)$$
$$= (1-xt)^\alpha (1-yt)^\beta \, {}_2F_1\left(-\alpha,-\beta,-\alpha-\beta,\frac{(x-1)(y-1)t}{(1-xt)(1-yt)}\right),$$
$$(6.73)$$

We need also the identity

$$\sum_n^\infty P_n^{(\alpha,\beta)}(x)z^n = \frac{2^{\alpha+\beta}}{R(1+R-z)^\alpha(1+R+z)^\beta}, \qquad R \equiv \sqrt{-2xz+z^2+1}.$$
$$(6.74)$$

Combining the previous formulas, with $y \to 1/y$, and other basic identities of hypergeometric functions, we can derive the following sum:

$$\sqrt{(1-x)(1-y)}^{2h} r^h s^h \sum_{k,\bar{k}=0}^\infty \frac{k!(2h+\bar{k}-1)!}{\bar{k}!(2h+k-1)!} r^k s^{\bar{k}}(xy)^{\frac{\bar{k}-k}{2}}$$

$$\times P_k^{(\bar{k}-k,2h-1)}(1-2x)P_k^{(\bar{k}-k,2h-1)}(1-2y) = \frac{\left(\sqrt{\sigma^2-1}+\sigma\right)^{1-2h}}{2\sqrt{\sigma^2-1}}.$$
$$(6.75)$$

where σ is defined as

$$\sigma \equiv \frac{-\sqrt{x}\sqrt{y}(r+s)+rs+1}{2\sqrt{1-x}\sqrt{1-y}\sqrt{rs}}.$$
$$(6.76)$$

For the examples worked out in section 3.4.3, σ is directly related to the geodesic distance between two endpoints.

6.9 Inner product with quasi-normal modes eigen-functions

In this appendix we explore what will happen if in (3.96), given by

$$\langle U(y_f)|U(y_i)\rangle = \sum_{k,\bar{k}}^\infty \Phi_{k,\bar{k}}(y_f)\Phi_{k,\bar{k}}^*(y_i).$$
$$(6.77)$$

we replaced (without justification) $\Phi_{k,\bar{k}}$ the more familiar quasi-normal modes for the BTZ black hole.

The quasi-normal modes are defined as the fields in black hole geometries that are purely ingoing at the horizon, and that vanish at infinity. For the BTZ black hole, solutions to $\Box^2\Phi = m^2\Phi$ with these conditions are found in [126], imposing separability in its variables:

$$
\Phi^{\text{QNM}}(y) = e^{-i\omega t}e^{il\phi}\left(\frac{r_+}{r}\right)^{2h}\left(1 - \frac{r_+^2}{r^2}\right)^{-\frac{i\omega}{2r_+}}
$$
$$
\times \ _2F_1\left(h + \frac{i}{2r_+}(l - \omega), h - \frac{i}{2r_+}(l + \omega), 2h, \frac{r_+^2}{r^2}\right) \qquad (6.78)
$$

where we have considered the non-rotating case ($r_- = 0$), and that the mass of the scalar field is related to the conformal dimension as $h = \frac{1}{2}(1 + \sqrt{1 + m^2})$. The vanishing boundary condition gives the left and right quasi-normal modes:

$$
\omega_\pm = \pm l - 2ir_+(n + h). \qquad (6.79)
$$

Using the positive root in (6.79), and defining $l = ir_+(k - \bar{k})$:

$$
\Phi_{k,\bar{k}}^{\text{QNM}}(y) = C_{k,\bar{k}}e^{-r_+(2ht+kx^++\bar{k}x^-)}
$$
$$
\times \left(\frac{r^2}{r_+^2} - 1\right)^{-h}\left(1 - \frac{r_+^2}{r^2}\right)^{\frac{k-\bar{k}}{2}} P_k^{(\bar{k}-k,2h-1)}\left(\frac{r_+^2 + r^2}{r_+^2 - r^2}\right), \qquad (6.80)
$$

We have named the previous field $\Phi_{k,\bar{k}}$ by analogy with the global case, but it does not follow (3.93) for the BTZ differential operators in (3.116).

Inspired by the global case, we will compute the overlap of two states (3.89) in the bulk. Evaluating (6.77) with (6.80) gives

$$
\langle U(y_f)|U(y_i)\rangle = \sum_{k,\bar{k}}^{\infty} \Phi_{k,\bar{k}}^{\text{QNM}}(y_f)\Phi_{k,\bar{k}}^{*\,\text{QNM}}(y_i)
$$
$$
= \sum_{k,\bar{k}=0}^{\infty} e^{-r_+h(\Delta x^++\Delta x^-)-r_+(k\Delta x^++\bar{k}\Delta x^-)}\frac{k!(2h+\bar{k}-1)!}{\bar{k}!(2h+k-1)!}\left(1 - \frac{r_+^2}{r_i^2}\right)^{\frac{k-\bar{k}}{2}}\left(1 - \frac{r_+^2}{r_f^2}\right)^{\frac{k-\bar{k}}{2}}
$$
$$
\times \left(\frac{r_i^2}{r_+^2} - 1\right)^{-h}\left(\frac{r_f^2}{r_+^2} - 1\right)^{-h} P_k^{(\bar{k}-k,\,2h-1)}\left(\frac{r_+^2 + r_f^2}{r_+^2 - r_f^2}\right) P_k^{(\bar{k}-k,\,2h-1)}\left(\frac{r_+^2 + r_i^2}{r_+^2 - r_i^2}\right).
$$
$$
(6.81)
$$

Using again (6.75), this time with $x = \left(1 - \frac{r_+^2}{r_i^2}\right)^{-1}, y = \left(1 - \frac{r_+^2}{r_f^2}\right)^{-1}, r = e^{-r_+\Delta x^-}$,

and $s = e^{-r_+ \Delta x^+}$, we see that the result for the results is as well (3.111), with the geodesic length for the BTZ in (6.68).

6.10   Integral kernels in CFT representation

In this Appendix we describe the mapping between a general $|U\rangle$ state at the boundary in Poincaré coordinates and a CFT smearing kernel (3.134) in Euclidean signature. Though our interpretation is different, the manipulations here are mathematically very similar to those in e.g. [136].

We parametrize the group element in terms of three parameters $(\sigma, w, \bar{w})$ as

$$U_1 = e^{-w_1 \frac{i}{2}(-2L_0 - L_1 - L_{-1})} e^{\sigma_1 (L_{-1} - L_1)} e^{+\bar{w}_1 \frac{i}{2}(-2L_0 + (L_1 + L_{-1}))} . \tag{6.82}$$

By acting on the Ishibashi state we can rotate it, where the splitting into G and $\overline{G}$ is arbitrary and was picked in this way for later convenience:

$$G(e^{-w_1 \frac{i}{2}(-2L_0 - L_1 - L_{-1})} e^{\sigma_1 (L_{-1} - L_1)}) \overline{G}(e^{-\bar{w}_1 \frac{i}{2}(-2L_0 + (L_1 + L_{-1}))}) |\Sigma_{\text{Ish}}\rangle = |U\rangle . \tag{6.83}$$

We now want to realize the $SL(2, \mathbb{R})$ generators geometrically in terms of differential operators acting on $\mathbb{R}^2$. We note that this assignment of generators to operators is not fixed by the algebra alone, as conjugation by any $SL(2, \mathbb{R})$ element (or an outer automorphism such as Σ_{Ish}) will leave the algebra invariant. The assignment is instead fixed by the boundary behavior of the gauge connection chosen to be the AdS$_3$ connection; for the choice (3.138) the assignment is:

$$\partial = \frac{i}{2} (2\ell_0 + \ell_1 + \ell_{-1}) , \qquad z\partial = -\frac{1}{2}(\ell_1 - \ell_{-1}) , \qquad z^2 \partial = \frac{i}{2}(2\ell_0 - \ell_1 - \ell_{-1})) ,$$
$$\bar{\partial} = \frac{i}{2} (2\bar{\ell}_0 - \bar{\ell}_1 - \bar{\ell}_{-1}) , \qquad \bar{z}\bar{\partial} = \frac{1}{2} (\bar{\ell}_1 - \bar{\ell}_{-1}) , \qquad \bar{z}^2 \bar{\partial} = \frac{i}{2} (2\bar{\ell}_0 + \bar{\ell}_1 + \bar{\ell}_{-1}) . \tag{6.84}$$

Thus the operation we want to realize is

$$\mathcal{O}_U^{(0)}(z_1, \bar{z}_1) = e^{w\partial_{z_1}} e^{2\sigma z_1 \partial_{z_1}} e^{\bar{w}\bar{\partial}_{z_1}} K(0, z_1, \bar{z}_1)[\mathcal{O}] . \tag{6.85}$$

We will now understand how these operators act on the integral kernel. Clearly two of them are just translations in z_1 and $\bar{z}_1$:

$$\exp(w\partial_1) K(\rho, z_1, \bar{z}_1)[\mathcal{O}] = K(\rho, z_1 + w, \bar{z}_1)[\mathcal{O}] ,$$
$$\exp(\bar{w}\bar{\partial}_1) K(\rho, z_1, \bar{z}_1)[\mathcal{O}] = K(\rho, z_1, \bar{z}_1 + \bar{w})[\mathcal{O}] , \tag{6.86}$$

where we use the notation from (3.132). The more interesting one is the dilatation, which acts by rescaling z_1 (note: actually z_1, not the second argument of K) by a factor of $e^{2\sigma}$:

$$\exp\left(2\sigma z_1 \partial_1\right) K(\rho, z_1, \bar{z}_1) = K(\rho, e^{2\sigma} z_1, \bar{z}_1)[\mathcal{O}] \ . \tag{6.87}$$

However, due to the form of the integral kernel, we have the following relation:

$$K(\rho, e^{2\sigma} z_1, \bar{z}_1) = K(\rho + \sigma, z_1, \bar{z}_1) \ . \tag{6.88}$$

(where this is now a relation that works for the arguments of K). To see this, note that

$$\int dz d\bar{z} \left(\frac{e^{-2\rho} - (z - e^{2\sigma} z_1)(\bar{z} - \bar{z}_1)}{e^{-\rho}} \right)^{2h-2} \mathcal{O}(iz, i\bar{z})$$
$$= \int dz' d\bar{z} \left(\frac{e^{-2\rho'} - (z' - z_1)(\bar{z} - \bar{z}_1)}{e^{-\rho'}} \right)^{2h-2} \mathcal{O}(iz', i\bar{z}) \ , \tag{6.89}$$

where $\rho' = \rho + \sigma$, $z' = e^{-2\sigma} z$ and we used the scaling property of $\mathcal{O}(\lambda z, \bar{z}) = \lambda^{-h} \mathcal{O}(z, \bar{z})$. Thus we conclude that

$$\exp\left(2\sigma z_1 \partial_1\right) K(\rho, z_1 + w, \bar{z}_1) = K(\rho + \sigma, z_1 + e^{-2\sigma} w, \bar{z}_1)[\mathcal{O}] \ . \tag{6.90}$$

We now construct the desired object:

$$\begin{aligned}
\mathcal{O}_U^{(0)}(z_1, \bar{z}_1) &= e^{w \partial_{z_1}} e^{-2\sigma z_1 \partial_{z_1}} e^{\bar{w} \bar{\partial}_{z_1}} K(0, z_1, \bar{z}_1)[\mathcal{O}] \\
&= e^{w \partial_{z_1}} e^{2\sigma z_1 \partial_{z_1}} K(0, z_1, \bar{z}_1 + \bar{w})[\mathcal{O}] \\
&= e^{w \partial_{z_1}} K(\sigma, z_1, \bar{z}_1 + \bar{w})[\mathcal{O}] \\
&= K(\sigma, z_1 + w, \bar{z}_1 + \bar{w})[\mathcal{O}] \ .
\end{aligned} \tag{6.91}$$

Now we finally need to act with the overall compensating ρ dilatation:

$$\begin{aligned}
\mathcal{O}_U^{(\rho)}(z_1, \bar{z}_1) &= e^{\rho z \partial_{z_1}} e^{\rho \bar{z} \partial_{\bar{z}_1}} K(\sigma, z_1 + w, \bar{z}_1 + w)[\mathcal{O}] \\
&= K(\sigma, e^{\rho} z_1 + w, e^{\rho} \bar{z}_1 + w)[\mathcal{O}] \\
&= K(\rho + \sigma, z_1 + e^{-\rho} w, \bar{z}_1 + e^{-\rho} w)[\mathcal{O}] \ .
\end{aligned} \tag{6.92}$$

The final relation is thus

$$\mathcal{O}_U^{(\rho)}(z_1, \bar{z}_1) = K(\rho + \sigma, z_1 + e^{-\rho} w, \bar{z}_1 + e^{-\rho} w)[\mathcal{O}] \ , \tag{6.93}$$

which is (3.134) in the text.

6.11 Wilson line operator in AdS$_3$ higher spin gravity

This appendix is a brief summary of the results in [4, 108] with emphasis on how to evaluate the Wilson line. To recap, the operator is defined as

$$W_{\mathcal{R}}(y_i, y_f) = \langle U_f | \mathcal{P} \exp\left(-\int_\gamma A\right) \mathcal{P} \exp\left(-\int_\gamma \bar{A}\right) |U_i\rangle \;, \qquad (6.94)$$

$\mathcal{R}$ is the infinite dimensional representation in (4.2), and γ is a curve with bulk endpoints (y_i, y_j). $U(y)$ is a probe field that lives in the worldline γ, and which quantum numbers are governed by $\mathcal{R}$. Its boundary values are chosen such that $U_i = U_f = \mathbb{1}$: this choice ensures that the Wilson line that the answer is Lorentz invariant. In a saddle point approximation, the value of the Wilson line is

$$-\log W_{\mathcal{R}}(y_i, y_f) \sim \text{tr}_f(\log(M)P_0) \;, \qquad (6.95)$$

where here $\sim$ denotes the saddle point approximation, and P_0 is the conjugated momentum of the probe field U. More importantly P_0 carries the data related to the Casimir's of the representation $\mathcal{R}$. In the highest weight representation of $sl(N, \mathbb{R}) \oplus sl(N, \mathbb{R})$ labelled by quantum numbers $(h, h_s) = (\bar{h}, \bar{h}_s)$ we would have

$$P_0 \equiv \frac{h}{2} L_0 + \sum_{s=2}^{N} h_s W_0^{(s)} \;. \qquad (6.96)$$

The matrix M in (6.95) contains the information about the background connections $(A, \bar{A})$:

$$M \equiv g_R(y_i) g_L(y_i) g_L^{-1}(y_f) g_R^{-1}(y_f) \;, \qquad (6.97)$$

with $g_R(y)$ and $g_L(y)$ are defined according to (4.5). This expression makes evident that the Wilson line is only sensitive to the endpoints of γ.

We will restrict now the discussion to Wilson lines in $sl(3, \mathbb{R}) \oplus sl(3, \mathbb{R})$. As we send the endpoints of the Wilson line to one of the two boundaries, located at $r \to \pm\infty$, we only need to consider the asymptotic behaviour of the eigenvalues of M to evaluate (6.95). If asymptotically we have

$$b(r) = \bar{b}(r) \underset{r\to\infty}{\to} e^{rL_0} \;, \qquad (6.98)$$

the eigenvalues of M will asymptote to

$$\lambda_M \sim \left(m_1 \, \epsilon^{-4}, \quad \frac{m_2}{m_1}, \quad \frac{\epsilon^4}{m_2}\right) \;, \qquad (6.99)$$

where $\epsilon = e^{-\rho}$ is the cutoff, and m_1 and m_2 are related to the coefficients of the characteristic polynomial as:

$$\text{Tr}_f(M) = m_1 \, \epsilon^{-4} + ... , \qquad \frac{1}{2} \left(\text{Tr}_f(M)^2 - \text{Tr}_f(M^2) \right) = m_2 \, \epsilon^{-4} + ... \quad (6.100)$$

Note that $m_1 = m_1(y_i, y_f)$ and $m_2 = m_2(y_i, y_f)$ depend on the endpoints and the background charges carried by the connections. The asymptotic behaviour of the Wilson line close to the boundary is given by

$$- \log W_{\mathcal{R}}(y_i, y_f) = \frac{h}{2} \, \log \left(\frac{m_1 m_2(y_i, y_f)}{\epsilon^8} \right) + h_3 \log \left(\frac{m_1(y_i, y_f)}{m_2(y_i, y_f)} \right) . \quad (6.101)$$

where we kept only universal terms as $\epsilon \to 0$. It is important to highlight that we have written an equal sign in (6.101), even though the expression is valid just in the the saddle-point approximation, and at $r \to \pm\infty$. For simplicity, we will use this notation through this chapter.

It will be useful to note that for $\Delta\phi = 0$, the solutions depends only a_t and $\bar{a}_t$, which are elements of $SL(2,\mathbb{R})$ subgroup in $SL(3,\mathbb{R})$ due to the holonomy condition (1.113). Therefore, M belongs as well to the $SL(2,\mathbb{R})$ subgroup, which implies that $m_1 = m_2$ and

$$- \log W_{\mathcal{R}}(t_i, t_f) = h \log \left(\frac{m_1(t_i, t_f)}{\epsilon^4} \right) . \quad (6.102)$$

In general we only need that at infinity

$$b(r), \, \bar{b}(r) \cong e^{-\log(\varepsilon)L_0} , \quad (6.103)$$

where $\cong$ means equal up to conjugation, and ε controls the UV cutoff as we approach the asymptotic boundaries. If the conjugation matrices do not depend on ε, the formulas (6.99)-(6.102) hold with the substitution ϵ by ε. This will be the case of the black hole gauge, detailed in Section 6.13.

We can perform a consistency check. When we have a just a theory pure gravity and not higher spin charges, and it can be shown that equation (6.95) reduces to:

$$- \log W_{\mathcal{R}} = 2h \cosh^{-1} \left(\frac{1}{2} \text{tr}_f(M) \right) . \quad (6.104)$$

where we take the trace in the fundamental representation of $SL(2,\mathbb{R})$. Using the explicit form $sl(2,\mathbb{R})$ connections in (1.125), and the parametrization (4.23), we show that

$$\cosh^{-1} \left(\frac{1}{2} \text{tr}_f(M) \right) = D(y_i, y_f) . \quad (6.105)$$

where $D(y_i, y_f)$ is the geodesic distance related to this background metric (6.63). Therefore, that (6.104) is equivalent to what we found in (3.5), when $U_i = U_f = \mathbb{1}$.

6.12   Thermofield states and KMS conditions

In this appendix we review the definition thermofield state, and properties of thermal correlations functions. We will denote the relations discussed below as "KMS conditions" (even though only one of them is strictly speaking *the* KMS condition).

Consider a system with a Hamiltonian H, and time-evolve operators in the Heisenberg picture:

$$\mathcal{O}(t) = e^{iHt}\mathcal{O}(0)e^{-iHt} . \tag{6.106}$$

It is very easy to show that for two operators $\mathcal{O}_1$ and $\mathcal{O}_2$, we have

$$\text{Tr}\left(e^{-\beta H}\mathcal{O}_1(t - i\beta)\mathcal{O}_2(0)\right) = \text{Tr}\left(e^{-\beta H}\mathcal{O}_2(0)\mathcal{O}_1(t)\right) . \tag{6.107}$$

This is what one normally calls the KMS condition.

Let us now try this for a different density matrix $\rho = e^{-\beta H - \beta\mu Q}$ with Q another conserved charge of the system; for example, it could be a $U(1)$ charge, or $Q = W_0$ where W_0 is the zero mode of the $\mathcal{W}_3$ algebra. In this case we find

$$\begin{aligned}
\text{Tr}\left(e^{-\beta H - \beta\mu Q}\mathcal{O}_2(0)\mathcal{O}_1(t)\right) &= \text{Tr}\left(e^{-\beta H - \beta\mu Q}\mathcal{O}_2(0)e^{-\beta H - \beta\mu Q}e^{+\beta H + \beta\mu Q}\mathcal{O}_1(t)\right) \\
&= \text{Tr}\left(\mathcal{O}_2(0)e^{-\beta H - \beta\mu Q}\left[e^{\beta\mu Q}\mathcal{O}_1(t - i\beta)e^{-\beta\mu Q}\right]\right) \\
&= \text{Tr}\left(e^{-\beta H - \beta\mu Q}\mathcal{O}_1(t - i\beta)\mathcal{O}_2(0)\right)e^{-\beta\mu q_1} ,
\end{aligned} \tag{6.108}$$

where in the last equality we have assumed that $\mathcal{O}_1$ is an operator with definite charge q_1. Note that if $\mathcal{O}_1$ was *not* a charge eigenstate we could stop at the line above and still get a useful (but more complicated) KMS relation. Thus the charged KMS relation is

$$\text{Tr}\left(e^{-\beta H - \beta\mu Q}\mathcal{O}_1(t - i\beta)\mathcal{O}_2(0)\right) = \text{Tr}\left(e^{-\beta H - \beta\mu Q}\mathcal{O}_2(0)\mathcal{O}_1(t)\right)e^{+\beta\mu q_1} . \tag{6.109}$$

The extra factor involving the charge on the right-hand side appeared because of the mismatch between the Hamiltonian used to evolve the system (i.e. just H) and the Hamiltonian used to construct the density matrix (i.e. $H + \mu Q$). If we evolve the system using $H + \mu Q$ then there will be no extra factor involving the charge, and the correlator will be strictly periodic, as in (6.107).

The thermofield double state is defined as follows. Let $\mathcal{H} = \mathcal{H}_L \otimes \mathcal{H}_R$ denote the full Hilbert space which is composed by two copies of the original CFT Hilbert

space. The thermofield state is defined by the following wave function on $\mathcal{H}$

$$|\psi\rangle = \frac{1}{\sqrt{Z}} \sum_n e^{-\frac{\beta}{2}(E_n + \mu Q_n)} |\mathcal{U}n\rangle_L \otimes |n\rangle_R \ . \tag{6.110}$$

Here we included a chemical potential, and the sum is over all energy eigenstates of the system which carry as well Q charge; Z is a suitable normalization. $\mathcal{U}$ is the anti-unitary operator that implements CPT; this is important since if one constructs the thermofield state by cutting open a path-integral then this CPT operator must be there (see e.g. [185, 186]). Anti-unitary implies that

$$\mathcal{U}^{-1} = \mathcal{U}^\dagger \qquad \langle \mathcal{U}\psi | \mathcal{U}\phi \rangle = \langle \phi | \psi \rangle \ , \tag{6.111}$$

and the fact that $\mathcal{U}$ implements CPT means

$$\mathcal{U}^{-1}(iH)\mathcal{U} = -iH \qquad \mathcal{U}^{-1}\mathcal{O}\mathcal{U} \equiv \mathcal{O}^{CPT} \ . \tag{6.112}$$

Note that $\mathcal{U}$ actually commutes with H, but anticommutes with i. We denote the CPT conjugate of an operator with a superscript. For sake of simplicity, in the following we will consider scalar operators and in this case $\mathcal{O}^{CPT} = \mathcal{O}^\dagger$.

Now let us carefully compute

$$\langle \psi | \mathcal{O}_{1,L}(t_L) \mathcal{O}_{2,R}(t_R) | \psi \rangle$$
$$= \frac{1}{Z} \sum_{m,n} \langle \mathcal{U}n | e^{i\hat{H}t_L} \mathcal{O}_1 e^{-i\hat{H}t_L} |\mathcal{U}m\rangle \langle n | e^{i\hat{H}t_R} \mathcal{O}_2 e^{-i\hat{H}t_R} |m\rangle e^{-\frac{\beta}{2}(\hat{E}_n + \hat{E}_m)} \ , \tag{6.113}$$

where $\hat{E}_n = E_n + \mu Q_n$. Note that we are evolving the system with $\hat{H} \equiv H + \mu Q$, which is the natural choice from the gravitational side. Looking at the first term, we find

$$\langle \mathcal{U}n | e^{i\hat{H}t_L} \mathcal{O}_1 e^{-i\hat{H}t_L} |\mathcal{U}m\rangle = \langle \mathcal{U}n | \mathcal{U} e^{-i\hat{H}t_L} \mathcal{O}_1^{CPT} e^{i\hat{H}t_L} m\rangle$$
$$= \langle e^{-i\hat{H}t_L} \mathcal{O}_1^{CPT} e^{i\hat{H}t_L} m | n\rangle$$
$$= \langle m | e^{-i\hat{H}t_L} (\mathcal{O}_1^{CPT})^\dagger e^{i\hat{H}t_L} |n\rangle$$
$$= \langle m | e^{-i\hat{H}t_L} \mathcal{O}_1 e^{i\hat{H}t_L} |n\rangle \ . \tag{6.114}$$

The first equality uses (6.112) and the second uses (6.111), the third equality follows from the definition of the adjoint, and in the last line we used that the

operator is scalar. Thus we find

$$
\begin{aligned}
\langle\psi|\mathcal{O}_{1,L}(t_L)\mathcal{O}_{2,R}(t_R)|\psi\rangle & \\
&= \sum_{m,n} e^{-\frac{\beta}{2}\left(\hat{E}_n+\hat{E}_m\right)+it_L\left(\hat{E}_n-\hat{E}_m\right)+it_R\left(\hat{E}_n-\hat{E}_m\right)}\langle m|\mathcal{O}_1|n\rangle\langle n|\mathcal{O}_2|m\rangle \\
&= \sum_{m,n}\langle m|e^{-\frac{\beta}{2}\left(\hat{H}-i\hat{H}(t_L+t_R)\right)}\mathcal{O}_1 e^{-\frac{\beta}{2}\left(\hat{H}+i\hat{H}(t_L+t_R)\right)}|n\rangle\langle n|\mathcal{O}_2|m\rangle \\
&= \mathrm{Tr}\left(e^{-\beta(H+\mu Q)}\mathcal{O}_1\left(-t_L-\frac{i\beta}{2}\right)\mathcal{O}_2(t_R)\right) \ .
\end{aligned}
$$

(6.115)

These manipulations shows how $\langle\psi|\mathcal{O}_{1,L}(t_L)\mathcal{O}_{2,R}(t_R)|\psi\rangle$ is related to the thermal correlation function. With some slight abuse of language, and in analogy to (6.107), we will refer to this relation as a KMS condition. Note that the sign of t_L is flipped: this relation explains what it means for "time to run backwards on the other side".

If instead we used H to evolve the system, instead of $\hat{H}$,

$$
\langle\psi|\mathcal{O}_{1,L}(t_L)\mathcal{O}_{2,R}(t_R)|\psi\rangle = \mathrm{Tr}\left(e^{-\beta H-\mu Q}\mathcal{O}_1\left(-t_L-\frac{i\beta}{2}\right)\mathcal{O}_2(t_R)\right)e^{-\frac{\beta\mu q_1}{2}} \ ,
$$

(6.116)

where we assumed that $\mathcal{O}_1$ is a scalar operator with a definite charge q_1. For operators with more complicated CPT conjugations or that are not charge eigenstates, we would find more complicated versions of (6.115).

From the above KMS conditions, we can derive further relation. Define the RR correlator as a 'one-sided' correlator in the thermofield state which involves only operators on $\mathcal{H}_R$. For $\mathcal{O}_1 = \mathcal{O}_2 \equiv \mathcal{O}$, we find

$$
\langle\psi|\mathcal{O}_R(t_f)\mathcal{O}_R(t_i)|\psi\rangle = \mathrm{Tr}\left(e^{-\beta\hat{H}}\mathcal{O}(t_f)\mathcal{O}(t_i)\right) \ ,
$$

(6.117)

where we have suppressed the indexes R in the right hand side of the equation since they are redundant. Analogously, the LL correlator is

$$
\langle\psi|\mathcal{O}_L(t_f)\mathcal{O}_L(t_i)|\psi\rangle = \mathrm{Tr}\left(e^{-\beta\hat{H}}\mathcal{O}(-t_f)\mathcal{O}(-t_i)\right) \ .
$$

(6.118)

For an LR correlator we have

$$
\langle\psi|\mathcal{O}_L(t_f)\mathcal{O}_R(t_i)|\psi\rangle = \mathrm{Tr}\left(e^{-\beta\hat{H}}\mathcal{O}(-t_f-i\beta/2)\mathcal{O}(t_i)\right) \ ,
$$

(6.119)

and obviously, the RL correlator is given by

$$
\langle\psi|\mathcal{O}_R(t_f)\mathcal{O}_L(t_i)|\psi\rangle = \mathrm{Tr}\left(e^{-\beta\hat{H}}\mathcal{O}(t_f)\mathcal{O}(-t_i-i\beta/2)\right) \ .
$$

(6.120)

These previous identities imply that the correlators should be related as

$$
\begin{aligned}
\langle\psi|\mathcal{O}_R(t_f)\mathcal{O}_R(t_i)|\psi\rangle &= \langle\psi|\mathcal{O}_R(t_f)\mathcal{O}_R(t_i - i\beta)|\psi\rangle \\
&= \langle\psi|\mathcal{O}_L(-t_f)\mathcal{O}_L(-t_i)|\psi\rangle \\
&= \langle\psi|\mathcal{O}_L(-t_f - i\beta/2)\mathcal{O}_R(t_i)|\psi\rangle \\
&= \langle\psi|\mathcal{O}_R(t_f)\mathcal{O}_L(-t_i - i\beta/2)|\psi\rangle\,,
\end{aligned}
\tag{6.121}
$$

The relations between the one-sided (RR and LL) and two-sided correlators (RL and LR) we denote as "KMS conditions".

6.13 Horizon gauge for $\mathcal{W}_3$ black hole

In this appendix we present the solution to the horizon condition constructed in [51]. This solution is valid for the non-rotating holomorphic black hole (1.126), however it is straight forward to check that it is also applicable for the non-rotating canonical black hole (1.127). The ansatz used there is

$$
\begin{aligned}
A &= g(r)^{-1}b(r)^{-1}(a_h + d)\,b(r)g(r)\,, \\
\bar{A} &= g(r)b(r)\,(\bar{a}_h + d)b(r)^{-1}g(r)^{-1}\,,
\end{aligned}
\tag{6.122}
$$

where $b(r) = e^{(r+r_0)L_0}$ with $e^{r_0} = \sqrt{2\pi\mathcal{L}/k}$, and they take

$$
\begin{aligned}
g(r) &= e^{F(r)(W_1 - W_{-1}) + G(r)L_0}\,, \\
h(r) &= e^{H(r)(W_1 + W_{-1})}\,,
\end{aligned}
\tag{6.123}
$$

with $F(r) = F(-r)$, $G(r) = G(-r)$, and $H(-r) = -H(-r)$; this implies that $g(r) = g(-r)$, $h(r) = h^{-1}(-r)$ and $h(0) = \mathbb{1}$. Using (6.123), a solution to (4.59)-(4.60) is

$$
\begin{aligned}
Y^2 &= 1 + C\,\cosh^2(r)\,, \tag{6.124} \\
X &= \sqrt{\frac{C - 1 + Y}{C - 1 - Y}}\,, \tag{6.125} \\
G &= -\frac{1}{Y}\log(X) \tag{6.126} \\
\frac{F}{G} &= \frac{\sqrt{C}}{2}\cosh(r)\,, \tag{6.127} \\
\tan H &= -\frac{\sinh(r)}{\sqrt{C - 2 - \cosh^2(r)}}\,. \tag{6.128}
\end{aligned}
$$

In this new radial parametrization, the asymptotic boundary is now located at $r = r_*$ which is given by

$$\cosh^2(r_*) = C - 2 \quad \longleftrightarrow \quad Y(r_*) = C - 1 \,. \tag{6.129}$$

In the BTZ limit, $C \to \infty$, we recover $r = r_* \to \infty$. From equations (6.124)-(6.127), we observe that the parameter X diverges when $r = r_*$, and Y, G, and F have an finite value. At the boundary, we consider X^{-1} as the cutoff ε, and we can express Y, G, and F in terms of C. With these considerations, we diagonalize $g(r_*)$, and find as eigenvalues:

$$\lambda_g(r_*) = \left(\varepsilon^{-1}, \quad 1, \quad \varepsilon \right) = e^{-\log(\varepsilon)L_0} \,, \tag{6.130}$$

The eigenvectors of $g(r_*)$ are finite, i.e., they do not depend in ε.

6.14 Computation of Kruskal gauge for higher spin black hole

Here we provide details of the computation of the radial functions $b(\rho)$ and $\bar{b}(\rho)$ that are required to put the higher spin black hole in Kruskal gauge. The basic constraint on these functions arises from the demand that the Euclidean objects defined as

$$B(r, \tau) = e^{a_\tau \tau} b(r) e^{-iL_0 \frac{2\pi\tau}{\beta}} \qquad \overline{B}(r, \tau) = e^{iL_0 \frac{2\pi\tau}{\beta}} \bar{b}(\rho) e^{-\bar{a}_\tau \tau} \tag{6.131}$$

 be smooth functions of the complex coordinates

$$w = r e^{\frac{2\pi i \tau}{\beta}} \qquad \bar{w} = r e^{-\frac{2\pi i \tau}{\beta}} \tag{6.132}$$

near the Euclidean origin. By smooth, we mean that the expansion of $B(w, \bar{w})$ contains only positive integer powers of $w, \bar{w}$. As described in the bulk text, this analyticity property guarantees that the gauge connections can be analytically continued to a Lorentzian section that describes a two-sided black hole with a smooth horizon.

On the other hand, to have a clean CFT interpretation of the bulk connections, we need to also demand that as it approaches the boundary $b(r)$ blow up as $b(r) \sim \exp(g(r)L_0)$ with $g(r)$ some function that tends to infinity at the boundary. Here we describe the construction of the functions $b, \bar{b}$ that satisfy these two requirements.

6.14.1   Setup

First, we use coordinates where the horizon is at $r = 0$, and which further match onto the more conventional ρ coordinate at large r as $\rho = e^r$. In other words the function $g(r) = e^r$. Now consider diagonalizing a and $\bar{a}$: the holonomy condition tells us that a_τ and $\bar{a}_\tau$ are conjugate to L_0, so we have

$$a_\tau = V \left(\frac{2\pi i L_0}{\beta} \right) V^{-1} \qquad \bar{a}_\tau = \bar{V} \left(\frac{2\pi i L_0}{\beta} \right) \bar{V}^{-1} . \tag{6.133}$$

Inserting these expansions into (6.131) we find

$$B(r, \tau) = V e^{\frac{2\pi i \tau}{\beta} L_0} V^{-1} b(r) e^{-i \frac{2\pi \tau}{\beta} L_0}, \tag{6.134}$$

and a similar expression for $\overline{B}$. We will focus for now on B. We expand

$$V^{-1} b(r) = \exp \left(\sum_a F_a(r) T^a \right) \tag{6.135}$$

where a runs over the generators of the algebra, $F_a(r)$ is a set of mode functions to be defined shortly, and the T^a are the generators. Note that the demand that B depend smoothly on $w, \bar{w}$ as defined in (6.132) ties together the time and radial dependence. In this basis the time-dependence is simply a conjugation by L_0, multiplying each generator by a factor of $e^{-\frac{2\pi i h(a)\tau}{\beta}}$, where $h(a)$ is the weight under L_0 of the generator T^a, i.e. $[L_0, T^a] = -h(a)T^a$. Thus the analyticity condition requires that near the origin we have:

$$F_a(r \to 0) \sim r^{|h(a)|} . \tag{6.136}$$

as well as a parity condition on r (i.e. $F_a(r)$ should be either even or odd).

We also require that at infinity we approach $b(r \to \infty) \sim \exp\left(e^r L_0\right)$. It is convenient to define a basis of functions $f_a^m(r)$ such that

$$f_a^m(r \to 0) \sim r^{|h(a)|} \qquad f_a^m(r \to \infty) \sim e^{-mr} . \tag{6.137}$$

Such a basis is presented explicitly below and is easy to find as the functions are otherwise unconstrained. We now further expand

$$F_a = \sum_{m=-1,0,\cdots} c_a^m f_a^m(r) \tag{6.138}$$

By adjusting the coefficients c_a^m we may reproduce any function at infinity to a prescribed order in an expansion in inverse powers in e^{-r}. We will calculate only the terms $m = -1, 0$ as this is sufficient to calculate any correlator in $SL(3)$ higher spin gravity: for $SL(N)$ we require $N - 1$ terms.

6.14.2   Diagonalization

We now explicitly calculate the matrix logarithm of

$$Q \equiv V^{-1} \exp(\rho L_0) \tag{6.139}$$

to the first two orders in inverse powers of $\rho \equiv e^r$ to find the expansion coefficients c_a^m.

It is easiest to diagonalize Q and take the logarithm of the eigenvalues. To diagonalize Q in the asymptotic limit we follow an algorithm somewhat similar to that normally used in quantum mechanical perturbation theory, with some modifications arising from the fact that Q is not Hermitian. Define $x \equiv e^\rho$. Denoting the i-th eigenvalue and eigenvector as $\lambda^{(i)}$ and $v^{(i)}$ respectively, we expand everything in powers of x to find:

$$\left(Q_1 x + Q_0 + Q_{-1} x^{-1} \cdots \right) \left(v_0^{(i)} + v_{-1}^{(i)} x^{-1} + \cdots \right)$$
$$= (\lambda_1^{(i)} x + \lambda_0^{(i)} + \cdots) \left(v^{(i)} + v_{-1}^{(i)} x^{-1} + \cdots \right), \tag{6.140}$$

The Q_α may be found explicitly and directly diagonalized without much difficulty. The challenge is to extract from the Q_α the behavior of the $v^{(i)}$. We assume the expansion in powers of the eigenvectors starts at $\mathcal{O}(x^0)$: this can always be arranged by rescaling the individual eigenvectors. We will determine each $v^{(i)}$ only to leading order, i.e. $v_0^{(i)}$.

We first need to first determine the scaling behavior of the eigenvalues. Note first that if we define $\mathcal{Q}_n \equiv \text{Tr}(Q^n)$, then the characteristic polynomial of Q is given by

$$P_Q(\lambda) = -\lambda^3 + \mathcal{Q}_1 \lambda^2 - \frac{1}{2}(\mathcal{Q}_1^2 - \mathcal{Q}_2)\lambda + 1, \tag{6.141}$$

where we have used the fact that product of the eigenvalues is 1 as $Q \in SL(3)$. From direct computation we now find that as $x \to \infty$, $\mathcal{Q}_1 \sim q_1 x + \mathcal{O}(1)$, $\frac{1}{2}(\mathcal{Q}_1^2 - \mathcal{Q}_2) \sim q_2 x + \mathcal{O}(1)$, where q_1 and q_2 are presented explicitly below. Now by balancing terms in the characteristic polynomial we find that the eigenvalues scale as

$$\lambda^{(i)}(x \to \infty) \sim \left(q_1 x, \frac{q_2}{q_1}, \frac{1}{q_2 x} \right), \tag{6.142}$$

Thus we see that the order of the starting term in $\lambda_\alpha^{(i)}$ depends on which eigenvalue we are studying, e.g. $\lambda_1^{(1)} = q_1$ but $\lambda_1^{(2)} = 0$.

We turn now to the eigenvectors. We begin with the largest eigenvalue, $\lambda^{(1)}$. The $\mathcal{O}(x^1)$ equation is

$$Q_1 v_0^{(1)} = \lambda_1^{(1)} v_0^{(1)} \tag{6.143}$$

In other words, $v_0^{(1)}$ is an eigenvector of Q_1 itself with eigenvalue $\lambda_1^{(1)} = q_1$. If we now examine the eigenvectors of Q_1 we see that it has two eigenvectors with zero eigenvalue, $\text{Dim}(\text{Ker}(Q_1)) = 2$, as well as a single nonzero eigenvector with eigenvalue q_1: thus $v_0^{(1)}$ is fixed to be this eigenvector.

We turn now to $\lambda^{(2)}$. The $\mathcal{O}(x^1)$ equation is now

$$Q_1 v_0^{(2)} = 0 \tag{6.144}$$

and thus we find only that $v_0^{(2)}$ belongs to the two-dimensional kernel of Q_1 discussed above. To narrow it down within this subspace, we study the $\mathcal{O}(x^0)$ equation, which is

$$Q_1 v_{-1}^{(2)} + \left(Q_0 - \lambda_0^{(2)} \mathbf{1}\right) v_0^{(2)} = 0 \tag{6.145}$$

Thus $\left(Q_0 - \lambda_0^{(2)} \mathbf{1}\right) v_0^{(2)}$ lies within the image of Q_1: but this means that it is proportional to the only eigenvector of Q_1 with nonzero eigenvalue, and so is proportional to $v_0^{(1)}$ found above. So we see that

$$v_0^{(2)} = \left(Q_0 - \lambda_0^{(2)} \mathbf{1}\right)^{-1} v_0^{(1)} \tag{6.146}$$

fixing it up to rescaling. We turn finally to the eigenvector corresponding to $\lambda^{(3)}$. While presumably the above procedure can be systematized to arbitrarily higher order, as $\lambda^{(3)}$ is the last eigenvalue, we may use a trick: the $\mathcal{O}(x^1)$ and $\mathcal{O}(x^0)$ equations are

$$Q_1 v_0^{(3)} = 0 \qquad Q_2 v_0^{(3)} = 0 \ . \tag{6.147}$$

and thus $v_0^{(3)}$ lies in the intersection of the kernel of Q_1 and the kernel of Q_2; we may explicitly check that this intersection is a one-dimensional subspace, fixing $v_0^{(3)}$.

Thus we have determined the eigenvalues and eigenvectors. We write now

$$Q(x \to \infty) \sim W \exp(D) W^{-1} = \exp(WDW^{-1}) \tag{6.148}$$

where W is the matrix whose columns are the $v^{(i)}$ and D is the following diagonal matrix:

$$D = \log(\text{diag}(\lambda^{(i)})) = L_0(\log x) + \Lambda \qquad \Lambda \equiv \text{diag}\left(\log q_1, \log\left(\frac{q_2}{q_1}\right), -\log(q_2)\right) \tag{6.149}$$

We now equate WDW^{-1} with $\sum_a F_a(r)T^a$ defined in (6.135), multiply by T^b, and take a trace to find

$$\sum_a \sum_{m=-1,0} \delta^{ab} c_a^m f_a^m (r \to \infty) = \text{Tr}(WDW^{-1}T^b) \qquad (6.150)$$

where we have defined the Killing metric on the Lie algebra as $\delta^{ab} \equiv \text{Tr}(T^aT^b)$ and its inverse by δ_{ab}. Now from the explicit form of the W's and of the mode functions f_a^m we can find the expansion coefficients c_a^m. Note that due to the judicious choice of the mode functions, the term $m = -1$ corresponds directly to the $L_0(\log x)$ term in (6.149) and the $m = 0$ term to the second (constant in x) term.

$$c_a^{-1} = \delta_{ab} \text{Tr}(WL_0W^{-1}T^b) \qquad c_a^0 = \delta_{ab} \text{Tr}(W\Lambda W^{-1}T^b) \qquad (6.151)$$

From (6.135) this fixes $b(r)$ as

$$b(r) = V \exp\left(\sum_a \sum_{m=-1,0} c_a^m f_a^m(r)\right) \qquad (6.152)$$

For the barred connection we follow precisely the same procedure to find instead

$$\bar{b}(r) = \exp\left(\sum_a \sum_{m=-1,0} \bar{c}_a^m f_a^m(r)\right) \bar{V}^{-1} . \qquad (6.153)$$

In Appendix E.3 in [3], we collect expressions for $b(r)$ and $\bar{b}(r)$ found by implementing this algorithm.

BIBLIOGRAPHY

[1] A. Castro, E. Llabrés, and F. Rejon-Barrera, "Geodesic Diagrams, Gravitational Interactions & OPE Structures," *JHEP* **06** (2017) 099, `arXiv:1702.06128 [hep-th]`.

[2] A. Castro, N. Iqbal, and E. Llabrés, "Wilson Lines and Ishibashi States in AdS_3/CFT_2," *JHEP* **09** (2018) 066, `arXiv:1805.05398 [hep-th]`.

[3] A. Castro, N. Iqbal, and E. Llabrés, "Eternal Higher Spin Black Holes: a Thermofield Interpretation," *JHEP* **08** (2016) 022, `arXiv:1602.09057 [hep-th]`.

[4] A. Castro and E. Llabrés, "Unravelling Holographic Entanglement Entropy in Higher Spin Theories," *JHEP* **03** (2015) 124, `arXiv:1410.2870 [hep-th]`.

[5] J. de Boer, E. Llabrés, J. F. Pedraza, and D. Vegh, "Chaotic strings in AdS/CFT," *Phys. Rev. Lett.* **120** no. 20, (2018) 201604, `arXiv:1709.01052 [hep-th]`.

[6] S. W. Hawking, "Black holes in general relativity," *Commun. Math. Phys.* **25** (1972) 152–166.

[7] J. D. Bekenstein, "Black holes and entropy," *Phys. Rev.* **D7** (1973) 2333–2346.

[8] S. W. Hawking, "Particle Creation by Black Holes," *Commun. Math. Phys.* **43** (1975) 199–220.

[9] G. 't Hooft, "Dimensional reduction in quantum gravity,"

arXiv:gr-qc/9310026.

[10] L. Susskind, "The World as a hologram," *J. Math. Phys.* **36** (1995) 6377–6396, arXiv:hep-th/9409089.

[11] J. M. Maldacena, "The large N limit of superconformal field theories and supergravity," *Adv. Theor. Math. Phys.* **2** (1998) 231–252, arXiv:hep-th/9711200.

[12] M. Van Raamsdonk, "Building up spacetime with quantum entanglement," *Gen. Rel. Grav.* **42** (2010) 2323–2329, arXiv:1005.3035 [hep-th]. [Int. J. Mod. Phys.D19,2429(2010)].

[13] S. Ferrara, A. F. Grillo, and R. Gatto, "Manifestly conformal covariant operator-product expansion," *Lett. Nuovo Cim.* **2S2** (1971) 1363–1369. [Lett. Nuovo Cim.2,1363(1971)].

[14] S. Ferrara, A. F. Grillo, G. Parisi, and R. Gatto, "Covariant expansion of the conformal four-point function," *Nucl. Phys.* **B49** (1972) 77–98. [Erratum: Nucl. Phys.B53,643(1973)].

[15] S. Ferrara, R. Gatto, and A. F. Grillo, "Properties of Partial Wave Amplitudes in Conformal Invariant Field Theories," *Nuovo Cim.* **A26** (1975) 226.

[16] F. A. Dolan and H. Osborn, "Conformal Partial Waves: Further Mathematical Results," arXiv:1108.6194 [hep-th].

[17] F. A. Dolan and H. Osborn, "Conformal partial waves and the operator product expansion," *Nucl. Phys.* **B678** (2004) 491–507, arXiv:hep-th/0309180 [hep-th].

[18] F. A. Dolan and H. Osborn, "Conformal four point functions and the operator product expansion," *Nucl. Phys.* **B599** (2001) 459–496, arXiv:hep-th/0011040 [hep-th].

[19] E. Witten, "Anti-de Sitter space and holography," *Adv. Theor. Math. Phys.* **2** (1998) 253–291, arXiv:hep-th/9802150.

[20] E. D'Hoker and D. Z. Freedman, "General scalar exchange in AdS(d+1)," *Nucl. Phys.* **B550** (1999) 261–288, arXiv:hep-th/9811257 [hep-th].

[21] E. D'Hoker, D. Z. Freedman, and L. Rastelli, "AdS / CFT four point functions: How to succeed at z integrals without really trying," *Nucl. Phys.* **B562** (1999) 395–411, arXiv:hep-th/9905049 [hep-th].

[22] E. D'Hoker, D. Z. Freedman, S. D. Mathur, A. Matusis, and L. Rastelli, "Graviton exchange and complete four point functions in the AdS / CFT correspondence," *Nucl. Phys.* **B562** (1999) 353–394, arXiv:hep-th/9903196 [hep-th].

[23] H. Liu, "Scattering in anti-de Sitter space and operator product expansion," *Phys. Rev.* **D60** (1999) 106005, arXiv:hep-th/9811152 [hep-th].

[24] I. Heemskerk, J. Penedones, J. Polchinski, and J. Sully, "Holography from Conformal Field Theory," *JHEP* **10** (2009) 079, arXiv:0907.0151 [hep-th].

[25] W. Pauli and M. Fierz, "On Relativistic Field Equations of Particles With Arbitrary Spin in an Electromagnetic Field," *Helv. Phys. Acta* **12** (1939) 297–300.

[26] A. L. Fitzpatrick and J. Kaplan, "Unitarity and the Holographic S-Matrix," *JHEP* **10** (2012) 032, arXiv:1112.4845 [hep-th].

[27] M. S. Costa, V. Goncalves, and J. Penedones, "Spinning AdS Propagators," *JHEP* **09** (2014) 064, arXiv:1404.5625 [hep-th].

[28] X. Bekaert, J. Erdmenger, D. Ponomarev, and C. Sleight, "Towards holographic higher-spin interactions: Four-point functions and higher-spin exchange," *JHEP* **03** (2015) 170, arXiv:1412.0016 [hep-th].

[29] P. H. Ginsparg, "APPLIED CONFORMAL FIELD THEORY," in *Les Houches Summer School in Theoretical Physics: Fields, Strings, Critical Phenomena Les Houches, France, June 28-August 5, 1988*, pp. 1–168. 1988. arXiv:hep-th/9108028 [hep-th]. http://inspirehep.net/record/265020/files/arXiv:hep-th_9108028.pdf.

[30] S. Carlip, "The (2+1)-Dimensional black hole," *Class.Quant.Grav.* **12** (1995) 2853–2880, arXiv:gr-qc/9506079 [gr-qc].

[31] V. Balasubramanian and P. Kraus, "A stress tensor for anti-de Sitter

gravity," *Commun. Math. Phys.* **208** (1999) 413–428, `hep-th/9902121`.

[32] J. D. Brown and J. W. York, Jr., "Quasilocal energy and conserved charges derived from the gravitational action," *Phys. Rev.* **D47** (1993) 1407–1419, `arXiv:gr-qc/9209012 [gr-qc]`.

[33] J. D. Brown and M. Henneaux, "Central Charges in the Canonical Realization of Asymptotic Symmetries: An Example from Three-Dimensional Gravity," *Commun.Math.Phys.* **104** (1986) 207–226.

[34] M. Banados, "Three-dimensional quantum geometry and black holes," `arXiv:hep-th/9901148 [hep-th]`.

[35] A. Achucarro and P. K. Townsend, "A Chern-Simons Action for Three-Dimensional anti-De Sitter Supergravity Theories," *Phys. Lett.* **B180** (1986) 89.

[36] E. Witten, "(2+1)-Dimensional Gravity as an Exactly Soluble System," *Nucl.Phys.* **B311** (1988) 46.

[37] M. Ammon, M. Gutperle, P. Kraus, and E. Perlmutter, "Black holes in three dimensional higher spin gravity: A review," *J.Phys.* **A46** (2013) 214001, `arXiv:1208.5182 [hep-th]`.

[38] A. Campoleoni, S. Fredenhagen, S. Pfenninger, and S. Theisen, "Asymptotic symmetries of three-dimensional gravity coupled to higher-spin fields," *JHEP* **1011** (2010) 007, `arXiv:1008.4744 [hep-th]`.

[39] M. Banados, "Global charges in Chern-Simons field theory and the (2+1) black hole," *Phys.Rev.* **D52** (1996) 5816, `arXiv:hep-th/9405171 [hep-th]`.

[40] M. Banados, T. Brotz, and M. E. Ortiz, "Quantum three-dimensional de Sitter space," *Phys. Rev.* **D59** (1999) 046002, `arXiv:hep-th/9807216 [hep-th]`.

[41] M. Gutperle and P. Kraus, "Higher Spin Black Holes," *JHEP* **1105** (2011) 022, `arXiv:1103.4304 [hep-th]`.

[42] I. Klebanov and A. Polyakov, "AdS dual of the critical O(N) vector model," *Phys.Lett.* **B550** (2002) 213–219, `arXiv:hep-th/0210114 [hep-th]`.

[43] E. Sezgin and P. Sundell, "Massless higher spins and holography," *Nucl. Phys.* **B644** (2002) 303–370, `arXiv:hep-th/0205131`.

[44] M. A. Vasiliev, "Consistent equation for interacting gauge fields of all spins in (3+1)-dimensions," *Phys.Lett.* **B243** (1990) 378–382.

[45] M. A. Vasiliev, "Nonlinear equations for symmetric massless higher spin fields in (A)dS(d)," *Phys. Lett.* **B567** (2003) 139–151, `arXiv:hep-th/0304049 [hep-th]`.

[46] C. Aragone and S. Deser, "HYPERSYMMETRY IN D = 3 OF COUPLED GRAVITY MASSLESS SPIN 5/2 SYSTEM," *Class. Quant. Grav.* **1** (1984) L9.

[47] C. Fronsdal, "Massless Fields with Integer Spin," *Phys. Rev.* **D18** (1978) 3624.

[48] M. Henneaux and S.-J. Rey, "Nonlinear $W_{infinity}$ as Asymptotic Symmetry of Three-Dimensional Higher Spin Anti-de Sitter Gravity," *JHEP* **1012** (2010) 007, `arXiv:1008.4579 [hep-th]`.

[49] A. Campoleoni, S. Fredenhagen, and S. Pfenninger, "Asymptotic W-symmetries in three-dimensional higher-spin gauge theories," *JHEP* **1109** (2011) 113, `arXiv:1107.0290 [hep-th]`.

[50] A. Castro, E. Hijano, A. Lepage-Jutier, and A. Maloney, "Black Holes and Singularity Resolution in Higher Spin Gravity," *JHEP* **1201** (2012) 031, `arXiv:1110.4117 [hep-th]`.

[51] M. Ammon, M. Gutperle, P. Kraus, and E. Perlmutter, "Spacetime Geometry in Higher Spin Gravity," *JHEP* **1110** (2011) 053, `arXiv:1106.4788 [hep-th]`.

[52] J. de Boer and J. I. Jottar, "Thermodynamics of higher spin black holes in AdS_3," *JHEP* **1401** (2014) 023, `arXiv:1302.0816 [hep-th]`.

[53] C. Bunster, M. Henneaux, A. Perez, D. Tempo, and R. Troncoso, "Generalized Black Holes in Three-dimensional Spacetime," `arXiv:1404.3305 [hep-th]`.

[54] J. de Boer and J. I. Jottar, "Boundary Conditions and Partition Functions

in Higher Spin AdS_3/CFT_2," `arXiv:1407.3844 [hep-th]`.

[55] M. Banados, R. Canto, and S. Theisen, "The Action for higher spin black holes in three dimensions," *JHEP* **1207** (2012) 147, `arXiv:1204.5105 [hep-th]`.

[56] A. Perez, D. Tempo, and R. Troncoso, "Higher spin gravity in 3D: Black holes, global charges and thermodynamics," *Phys.Lett.* **B726** (2013) 444–449, `arXiv:1207.2844 [hep-th]`.

[57] G. Compère, J. I. Jottar, and W. Song, "Observables and Microscopic Entropy of Higher Spin Black Holes," *JHEP* **1311** (2013) 054, `arXiv:1308.2175 [hep-th]`.

[58] M. Henneaux, A. Perez, D. Tempo, and R. Troncoso, "Chemical potentials in three-dimensional higher spin anti-de Sitter gravity," *JHEP* **1312** (2013) 048, `arXiv:1309.4362 [hep-th]`.

[59] A. Castro, R. Gopakumar, M. Gutperle, and J. Raeymaekers, "Conical Defects in Higher Spin Theories," *JHEP* **1202** (2012) 096, `arXiv:1111.3381 [hep-th]`.

[60] E. Hijano and P. Kraus, "A new spin on entanglement entropy," *JHEP* **12** (2014) 041, `arXiv:1406.1804 [hep-th]`.

[61] J. de Boer, A. Castro, E. Hijano, J. I. Jottar, and P. Kraus, "Higher spin entanglement and $\mathcal{W}_N$ conformal blocks," *JHEP* **07** (2015) 168, `arXiv:1412.7520 [hep-th]`.

[62] E. Hijano, P. Kraus, E. Perlmutter, and R. Snively, "Witten Diagrams Revisited: The AdS Geometry of Conformal Blocks," *JHEP* **01** (2016) 146, `arXiv:1508.00501 [hep-th]`.

[63] R. Rattazzi, V. S. Rychkov, E. Tonni, and A. Vichi, "Bounding scalar operator dimensions in 4D CFT," *JHEP* **12** (2008) 031, `arXiv:0807.0004 [hep-th]`.

[64] D. Poland, D. Simmons-Duffin, and A. Vichi, "Carving Out the Space of 4D CFTs," *JHEP* **05** (2012) 110, `arXiv:1109.5176 [hep-th]`.

[65] S. El-Showk, M. F. Paulos, D. Poland, S. Rychkov, D. Simmons-Duffin,

and A. Vichi, "Solving the 3D Ising Model with the Conformal Bootstrap,"
Phys. Rev. **D86** (2012) 025022, `arXiv:1203.6064 [hep-th]`.

[66] S. Rychkov, *EPFL Lectures on Conformal Field Theory in D ≥ 3
Dimensions.* SpringerBriefs in Physics. 2016. `arXiv:1601.05000
[hep-th]`. `http://inspirehep.net/record/1415968/files/arXiv:
1601.05000.pdf`.

[67] D. Simmons-Duffin, "TASI Lectures on the Conformal Bootstrap,"
`arXiv:1602.07982 [hep-th]`.

[68] D. Poland and D. Simmons-Duffin, "The conformal bootstrap," *Nature
Phys.* **12** no. 6, (2016) 535–539.

[69] J. M. Maldacena, "The Large N limit of superconformal field theories and
supergravity," *Int. J. Theor. Phys.* **38** (1999) 1113–1133,
`arXiv:hep-th/9711200 [hep-th]`. [Adv. Theor. Math. Phys.2,231(1998)].

[70] S. S. Gubser, I. R. Klebanov, and A. M. Polyakov, "Gauge theory
correlators from noncritical string theory," *Phys. Lett.* **B428** (1998)
105–114, `arXiv:hep-th/9802109 [hep-th]`.

[71] M. Nishida and K. Tamaoka, "Geodesic Witten diagrams with an external
spinning field," `arXiv:1609.04563 [hep-th]`.

[72] M. S. Costa, J. Penedones, D. Poland, and S. Rychkov, "Spinning
Conformal Blocks," *JHEP* **11** (2011) 154, `arXiv:1109.6321 [hep-th]`.

[73] H. Liu and A. A. Tseytlin, "On four point functions in the CFT / AdS
correspondence," *Phys. Rev.* **D59** (1999) 086002, `arXiv:hep-th/9807097
[hep-th]`.

[74] D. Z. Freedman, S. D. Mathur, A. Matusis, and L. Rastelli, "Comments on
4 point functions in the CFT / AdS correspondence," *Phys. Lett.* **B452**
(1999) 61–68, `arXiv:hep-th/9808006 [hep-th]`.

[75] E. D'Hoker, S. D. Mathur, A. Matusis, and L. Rastelli, "The Operator
product expansion of N=4 SYM and the 4 point functions of supergravity,"
Nucl. Phys. **B589** (2000) 38–74, `arXiv:hep-th/9911222 [hep-th]`.

[76] L. Hoffmann, A. C. Petkou, and W. Ruhl, "Aspects of the conformal

operator product expansion in AdS / CFT correspondence," *Adv. Theor. Math. Phys.* **4** (2002) 571–615, `arXiv:hep-th/0002154 [hep-th]`.

[77] L. Hoffmann, A. C. Petkou, and W. Ruhl, "A Note on the analyticity of AdS scalar exchange graphs in the crossed channel," *Phys. Lett.* **B478** (2000) 320–326, `arXiv:hep-th/0002025 [hep-th]`.

[78] J. Penedones, "Writing CFT correlation functions as AdS scattering amplitudes," *JHEP* **03** (2011) 025, `arXiv:1011.1485 [hep-th]`.

[79] M. F. Paulos, "Towards Feynman rules for Mellin amplitudes," *JHEP* **10** (2011) 074, `arXiv:1107.1504 [hep-th]`.

[80] A. L. Fitzpatrick, J. Kaplan, J. Penedones, S. Raju, and B. C. van Rees, "A Natural Language for AdS/CFT Correlators," *JHEP* **11** (2011) 095, `arXiv:1107.1499 [hep-th]`.

[81] M. S. Costa, V. Goncalves, and J. Penedones, "Conformal Regge theory," *JHEP* **12** (2012) 091, `arXiv:1209.4355 [hep-th]`.

[82] V. Goncalves, J. Penedones, and E. Trevisani, "Factorization of Mellin amplitudes," *JHEP* **10** (2015) 040, `arXiv:1410.4185 [hep-th]`.

[83] R. Gopakumar, A. Kaviraj, K. Sen, and A. Sinha, "A Mellin space approach to the conformal bootstrap," `arXiv:1611.08407 [hep-th]`.

[84] M. S. Costa, J. Penedones, D. Poland, and S. Rychkov, "Spinning Conformal Correlators," *JHEP* **11** (2011) 071, `arXiv:1107.3554 [hep-th]`.

[85] C. Sleight and M. Taronna, "Higher Spin Interactions from Conformal Field Theory: The Complete Cubic Couplings," *Phys. Rev. Lett.* **116** no. 18, (2016) 181602, `arXiv:1603.00022 [hep-th]`.

[86] M. Taronna, *Higher-Spin Interactions: three-point functions and beyond*. PhD thesis, Pisa, Scuola Normale Superiore, 2012. `arXiv:1209.5755 [hep-th]`. `http://inspirehep.net/record/1188191/files/arXiv:1209.5755.pdf`.

[87] X. Bekaert, J. Erdmenger, D. Ponomarev, and C. Sleight, "Quartic AdS

Interactions in Higher-Spin Gravity from Conformal Field Theory," *JHEP* **11** (2015) 149, `arXiv:1508.04292 [hep-th]`.

[88] J. Erdmenger, M. Flory, and C. Sleight, "Conditions on holographic entangling surfaces in higher curvature gravity," *JHEP* **06** (2014) 104, `arXiv:1401.5075 [hep-th]`.

[89] M. S. Costa, T. Hansen, J. Penedones, and E. Trevisani, "Projectors and seed conformal blocks for traceless mixed-symmetry tensors," *JHEP* **07** (2016) 018, `arXiv:1603.05551 [hep-th]`.

[90] E. Joung, L. Lopez, and M. Taronna, "On the cubic interactions of massive and partially-massless higher spins in (A)dS," *JHEP* **07** (2012) 041, `arXiv:1203.6578 [hep-th]`.

[91] E. Joung, L. Lopez, and M. Taronna, "Generating functions of (partially-)massless higher-spin cubic interactions," *JHEP* **01** (2013) 168, `arXiv:1211.5912 [hep-th]`.

[92] B. Czech, L. Lamprou, S. McCandlish, B. Mosk, and J. Sully, "A Stereoscopic Look into the Bulk," *JHEP* **07** (2016) 129, `arXiv:1604.03110 [hep-th]`.

[93] J. de Boer, F. M. Haehl, M. P. Heller, and R. C. Myers, "Entanglement, holography and causal diamonds," *JHEP* **08** (2016) 162, `arXiv:1606.03307 [hep-th]`.

[94] M. Guica, "Bulk fields from the boundary OPE," `arXiv:1610.08952 [hep-th]`.

[95] C. Sleight and M. Taronna, "Higher-Spin Algebras, Holography and Flat Space," `arXiv:1609.00991 [hep-th]`.

[96] M. S. Costa and T. Hansen, "Conformal correlators of mixed-symmetry tensors," *JHEP* **02** (2015) 151, `arXiv:1411.7351 [hep-th]`.

[97] A. Castedo Echeverri, E. Elkhidir, D. Karateev, and M. Serone, "Deconstructing Conformal Blocks in 4D CFT," *JHEP* **08** (2015) 101, `arXiv:1505.03750 [hep-th]`.

[98] F. Rejon-Barrera and D. Robbins, "Scalar-Vector Bootstrap," *JHEP* **01**

(2016) 139, `arXiv:1508.02676 [hep-th]`.

[99] L. Iliesiu, F. Kos, D. Poland, S. S. Pufu, D. Simmons-Duffin, and R. Yacoby, "Fermion-Scalar Conformal Blocks," *JHEP* **04** (2016) 074, `arXiv:1511.01497 [hep-th]`.

[100] A. Castedo Echeverri, E. Elkhidir, D. Karateev, and M. Serone, "Seed Conformal Blocks in 4D CFT," *JHEP* **02** (2016) 183, `arXiv:1601.05325 [hep-th]`.

[101] M. S. Costa, T. Hansen, J. Penedones, and E. Trevisani, "Radial expansion for spinning conformal blocks," *JHEP* **07** (2016) 057, `arXiv:1603.05552 [hep-th]`.

[102] V. Schomerus, E. Sobko, and M. Isachenkov, "Harmony of Spinning Conformal Blocks," `arXiv:1612.02479 [hep-th]`.

[103] O. Aharony, L. F. Alday, A. Bissi, and E. Perlmutter, "Loops in AdS from Conformal Field Theory," `arXiv:1612.03891 [hep-th]`.

[104] S. Giombi, C. Sleight, and M. Taronna, "Spinning AdS Loop Diagrams: Two Point Functions," *JHEP* **06** (2018) 030, `arXiv:1708.08404 [hep-th]`.

[105] E. Witten, "Quantum field theory and the Jones polynomial," *Commun. Math. Phys.* **121** (1989) 351.

[106] E. Witten, "Topology Changing Amplitudes in (2+1)-Dimensional Gravity," *Nucl.Phys.* **B323** (1989) 113.

[107] S. Carlip, "Exact Quantum Scattering in (2+1)-Dimensional Gravity," *Nucl.Phys.* **B324** (1989) 106.

[108] M. Ammon, A. Castro, and N. Iqbal, "Wilson Lines and Entanglement Entropy in Higher Spin Gravity," *JHEP* **1310** (2013) 110, `arXiv:1306.4338 [hep-th]`.

[109] M. Blencowe, "A Consistent Interacting Massless Higher Spin Field Theory In D = (2+1)," *Class.Quant.Grav.* **6** (1989) 443.

[110] E. Bergshoeff, M. Blencowe, and K. Stelle, "Area Preserving Diffeomorphisms and Higher Spin Algebra," *Commun.Math.Phys.* **128**

(1990) 213.

[111] J. de Boer and J. I. Jottar, "Entanglement Entropy and Higher Spin Holography in AdS$_3$," *JHEP* **1404** (2013) , `arXiv:1306.4347 [hep-th]`.

[112] A. Hegde, P. Kraus, and E. Perlmutter, "General results for higher spin Wilson lines and entanglement in Vasiliev theory," *Journal of High Energy Physics* **2016** no. 1, (2016) 176.

[113] A. Castro, S. Detournay, N. Iqbal, and E. Perlmutter, "Holographic entanglement entropy and gravitational anomalies," *JHEP* **1407** (2014) 114, `arXiv:1405.2792 [hep-th]`.

[114] A. Castro, D. M. Hofman, and N. Iqbal, "Entanglement entropy in warped conformal field theories," *Journal of High Energy Physics* **2016** no. 2, (2016) 33.

[115] N. Ishibashi, "The Boundary and Crosscap States in Conformal Field Theories," *Mod. Phys. Lett.* **A4** (1989) 251.

[116] J. L. Cardy, "Boundary conformal field theory," `arXiv:hep-th/0411189 [hep-th]`.

[117] D. E. Berenstein, R. Corrado, W. Fischler, and J. M. Maldacena, "The Operator product expansion for Wilson loops and surfaces in the large N limit," *Phys. Rev.* **D59** (1999) 105023, `arXiv:hep-th/9809188 [hep-th]`.

[118] U. H. Danielsson, E. Keski-Vakkuri, and M. Kruczenski, "Vacua, propagators, and holographic probes in AdS / CFT," *JHEP* **01** (1999) 002, `arXiv:hep-th/9812007 [hep-th]`.

[119] J. M. Maldacena, "Eternal black holes in anti-de Sitter," *JHEP* **0304** (2003) 021, `arXiv:hep-th/0106112 [hep-th]`.

[120] M. Miyaji, T. Numasawa, N. Shiba, T. Takayanagi, and K. Watanabe, "Continuous Multiscale Entanglement Renormalization Ansatz as Holographic Surface-State Correspondence," *Phys. Rev. Lett.* **115** no. 17, (2015) 171602, `arXiv:1506.01353 [hep-th]`.

[121] H. Verlinde, "Poking Holes in AdS/CFT: Bulk Fields from Boundary States," `arXiv:1505.05069 [hep-th]`.

[122] Y. Nakayama and H. Ooguri, "Bulk Locality and Boundary Creating Operators," *JHEP* **10** (2015) 114, `arXiv:1507.04130 [hep-th]`.

[123] J. M. Maldacena and A. Strominger, "AdS(3) black holes and a stringy exclusion principle," *JHEP* **9812** (1998) 005, `arXiv:hep-th/9804085 [hep-th]`.

[124] V. Balasubramanian, P. Kraus, and A. E. Lawrence, "Bulk versus boundary dynamics in anti-de Sitter space-time," *Phys. Rev.* **D59** (1999) 046003, `arXiv:hep-th/9805171 [hep-th]`.

[125] J. S. F. Chan and R. B. Mann, "Scalar wave falloff in asymptotically anti-de Sitter backgrounds," *Phys. Rev.* **D55** (1997) 7546–7562, `arXiv:gr-qc/9612026 [gr-qc]`.

[126] D. Birmingham, "Choptuik scaling and quasinormal modes in the AdS / CFT correspondence," *Phys. Rev.* **D64** (2001) 064024, `arXiv:hep-th/0101194 [hep-th]`.

[127] V. Cardoso and J. P. S. Lemos, "Scalar, electromagnetic and Weyl perturbations of BTZ black holes: Quasinormal modes," *Phys. Rev.* **D63** (2001) 124015, `arXiv:gr-qc/0101052 [gr-qc]`.

[128] D. Birmingham, I. Sachs, and S. N. Solodukhin, "Conformal field theory interpretation of black hole quasinormal modes," *Phys. Rev. Lett.* **88** (2002) 151301, `arXiv:hep-th/0112055 [hep-th]`.

[129] B. Chen and J. Long, "Hidden Conformal Symmetry and Quasi-normal Modes," *Phys. Rev.* **D82** (2010) 126013, `arXiv:1009.1010 [hep-th]`.

[130] H.-b. Zhang, "$SL(2, R)$ symmetry and quasi-normal modes in the BTZ black hole," *JHEP* **03** (2011) 009, `arXiv:1102.4721 [hep-th]`.

[131] M. Banados, *Agujero Negro en Tres Dimensiones*. PhD thesis, Universidad de Chile, 1993.

[132] A. Hamilton, D. N. Kabat, G. Lifschytz, and D. A. Lowe, "Holographic representation of local bulk operators," *Phys. Rev.* **D74** (2006) 066009, `arXiv:hep-th/0606141 [hep-th]`.

[133] A. Hamilton, D. N. Kabat, G. Lifschytz, and D. A. Lowe, "Local bulk

operators in AdS/CFT: A Boundary view of horizons and locality," *Phys. Rev.* **D73** (2006) 086003, `arXiv:hep-th/0506118 [hep-th]`.

[134] Y. Nakayama and H. Ooguri, "Bulk Local States and Crosscaps in Holographic CFT," *JHEP* **10** (2016) 085, `arXiv:1605.00334 [hep-th]`.

[135] A. Lewkowycz, G. J. Turiaci, and H. Verlinde, "A CFT Perspective on Gravitational Dressing and Bulk Locality," *JHEP* **01** (2017) 004, `arXiv:1608.08977 [hep-th]`.

[136] K. Goto and T. Takayanagi, "CFT descriptions of bulk local states in the AdS black holes," `arXiv:1704.00053 [hep-th]`.

[137] N. Anand, H. Chen, A. L. Fitzpatrick, J. Kaplan, and D. Li, "An Exact Operator That Knows Its Location," *JHEP* **02** (2018) 012, `arXiv:1708.04246 [hep-th]`.

[138] A. Hamilton, D. N. Kabat, G. Lifschytz, and D. A. Lowe, "Local bulk operators in AdS/CFT: A Holographic description of the black hole interior," *Phys. Rev.* **D75** (2007) 106001, `arXiv:hep-th/0612053 [hep-th]`. [Erratum: Phys. Rev.D75,129902(2007)].

[139] K. Papadodimas and S. Raju, "Black Hole Interior in the Holographic Correspondence and the Information Paradox," *Phys. Rev. Lett.* **112** no. 5, (2014) 051301, `arXiv:1310.6334 [hep-th]`.

[140] M. Guica and D. L. Jafferis, "On the construction of charged operators inside an eternal black hole," *SciPost Phys.* **3** no. 2, (2017) 016, `arXiv:1511.05627 [hep-th]`.

[141] B. Carneiro da Cunha and M. Guica, "Exploring the BTZ bulk with boundary conformal blocks," `arXiv:1604.07383 [hep-th]`.

[142] S. Giombi, A. Maloney, and X. Yin, "One-loop Partition Functions of 3D Gravity," *JHEP* **08** (2008) 007, `arXiv:0804.1773 [hep-th]`.

[143] H. L. Verlinde, "Conformal Field Theory, 2-*D* Quantum Gravity and Quantization of Teichmuller Space," *Nucl. Phys.* **B337** (1990) 652–680.

[144] S. Elitzur, G. W. Moore, A. Schwimmer, and N. Seiberg, "Remarks on the Canonical Quantization of the Chern-Simons-Witten Theory," *Nucl. Phys.*

B326 (1989) 108–134.

[145] K. B. Alkalaev and V. A. Belavin, "Classical conformal blocks via AdS/CFT correspondence," *JHEP* **08** (2015) 049, `arXiv:1504.05943 [hep-th]`.

[146] E. Hijano, P. Kraus, E. Perlmutter, and R. Snively, "Semiclassical Virasoro blocks from AdS$_3$ gravity," *JHEP* **12** (2015) 077, `arXiv:1508.04987 [hep-th]`.

[147] K. B. Alkalaev and V. A. Belavin, "Monodromic vs geodesic computation of Virasoro classical conformal blocks," *Nucl. Phys.* **B904** (2016) 367–385, `arXiv:1510.06685 [hep-th]`.

[148] M. Besken, A. Hegde, E. Hijano, and P. Kraus, "Holographic conformal blocks from interacting Wilson lines," *JHEP* **08** (2016) 099, `arXiv:1603.07317 [hep-th]`.

[149] A. L. Fitzpatrick, J. Kaplan, D. Li, and J. Wang, "Exact Virasoro Blocks from Wilson Lines and Background-Independent Operators," *JHEP* **07** (2017) 092, `arXiv:1612.06385 [hep-th]`.

[150] R. Nakayama and T. Suzuki, "A Bulk Localized State and New Holographic Renormalization Group Flow in 3D Spin-3 Gravity," *Int. J. Mod. Phys.* **A33** no. 12, (2018) 1850061, `arXiv:1712.04678 [hep-th]`.

[151] M. Banados, R. Canto, and S. Theisen, "Higher Spin Black Holes in Three Dimensions: Comments on Asymptotics and Regularity," `arXiv:1601.05827 [hep-th]`.

[152] A. Lewkowycz and J. Maldacena, "Generalized gravitational entropy," *JHEP* **1308** (2013) 090, `arXiv:1304.4926 [hep-th]`.

[153] S. Datta, J. R. David, M. Ferlaino, and S. P. Kumar, "Higher spin entanglement entropy from CFT," `arXiv:1402.0007 [hep-th]`.

[154] S. Ryu and T. Takayanagi, "Holographic derivation of entanglement entropy from AdS/CFT," *Phys.Rev.Lett.* **96** (2006) 181602, `arXiv:hep-th/0603001 [hep-th]`.

[155] W. Israel, "Thermo field dynamics of black holes," *Phys. Lett.* **A57** (1976)

107–110.

[156] P. Kraus and E. Perlmutter, "Probing higher spin black holes," *JHEP* **1302** (2013) 096, arXiv:1209.4937 [hep-th].

[157] A. Chamblin, R. Emparan, C. V. Johnson, and R. C. Myers, "Charged AdS black holes and catastrophic holography," *Phys. Rev.* **D60** (1999) 064018, arXiv:hep-th/9902170 [hep-th].

[158] S. A. Hartnoll, "Lectures on holographic methods for condensed matter physics," *Class. Quant. Grav.* **26** (2009) 224002, arXiv:0903.3246 [hep-th].

[159] A. Castro, D. M. Hofman, and N. Iqbal, "Entanglement Entropy in Warped Conformal Field Theories," *JHEP* **02** (2016) 033, arXiv:1511.00707 [hep-th].

[160] M. Banados, M. Henneaux, C. Teitelboim, and J. Zanelli, "Geometry of the (2+1) black hole," *Phys.Rev.* **D48** (1993) 1506–1525, arXiv:gr-qc/9302012 [gr-qc].

[161] P. Kraus, H. Ooguri, and S. Shenker, "Inside the horizon with AdS / CFT," *Phys. Rev.* **D67** (2003) 124022, arXiv:hep-th/0212277 [hep-th].

[162] R. Callan, J.-Y. He, and M. Headrick, "Strong subadditivity and the covariant holographic entanglement entropy formula," *JHEP* **1206** (2012) 081, arXiv:1204.2309 [hep-th].

[163] J. Knuttel, "Entanglement Entropy and Black Holes in (2+1)-Dimensional Higher Spin Gravity," Master's thesis, University of Amsterdam, The Netherlands, 2014.

[164] M. R. Gaberdiel, K. Jin, and E. Perlmutter, "Probing higher spin black holes from CFT," *JHEP* **1310** (2013) 045, arXiv:1307.2221 [hep-th].

[165] T. Hartman and J. Maldacena, "Time Evolution of Entanglement Entropy from Black Hole Interiors," *JHEP* **05** (2013) 014, arXiv:1303.1080 [hep-th].

[166] P. Calabrese and J. L. Cardy, "Evolution of entanglement entropy in one-dimensional systems," *J. Stat. Mech.* **0504** (2005) P04010,

arXiv:cond-mat/0503393 [cond-mat].

[167] H. Liu and S. J. Suh, "Entanglement Tsunami: Universal Scaling in Holographic Thermalization," *Phys. Rev. Lett.* **112** (2014) 011601, arXiv:1305.7244 [hep-th].

[168] H. Liu and S. J. Suh, "Entanglement growth during thermalization in holographic systems," *Phys. Rev.* **D89** no. 6, (2014) 066012, arXiv:1311.1200 [hep-th].

[169] D. A. Roberts and D. Stanford, "Two-dimensional conformal field theory and the butterfly effect," *Phys. Rev. Lett.* **115** no. 13, (2015) 131603, arXiv:1412.5123 [hep-th].

[170] J. Maldacena, S. H. Shenker, and D. Stanford, "A bound on chaos," arXiv:1503.01409 [hep-th].

[171] E. Perlmutter, "Bounding the Space of Holographic CFTs with Chaos," arXiv:1602.08272 [hep-th].

[172] N. Iqbal, H. Liu, and M. Mezei, "Semi-local quantum liquids," *JHEP* **04** (2012) 086, arXiv:1105.4621 [hep-th].

[173] T. Faulkner, N. Iqbal, H. Liu, J. McGreevy, and D. Vegh, "Holographic non-Fermi liquid fixed points," *Phil. Trans. Roy. Soc.* **A 369** (2011) 1640, arXiv:1101.0597 [hep-th].

[174] T. Faulkner, H. Liu, J. McGreevy, and D. Vegh, "Emergent quantum criticality, Fermi surfaces, and AdS(2)," *Phys. Rev.* **D83** (2011) 125002, arXiv:0907.2694 [hep-th].

[175] M. Banados, A. Castro, A. Faraggi, and J. I. Jottar, "Extremal Higher Spin Black Holes," arXiv:1512.00073 [hep-th].

[176] A. L. Fitzpatrick, J. Kaplan, and M. T. Walters, "Universality of Long-Distance AdS Physics from the CFT Bootstrap," *JHEP* **1408** (2014) 145, arXiv:1403.6829 [hep-th].

[177] Y. Hikida and T. Uetoko, "Conformal blocks from Wilson lines with loop corrections," *Phys. Rev.* **D97** no. 8, (2018) 086014, arXiv:1801.08549 [hep-th].

[178] A. Bhatta, P. Raman, and N. V. Suryanarayana, "Holographic Conformal Partial Waves as Gravitational Open Wilson Networks," `arXiv:1602.02962 [hep-th]`.

[179] A. Bhatta, P. Raman, and N. V. Suryanarayana, "Scalar Blocks as Gravitational Wilson Networks," `arXiv:1806.05475 [hep-th]`.

[180] C. Sleight, *Interactions in Higher-Spin Gravity: a Holographic Perspective*. PhD thesis, Munich U., 2016. `arXiv:1610.01318 [hep-th]`. `http://inspirehep.net/record/1489652/files/arXiv:1610.01318.pdf`.

[181] D. Z. Freedman, S. D. Mathur, A. Matusis, and L. Rastelli, "Correlation functions in the CFT(d) / AdS(d+1) correspondence," *Nucl. Phys.* **B546** (1999) 96–118, `arXiv:hep-th/9804058 [hep-th]`.

[182] E. D'Hoker and D. Z. Freedman, "Supersymmetric gauge theories and the AdS / CFT correspondence," in *Strings, Branes and Extra Dimensions: TASI 2001: Proceedings*, pp. 3–158. 2002. `arXiv:hep-th/0201253 [hep-th]`.

[183] A. Zhiboedov, "A note on three-point functions of conserved currents," `arXiv:1206.6370 [hep-th]`.

[184] H. Srivastava and H. Manocha, *A treatise on generating functions*. Ellis Horwood limited, 1984.

[185] D. Marolf and J. Polchinski, "Gauge/Gravity Duality and the Black Hole Interior," *Phys. Rev. Lett.* **111** (2013) 171301, `arXiv:1307.4706 [hep-th]`.

[186] D. Harlow, "Jerusalem Lectures on Black Holes and Quantum Information," `arXiv:1409.1231 [hep-th]`.

Samenvatting

Dit proefschrift gaat over aspecten van de AdS/CFT-correspondentie die direct belangrijk zijn voor problemen in klassieke- en kwantumzwaartekracht. In het bijzonder gebruiken we geodetische Wittendiagrammen en Wilsonlijnen in AdS/CFT om zwaartekracht te onderzoeken. Wat volgt is een samenvatting van onze resultaten.

Inleidein

In hoofdstuk 1 beginnen we met en overzicht van de holografische correspondentie, met nadruk op de kenmerken die onmisbaar zijn voor dit proefschrift. Dit zal de context scheppen voor de nieuwe resultaten die in de rest van de hoofdstukken worden gepresenteerd. Deze inleiding, evenals het proefschrift, heeft twee te onderscheiden delen. Het eerste delen onderzoekt enkele aspecten van de dualiteit in algemene dimensies en het tweede delen focus op de eigenaardigheden van AdS_3/CFT_2. Een terugkerend leidmotief is hogere spinvelden. We zullen theorieën gebruiken die spinnende velden bevatten, als een raamwerk om de AdS/CFT-correspondentie te bestuderen.

Spinnende geodetische-Wittendiagrammen

Symmetrieën spelen een cruciale rol in conforme veldtheorieën. De exploitatie van de conforme groep geeft een efficiënt organisatieprincipe voitie van vierpuntscorrelatiefuncties, die een expliciet onderscheid maakt tussen delen die puur bepaald wordor de waarneembare theorieën. Een voorbeeld van een dergelijk principe is de conforme blokdecomposen door symmetrieën en de theorieafhankelijke gege-

vens. Een heel natuurlijke vraag doet zich voor in holografie: kunnen we obser-
vabelen in zwaartekracht even efficiënt organiseren als in de duaal CFT's? Dit
probleem is sinds het begin van holografie aangepalst met behulp van bijvoor-
beeld Wittendiagrammen. Pas onlangs werden, geodetische Wittendiagrammen
werden voorgesteld als de duaal van de conforme blokken. Geodetische Witten-
diagrammen werpen nieuw licht op het idëe van holografische reconstructie: ze
geven een holografische betekenis aan de conforme blokdecompositie van vierpunts
Wittendiagrammen en ze stellen ons in staat de gecompliceerde d-dimensionale vo-
lumeintegralen van de Wittendiagrammen te schrijven in termen van eenvoudigere
lijnintegralen. Het oorspronkelijke voorstel van geodetisch Wittendiagrammen was
alleen voor externe scalaire velden geformuleerd. In hoofdstuk 2 hebben we dit uit-
gebreid tot spinnende velden in de externe vertices. We hebben een systematische
manier gevonden om geodetische Wittendiagrammen voor externe velden met al-
gemene spin te evalueren en we hebben de originele Wittendiagrammen ontleed in
termen daarvan. Ondanks het succes van geodetische Wittendiagrammen vonden
we enkele problemen die onopgelost bleven. We hebben waargenomen dat het-
zelfde conforme blok met spin kan worden uitgedrukt in termen van verschillende
geodetische Wittendiagrammen met ongelijke bulkinteracties. Dit toont aan dat
geodetische Wittendiagrammen bulkinteracties niet als fundamenteel behandelen.

Wilsonlijnen in AdS$_3$/CFT$_2$

In hoofdstuk 3 en 4 concentreren we ons op zwaartekracht in drie dimensies. In dit
geval heeft de zwaartekracht geen propagerende vrijheidsgraden en kan ze worden
herschreven als een Chern-Simons theorie. Dit is in het algemeen veel eenvoudiger
om het formalisme van Einstein algemene relativiteit theorie te manipuleren. In
de Chern-Simons formulering wordt de koppeling van materie gedaan met behulp
van Wilsonlijnen. In de context van AdS/CFT zijn deze objecten belangrijk om de
vrijheidsgraden van de theorie op de rand te analyseren omdat ze gerelateerd zijn
aan grootheden zoals CFT-correlatiefuncties en verstrengelings-entropie. In dit
proefschrift zullen we Wilson lijnen in AdS$_3$/ CFT$_2$ gebruiken voor twee verschil-
lende, maar gerelateerde doeleinden. In hoofdstuk 3 laten we zien dat ze kunnen
worden gebruikt om de overlap van twee lokale bulktoestanden te berekenen. Dit
geeft ons een recept om lokale bulkvelden te reconstrueren van CFT$_2$-operators in
globale AdS$_3$- en BTZ-geometrieën. In hoofdstuk 4 gebruiken we de Wilsonlijn in
de context van hogere spintheorieën. We gebruiken ze om een idee expliciet van
causaliteit te bieden in hogere spinzwaartekracht, waardoor we een Penrosedia-
gram kunnen toewijzen aan hogere-spin zwarte gaten.

ACKNOWLEDGEMENTS

You go to my head,
and you linger like a haunting refrain,
and I find you spinning round in my brain,
like the bubbles in a glass of champagne.

Billie Holiday

The role of an advisor in the life of a PhD student is more important than one can think. There are generally not bad or good supervisors; and it is all about the pairing between both parts. I feel that Alejandra Castro was the perfect match for me. I owe this thesis to her. Not only did she teach me physics, but she gave me great career and personal guidance, pushing me further when I was too distracted. I am really grateful for her feedback about presentations and writing, which was much more useful than any course in soft skills. Moreover, I felt very confortable approaching her for any reason, anytime. We had many long discussions, but sometimes crossing some words at the coffee machine was enough to get some inspiration to keep going with my computations. I am very lucky to have had her as a supervisor.

This thesis would not have been possible without my great collaborators Nabil, Fernando, Jan, David, and Juan, from whom I learnt so much. Moreover, the String Theory group of Amsterdam was a very inspiring and welcoming environment to work in. Specially, I would like to thank the other PhD students, Francesca, Gerben, Jaco, Ido, Laurens, Sam, Jorrit, Lars, Sagar, Beatrix, Greg, and Antonio, for their friendships, the nice coffee breaks, and for making this way a lot easier. To Damian, and Adolfo, for the mates and alfajores. To Alex, for having answers to my questions, and being so fun. To Ben, for taking me as his teaching assistant so many times, and for his constant support. During the master, Alex, Jochem, and Manus were the best friends, and study mates. Thanks for all

the Sunday evening rotis, for visiting me in Menorca, and for being so welcoming. There is also beautiful people at the other side of the street: Sabrina, and Jacopo, you cannot imagine how happy I am that I do not have to say goodbye to you, and Michael, I will miss our kitchen conversations while cooking. Fortunately, the life of a PhD student does not happen only at the university, and you get to know different countries and continents, where you meet incredible people. I would like to particularly highlight Pierre, and, of course, Celine, who is the best conference travel mate.

After these six years, Amsterdam has become a home to me. This would not have been the case without my friends: Bernat, Cris, Clemente, Guille, Miguel, Vanessa, and the already long gone Michael and Pablo. We form an amazing unstoppable team; you do not know how much I will miss drinking Chouffe with you. Another cornerstone has been Bilderdachio, where people like Bernardo, Carlo, Claudia, Eugenio, and Robbie created an Italian home in the heart of Amsterdam. Thanks to them I met Andrea, who turned out to be very special after all, and whose stupidity makes me smile widely. The chileans have had also an important role in this journey, with Nataly, and Pablo topping the list for always wanting to have one last drink. A honorary mention goes to Diego, with whom I very happily shared flat, friends, parties, travels, and even supervisor. Without you would not have been half as good. The Lindy Hop community has also brought me a lot of pleasure. I learned a lot about dancing, playfulness, and perseverance. I would like to particularly thank Juan, who apart from being a great collaborator, drag me back in the dancing scene. Prepare all your couches, I will come back often.

Everyone that knows me a little realises my profound love to my homeland, Menorca. It is hard to be far away, but at the same time it is comforting to know that, no matter what, there is a safe place that you will go back to. I want to thank my friends, Dowy and Lluís, who are still able to get the Rambo face paint when it is necessary. And to Carol, who will always be the MVP. I would like to ask my sincere apologies to Tomeu and Adrià, for always intruding their romantic summer nights. I want to thank my family for their support, and for the unmovable long Sunday lunches with my parents, aunts, my sister, who has become a great party companion, and my cousin Helena, who is the best. Finally, I specially dedicate this thesis to my grandparents, l'avi en José, i s'àvia Sita, who are greatly missed.